APPENDIX F. TEST-TRACK RESULTS

F.1 VEHICLE INDUCED FALSE ALARMS—STRAIGHT ROADWAY

F.1.1 Purpose

The purpose of the following two tests ("Roadside Vehicle" and "Adjacent Lane Vehicle") is to determine the Primary vehicle's ability to ignore an out-of-lane Secondary vehicle on a straight section of roadway. In one case, the Secondary (target) vehicle is parked on the roadside shoulder; in the second it is traveling in an adjacent lane in front of the Primary (or host) vehicle. Only the Primary and Secondary vehicles will be present on the roadway.

These tests were designed to measure the return levels, if any, observed in the raw radar return signal from the "non-threatening" secondary vehicle. We refer to these "non-threatening" vehicles as "clutter," that produce returns which are not of primary interest to the radar system. In the automotive radar application, the Secondary vehicles in these tests are clutter because they are not located in the operating lane of the Primary vehicle and therefore, do not constitute a collision threat under normal driving conditions.

F.1.1.1 Roadside Vehicle

Procedure

The Secondary vehicle was parked on the roadside shoulder approximately 1/4 of a mile in front of the Primary vehicle. The Primary vehicle accelerated to freeway speeds and passed the Secondary vehicle, completing the test.

This test procedure was repeated a number of times using both a Honda Accord and a Semi-Tractor/Trailer as the Secondary vehicles. Also, runs were made with the FLAR sensor's center beam active. The center beam has a 3 degree azimuth and 3 degree elevation beamwidth.

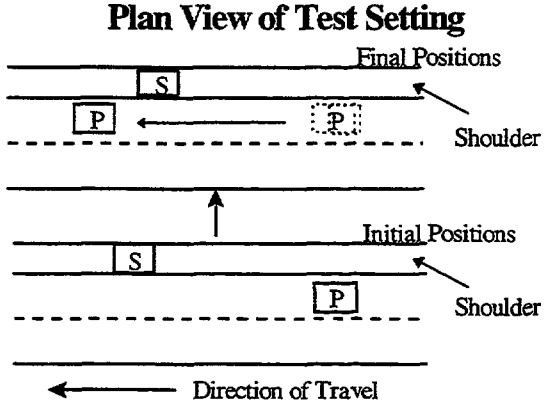

Results

Data from these tests was screened using the ERIM Analysis PC software to identify data sets for further analysis. Several data sets were selected and the raw radar returns (prior to any digitization in the FLAR) were processed using custom Matlab scripts.

The Matlab processing of data from both the Honda Accord runs and Semi-Tractor/Trailer runs showed evidence that the FLAR raw data detected these roadside vehicles. The Semi-Tractor/Trailer vehicle provided a stronger return under the geometric conditions of the test than the Honda Accord. The data from one of the test runs with the Semi-Tractor/Trailer as the Secondary vehicle will be used to illustrate these findings.

Figure F-1 shows the FLAR signal returns for one of the test runs. The returns resulting from the roadside vehicle are annotated in the figure. As expected, the radar initially detects' the target at a long range. As time progresses and the Primary vehicle approaches the Secondary vehicle, the range of the radar returns correspondingly decreases and their amplitude increases. Finally, the radar returns from the Secondary vehicle fall off sharply and are not evident above the baseline returns of the system.

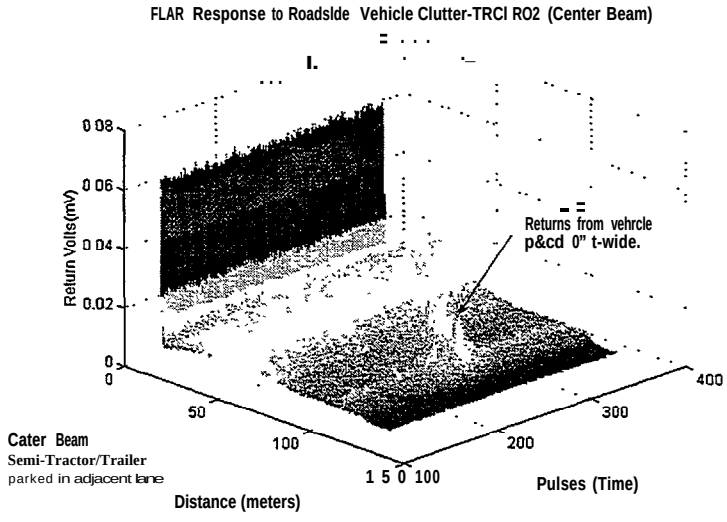

Figure F-1. FLAR Response to Roadside Vehicle Clutter

Quantitative analysis indicates that for the given geometries in this test, the tractor/trailer RCS levels varied from -3 to +3 dBsm. These levels are highly dependent on the orientation between the radar and the target, and also the positioning of the target within the illuminating radar beam pattern as discussed below.

The range at which the Secondary vehicle was first detected was approximately 90 meters and the range at which the returns fell off was approximately 50 meters. Figure F-2 illustrates the geometric orientations which induced the radar returns. Simple trigonometric anaIysis indicates that the roadside vehicle produced radar returns during the period at which it was at an azimuthal heading of 1.3 to 2.3 degrees (referenced to the Primary vehicle's radar beam boresight).

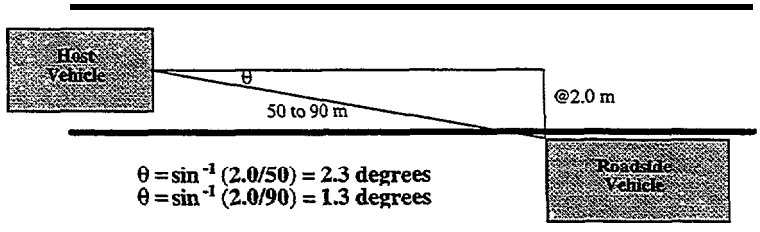

Figure F-2. Object Orientation Roadside Clutter Analysis

'Throughout the discussions in this report, the term "detects" refers to the observable presence of radar returns from a particular object in the radar's raw IF signal. This is different than stating that the FLAR "locked-on" and tracked a target. The term "locked-on" refers to the fact that the FLAR (and its internal TRW-proprietary processing algorithms) identified and tracked the object.

Results

As in the roadside vehicle experiments, data from these tests was screened using the ERIM Analysis PC software to identify data sets for further analysis. Several data sets were selected and the raw radar returns (prior to any digitization in the FLAR) were processed using custom Matlab scripts.

For test runs with the radar's center beam active, the adjacent lane tests showed that returns from the Secondary adjacent lane vehicles were not present. While this result does not appear consistent with the roadside vehicle tests, the difference can be attributed to slightly different geometric orientations, which resulted in the Secondary vehicle being located outside the mainlobe of the center beam.

For test runs with the radar's left beam active, the adjacent lane vehicles produced clear radar returns. By having the left beam active, the FLAR's effective field-of-view is skewed to the left by approximately 2.7 degrees. This multiple beam approach, to increase the FLAR's overall field-of-view, was employed primarily to support tracking vehicles while the primary vehicle was in a curve. From this test, it is evident that this multiple beam approach can help detect vehicles in an adjacent lane.

Figure F-4 is an example run with a semi-tractor/trailer as the Secondary vehicle. Here we see that the radar detected the Secondary vehicle at ranges varying from approximately 45 to 65 meters. These return levels are lower than one might expect with the Ieft beam being active, however considering that the orientation and shape of the semi-tractor/trailer, it is reasonable to assume that a large portion of the ener,v is being reflected away from the FLAR receiver. Quantitative analysis indicated that for the given orientations, the truck returns correlated to a target with an RCS of approximately -5 dBsm. Tests run with the Accord resulted in similar RCS measurements.

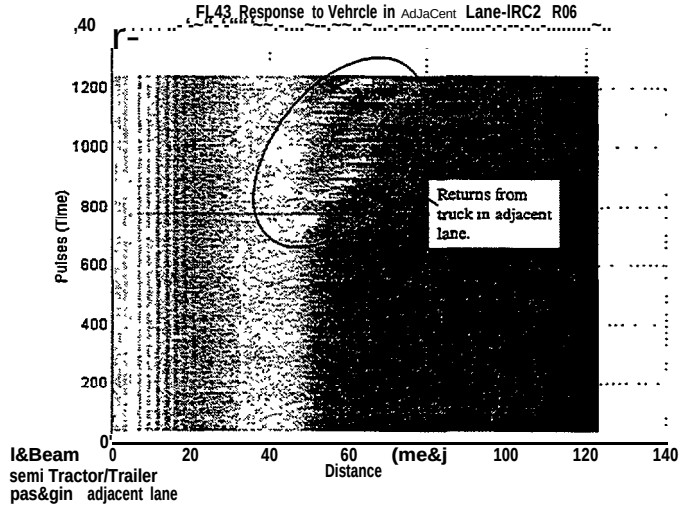

Figure F-4. FLAR Response to Vehicle in Adjacent Lane

This figure also illustrates another interesting phenomena -- the radar has detected two separate groups of scatterers on the same vehicle, which appear as two totally separate returns. Analysis of the collected data determined that the first return (the lower return in the figure) is coming from a scatterer located on the front part of the Secondary vehicle, probably the front set of wheels. The second return (the top return in the figure), which is separated from the first by approximately 55 feet, is coming from the rear portion of the vehicle, probably the rear set of wheels.

Figure F-5 illustrates the geometric orientation corresponding to the range over which the Secondary vehicle was detected by the left beam. These are consistent with the measured beam patterns of the FLAR as shown in Figure F -6. The range of azimuth angle over which the vehicle in the adjacent lane

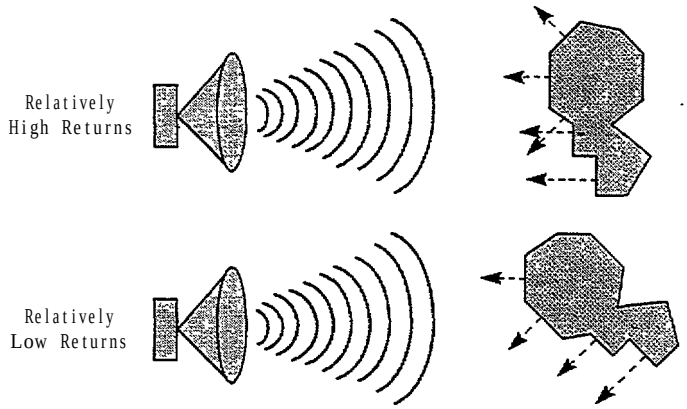

Figure F-7. **How Target Orientation Affects Return Levels**

Conclusions

Conclusions derived from the experiments are summarized below.

- Some automotive radar system designers have used a 3 degree 3 dB beamwidth since it covers one lane width at approximately 100 m (the specified detection range). These test show that large RCS objects outside the stated beamwidth will produce returns in the radar sensor.
- Even though automotive radars may have an extended FOV (either through beam switching or scanning), the orientation and shape of vehicles in the adjacent lanes can produce return levels much lower than expected.
- While the return levels from the Secondary vehicles in these tests are relatively low, the specific orientation and structure of roadside/adjacent lane clutter can produce relatively high return levels. Quantitatively speaking, the geometries and orientations of the experiments resulted in observed RCS levels from both the Accord and tractor/trailer on the order of -5 to 0 dBsm.
- The radar would interpret returns witnessed in these experiments an object in the direct path of the primary vehicle.
- Threat algorithms must take into account returns from objects located outside the stated beamwidth of the antenna (3 dB width)
- The results indicate that some form of azimuth resolution, at least half a lane width, would be highly beneficial for collision avoidance systems.

F.2 BRAKING SECONDARY VEHICLE-STRAIGHT ROADWAY

F.2.1 Purpose

The purposeof this test is to evaluate the Primary vehicle's response to a target vehicle which braked after the Primary vehicle had been tracking it. Events of interest are loss of target tracking and the return levels from target vehicle.

Procedure

During the test, the Primary vehicle maintained a constant speed (45 MPH), while the target vehicle accelerated and braked to vary the range between the two vehicles. The range was varied from approximately 20 to 50 meters. The test took place on a closed test track with only the primary and secondary vehicles present. Only the FLAR center beam was active during the test. The center beam has a 3 dB beamwidth of 3 degrees in both azimuth and elevation.

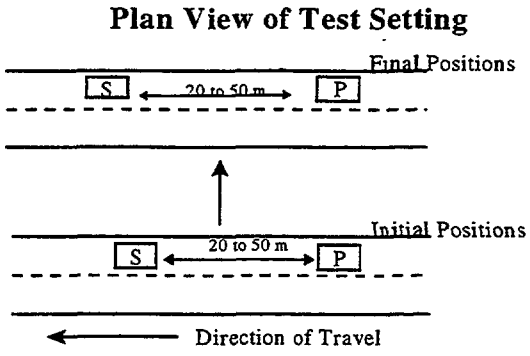

Results

Several runs were made following the procedure described above. The results were found to be consistent from run to run. Plots from one run will be used in the discussion below to illustrate the results.

Figure F-8 illustrates the raw (IF) radar return signals received by the FLAR system. Figure F-8(a) shows that in this fairly low clutter environment, the return signal levels from the target vehicle were clearly visible above the noise floor of the system for most of the time (note that the signal level shown in the plot consists of integrating the energy from six consecutive radar pulses). The dynamics between the host and target vehicles are easily seen in Figure F-8(b). The target vehicle continuously approached and receded from the host vehicle in a sinusoidal pattern.

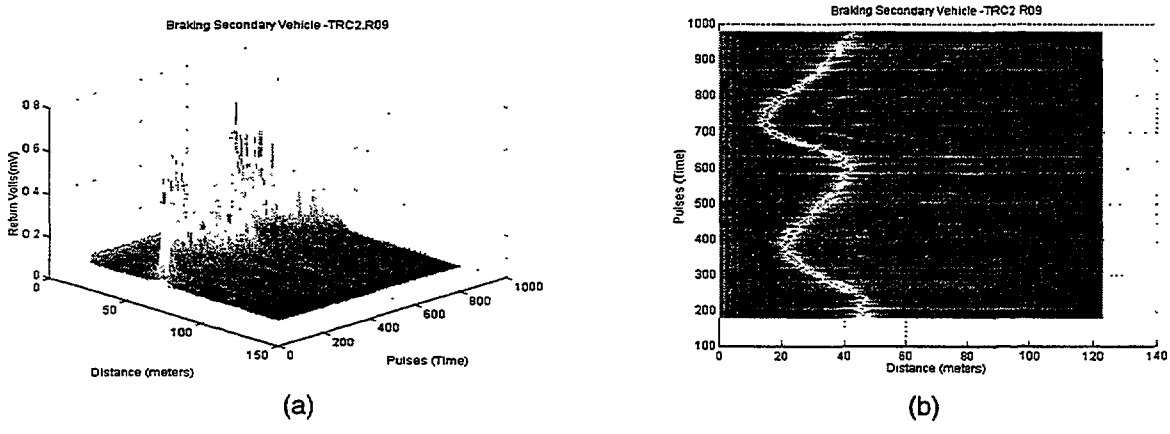

Figure F-8. Braking Secondary Vehicle

Return Levels

The return signal levels followed a pattern which would be expected from the experiment dynamics. As the range to the target vehicle decreased, the return levels increased and as the range to the target vehicle increased, the return levels decreased. A plot showing the peak return level for each group of processed radar pulses is provided in Figure F-9.

Quantitative analysis showed that the target vehicle, a Honda Accord exhibited average radar cross section (RCS) values ranging from +3 to +8 dBsm. Average RCS must be emphasized, because short term (pulse-to-pulse) variations in the calculated RCS were observed to vary by as much as 10 dB.

These short term variations in exhibited RCS levels can be attributed to scintillation and directive reflectivity effects. The scintillation effects are caused by the interaction of the electromagnetic waves reflected by individual radar scatterers which are distributed across the target vehicle. Due to the very short wavelength of the energy emitted by the FLAR, minute changes in the distance between the radar and the various scatterers causes the reflected waves to interact in constructive and destructive manners. When the waves add together constructively, the return 1evel increases; when they interact destructively, the return levels decrease.

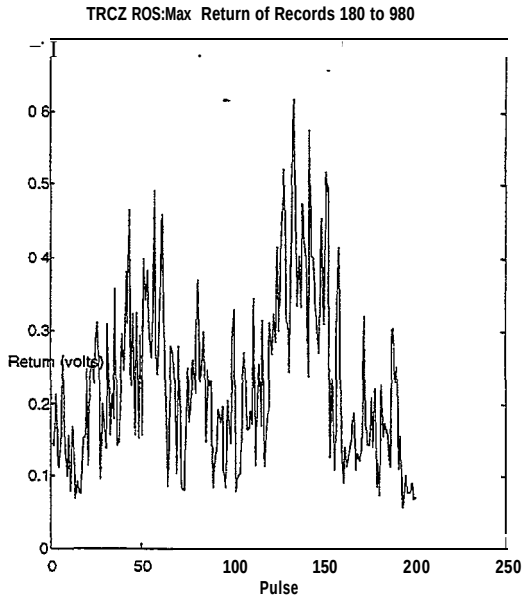

Figure F-9. Peak Return Levels

Directive reflectivity simply refers to the level at which a scatterer directs energy back at the illuminating radar. As the orientation between a complex shaped scatterer and an illuminating radar varies, the amount of energy reflected back at the illuminating radar can change drastically. A simple example of this effect is the glint of the sun off of a mirror.

Ability to Maintain Lock on Target Vehicle

Fortunately, these short term variations average out aud simple processing techniques will allow the radar sensor to maintain a consistent lock on the target, provided the target's average RCS results in return levels sufficiently above the sensor's noise floor.

In analyzing the processed outputs of the FLAR (which utilizes TRW's proprietary algorithms), it was found that the sensor did maintain a consistent lock on the target vehicle throughout the test collections. It should be noted though, that even the lowest returns from the target vehicle were above the baseline noise floor of the FLAR.

Accuracy of FLAR Tracking

In addition to evaluating the return levels and the ability of the FLAR to maintain lock on the target vehicle, a differential GPS (DGPS) truthing mechanism was utilized to evaluate the accuracy with which the FLAR reported the range to the target vehicle. During the tests, the reported range outputs from the FLAR were recorded. These ranges were calculated by TRW's proprietary processing algorithms and updated by the FLAR every 50 milliseconds.

Figure F-10 shows the results of the DGPS truthing analysis. Comparing the DGPS 'true' range with the range reported from the FLAR indicates that the FLAR was able to track the target vehicle to within 1 meter for the particular scenarios created during the test runs. This accuracy meets the reported specification of the FLAR.

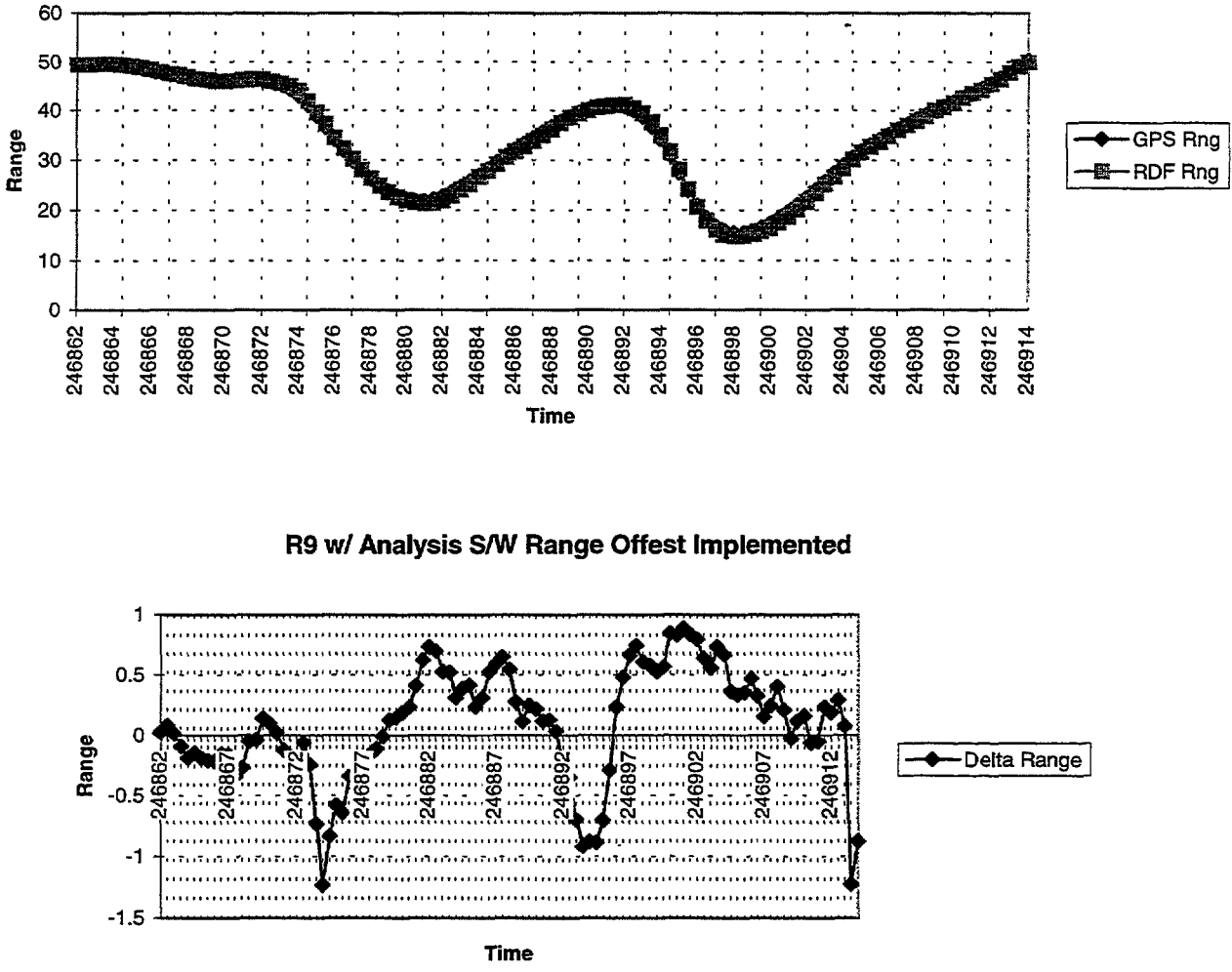

Figure F-10. GPS Truth for R9

Conclusions

The braking target vehicle test analysis did not produce any unanticipated results. In the relatively simple environment created during these tests, the radar returns accurately depicted the dynamics of the target vehicle.

The actual RCS levels were seen to vary by over 10 dB over the short term (500 msec), but tended to average out to a +3 to +8 dBsm RCS for the target vehicle (a Honda Accord). These levels are well correlated to the RCS measurements made on similar vehicles as part of this program. The variations in signal levels observed in this test can be expected to occur to differing degrees for most objects an automotive radar will encounter on the roadway.

Scintillation and directive reflectivity characteristics play a key role in the variations of the signal return levels seen by the radar sensor, as a result of the simple dynamics between the host and target vehicles. In many cases, these effects will actually help automotive radar detect low RCS targets by

sporadically generating relatively high level returns as a result of glint and constructive wave interactions.

Finally, the DGPS truthing mechanism was found to have a very high degree of correlation with the reported range values from the FLAR sensor. In fact, during the braking target vehicle tests, the FLAR was found to be accurate to within 1 meter for the duration of the collections.

F.3 OUT-OF-LANE VEHICLE CLUTTER—STRAIGHT ROADWAY

Purpose

The purpose of this test is to determine the Primary vehicle's ability to track the in-lane target vehicle when there is an out-of-lane "clutter" vehicle that should be ignored. These tests begin to address the issue of "clutter" vehicles interfering with the returns from target vehicles and causing errors in the reported ranges of the target vehicles. Events to watch for in this test are loss of lock on the target vehicle, returns from the clutter vehicle, and errors in reported range to the target vehicle.

Procedure

The test begins with the Primary vehicle maintaining a constant distance of approximately 30 meters from the in-lane target vehicle, (S1) and an out-of-lane "clutter" vehicle (S2) next to the Primary vehicle. The Primary and target vehicles maintain their lane positions throughout the test. The out-of-lane clutter vehicle accelerates to a position approximately 50 meters in front of the Primary vehicle and maintains this position (in the outside lane) for the remainder of the test.

A Honda Accord was used a the target vehicle and a semi-tractor/trailer was used as the clutter vehicle.

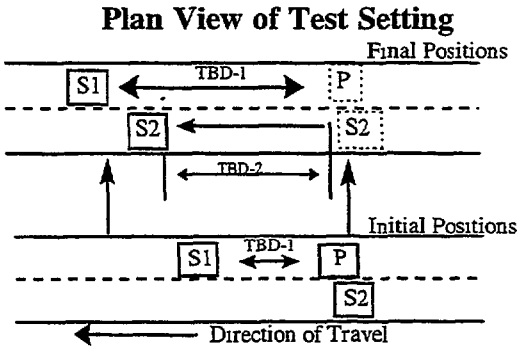

Results

Several test runs were made using the procedure described above. Test runs were made with both the center beam and left beams active. Figure F-11 is a data plot resulting from a run in which the left beam of the FLAR was active and will be used here to summarize the results of these tests.

As was the case in all the test runs, returns from the target vehicle were always observable in the raw radar data. Also, the TRW-proprietary algorithms used in the FLAR always maintained lock on the target vehicle whether the center or left beam was active.

Analysis of the DGPS data indicated that the presence of the clutter vehicle did not cause any erroneous range data to be reported

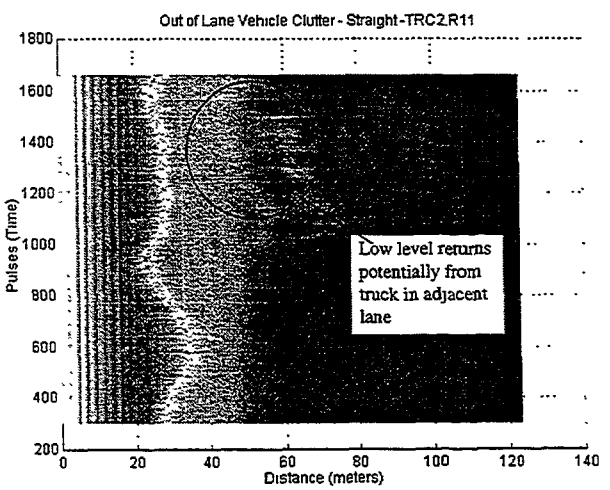

Figure F-11. Out of Lane Vehicle Clutter—Straight

by the FLAR for the given scenario. Likewise, no sudden shifts in IF frequency were observed in the raw radar data; this would have indicated some multipath interference induced by the clutter vehicle.

Returns from the clutter vehicle were only evident during runs in which the left beam was active. The annotations in Figure F- 11 highlight the returns attributed **to** the clutter vehicle; they are consistent with those observed during tests with the semi-tractor/trailer in a similar orientation. These returns were of a very low level and barely rose above the radar system noise floor.

Upon analyzing the video data which was collected along with the radar data, it was observed that the target vehicle had actually drifted to the right portion of its lane during the period when the returns from the clutter vehicle were present. Geometric analysis of the vehicle locations with respect to the radar during the collection show that the radar's field of view provided by the left beam was limited to roughly the left-most portion of the lane occupied by the Primary vehicle. Therefore, the clutter vehicle was being "occluded" by the target vehicle when the target vehicle was in the left or center portion of its lane. However, as the target vehicle drifted to the right, the clutter vehicle was being illuminated by the radar and thus provided the returns observed in Figure F-l 1.

Conclusions

For the given test scenarios, no significant effects from clutter vehicles on a straight roadway were observed. However, observations do lead to the conclusion that different scenarios may produce somewhat different results. In particular, target vehicles located at longer ranges than those tested in these experiments would allow the FLAR's left beam to more intensely illuminate the clutter vehicle, producing higher level returns. It is unlikely, at least on straight roadways, that these clutter returns would compete with or those from the target vehicles.

Unfortunately, the infinite combinations of vehicle positions could not be tested in this program. As a result, another potential effect of adjacent lane vehicle clutter which was not exhaustively tested for was that of multipath. Certain geometries between the radar, the target vehicle, and the clutter vehicle may produce returns resulting from "indirect" reflections off the vehicles. For example, the transmitted radar ener-7 may first reflect off the target vehicle toward the clutter vehicle, and reflect off the clutter vehicle and return to the radar. The result would be a return which would appear to come from the target vehicle, but at a longer range. It is suggested that more testing, to address empirical or simulated, to address multipath effects be conducted in the future.

These tests also provide some insight into results which could be expected for automotive radars which employ scanning antenna technology and larger field of views. As the antenna is directed towards the edges of its FOV, it will probably pick up returns from clutter vehicles in adjacent lanes. The scanning antenna mechanism will give system designers the ability to employ algorithms to help discriminate and identify clutter target returns based on the antenna's position within the scanning range.

F.4 INTENTIONAL LANE CHANGES-STRAIGHT ROADWAY

Purpose

The purpose of this test was to determine the radar's response to vehicle lane changes. Response time is an important performance parameter that was monitored.

Procedure

Only the Primary and target (Secondary) vehicles were present on the freeway. Two different types of lane changes were evaluated. In the first test, the Primary vehicle changed its lane to pass the target vehicle. In the second test, the target vehicle moved out of the Primary vehicle's lane.

Primary Passes Target

The test began with the Primary vehicle maintaining a constant distance to the target vehicle. The Primary vehicle then accelerated moderately and changed its lane to pass the target vehicle. The test terminates after the Primary vehicle passes the target vehicle.

Plan View of Test Setting

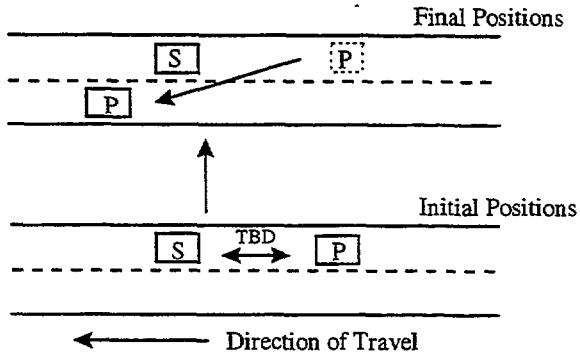

Target Leaves Lane

The test began with the Primary vehicle maintaining a constant distance to the target vehicle. The target vehicle accelerated moderately and changed its lane, then decelerated to approximately the same distance as at the beginning of the test. The test terminated after the Secondary vehicle had achieved and maintained the original headway.

Plan View of Test Setting

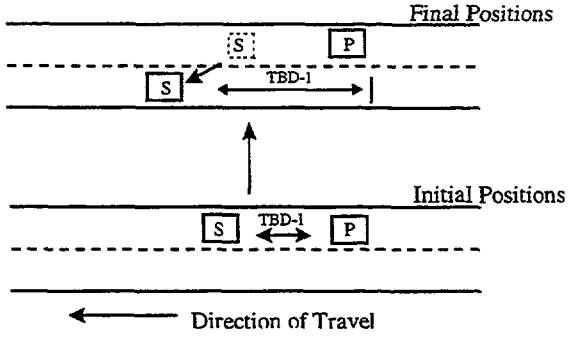

Results

In general, the radar sensor performed very well under the low-clutter environment created during these tests. The response time for the radar to react to the lane change appeared to be very good based on analysis of the video data, raw radar data, and GPS data. The analog video collection system limited the amount of quantitative analysis that could be done in terms of absolute response times, but the raw radar data and dynamic movements captured by the video system appeared to correlate to within a second. Performance was consistent over all the tests conducted and no significant differences were observed between the host lane change and target lane change dynamics.

A set of collection data taken during a host vehicle lane change maneuver will be used to summarize the results. The data plots in Figure F-12 are from a run in which the Primary vehicle was following a Honda Accord, and the Primary vehicle made a lane change. Figure F-12(a) illustrates the typical return characteristics as the Primary vehicle approaches the target vehicle, namely, the return levels increase as range decreases. The Accord measured to be approximately 3 to 7 dBsm through the run.

Procedure

The test began with the Primary (host) vehicle maintaining a constant distance to the first target vehicle (S1), with the second target vehicle adjacent to the Primary vehicle and traveling at the same speed. The second target vehicle then accelerated and moved into the right-hand lane between the other two vehicles. The distance between vehicles was selected for safe operation and to be within the FLAR's minimum operating range.

Plan View of Test Setting

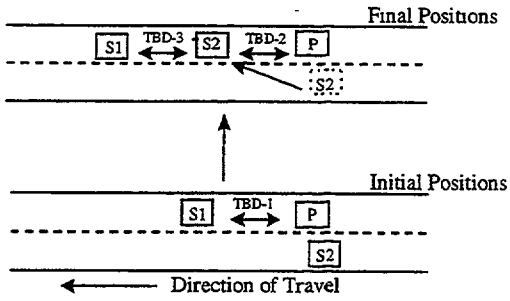

Results

The results of these tests parallel those described in the previous section, "Tracking New Target Vehicle—Straight Roadway." The primary difference was in the vehicle dynamics which produced the result. In the previous the first targeted vehicle departed from the Primary vehicle's lane, presenting the radar with a second target vehicle at a greater range than the first. In these tests, the second target cuts into the land and is presented to the radar at a range less than the first target vehicle by a maneuver.

The end result for both are similar in that the radar performed well. Sample data plots for one of the test runs conducted as part of this series of tests are provided below. The reader should refer to the discussion in "F.5: Tracking New Target Vehicle—Straight Roadway" for a more detailed discussion.

Figure F-16 plots the raw radar data collected throughout the duration of a test conducted using two Honda Accords as the target vehicles. Figure F-16(a) includes a time line of events and annotation indicating the sources of the respective returns. Figure F-16(b) shows the amplitudes of the relative return levels which correlate to an expected RCS of a Honda Accord of between +3 to +7 dBsm.

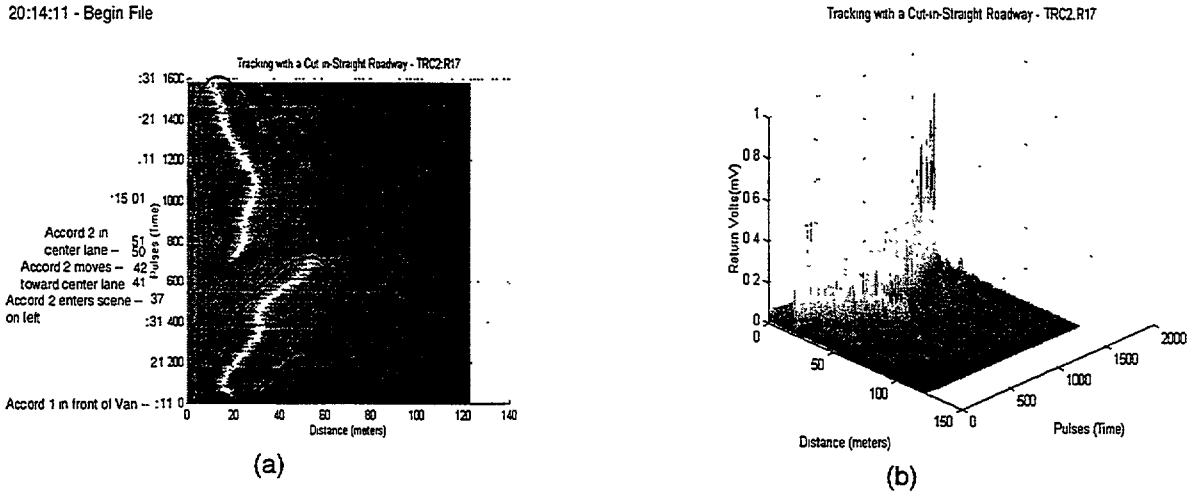

Figure F-16. Tracking With a Cut-In Straight Roadway

Figure F-17 is a plot of the GPS truth data and the FLAR reported range data. As in the lane departure tests, the FLAR produced no dropouts or jitter in the transition from one target vehicle to the other.

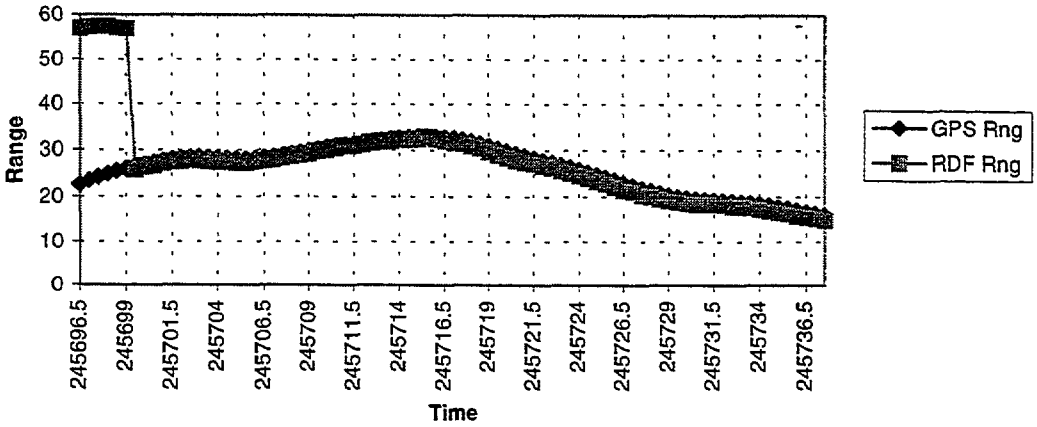

Figure F-17. GPS Truth for R17

Conclusions

The important issue to note in these tests is that during the cut-in process, the second target vehicle was actually in a position such that a collision could occur with the host vehicle, but the radar sensor would never "see" the target vehicle. Again this is a limitation of the FLAR's field of view.

Figure F-18 illustrates the problem in which the radar beam is not illuminating the target vehicle although the target vehicle is obviously within the primary vehicle's path. For the Adaptive Cruise Control Application, the operator may actually find himself accelerating into a collision with the undetected target vehicle. Two options for this situation are available. The first is to increase the field-of-view of the forward-looking sensor, and the second is to install simple supplemental sensors which work at close range but have a wide field-of-view. These supplemental near-range sensors could be strategically placed in areas near the edge of the vehicle, such as the headlight area.

Both of the solutions to this problem add both cost and complexity to the system and require a detailed trade-off analysis.

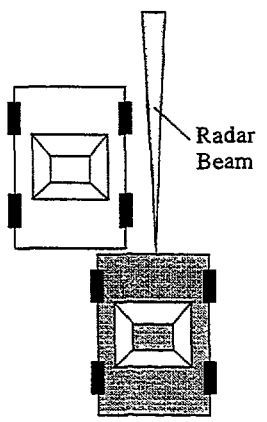

Figure F-18. Beam Illumination

F.7 STRONG VEHICLE CLUTTER IN RANGE—STRAIGHT ROADWAY

Purpose

The purpose of this test is to determine the radar's ability to acquire and maintain track on a fixed target vehicle in the presence of a relatively stronger (in terms of RCS), in-lane Secondary vehicle, but at a greater range. This will test the FLAR's ability to discriminate vehicles in the same lane, but with varying RCS and range.

Procedure

The nearer range target vehicle was a motorcycle (MC). The clutter vehicle was a semi-tractor/trailer with a radar cross-section significantly greater than that of the motorcycle. The FLAR's task was to detect and maintain track on the motorcycle and ignore the presence of the clutter vehicle. The test began with the motorcycle and clutter Secondary vehicle in the adjacent lane to the Primary, with all the vehicles traveling at the same speed. The motorcycle then accelerated, moves into the Primary vehicle's lane, and maintained a position in front of the Primary vehicle. The position of the motorcycle with respect to the primary vehicle was varied on a run-by-run basis. The clutter Secondary vehicle then accelerated, moved into the same lane, and varied its position from 5 to 80 meters in front of the motorcycle. The distances were selected for safe operation; their sum was less than the maximum operating range of the FLAR. The test continued for several minutes with the motorcycle varying its position within its lane.

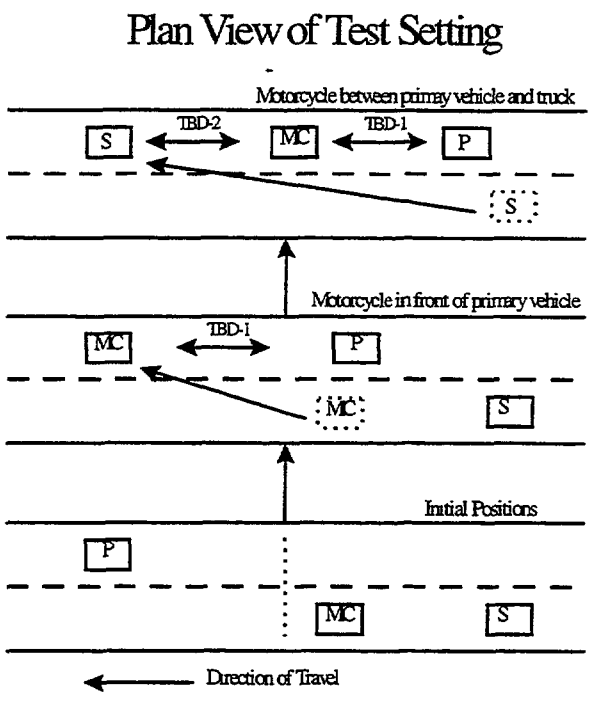

Results

These tests yielded some of the more interesting results in the program. Two separate data sets will be used to illustrate the effects of strong range clutter on the radar's response. Both data sets are taken from collections in which the motorcycle was located between the host vehicle and a semi-tractor/trailer.

Data Set #1: Radar Maintains Lock on Motorcycle

Figure F-19 is a plot of the radar return signals collected during the test. The figure also provides a time line of events which occurred during the collection and annotation of the respective sources which created the returns.

The motorcycle entered the primary vehicles lane approximately 10 seconds into the test and the radar's field of view approximately 13 seconds into the test. The initial range to the motorcycle was about 15 meters. The motorcycle continued accelerating until it reached a range of approximately 25 meters. This range was roughly maintained for the duration of the test. Approximately 30 seconds after the motorcycle entered the radar's field of view, the clutter vehicle (i.e., the truck) entered the lane in front of the primary vehicle. The radar returns generated by the truck are clearly seen on Figure F-19.

With both the motorcycle and truck with the radar's field of view, returns from both targets could be frequently observed. Occasionally, the motorcycle would be in a position such that it totally occluded the returns from the truck. This is observed in Figure F-19 at approximately 14:53:48 (or pulse 1500). The interesting point to note is that as the motorcycle drifted to the side of the lane, its return levels decreased, but were still observable, and those from the truck increased significantly. This is of course

due to the fact that as the motorcycle moved off of the radar beam's boresight, more of the energy illuminated the truck and less illuminated the motorcycle.

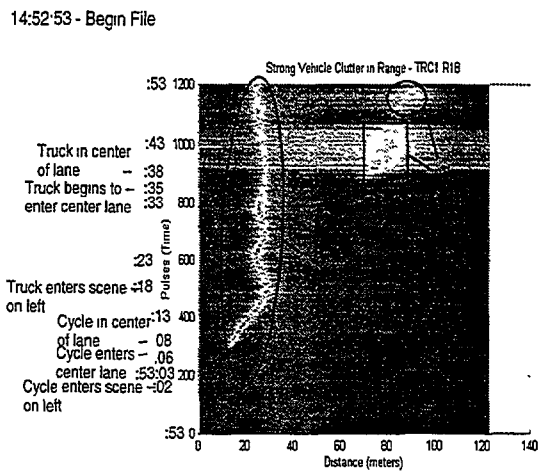

Figure F-19. Strong Vehicle Clutter in Range

The key performance attribute in this type of scenario is whether or not the radar can maintain lock on the motorcycle as it drifts to the edges of its lane, even in the presence of the truck returns. Based on the plot in Figure F-19, it is reasonable to conclude that a moderately robust tracking algorithm should be able to maintain lock on the motorcycle.

Figure F-20 shows that the FLAR and its TRW-proprietary processing algorithm did, in fact, maintain lock on the motorcycle. The line labeled "GPS Rng" in Figure F-20 corresponds to the measured range to the truck utilizing the DGPS truthing mechanism. The line labeled "RDF Rng" corresponds to the range reported by the FLAR. The TRW FLAR was designed to operate as an Adaptive Cruise Control sensor and, therefore, its primary function is to identify the target in front of the host vehicle and track its range. It is obvious from this plot that once the FLAR began tracking the motorcycle, it was able to maintain track throughout the test even in the presence of returns from the clutter vehicle which were stronger than that of the motorcycle.

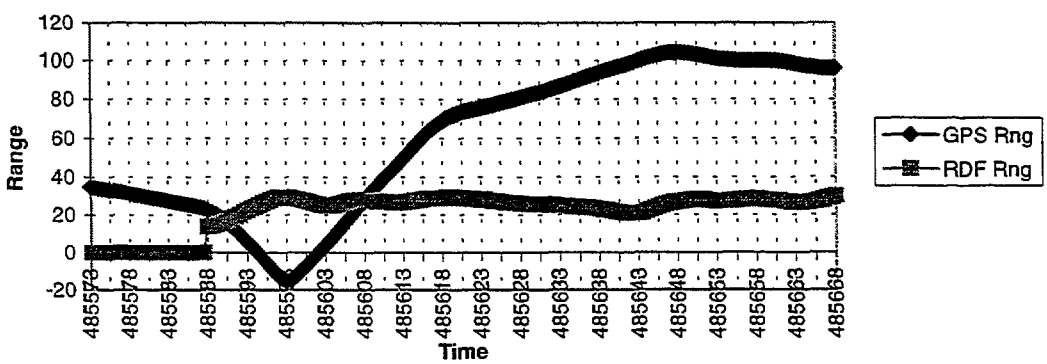

Figure F-20. GPS Truth for R18

Figure F-21 is another plot which contains the same data shown in Figure F-19; however, the differences in the relative return levels can be more clearly seen. MATLAB processing of this type of data allowed numerical analysis to estimate the radar cross-sections exhibited by both the motorcycle and the truck during the test.

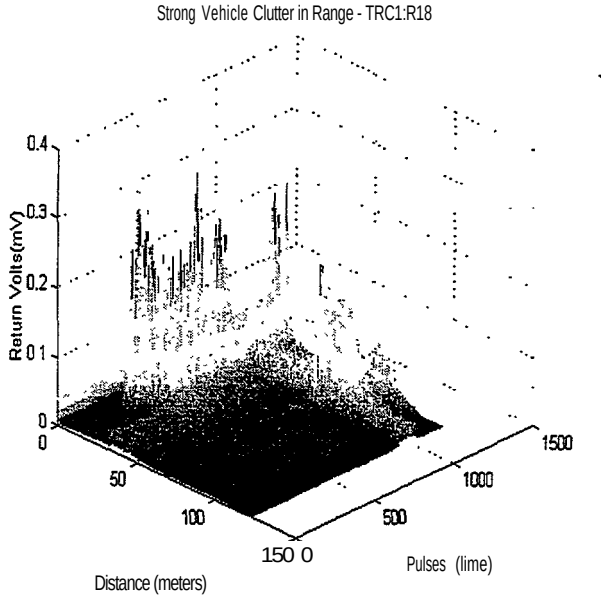

Figure F-21. Strong Vehicle Clutter in Range

Table F-1 summarizes the results of the radar cross section (RCS) analysis. The motorcycle was seen to vary from -6 to +3 dBsm depending upon its location within the lane. The truck exhibited RCS levels of 20 to 25 dBsm during periods when the motorcycle was positioned on the left side of the lane. As mentioned earlier, the motorcycle blocked nearly all of the truck returns when it was positioned in the center of the lane.

Table F-1. RCS Analysis Results

Target	Estimated RCS
Motorcycle in Center of Lane	0 to 3 dBsm
Motorcycle on Left Side of Lane	-6 to 0 dBsm
Truck with Cycle on Left Side of Lane	**20** to 25 dBsm

The RCS levels are quite consistent with the measurements taken during the "Roadway Object RCS Characteristics" phase of this program. The reader is referred to the "Catalog of RCS Characteristics for Common Roadway Objects" for more information on typical RCS levels. The catalog is available from both ERIM and NHTSA.

Data Set #2: Radar Loses Lock on Motorcycle

Figure F-22 is a plot of another test run made with the motorcycle and truck as the target vehicles. Again, a time line of events is provided in the figure and the source for the returns is annotated on the plot. Note **that** during pulses 1200 to 1400, both motorcycle and truck returns can be observed.

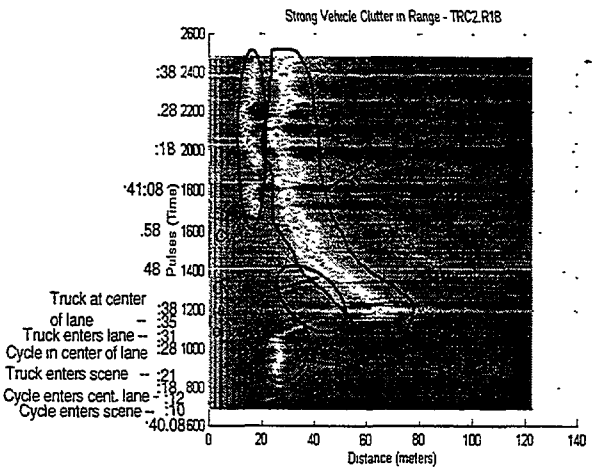

Figure F-22. Strong Vehicle Clutter in Range

Approximately 13 seconds into the test, the motorcycle enters the radar's FOV at a range of about 25 meters. The motorcycle then continues to accelerate as the truck enters the primary vehicle's lane. At about 30 seconds into the test (around pulse 1100), returns from both the motorcycle and the truck can be observed. The motorcycle is approximately 50 meters away, and the truck is 10 meters beyond the motorcycle. At this point, as expected, the returns from the motorcycle appear to be relatively low compared to that of the truck.

As both the truck and motorcycle decelerated with respect to the primary vehicle, the motorcycle was observed to drift to the left side of the lane. The plot in Figure F-22, illustrates that for a substantial period of time (about 15 seconds), the motorcycle returns were no longer observable. Subsequently, the motorcycle drifted back toward the center of the lane and was once again detected by the radar. The motorcycle stayed fairly close to the center of the lane, with some small deviations, for the duration of the collection.

The results of this test run contrast to those described for the previous data set in that the truck returns remained much more prominent throughout the run. In fact, once the truck entered the primary vehicle's lane, there were only several short periods during which the truck was fully occluded by the motorcycle.

As was the case with the previous data set, the critical performance parameter from the radar standpoint is whether or not the a consistent lock on the motorcycle can be held. Observing the raw radar returns indicates that there are two periods of time during which the radar may have had trouble maintaining a lock on the motorcycle. The largest gap occurs from 15:40:48 to 15:41:02 (pulses 1400 to 1650 in Figure F-22). The smaller gap occurs from 15:41:10 to 15:41:12 (pulses 1820 to 1900 in Figure F-22).

Figure F-23 is the corresponding GPS truthing plot to the test run. The truck range is represented by the line labeled "GPS Rng" and the reported FLAR range is represented by the line labeled "RDF Rng". It is clearly evident in the plot that the FLAR (utilizing the TRW-proprietary processing algorithms) did in fact lose lock on the motorcycle during the larger of the two gaps mentioned in the preceding paragraph. During this period, the FLAR began tracking the truck rather than the motorcycle. The transitions from tracking one vehicle as opposed to the other were not gradual transitions, but rather abrupt, in that the report range showed no residual effects from the previously tracked vehicle's position.

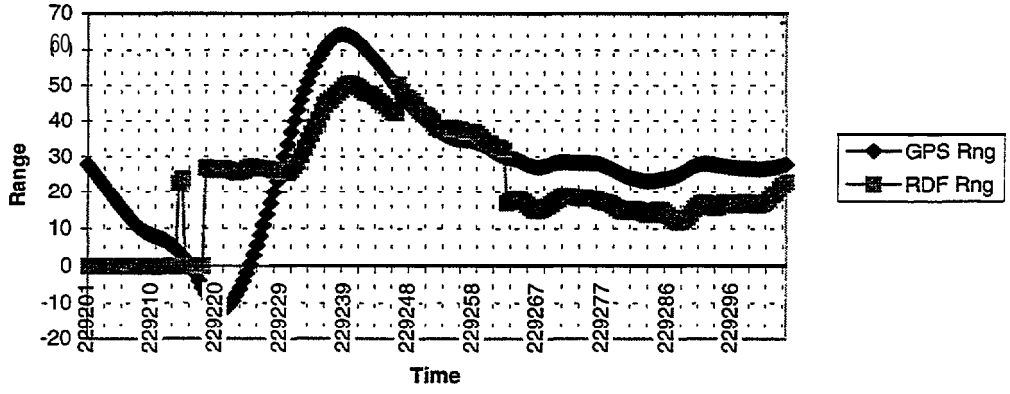

Figure F-23. GPS Truth for R18

Figure F-24 provides a better view of the relative return levels seen in the raw radar data during the collection. Peak level returns were evaluated to estimate the radar cross section (RCS) exhibited by each of the vehicles. These levels were found to be consistent with those listed in Table F-1,as expected.

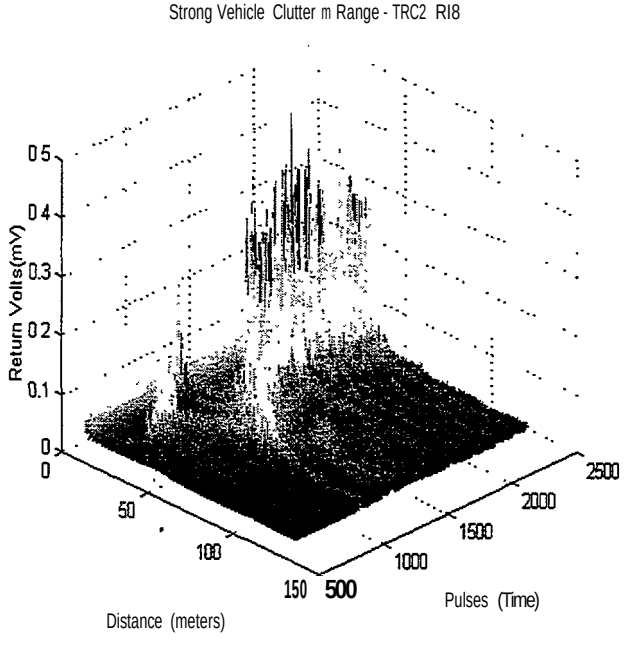

Figure F-24. Strong Vehicle Clutter in Range

Conclusions

The empirical data discussed in this test report indicate that automotive radar designs must carefully address the scenario of having a relatively small target located between the host vehicle and a relatively large target. Motorcycles and narrow cars pose the worst problems because they allow much of the radar energy to illuminate the large target located in front of them.

It was frequently observed in the empirical data that returns from both the motorcycle and truck targets within the host vehicle's lane were present. Furthermore, as the motorcycle drifted within its lane, its returns could actually dissipate to the point where the FLAR began tracking the truck which was at a greater range than the motorcycle. Obviously, this series of events could-have disastrous consequences in an ACC application. The driver could find himself accelerating to achieve a set headway behind the truck while colliding with the motorcycle.

These results emphasize the need for some form of scanning beam, in order to increase the radar's field of view and concentrate the highest gain portion of the beam across the path of the host vehicle.

One final issue of concern for this scenario deals with the use of automatic gain control (AGC) in the radar receiver circuitry. AGC implementations may be used to increase the effective dynamic range of a radar receiver and also protect it from saturation. However, there is a risk that a large vehicle, like the truck, may cause the AGC circuitry to reduce the sensitivity of the receiver to low level returns like those generated by the motorcycle.

The raw radar data in these tests was analyzed for AGC activity. The truck was found to induce a decrease in the FLAR receiver sensitivity by reducing the gain in the AGC circuitry. However, further analysis showed that the decrease in sensitivity did not, in and of itself, cause the loss of lock on the motorcycle. Instead, the primary cause for loss of track on the motorcycle was its position within the radar's beam.

F.8 VEHICLE CLUTTER IN AZIMUTH-STRAIGHT ROADWAY

Purpose

The purpose of these tests were to evaluate the radar's response to "clutter" vehicles positioned in azimuth (i.e., in adjacent lanes) while tracking a target vehicle located in the host vehicle's lane. This tests the FLAR's ability to discriminate between in-lane and out-of-lane vehicles.

Procedure

The FLAR's center beam (3 dB width of 3 degrees in azimuth and elevation) was activated during these tests.

The two out-of-lane Secondary vehicles (S2 and S3) had radar cross-sections equal to or greater than that of the in-lane Secondary vehicle. The test began with the Primary vehicle maintaining a constant distance from the in-lane target vehicle; the out-of-lane clutter vehicles were adjacent to the Primary vehicle and traveling at the same speed. The out-of-lane clutter vehicles then accelerated until they were adjacent to the in-lane Secondary vehicle. They maintained this position for several seconds and then decelerated until they were again adjacent to the Primary vehicle. The test terminated when the initial, relative vehicle positions had been achieved.

Plan View of Test Setting

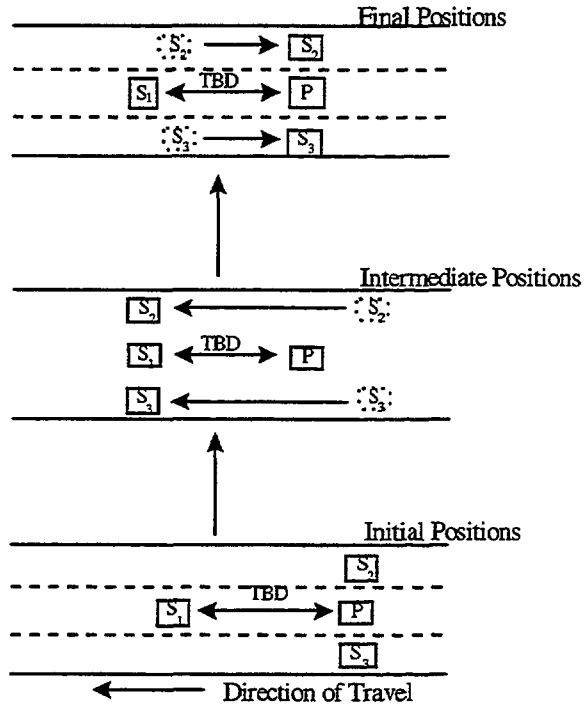

Results

The results for this test scenario are provided in the next section.

F.9 MERGING TRAFFIC-STRAIGHT ROADWAY

Another version of this test was conducted using a single clutter vehicle in the adjacent lane to simulate the situation frequently observed near a freeway entrance ramp. The vehicle dynamics are similar detailed in Section F.8 "Vehicle Clutter in Azimuth—Straight Roadway" tests described above.

Results

The results of both sets of tests were found to be very benign. Over six different test runs of varying target vehicle ranges up to 50 meters, the clutter vehicles never invoked a response in the raw radar data or the FLAR processed outputs. The plots in Figure F-25 summarize the empirical data collected in the tests.

The radar data accurately tracked the target vehicle's location throughout the test. The return levels from the Honda Accord target vehicle consistent with measurements made during other tests (at 3 to 7 dBsm).

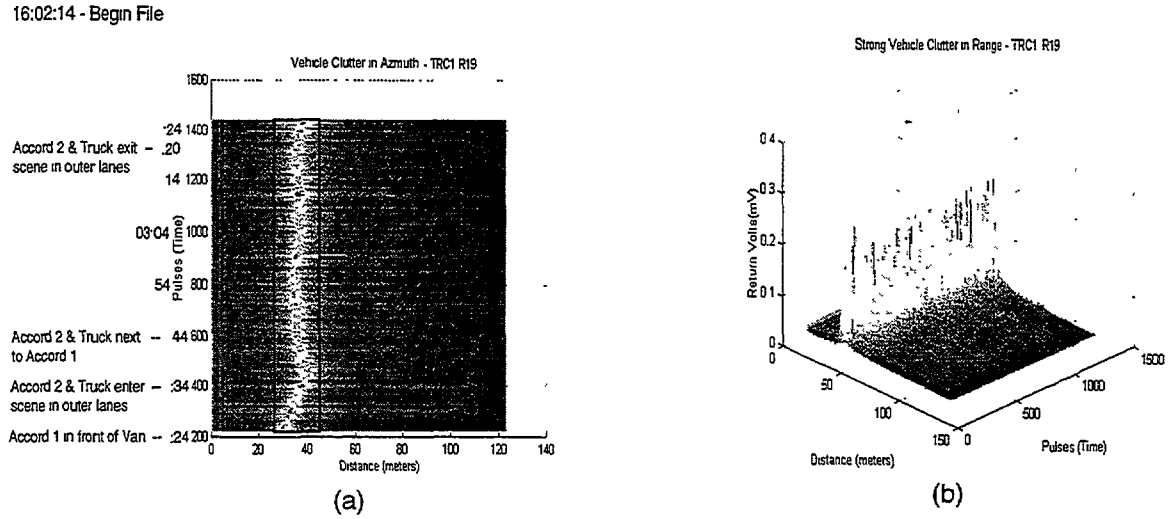

Figure F-25. Vehicle Clutter in Azimuth

Conclusions

For ranges up to 50 meters, vehicles in adjacent lanes do not appear to affect the raw returns of the radar sensor, given the 3 degree beamwidth of the FLAR. These tests did not extend to ranges beyond 50 meters, and further testing should be conducted.

F.10 VEHICLE INDUCED FALSE ALARMS—CURVED ROADWAY

F.10.1 Purpose

The purpose of the following two tests ("Stationary Target Vehicle on Shoulder" and "Moving Adjacent Lane Target Vehicle") is to evaluate the effect of guard rails and out-of-lane target vehicles located on a curved roadway. In one case the vehicle was parked on the roadside shoulder and in the other it was traveling in an adjacent lane in front of the Primary vehicle. Only the Primary and Secondary vehicles were present on the roadway.

These tests were designed to measure the return levels, if any, observed in the raw radar return signal from the "non-threatening" secondary vehicle and the guard rail.

F.10.1.1 Stationary Target Vehicle on Shoulder

Procedure

The Secondary vehicle was parked on the outside lane of a curved roadway which included a guard rail. The Primary vehicle began in the straight portion of the roadway, accelerated to freeway speed, passed the Secondary vehicle, and continued on until it exited the curved portion of the roadway completing the test.

This test procedure was repeated a number of times using both a Honda Accord and a Semi-Tractor/Trailer as the Secondary vehicles. Runs were also made with the FLAR sensor's center beam active. The center beam has a 3 degree azimuth and 3 degree elevation beamwidth.

Results

The ERIM Analysis PC software was used to screen the data and identify the data sets worthy of further analysis. Several data sets were selected and the raw radar returns (prior to any digitization in the FLAR) were processed using custom Matlab scripts. Several of the MATLAB output plots will be used here to illustrate the results. A complete set of plots from all MATLAB processed tests are included at the end of this document.

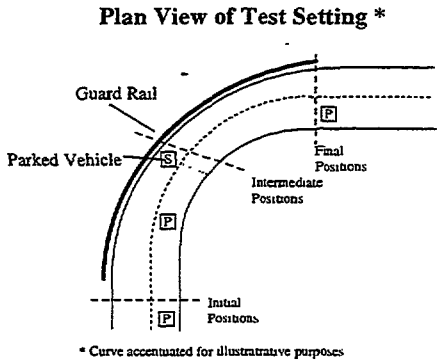

In general, radar returns form both the roadside guard rail and target vehicles were observed in the MATLAB processed data. The signal levels were well above the noise floor as will be illustrated below. Interestingly, the FLAR processed data (i.e., the TRW processing algorithm within the FLAR) never "locked-on" and tracked the returns from the guard rail or parked target vehicles for any significant period of time.

F.10.1.2 Characteristic Return From Guard Rail

Figure F-26 illustrates the characteristic return from a guard rail located on a curved section of roadway. As the primary vehicle approaches the curve, the radar beam remains fixed on a single section of guard rail which is located directly in front of the vehicle. Therefore, the reflection from the guard rail "appears" to the radar as a stationary object located directly in front of the radar, and approaching the radar at a rate equal to the vehicle's velocity. This portion of the guard rail characteristic is illustrated by the returns occurring during pulses 2100 to 2200 in Figure F-26.

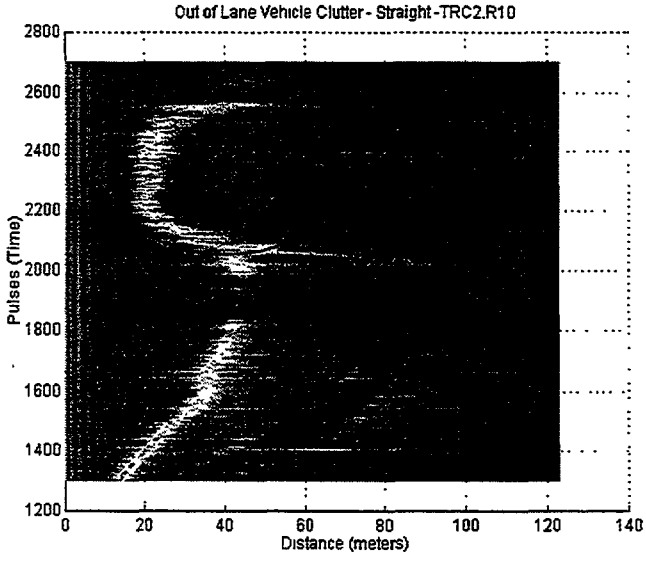

Figure F-26. Out of Lane Vehicle Clutter—Straight

Once the vehicle itself enters the curve, the radar beam begins traveling along the horizontal extent of the guard rail as the vehicle's heading constantly changes. Therefore, provided that the guard rail and roadway have similar curvatures, the portion of the guard rail being illuminated by the radar remains at a constant range as the vehicle proceeds through the curve. The guard rail returns of this type are observed for pulses 2200 through 2500 in Figure F-26.

Just prior to exiting the curve, the radar beam illuminates portions of the guard rail that do not have a similar curvature to that of the roadway. These portions of guard rail are actually straight. Therefore, as the vehicle exits the curve, the distance to the guard rail rapidly increases until the radar beam is no longer illuminating the guard rail, but instead is directed down the lane occupied by the host vehicle. This is illustrated during pulses 2500 and up in Figure F-26.

This dynamic sequence of events (see Figure F-27) creates the characteristic "C-shaped" return from the guard rail. Analysis of the guard rail experiments conducted under this program have resulted in RCS values for guard rails on the order of 0 to 5 dBsm. Of course these values are heavily dependent upon specific configuration of the guard rail, but it is evident that these RCS levels can compete with those from vehicles, pedestrians, and other roadway objects (see Section 3 of the final report for a description of RCS measurements on common roadway objects).

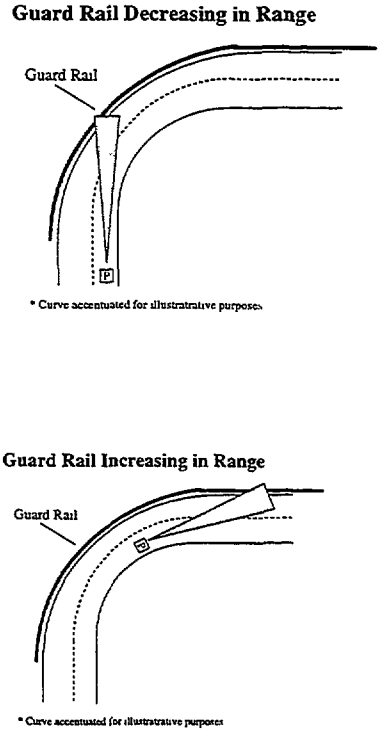

Figure F-27. Sequence of Guard Rail Returns

The final observation from the guard rail return is that due to the radar footprint which illuminates the curved portion of the rail, the returns indicate that the target has significant range extent. This attribute may be the cause for the FLAR's inability to "lock-on" and track the target as mentioned above.

F.10.1.3 Returns from Stationary Honda Accord

Figure F-28 shows are plots taken from experiments run with the Honda Accord used as the stationary target vehicle. The return from the Accord is annotated in Figure F-28(a). The return from the vehicle is brief due to the radar illumination beam sweeping horizontally through the scene as the host vehicle proceeds through the turn (see Figure F-27 for illustration of beam dynamics). Figure F-28(b) illustrates the relative return level from the Accord as compared to the guard rail and noise floor.

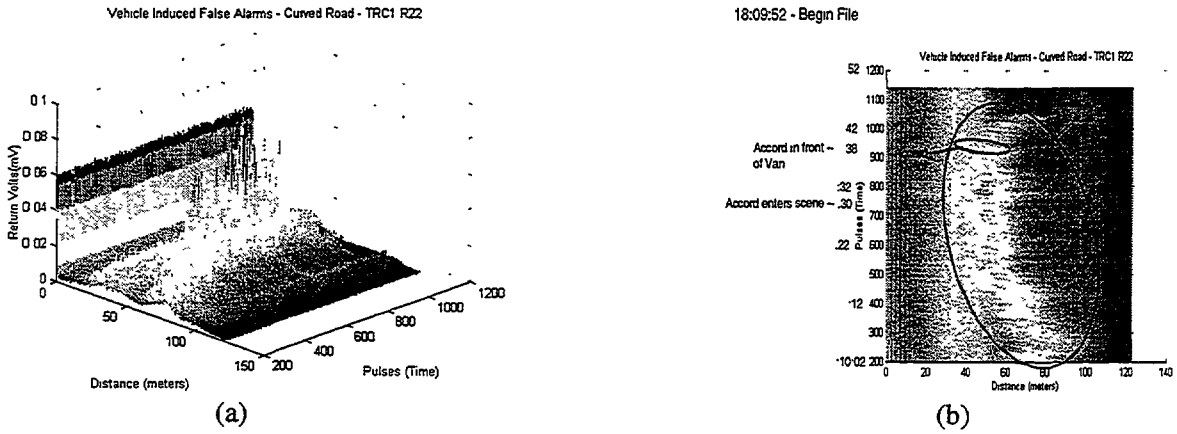

Figure F-28. Vehicle Induced False Alarms—Curved Road

Quantitative analysis of the returns from the Accord result in an RCS measurement of 2 to 3 dBsm. The value for the Accord correlates well to the RCS measurements made on similar vehicles in this program. This return level is slightly above that of the guard rail itself. During this test, the FLAR itself, utilizing the TRW processing algorithms, sporadically "locked-on" and tracked the returns from the guard rail for very brief periods of time (less than 500 msec). None of these brief "lock-on" periods corresponded to the returns from the Accord.

F.10.1.4 Returns from Stationary Tractor/Trailer

Figure F-29 shows plots taken from experiments run with the semi-tractor/trailer used as the stationary target vehicle. The return from the tractor/trailer is annotated in Figure F-29(a). The return from the vehicle is still fairly brief, but significantly longer than that from the Accord—approximately 1.25 second as opposed to 500 msec. The longer duration is due to the greater length of the truck compared to the Accord. This difference in length causes the horizontally sweeping radar beam to illuminate the truck for a longer period of time than it illuminated the Accord turn (see Figure F-27 for illustration of beam dynamics). Figure F-29(b) illustrates the relative return level from the Tractor/Trailer as compared to the guard rail and noise floor.

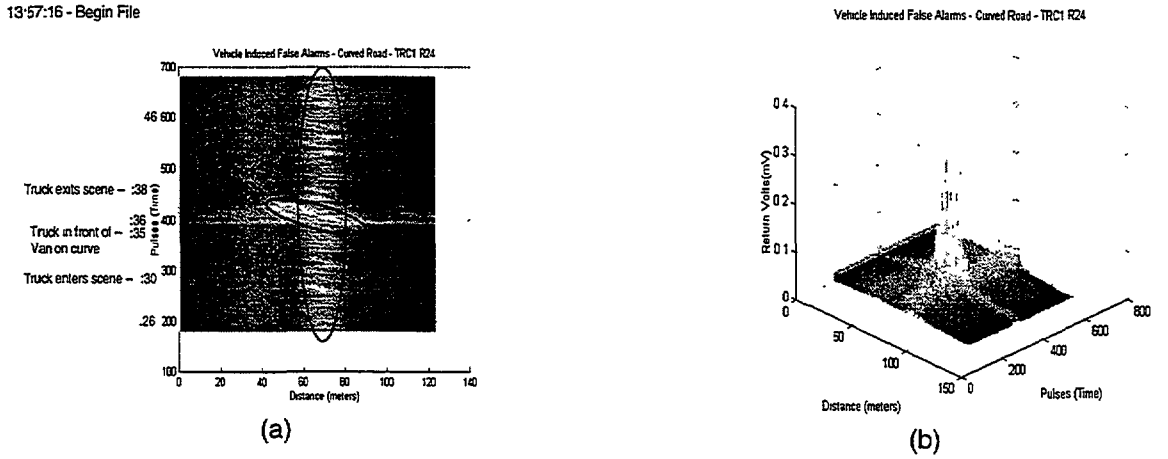

Figure F-29. Vehicle Induced False Alarms—Curved Road

Quantitative analysis of the returns from the tractor/trailer returns result in an RCS measurement of over 12 dBsm. The value for the tractor/trailer correlates well to the RCS measurements made on similar vehicles in this program. The truck's high RCS causes its return levels to rise substantially above those from the guard rail. During this particular test, the FLAR itself, utilizing the TRW processing algorithms, never "locked-on" and tracked the returns from the guard rail or the large brief return from the truck.

Conclusions for Stationary Target Vehicle on Shoulder

The test results discussed above illustrate how the dynamic movement of the radar through a typical roadway curve produces a characteristic return pattern (the 'C-shape') from a guard rail located on that curve.

Table F-2 provides quantitative information regarding the return levels observed in these measurements. Clearly, these levels of returns could certainly induce false alarms under specific scenarios.

Table F-2. Return Levels of Stationary Clutter

Description	Filename	RCSs (dBsm)
Guard Rail	TRC2:R10	0.9986449
Accord on Shoulder	TRC1:R22	2.5822699
Truck on Shoulder	TRC1:R24	12.37137

F.10.1.5 Moving Adjacent Lane Target Vehicle

Procedure

The Primary and Secondary vehicles were traveling at freeway speeds in adjacent lanes as they proceeded through the curve. A number of runs were made during which the range between the vehicles was held relatively constant. This range was varied from 10 to 70 meters on a per experiment basis. Runs were also made in which the range varied during the run. The Primary vehicle maintained a constant speed and the Secondary vehicle varied its speed to achieve the desired range profiles.

Plan View of Test Setting *

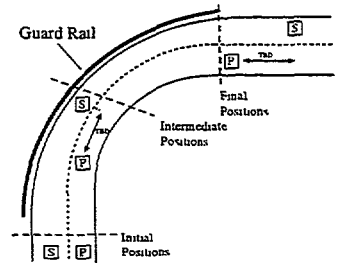

Multiple runs of this test were made using a Honda Accord and semi-tractor/trailer as the Secondary vehicle. Also, some runs were made with the FLAR center beam active, and some with the left beam active. Refer to the discussion on the FLAR antenna beam analysis for the description of these beam patterns.

Results

Data from these tests was screened using the ERIM Analysis PC software to identify the data sets worthy of further analysis. Several data sets were selected and the raw radar returns (prior to any digitization in the FLAR) were processed using custom Matlab scripts. Several of the MATLAB output

plots will be used here to illustrate the results. A complete set of plots from all MATLAR processed tests are included at the end of this document.

The plots provided in Figure F-30 are indicative of the results obtained with a moving target vehicle in an adjacent lane on a curved road. In this particular case, the secondary vehicle, a semi-tractor with trailer, provided a strong and consistent return throughout the majority of the curve maneuver,

For the given dynamics of this test, the raw radar return which was collected from the FXAR's center beam could be interpreted as though the host vehicle was directly behind the primary vehicle at a fairly consistent 40 to 50 meter range. For an ACC system, this would mean that the primary vehicle should track and maintain a specified headway to the secondary vehicle. However, this would of course be an operational error since the secondary vehicle is actually located in the adjacent lane.

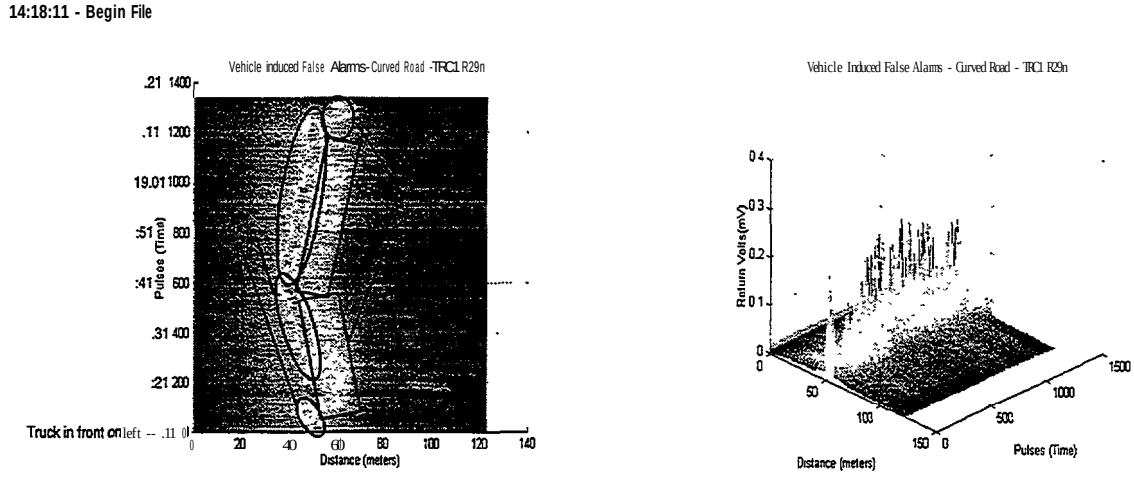

Figure F-30. Adjacent Lane Vehicle on Curve

Conclusions for Adjacent Lane Target Vehicle on Curve

The results of the adjacent lane vehicle tests have shown that without knowledge of the host vehicle dynamics or of the lane geometry in front of the host vehicle, it is very probable that a FLAR unit would incorrectly lock on to an adjacent lane vehicle. If additional information about the host vehicle's environment and activities were available, these could be utilized by the processing electronics to significantly decrease these types of false alarms.

For instance, an angular rate sensor on-board the host vehicle would provide information related to the current trajectory of the vehicle. If the radar system is aware that the vehicle is currently maneuvering through a curve, and the approximate curvature of the curve could be derived, then the radar data processing algorithm and threat assessment algorithm could use this information to filter out returns from adjacent lane vehicles based on the range and azimuthal location of the returns. This of course assumes that the radar system possesses the necessary azimuthal resolution.

F.1 1 TRACKING THROUGH A CURVE

Purpose

The purpose of this test was to determine the FLAR's ability to maintain track on a target vehicle through a standard freeway curve on a dry, flat section of roadway. The test was performed under good driving conditions. Roadway was selected that had guard rails in the scene.

Issues that were considered in these tests included the loss of returns from the target vehicle, and the returns induced by the guard rail around the curve.

Procedure

The test commenced when the Primary vehicle was tracking the target vehicle (a Honda Accord) in a straight section of roadway prior to entering a curve. Both vehicles were traveling at approximately the same speed, attempting to maintain those speeds and the initial separation of 10,40, and 70 meters throughout the test maneuver. The test terminated when both vehicles were again on a straight section of roadway.

As implied above, several tests were conducted, with the distance between the host and target vehicle being 10,40, and greater than 70 meters in individuaI runs.

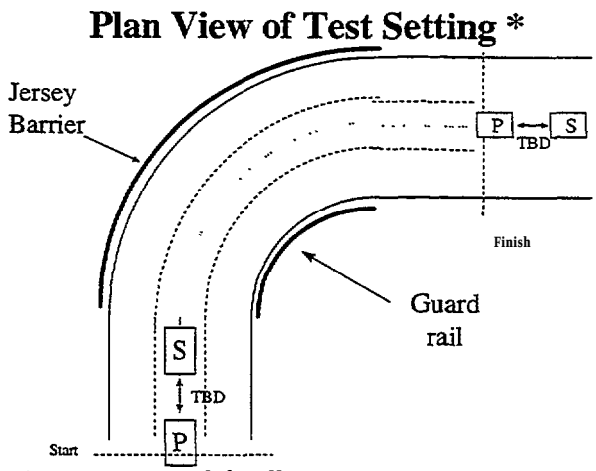

* Curve accentuated for illustratrative purposes

Results

The raw radar data plots for the mns conducted with target vehicles at 10,40, and 70 meters are provided in Figures F-3 1 and F-32. Figure F-3 1 is annotated to identify the source for each of the radar returns. Figure F-32 provides information on the relative return levels which can be used for more numerical analysis.

The remainder of this section will contrast the results from the three different test runs.

Ability to Maintain Track on Target Vehicle

The data plots shown in Figure F-3 1 clearly indicate that the return levels from the target vehicle were not impacted during the turn maneuver when the target vehicle was at a nominal 10 meter range [see Figure F-31(a)]. However, the reuim levels did exhibit significant impact when the target vehicle was at the nominal 40 and 70 meter ranges [see Figures F-31(b) and (c)]. At a 40 meter range, the target's vehicle's return levels were observed throughout the turn maneuver at a much lower level than on a straight roadway. At 70 meters, the target vehicle was not observed at all throughout the turn maneuver. For a more quantitative assessment of the impact on the return levels, see the analysis of the relative return levels provided below.

The radius of the curve used on these tests was approximately 238 meters which is a relatively tight turning radius at normal highway speeds. Table F-3 shows the angular departure from the radar antenna boresight at which the target vehicle is located, given the target vehicle range and a 780 feet radius curve. These values correlate very well with the observations. At a 10 meter range, the target vehicle is located 1.2 degrees off of the antenna boresight. This is within the 3 degree (1.5 degrees on either side of the boresight) PLAR center beam which was active on these tests.

Table F-3. Angular Departure for 238 Meter Radius Curve

Range to Target	**Angular Departure From Boresight**
10 meters	1.2 degees
40 meters	4.8 degrees
70 meters	8.5 degees

On the other hand, at 40 meters the target vehicle is 4.8 degrees off the boresight. As explained in 'Section F. 1: Vehicle Induced False Alarms-Straight Roadway," the real antenna beam extends beyond the 3 degree specification with much lower gain. Therefore, it makes sense that the target vehicle is still visible at 40 meters, but at much lower levels.

At 70 meters, the vehicle is located 8.5 degrees off of the antenna boresight. At this level of departure, the antenna beam gain is extremely low and the target vehicle is effectively out of the radar's field of view. As Figure F-31(c) ilhtstrates, radar returns from the target vehicle given this scenario were not evident.

This data leads to the conclusion: The ability of an automotive radar to maintain lock on a target vehicle is dependent upon the range to the target vehicle and the radius of the curve. In evaluating the raw radar returns under this test scenario, one could conclude that a radar should be able to track the vehicle at 10 meters, may be able to track the vehicle at 40 meters, and probably could not track the vehicle at 70 meters.

The GPS truthing plots provided in Figure F-33 correspond to the data plots from the three tests runs. The range to the target vehicle is represented by the curve labeled "GPS Rng" and the reported range from the FLAR (using the TRW-proprietary algorithms) is represented by the curve labeled "RDF Rng".

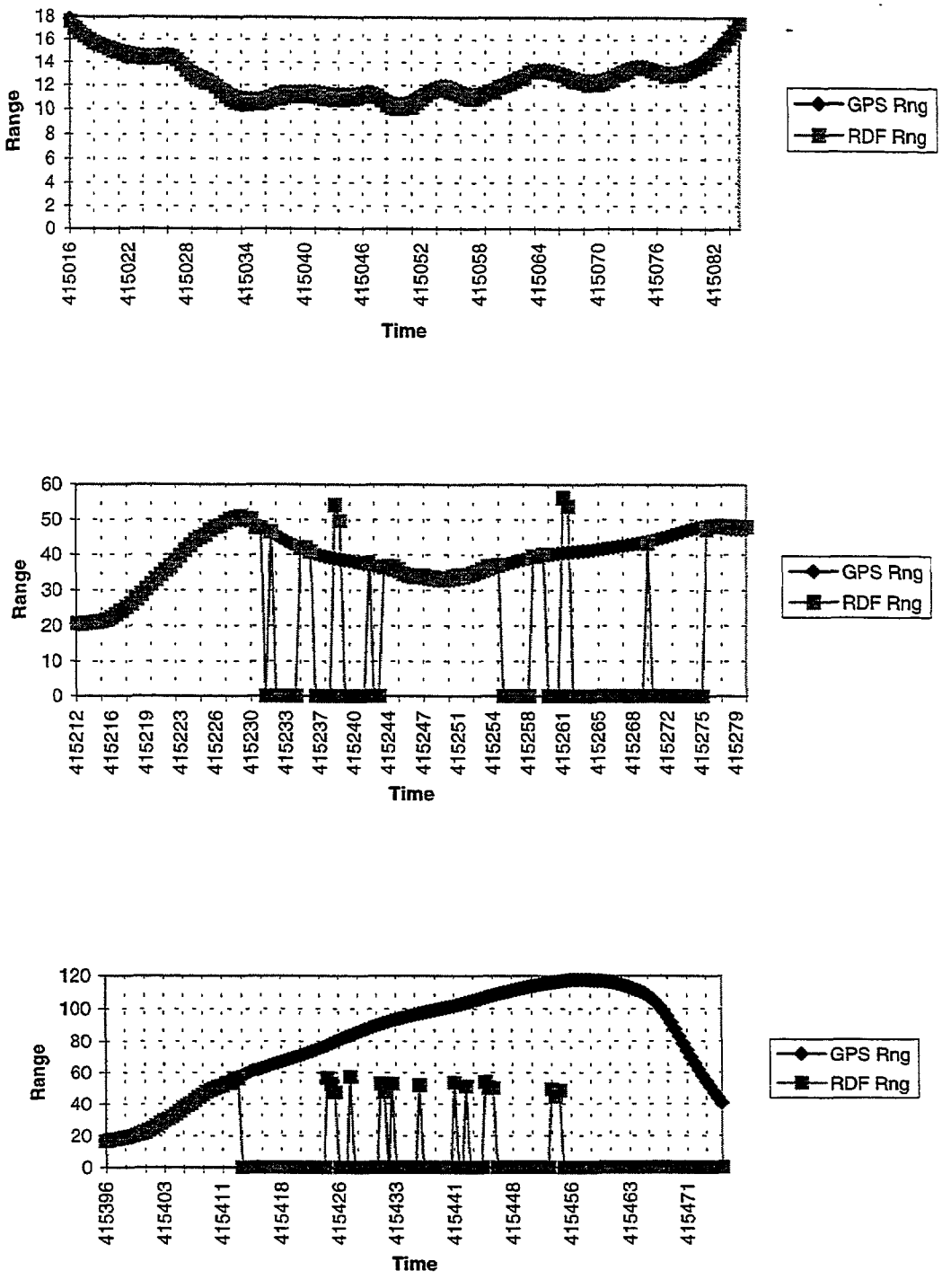

Figure F-33. GPS Truth for R30r, R31r, and R32r

As expected, the FLAR had no trouble tracking the target vehicle through the curve at a 10 meter range. Also as expected, the FLAR was unable to track the target vehicle at 70 meters once it entered the

curve. Between those two extremes is the test with the target vehicle at 40 meters. The middle plot in Figure F-33 clearly shows that when the range to the target dropped below 40 meters, the F'LAR was able to acquire and track the vehicle. However, as the target range exceeded 40 meters, the FLAR was very unreliable in providing an accurate measurement to the target vehicle.

The other interesting information contained in the plots of Figure F-33, is that the radar intermittently identifies the guard rail as a target to be tracked (indicated by the non-zero "RDF Rng" readings which do not correspond to "GPS Rng" values). It was originally expected that the radar would track the guard rail throughout the turn maneuver since the returns were consistently present. However, it is suspected that the TRW algorithms resident within the FLAR may have had difficulty identifying the centroid of the guard rail returns since they were spread over a 15 meter range.

Analysis of Relative Return Levels

The plots provided in Figure F-32 indicate the sizes of the relative return levels between the Honda Accord on the straight path, the Honda Accord around the curve, and the guard rail. Table F-4 summarizes the numerical analysis aimed at generating quantitative results on typical RCS values which can be expected in a scenario similar to the one tested here. Note again that this particular scenario used a curve with an approximately 238 meter radius.

Table F-4. RCS Numerical Analysis

Target	Empirically Estimated RCS
Accord on Straight Road	0 to 5 dBsm
Accord at 10 m Range on Curve	0 to 5 dBsm
Accord at 40 m Range on Curve	-3 dBsm and below
Accord at 70 m Range on Curve	No Returns Observed
Guard Rail on Curve	Typically 0 dBsm, 4 dF3sm peaks

The Accord on the straight roadway exhibited RCS levels consistent with those observed during other tests and measured during the RCS Characteristics task of this program. There was very little difference in the RCS of the Accord on a straight and at a 10 meter range on the curve. At the 40 meter range, the RCS of the Accord dropped significantly.

Characteristic Return from Guard Rail

The return from the guard rail was consistent throughout the curve maneuver, in that it was always present. The RCS averaged around 0 dBsm and occasionally peaked up near 4 dBsm. Comparison of these numbers shows that in terms of the magnitude, the guard rail can appear similar to a car.

The shape of the return from the guard rail (see Figure F-3 1) has significant range or depth to it. The radar returns from the guard rail are spread over approximateIy 10 to 15 meters in range. Figure F-34 shows how the incident radar energy will illuminate targets on curved roadways, such as guard rails.

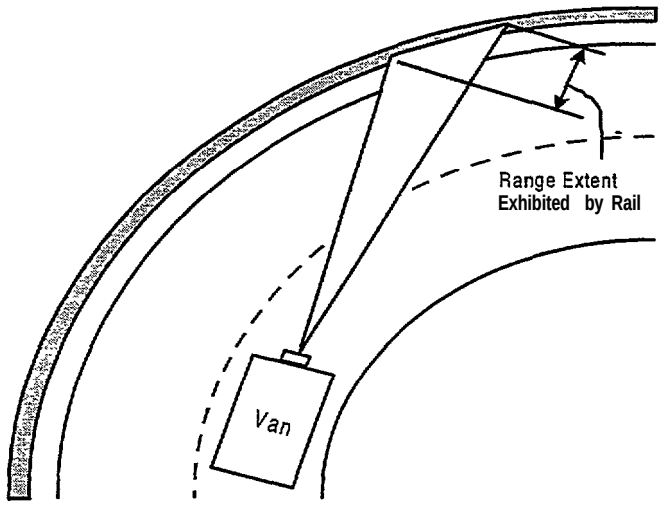

Figure F-34. illumination of **Targets on Curved Roadways**

The other interesting characteristic of the guardrail return is its "C-shaped" profile over time. The reason for this profile is discussed in detail in Section 6.10, "Vehicle Induced False Alarms-Curved Roadway.

Conclusions

The change in return levels from preceding vehicles on a straight roadway to those on a curved roadway is dependent upon the radius of the curve and the range to the vehicle. These tests showed that for a curve with an approximate 238 meter radius, vehicle ranges above 40 meters lead to a loss of track on the target (note that this is for an antenna beam with a 3 degree 3 dB width). The differences in return levels can be attributed to a combination of the target vehicle being located off of the antenna beam boresight, and the aspect angle being less than or greater than 180 degrees.

Guard rails located at the outer extent of the curved roadway were observed to exhibit RCS levels comparable to that of the vehicle tested. The vehicle tested was a Honda Accord with a 0 to 5 dBsm RCS characteristic for 180 degree aspect angle. Although returns from the guard rail were consistently observed in the radar raw data, the FLAR did not consistently track the guard rail as a target.

The results of these tests indicate the value that could be provided by lmowledge of the vehicle dynamics for a collision avoidance or ACC system. Knowing when a vehicle is in a curve, whether from yaw rate sensing or steering wheel angle, would be an important input to a system's threat assessment algorithm. The information could be useful in identifying certain returns as those from roadside objects, such as guard rails. The information could also be used to adjust the radar's field of view in the direction of the curve to aid in maintaining track on the preceding vehicle.

F.12 VEHICLE CLUTTER IN AZIMUTH-CURVED ROADWAY

Purpose

The purpose of this test was to determine the FLAR's ability to maintain track on a target vehicle through a standard freeway curve with other vehicles present in adjacent lanes. The test was performed under good driving conditions.

Issues considered in these tests included the loss of returns from the target vehicle, the FLAR's ability to discriminate between in-lane and out-of-lane target vehicles, and the returns induced by the vehicles in the adjacent lanes.

Procedure

For these tests, four different vehicles were used on a circular track with an approximate 500 foot radius. The primary vehicle (P) and target vehicle (Sl) were driven in the center lane of the circle. The two other vehicles were clutter vehicles (S2 and S3) driven in the inner and outer lanes of the circle. The two out-of-lane clutter vehicles were selected to have radar cross-sections similar that of the in-lane target vehicle. Actually, all three secondary vehicles were Honda Accords.

The test began with the Primary vehicle maintaining a constant distance from the m-lane target vehicle; the out-of-lane clutter vehicles were adjacent to the Primary vehicle and traveling at the same speed. The out-of-lane clutter vehicles accelerated until they were adjacent to the in-lane Secondary vehicle. They maintained this position for several seconds and then decelerated until they were again adjacent to the Primary vehicle.

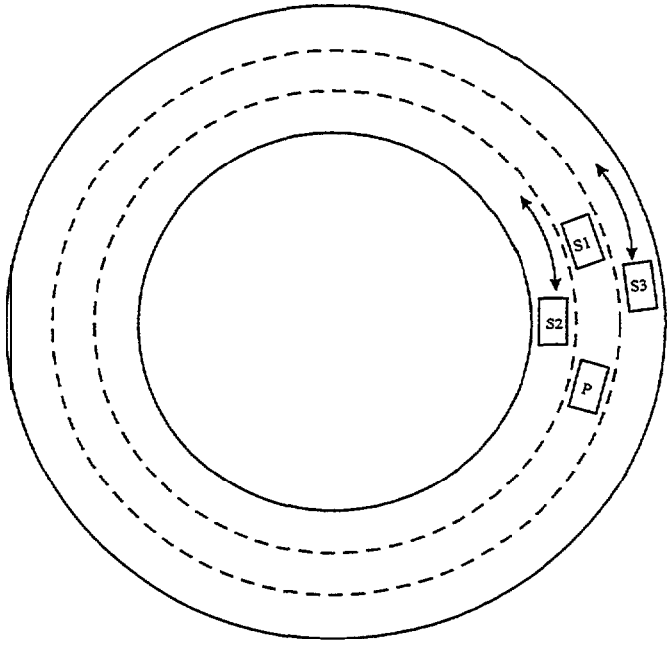

Figure F-35. Vehicle Clutter on Curved Roadway Scenario

These types of maneuvers were repeated several times during the course of a test run. Sometimes the clutter vehicles maneuvered together, and some times individually. The distance between the primary and target vehicles was varied during each test runs. Also, the FLAR's active beam (left, center, or right) was varied on separate runs.

Results

To illustrate and discuss the results of this series of tests, data from one of the test runs in which the FLAR's center beam was active will be used. Observations from test runs in which the left and right beam were active will also be discussed.

The series of plots shown in Figure F-36 are all from the same data set. Each plot consists of a different time interval of the test, which lasted for almost 5 minutes. The time sequence begins with the bottom plot in Figure F-36, proceeds up to the middle plot and then is completed with the top plot.

The returns which are visible in the data plots are annotated to indicate the vehicle which induced them. Accord 1 is the actual target vehicle located in the same lane as the host vehicle. Accord 2 was driving on the inside lane and Accord 3 was driving on the outside lane. The radius of curvature was approximately 500 feet in the middle lane.

To analyze these tests, extensive use was made of the ERIM Analysis Software which includes a video playback of the test which is synchronized to the radar data. Without the video playback, it is difficult to convey the exact vehicle maneuvers being conducted throughout the test. In an effort to convey the vehicle positions during the test to the reader, the line labeled "GPS Rng" in Figure F-37 indicates the range from the radar to the target vehicle throughout the test. The pulse number on the x-axis of Figure F-37 corresponds to the pulse number on the y-axis of the radar return plots in Figure F-36. Also, Table F-5 provides a sequence of events for the target and two clutter vehicles referenced to radar pulse number.

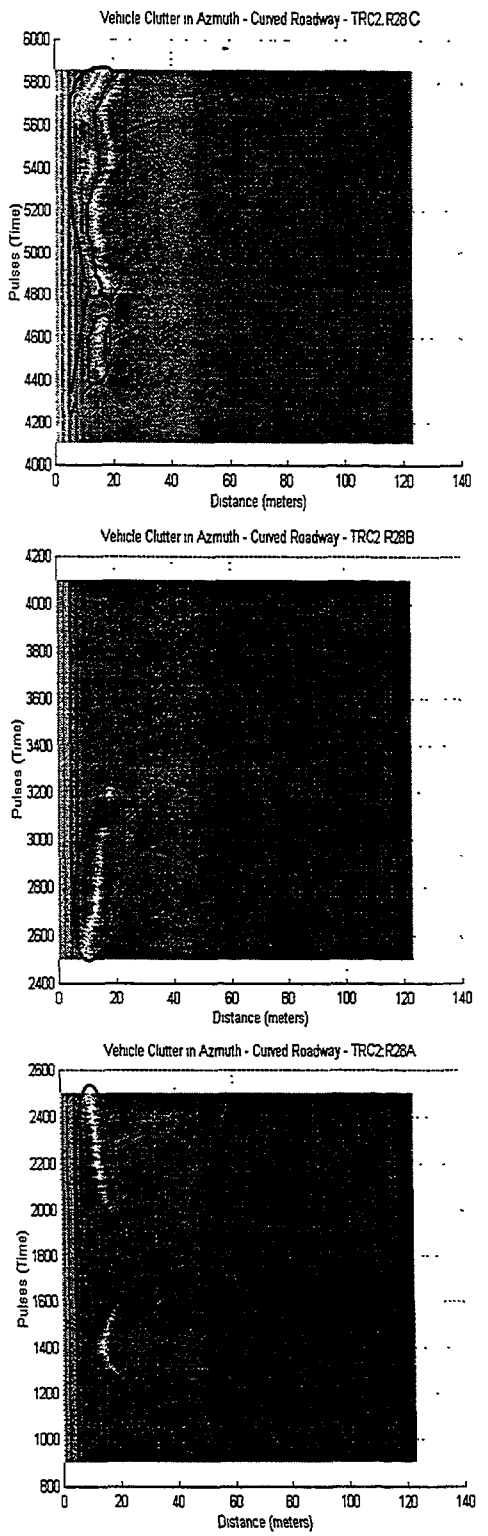

Figure F-36. Radar Data Curved —Roadway

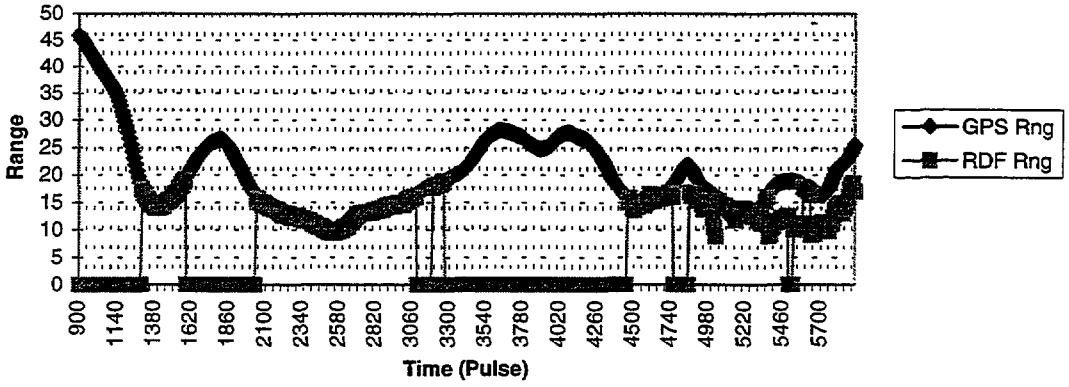

Figure F-37. GPS Truth for R28

Table F-5. Curved Roadway Test Analysis Summary

Pulse #	Vehicle Activity	Radar Response
900-2600	Accord 1 is only vehicle in scene	Radar ability to track Accord 1 position dependent upon range
2500-2700	Accords 2/3 enter scene and accelerate to positions adjacent to Accord 1	Accords 2/3 appeared to have no effect on raw radar data and ability of FLAR to track Accord 1
2700-3000	Accords 2/3 maintain positions adjacent to Accord 1	same as above
3000-3100	Accords 2/3 split-off and drop out of scene	same as above
3000-4200	Accord 1 is only vehicle in scene	Radar ability to track Accord 1 position dependent upon range
4200-4400	Accord 3 enters scene and accelerates to position in outside lane and 1 car length behind Accord 1	Accord 3 position has effect on raw radar returns. As Accord 1 and Accord 3 maneuver, returns from both vehicles are observed.
4400-end	Accord 3 maintains position in outside lane, 1 car length behind Accord 1	same as above

Correlation between the information in Figure F-36, Figure F-37, and Table F-5 is necessary to establish the cause and effect of vehicle maneuvers on the radar sensor. The third column in Table F-5 summarizes the radar response to the various events conducted during the test.

As observed in other tests conducted on curved roadways, the radar returns from preceding vehicles are dependent upon the radius of curvature in the roadway and the target vehicle's range from the radar. These two variables dictate whether or not the target vehicle position is located within the FLAR's field of view. Considering pulses 900 to 2600, where the only vehicle in the scene was Accord 1, Figure F-36 indicates that the vehicle both entered and withdrew from the FLAR's FOV. This information can be correlated with the GPS truthing information included in Figure F-37. The line labeled "GPS Rng" is the

actual range to Accord 1, and the line labeled "RDF Rng" is the FLAR's reported range to target vehicle output. It is clear that the FLAR's ability to track the target vehicle coincided with time intervals when the raw radar data indicates the vehicle was within the FOV.

The time period during which the returns from the target vehicle were not evident in the raw radar data correspond to intervals in which the target vehicle range exceeded more than 15 to 20 meters. Table F-6 shows at what angle from the antenna boresight a vehicle would be located on a 500 foot radius curve given a particular range to that vehicle. These numbers are in agreement with the configuration of the FLAR and the empirical observations made during this test.

Table F-6. Vehicle Location Versus Range to Vehicle

Range to Target Vehicle	Vehicle Location Off Antenna Boresight
10 meters	1.9 degrees
15 meters	2.8 degrees
20 meters	3.8 degrees

A plot of the FLAR's center beam pattern is provided in Figure F-38. A line has been drawn to indicate where in the beam pattern a target would fall if it was located four degrees off the antenna boresight.

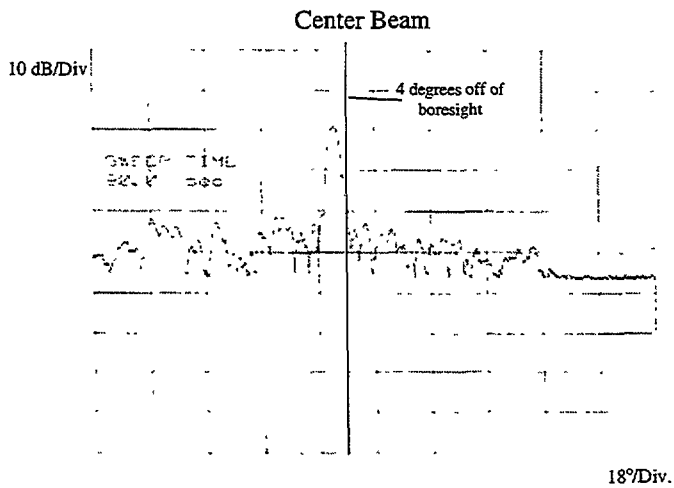

Figure F-38. Center Beam Patterns

It is obvious that the antenna gain in this region is extremely low. This explains why the returns from Accord 1 are not visible in the raw radar data when its range exceeds 15 to 20 meters on a 500 foot radius curve.

This also helps to explain why Accords 2 and 3 did not induce any returns in the radar during pulses 2500 to 3000. The data in Figure F-37 shows that the range to Accord 1 during that period was under 20 meters. Therefore, Accord 1's position prevented the radar beam from being reflected off any other objects, as pictured in Figure F-39. Here the radar beam is incident on Accord 1, but not on any other objects in the scene. This is verified by the raw radar plots in Figure F-36.

The observations and results made during pulses 3000 to 4200 are similar to those made during pulses 900 to 2600 described above.

From pulse 4200 to the end of the test run (pulse 5850), things start to get interesting. Here, the relative positioning of Accords 1 and 3 begins to have an effect on the raw radar returns and the ability of the FLAR to accurately track the target vehicle within its own lane.

The same dependency of the FLAR's ability to detect targets on radius of curvature and range to target still holds true. Figure F-38 shows that targets are still detected by the FLAR only when their range drops below 20 meters or so. The truthing information for pulses 4300 and up from Figure F-38 is reproduced in Figure F-40 for greater clarity.

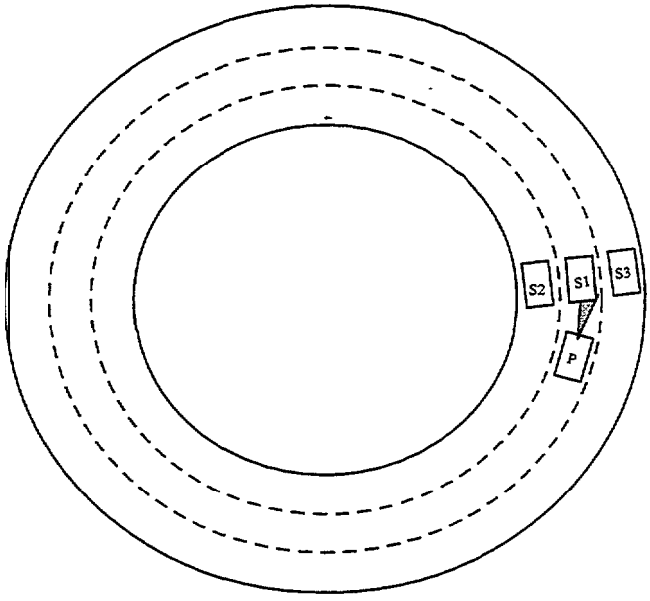

Figure F-39. Short Range Illumination

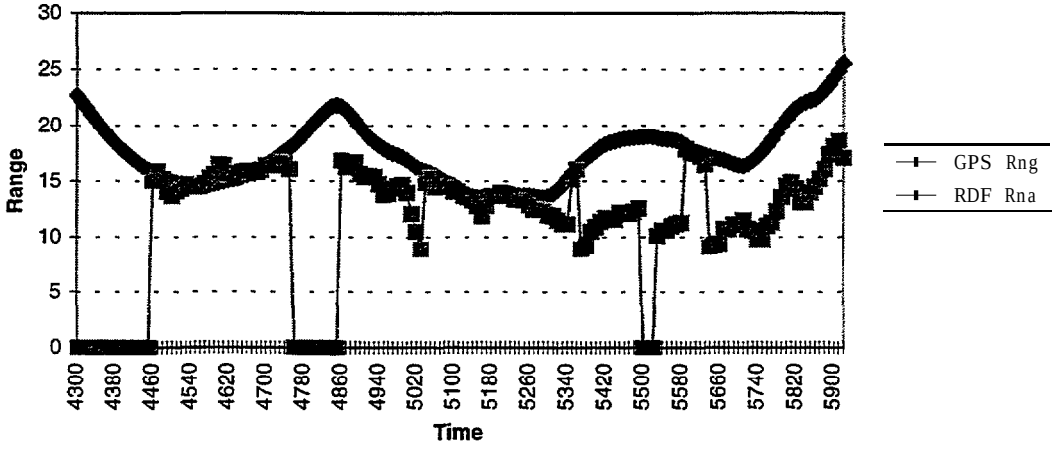

Figure F-40. GPS Truth for R28

The data in Figure F-40 shows that the FLAR (and the TRW-proprietary processing algorithm) detected an object inside the actual range of Accord 1. Comparison of this data in Figure F-40 with the raw radar data plots provided in Figure F-36 verifies that the FLAR is indeed tracking Accord 3. Figure F-41 shows a diagram of the situation.

Referring back to the top plot in Figure F-36, returns from both vehicles can be frequently observed. Due to the orientation of the vehicles, the returns from Accord 3 appear at a nearer range. Therefore, the FLAR treats this return as the **target to** be tracked. The FLAR has no knowledge of which lane Accord 3 is actually in.

Also referring to the raw radar plots in Figure F-36, it appears that returns are coming from different scattering centers located on Accord 3, perhaps the rear and front wheel wells.

The return levels observed from the Honda Accords during this test were typical of other tests with these vehicles. In general, the Accords exhibited a -2 to +5 dBsm radar cross section. This is slightly lower than tests conducted with the Accords on a straight roadway. The explanation for the difference lies in the orientation between the radar and the targets. On curved roadway less return is expected, since the relatively flat sides of the vehicle tend to reflect energy away from the radar.

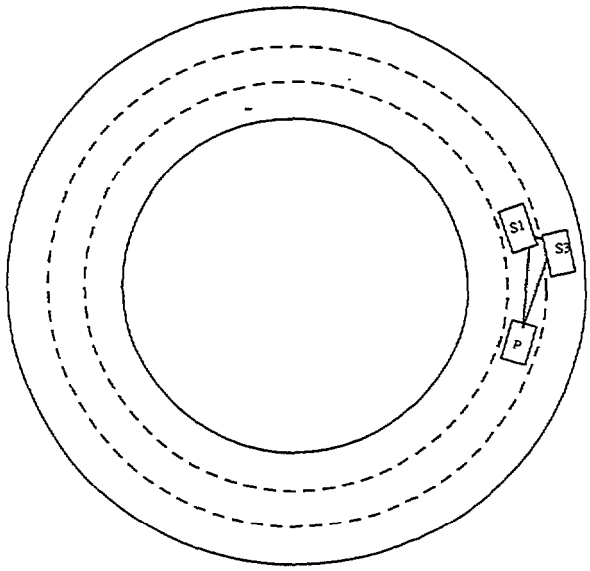

Figure F-41. Medium Range Illumination

The other collections made using this test scenario, but with the left or right beams activated, produced similar results in terms of the field-of-view limitations. It was found that collections with the left beam active allowed the FLAR to track the target vehicle out to a range of 40 meters versus the 20 meter limitation with the center beam. Also, neither Accord 2 or 3 was detected during the "left beam" tests.

On the other hand, "right beam" tests reduced the FLAR's ability to track the in-lane target vehicle down to around 10 meters. However Accord 3, located in the outside lane, could be tracked out to 35 meters or so. These "side beam" tests show how adjusting the FLAR's field of view will affect its performance, especially in curved roadway scenarios.

Conclusions

The empirical data in these tests showed that the ability of the FLAR to accurately track preceding vehicles in a curve depends on the curvature of the roadway and the range to the target vehicles. The diagrams provided the in the "Results" section of this document illustrate this dependency.

The FLAR center beam with its 3 degree 3dB azimuth width limited the detection range to the in-lane target vehicle to around 20 meters in a 500 foot radius curve. Given that 20 meters is not a very great distance, this limitation needs to be addressed by either steering the beam during a curve maneuver or increasing the radar's field of view by scanning the antenna across the scene. The tests conducted with the side beams indicates the gains that can be made in terms of increasing the detection ranges.

The results of these tests, combined with those from curved road tests with a guard rail present, indicate that it will be extremely difficult for an automotive radar to accurately assess the environmental dangers during a curve maneuver without other inputs into the system. Inputs such as yaw rate, steering wheel angIe, and any information regarding the azimuth positioning of objects in the scene would greatly enhance the robustness of the threat assessment algorithm. Yaw rate and steering wheel angle information could be easily gathered from sensors installed on the car. As for azimuthal positioning of objects, two options exist. The first is to create an even narrower **antenna** beam and scan it across the

scene. The other is to perform a data fusion function from a separate sensor such as an IR or optical camera to identify object positioning within the scene.

Obviously, adding another sensor beyond the radar for collision avoidance or ACC applications would make the system cost prohibitive. However, as night driving enhancement systems and lane sensing systems evolve, the possibility of sharing information among sensors becomes viable.

TEST TRACK DATA PLOTS

The following pages are selected raw data plots generated from the Test Track collections. The plots are presented by the test scenario being addressed as described in the test plan provided in Appendix E. Each plot is labeled with the appropriate test identification and annotation on the plots is provided where appropriate. The reader is referred to the test plan and test results descriptions in Appendices E and F, respectively.

These plots are provided to assist developers in quantitatively assessing the radar response to the scenarios tested. Of course these results are specific to the TRW FLAR sensor configuration (e.g., antenna gain and beam shape). The reader is referred to Section 4 of the final report which discusses the FLAR sensor characteristics in order to extrapolate the results to other configurations.

6.1 Vehicle Induced False Alarm - Vehicle At Roadside

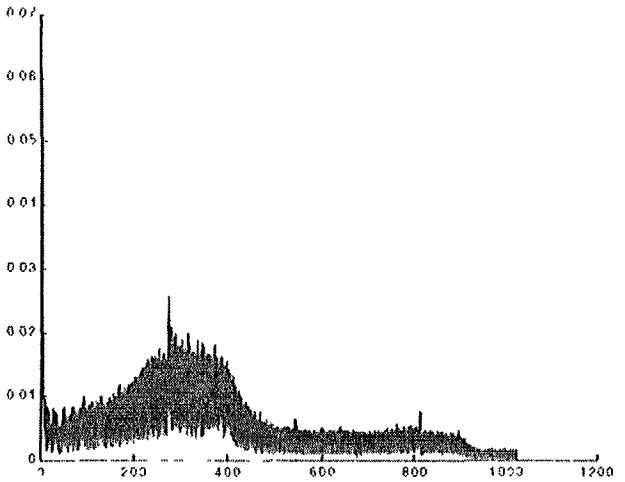

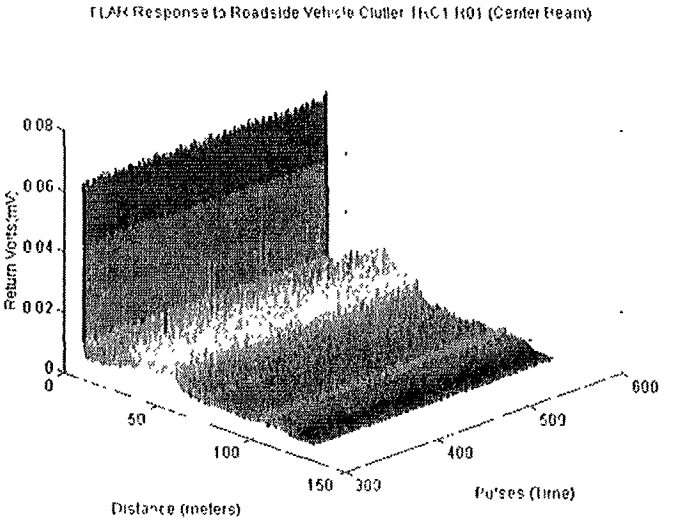

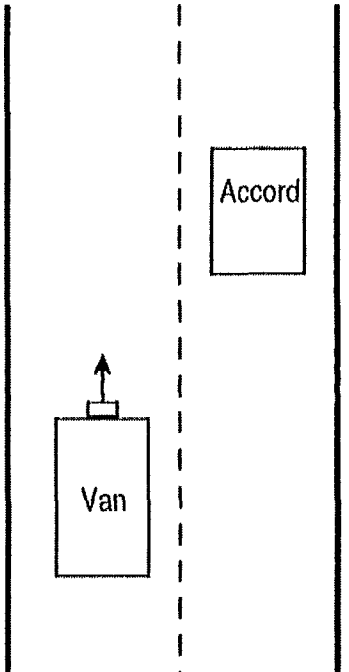

Center Beam
Honda Accord
parked in adjacent lane

6.1 Vehicle Induced False Alarm - Vehicle At Roadside

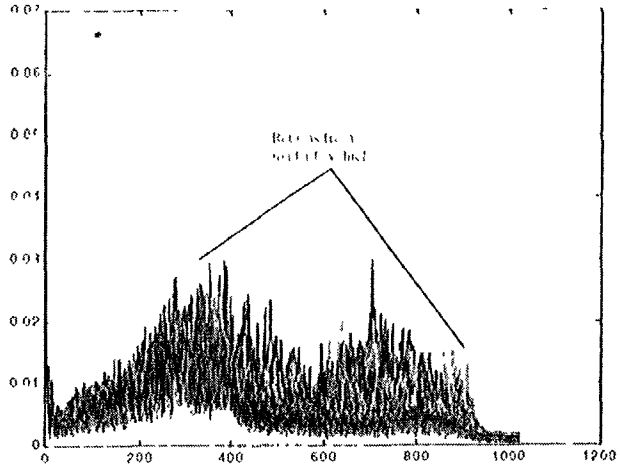

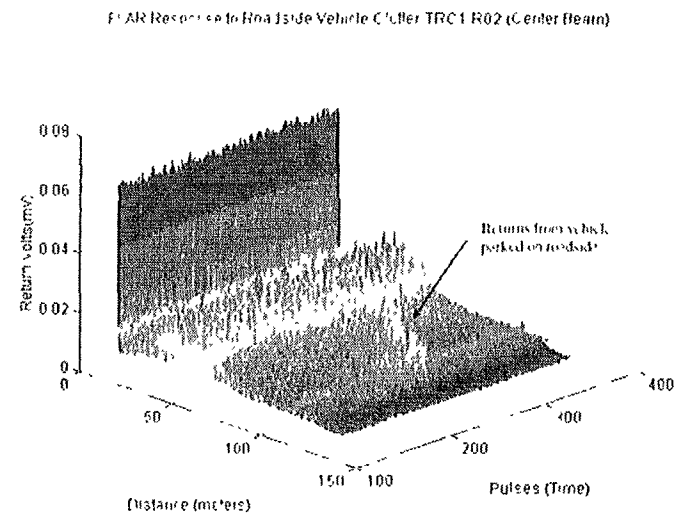

Center Beam
Semi-Tractor/Trailer
parked in adjacent lane

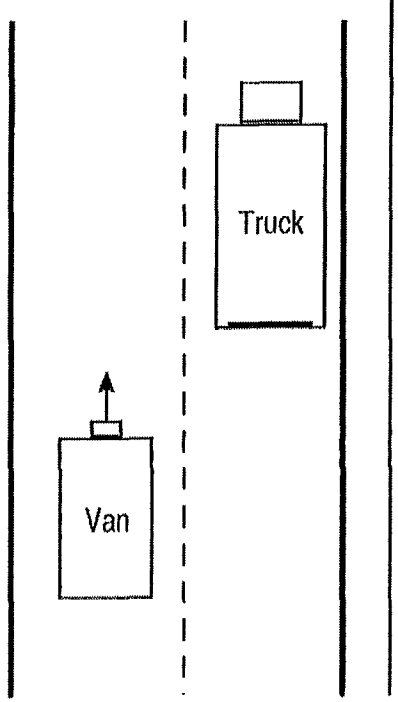

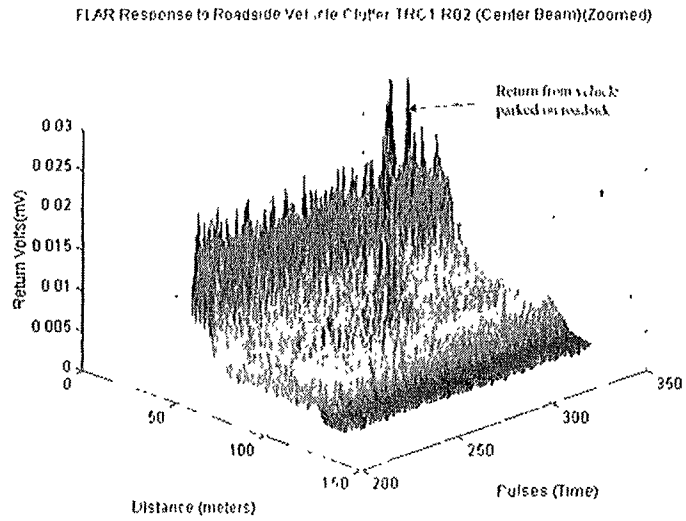

6.1 Vehicle Induced False Alarm - Vehicle At Roadside

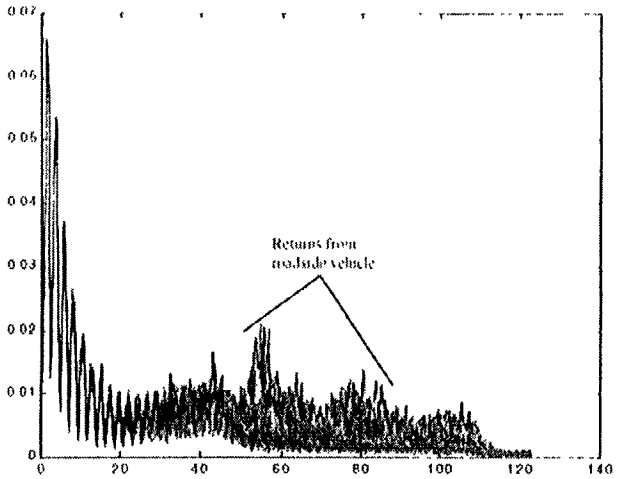

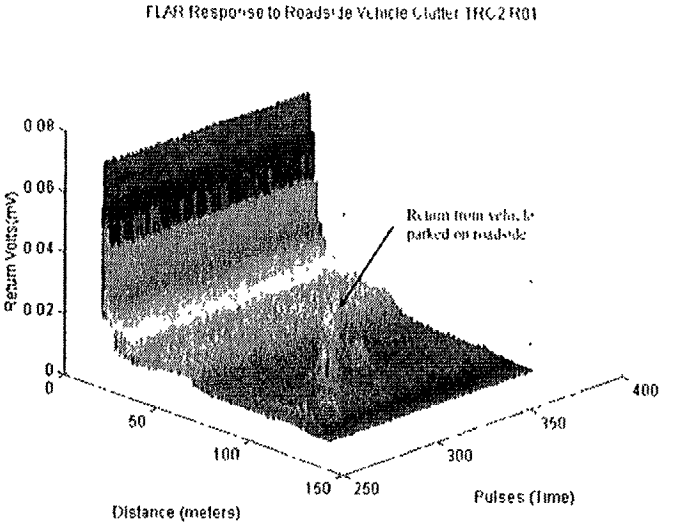

Center Beam
Semi-Tractor/Trailer
parked in adjacent lane

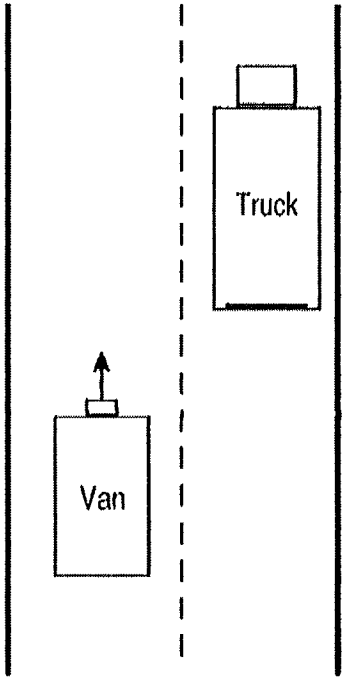

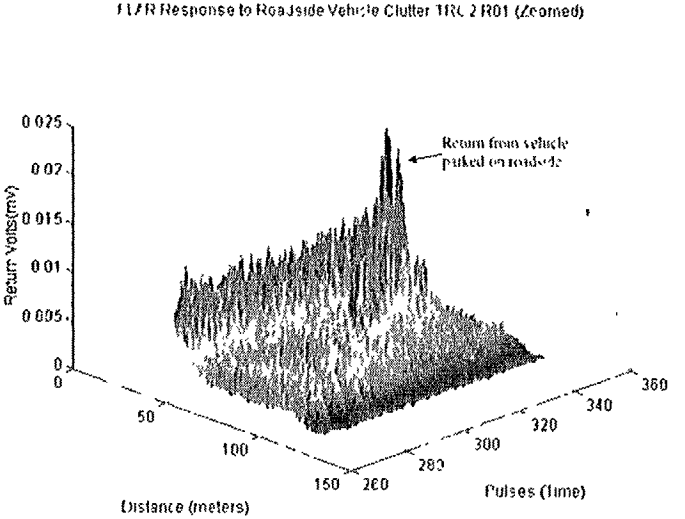

6.1 Vehicle Induced False Alarm - Vehicle At Roadside

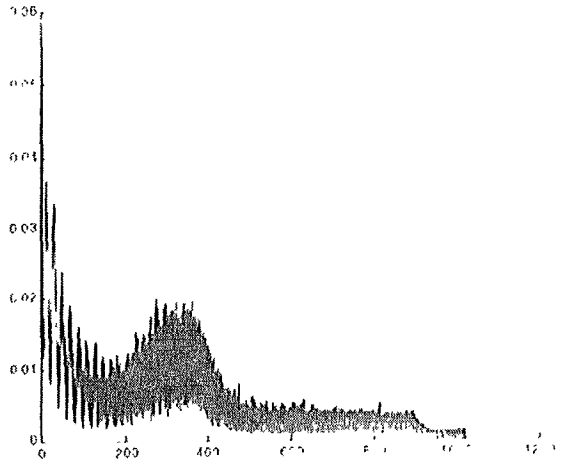

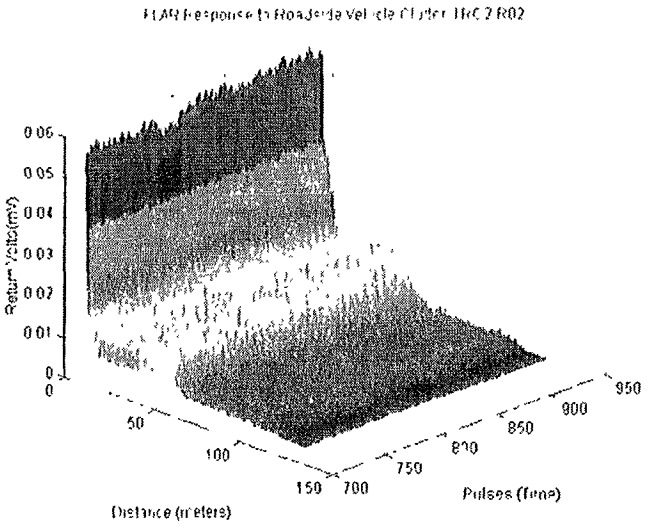

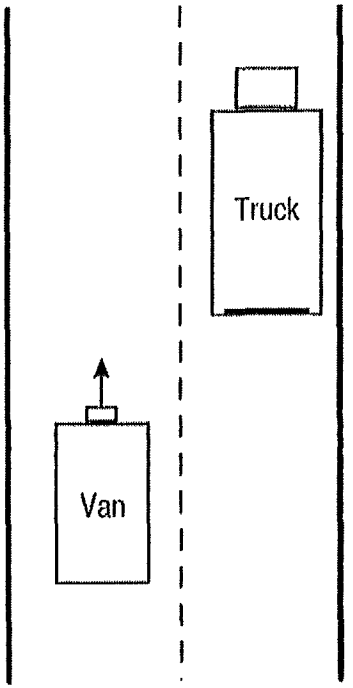

Right Beam
Semi-Tractor/Trailer
parked in adjacent lane

6.1 Vehicle Induced False Alarm - Vehicle At Roadside

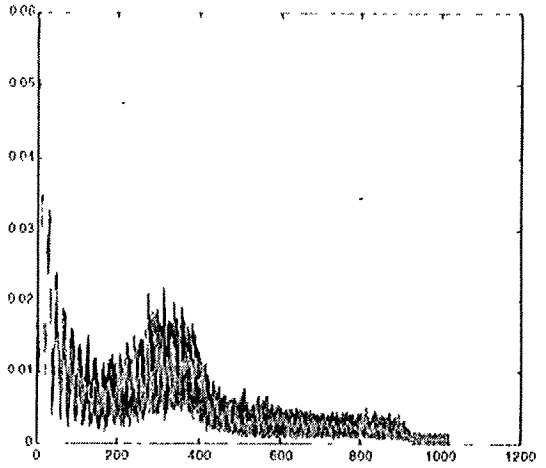

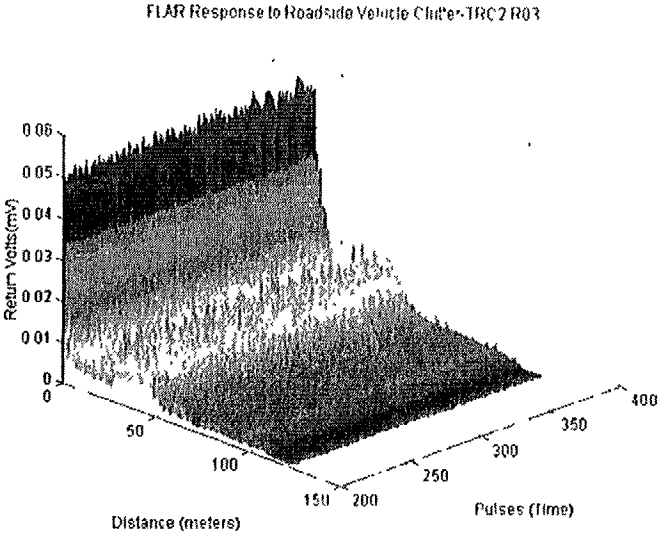

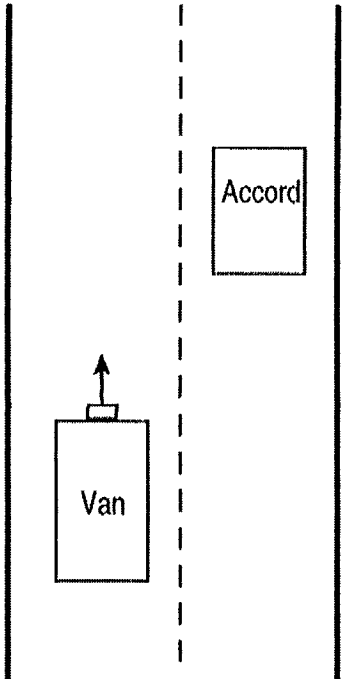

Center Beam
Honda Accord
parked in adjacent lane

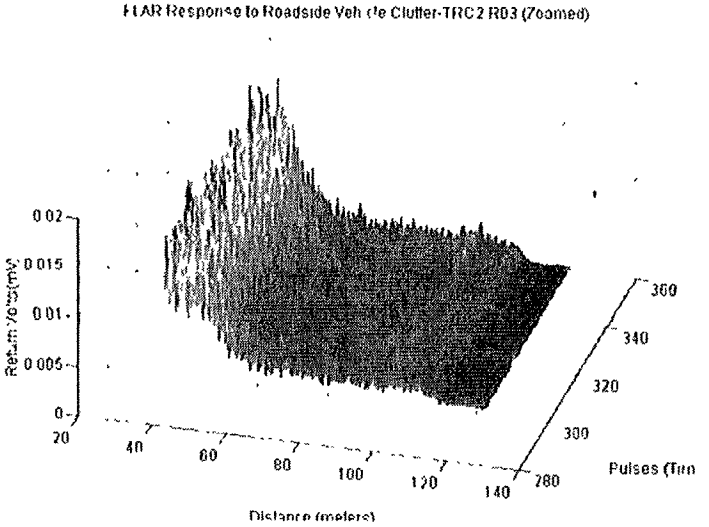

6.1 Vehicle Induced False Alarm - Vehicle At Roadside

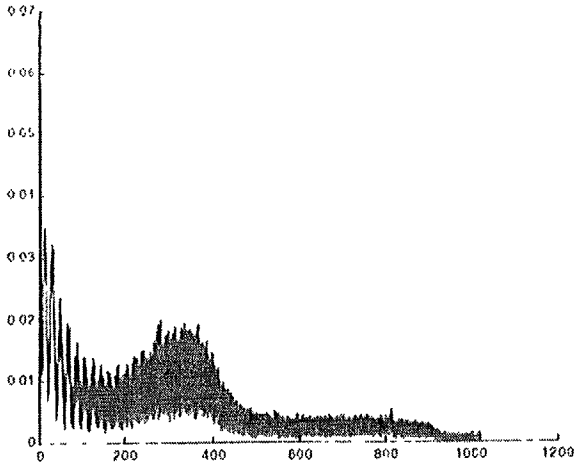

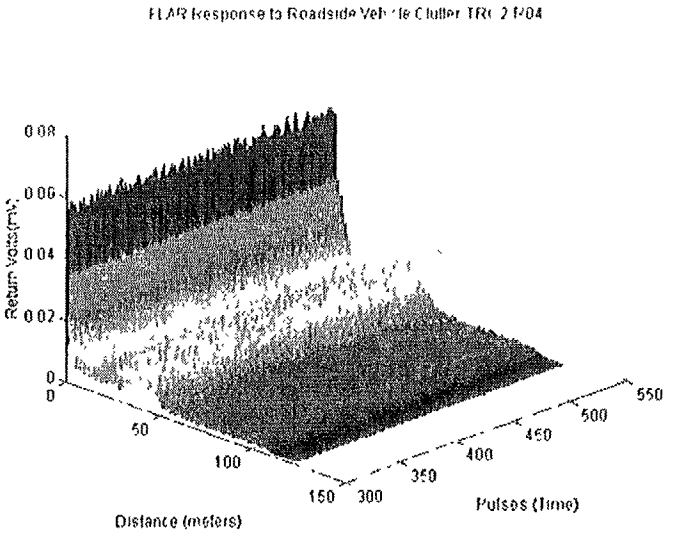

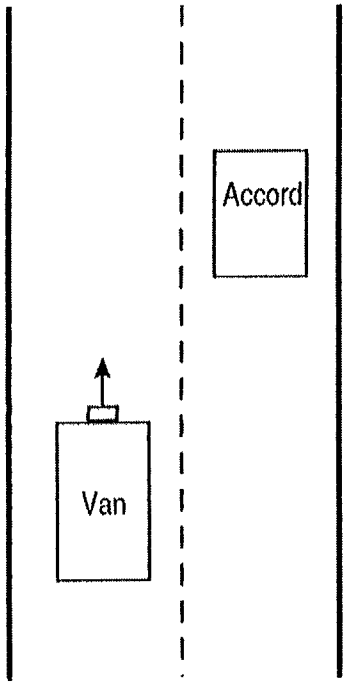

Right Beam
Honda Accord
parked in adjacent lane

Object Orientation Roadside Clutter Analysis

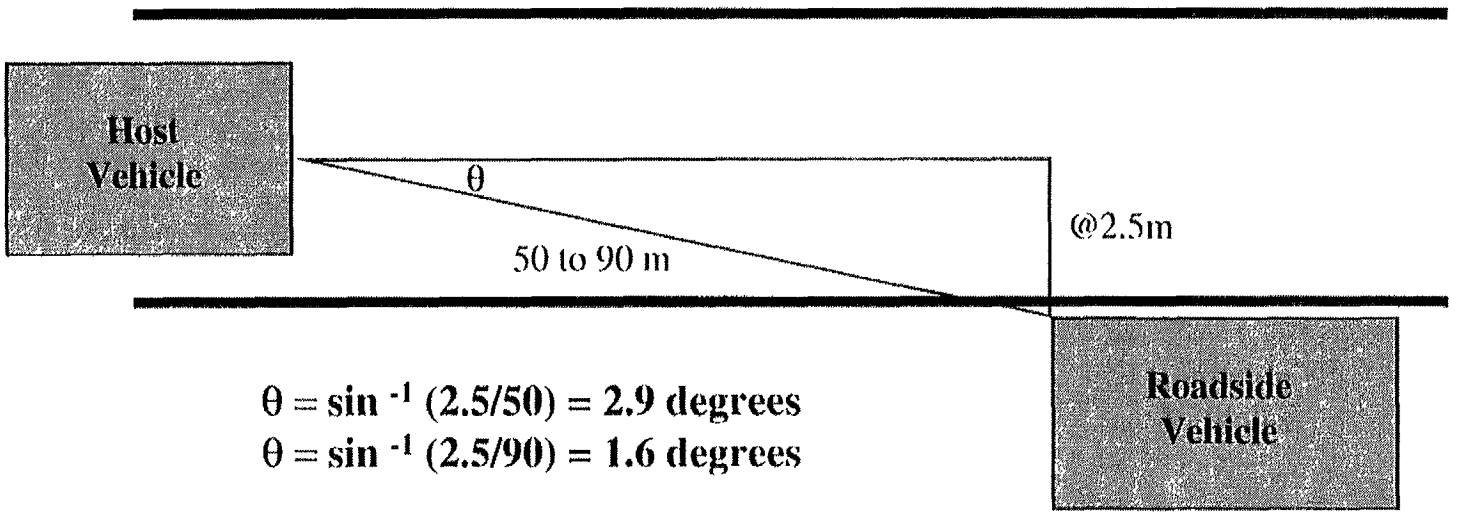

$\theta = \sin^{-1}(2.5/50) = 2.9$ degrees

$\theta = \sin^{-1}(2.5/90) = 1.6$ degrees

6.1b Vehicle Induced False Alarm - Vehicle in Adjacent Lane

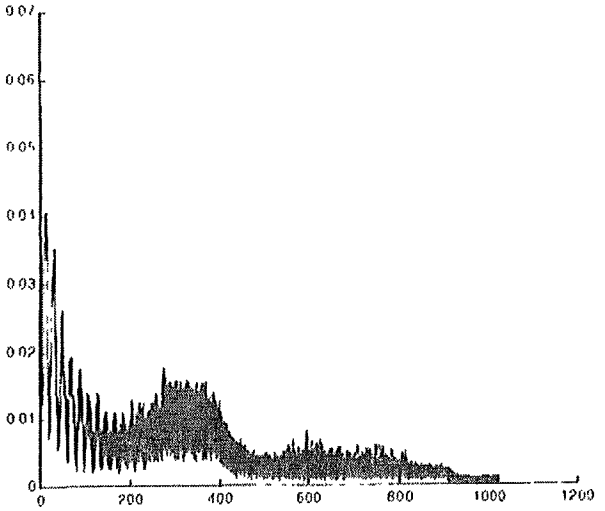

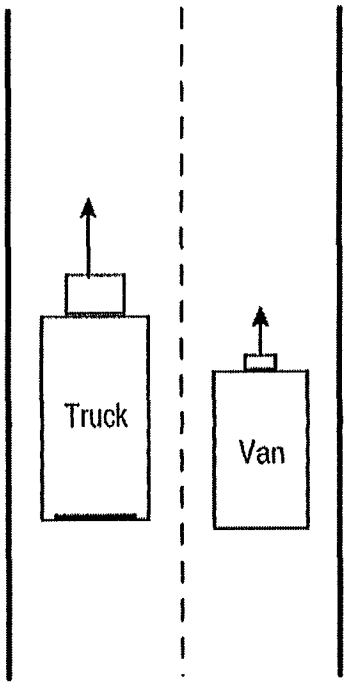

Center Beam
Semi Tractor/Trailer
passing in adjacent lane

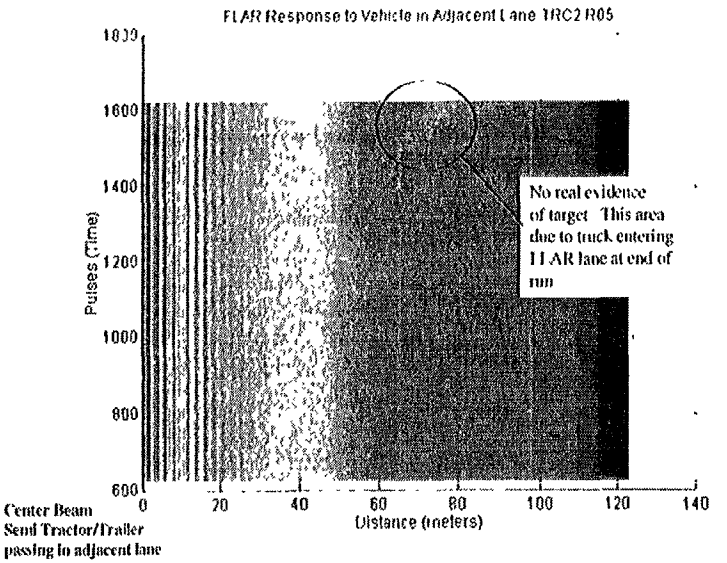

6.1b Vehicle Induced False Alarm - Vehicle in Adjacent Lane

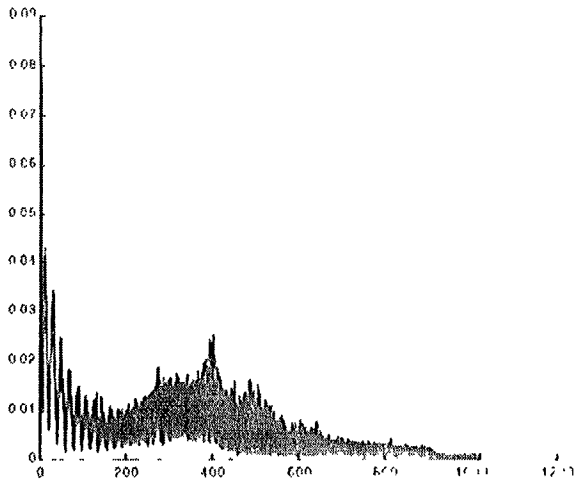

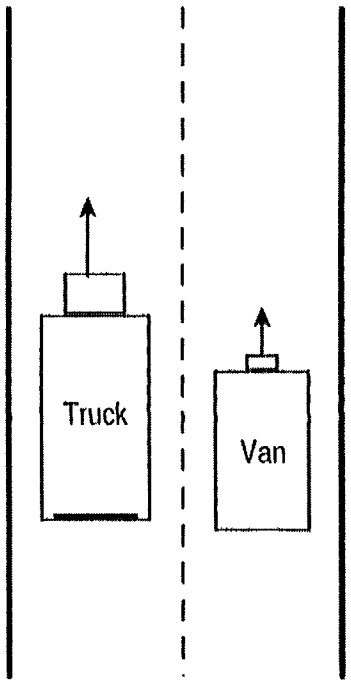

Left Beam
Semi Tractor/Trailer
passing in adjacent lane

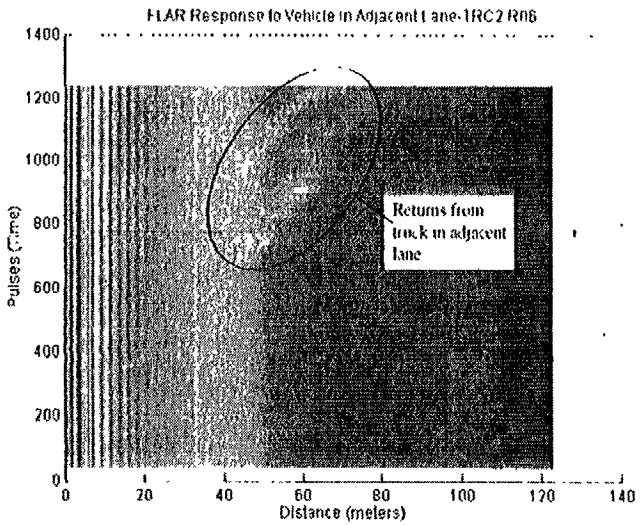

6.1b Vehicle Induced False Alarm - Vehicle in Adjacent Lane

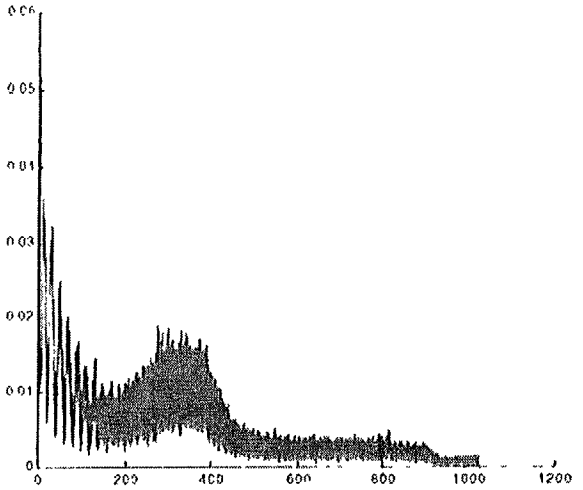

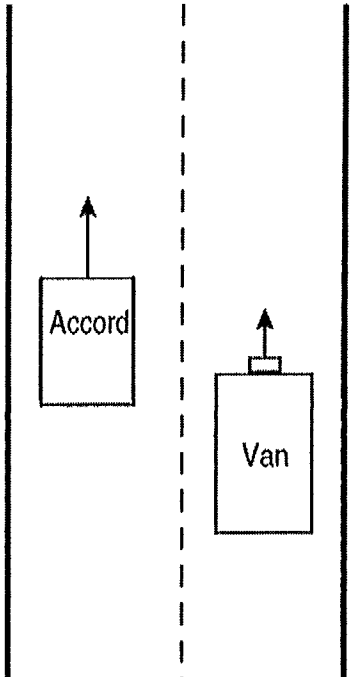

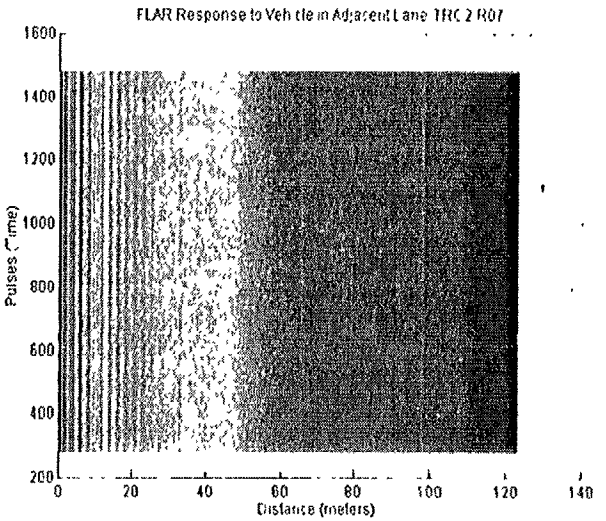

Center Beam
Accord
passing in adjacent lane

6.1b Vehicle Induced False Alarm - Vehicle in Adjacent Lane

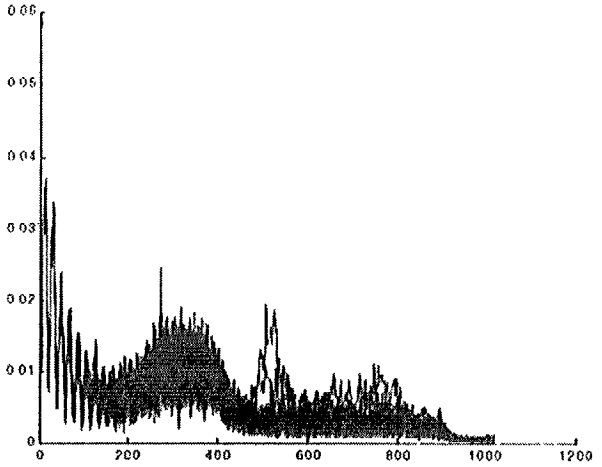

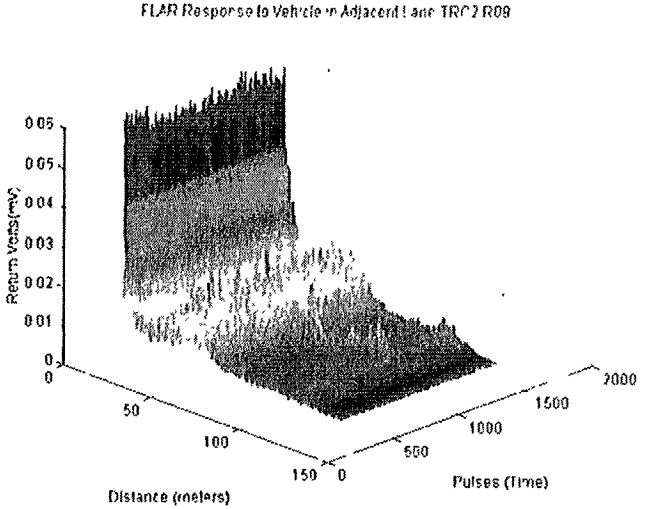

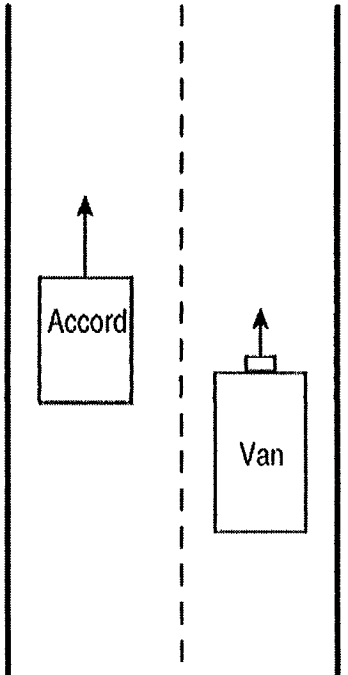

Left Beam
Accord
passing in adjacent lane

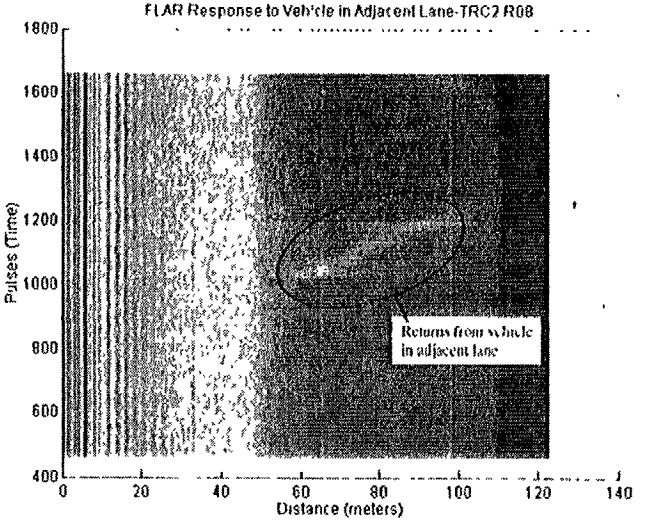

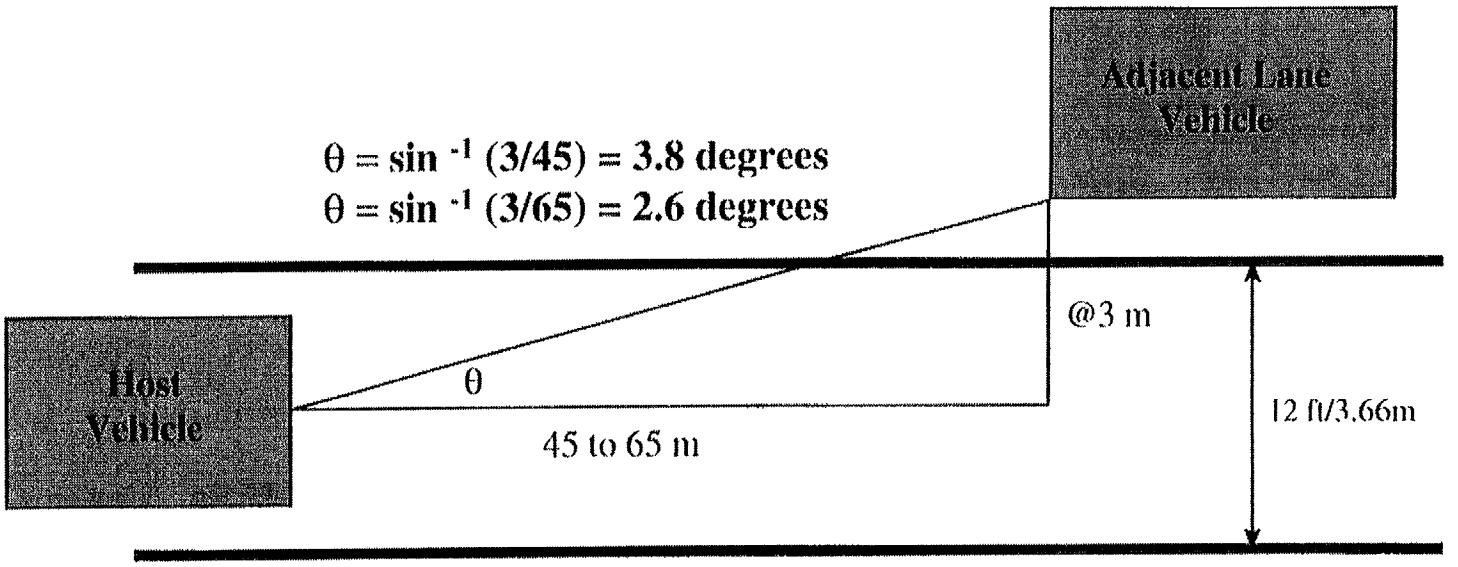

Object Orientation Adjacent Lane Clutter Analysis

6.2 Braking Secondary Vehicle - Straight Roadway

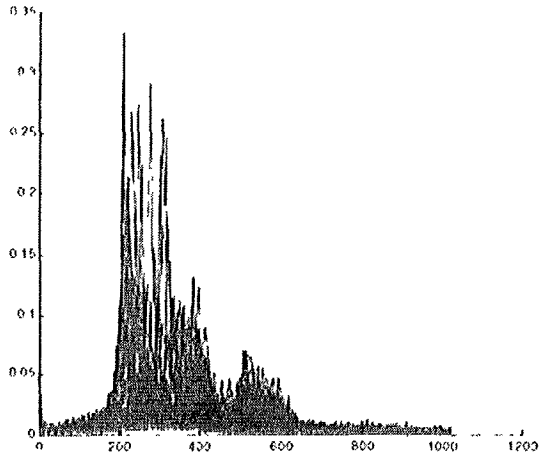

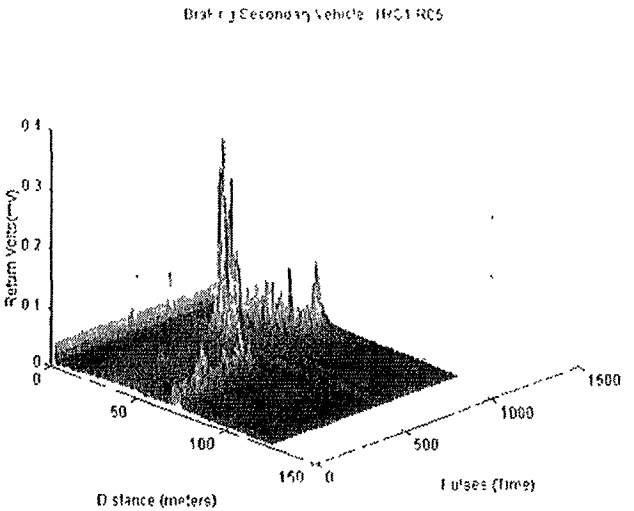

Center Beam
Braking Lead Vehicle
(Accord)
Straight Roadway

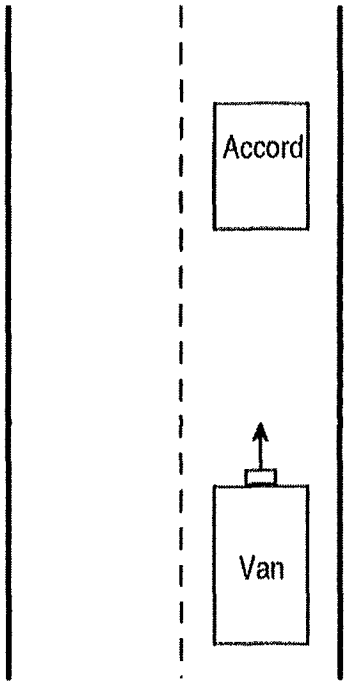

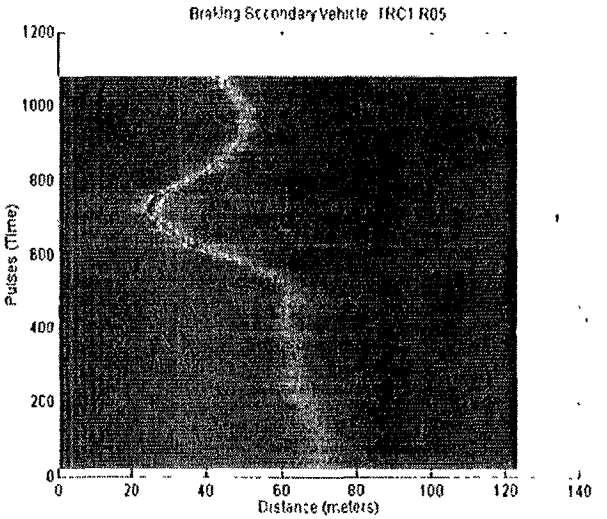

6.2 Braking Secondary Vehicle - Straight Roadway

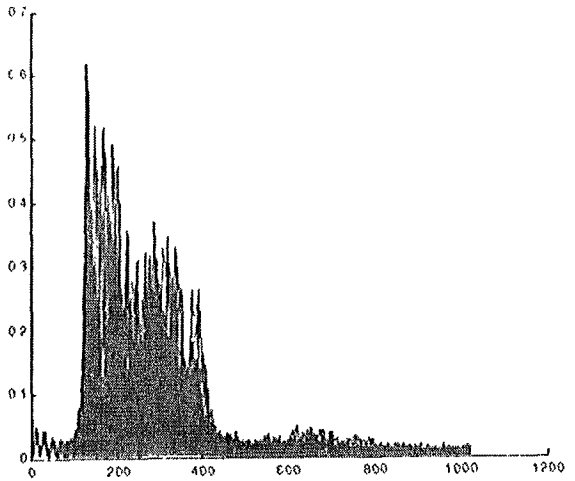

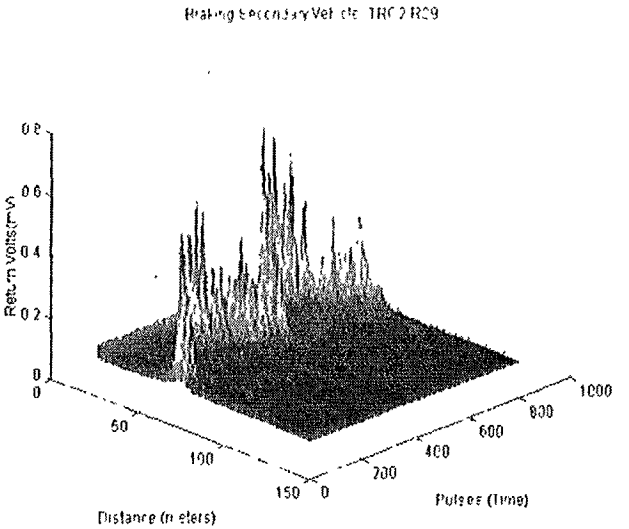

Center Beam
Braking Lead Vehicle
(Accord)
Straight Roadway

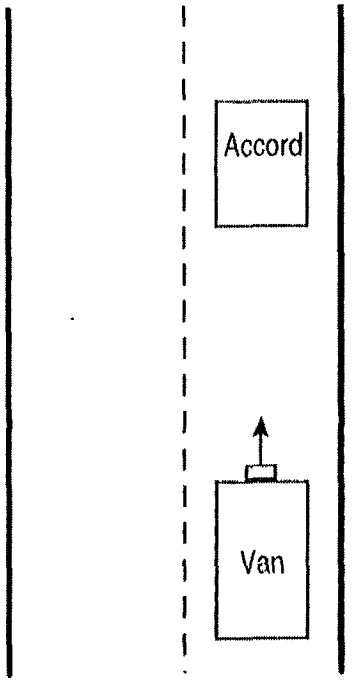

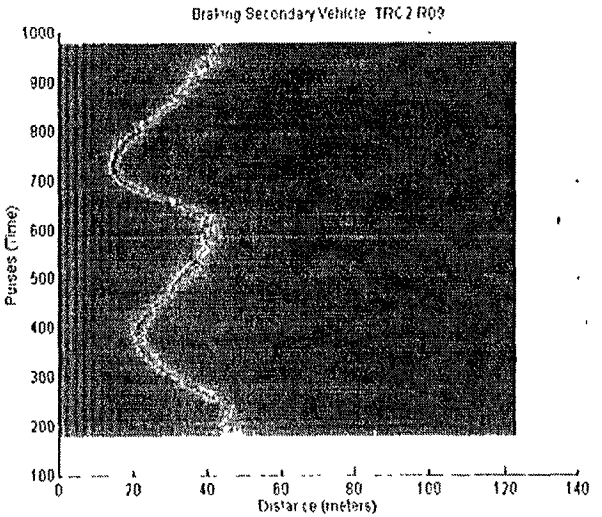

6.3 Out-of-Lane Vehicle Clutter - Straight Roadway

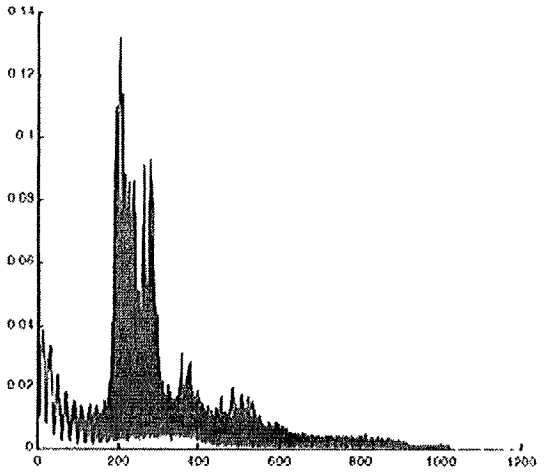

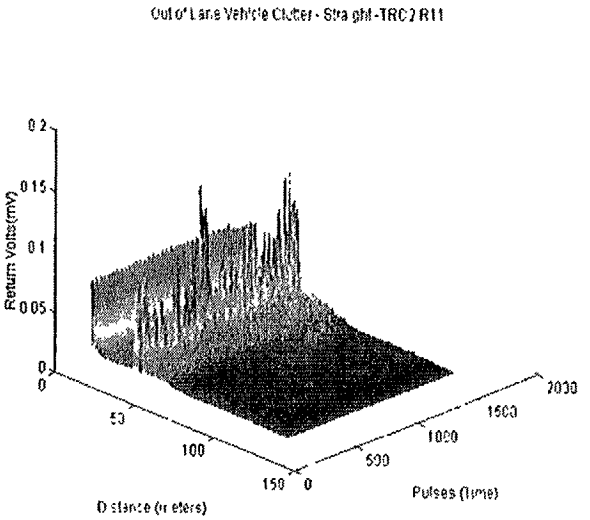

Left Beam
Accord Passed on Left
by Truck/Trailer
17:37:28 to 17:38:36

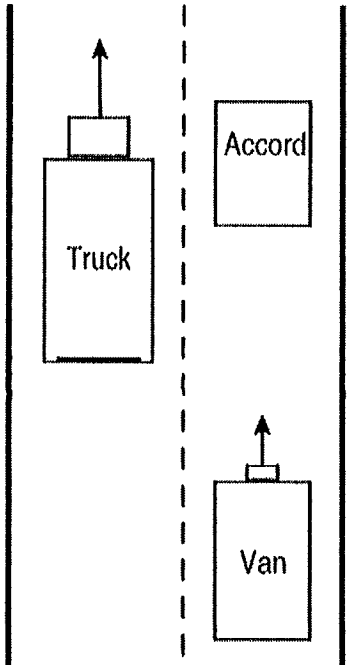

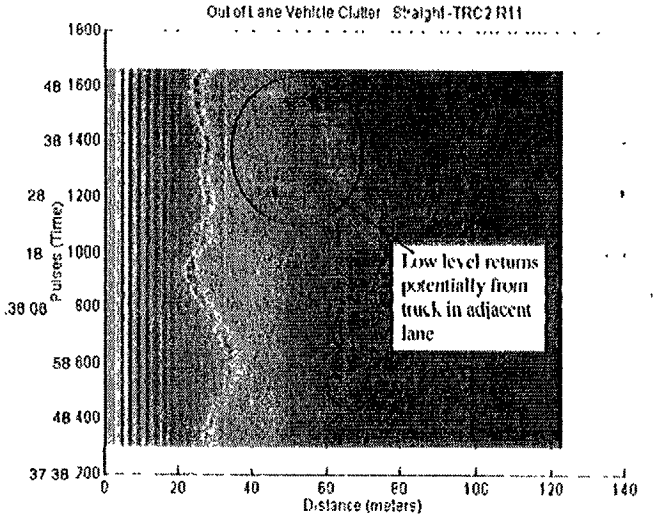

6.3 Out-of-Lane Vehicle Clutter - Straight Roadway

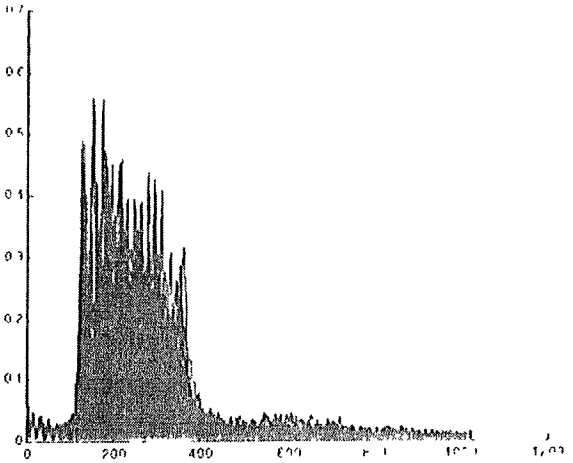

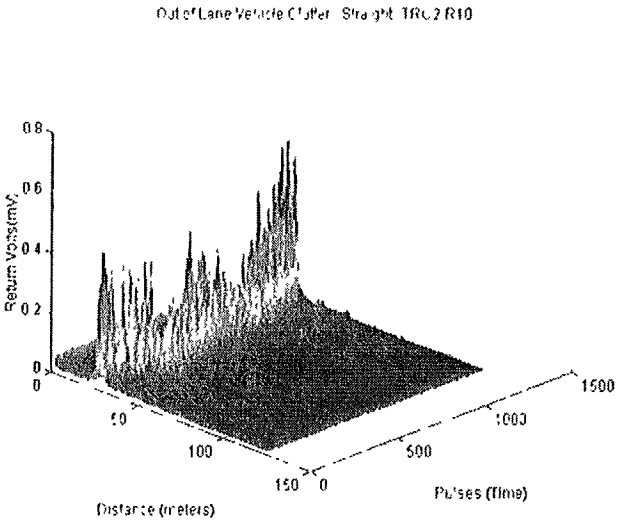

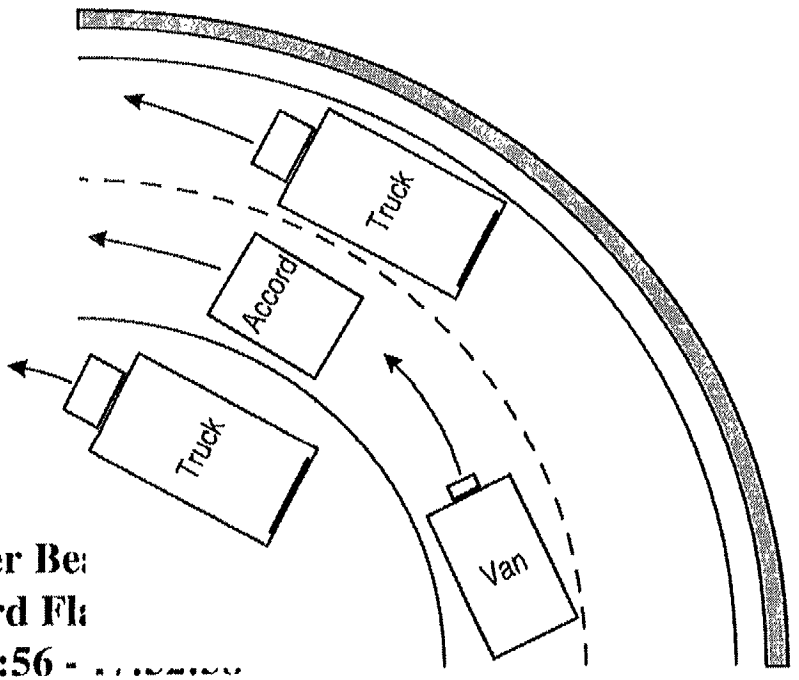

Center Be:
Accord Fl:
17:51:56 -

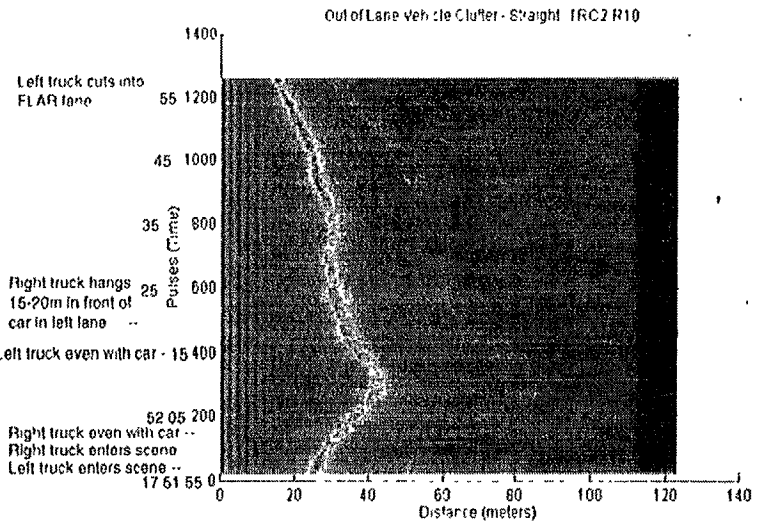

6.3 Out-of-Lane Vehicle Clutter - Straight Roadway

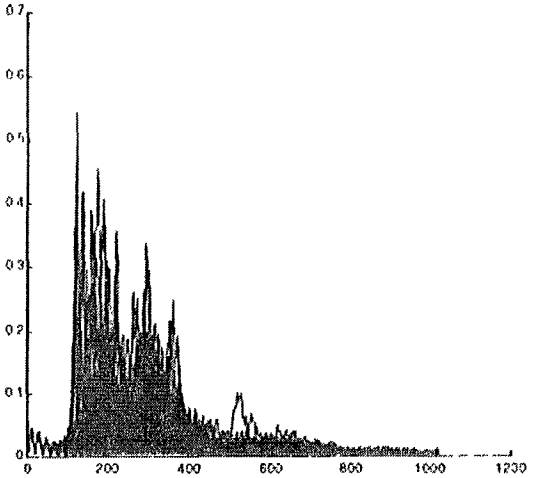

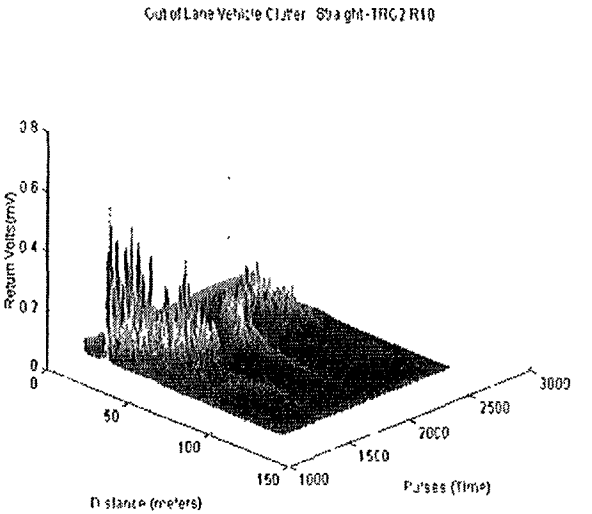

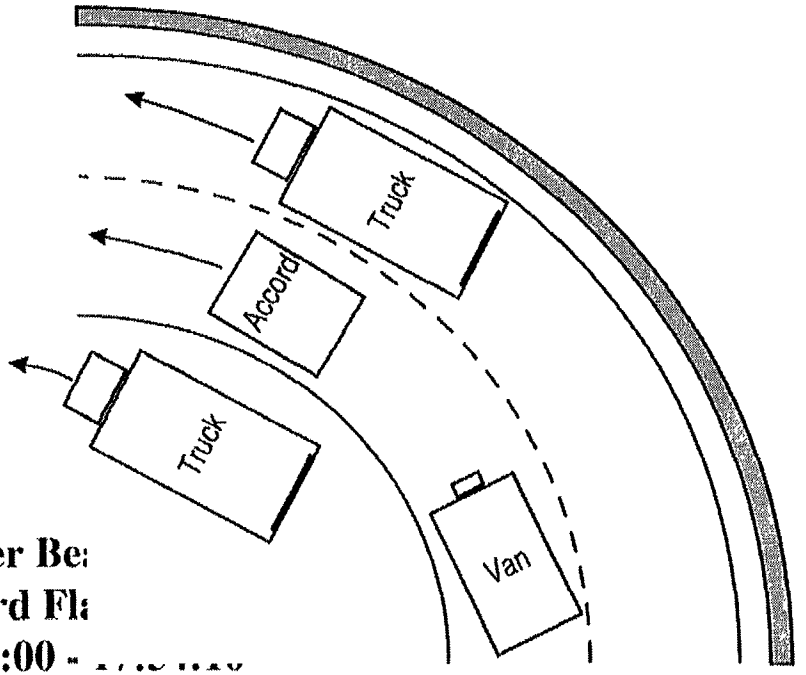

Center Be:
Accord Fl:
17:53:00 -

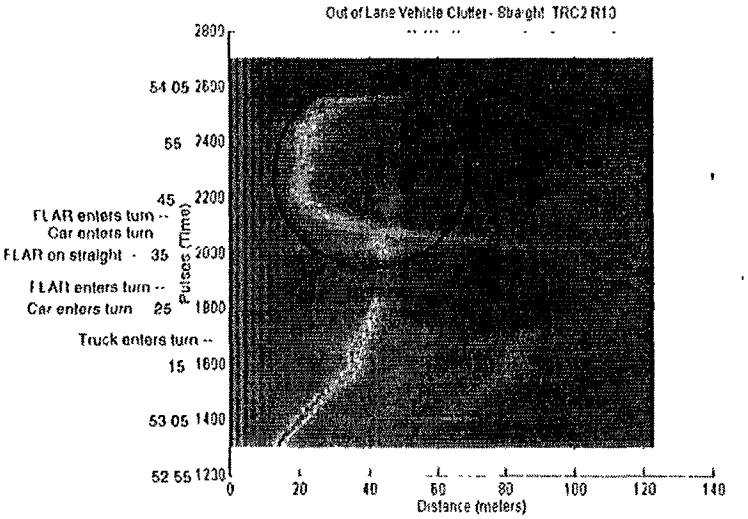

6.4 Intentional Lane Changes - Straight Roadway

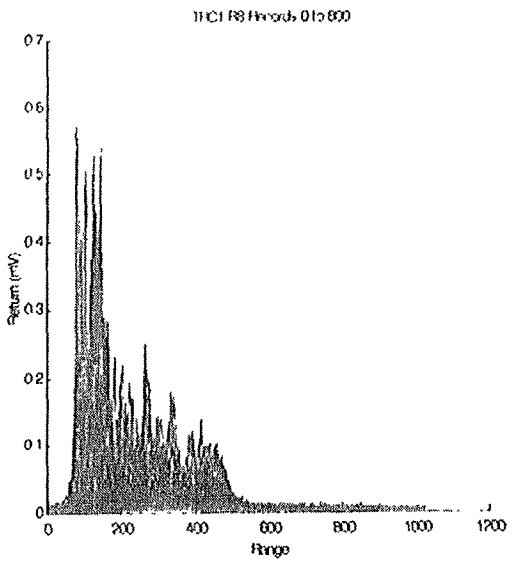

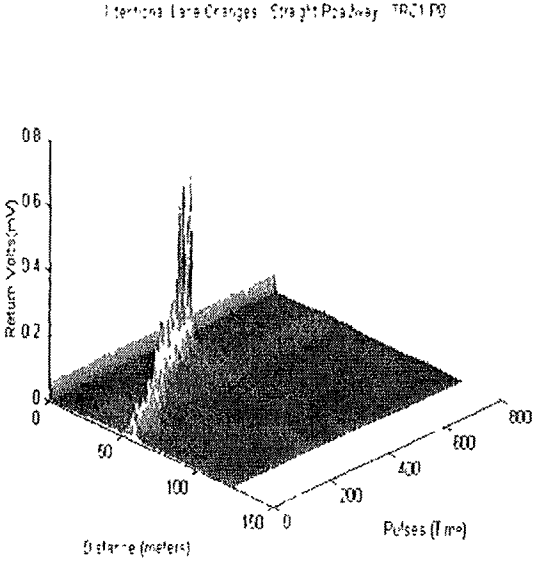

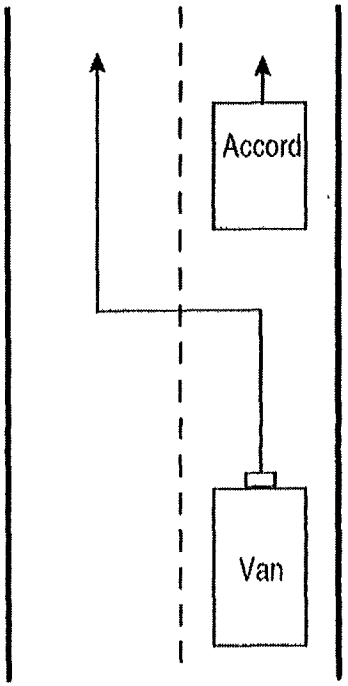

18:48:37 - Begin File

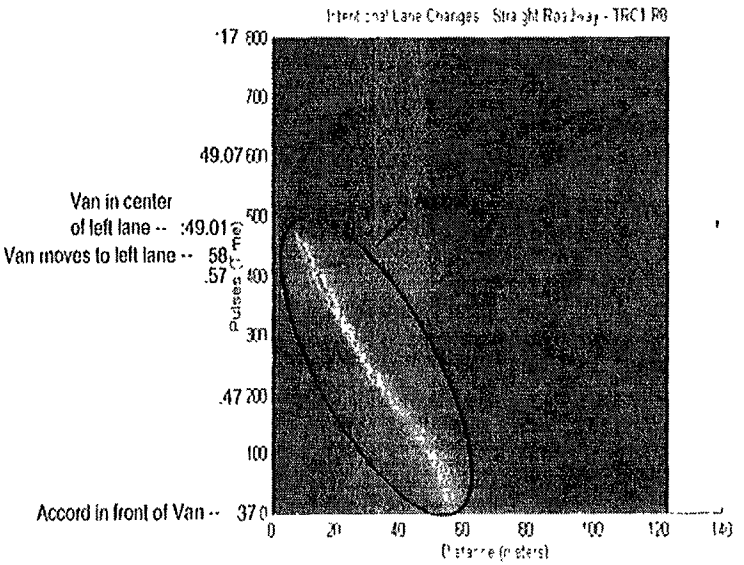

6.4 Intentional Lane Changes - Straight Roadway

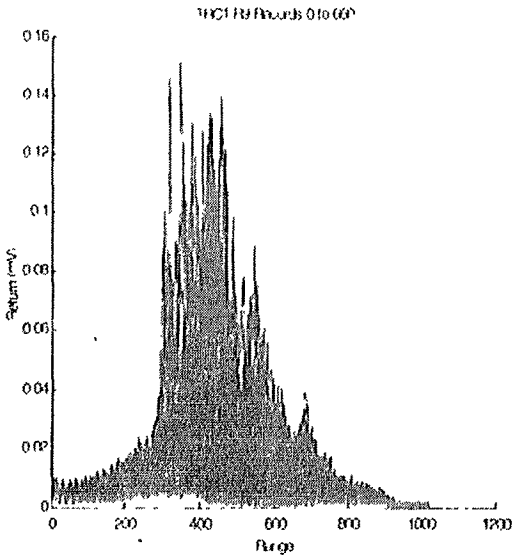

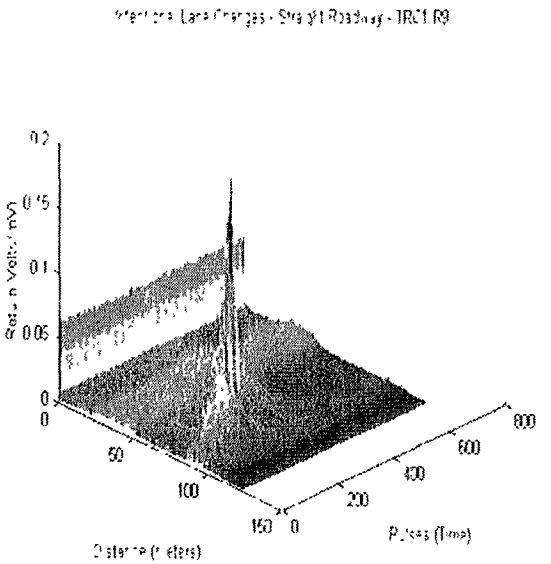

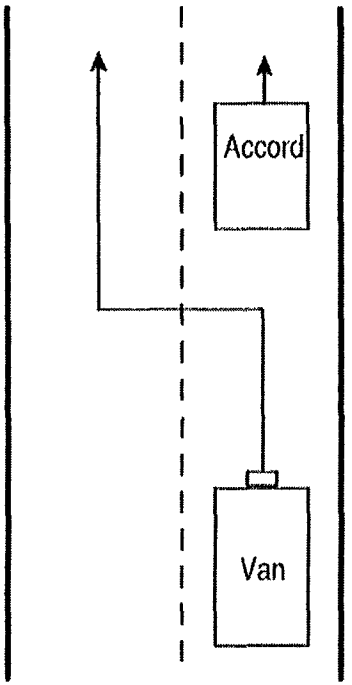

18:56:44 - Begin File

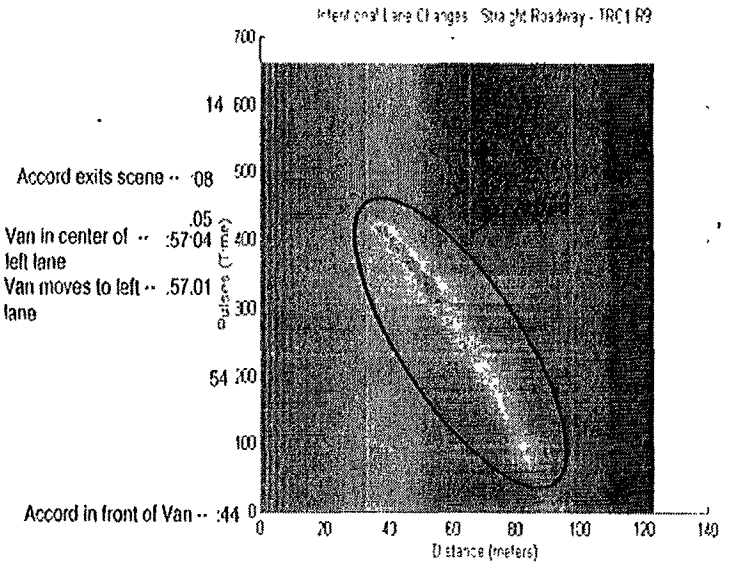

6.4 Intentional Lane Changes - Straight Roadway

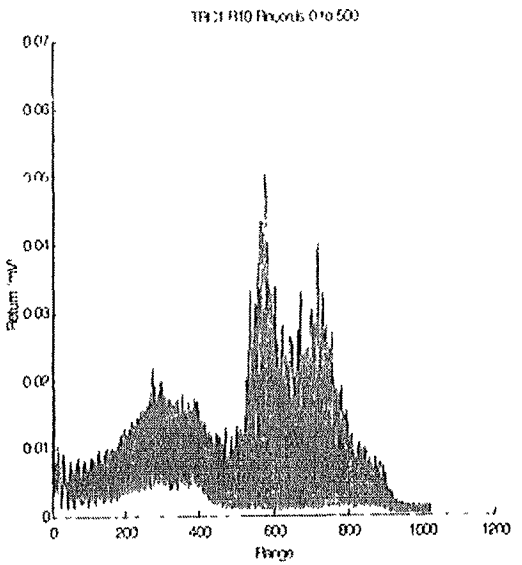

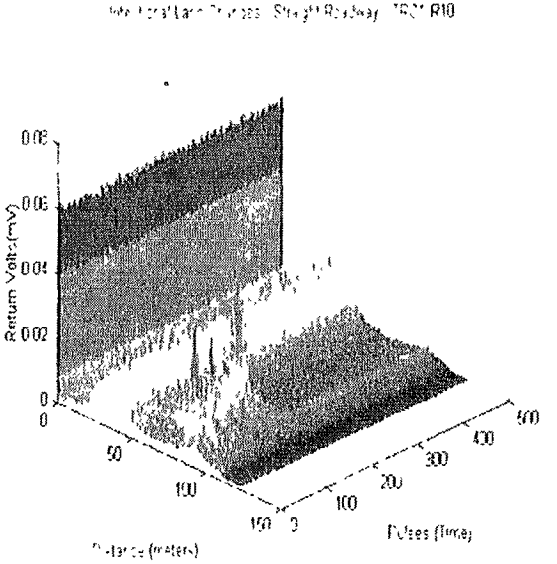

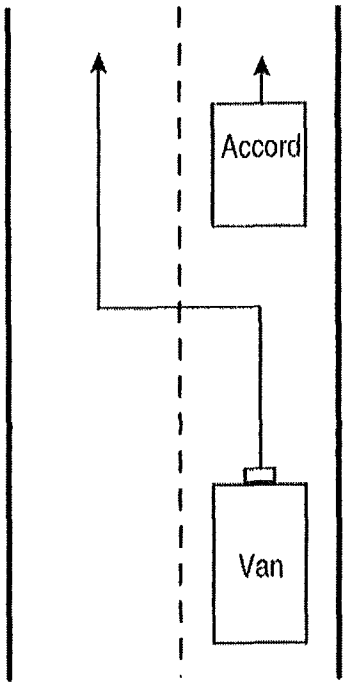

19:05:32 - Begin File

Van in center of left lane -- .43 .42

Van moves to left lane -- .39

Accord in front of Van -- .32

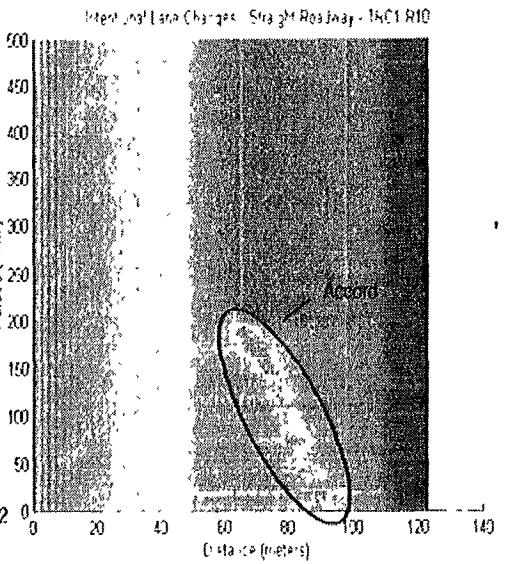

6.4 Intentional Lane Changes - Straight Roadway

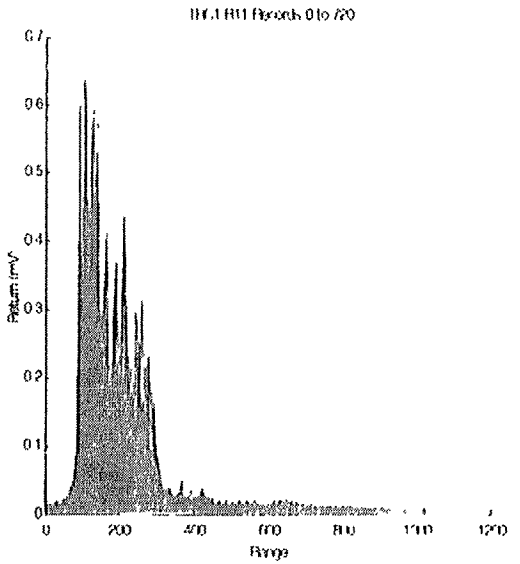

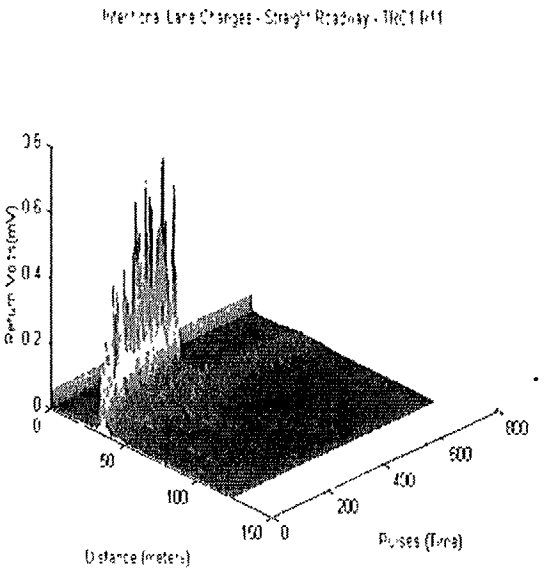

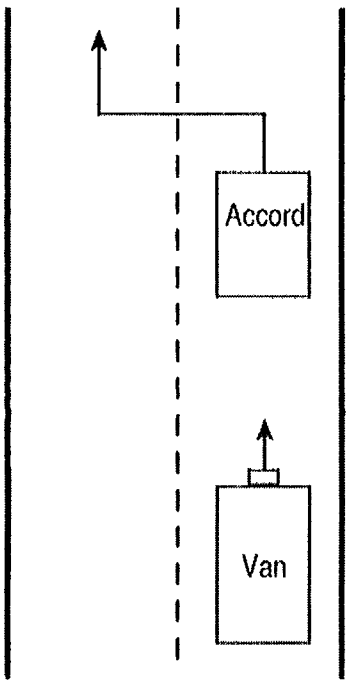

19.18:15 - Begin File

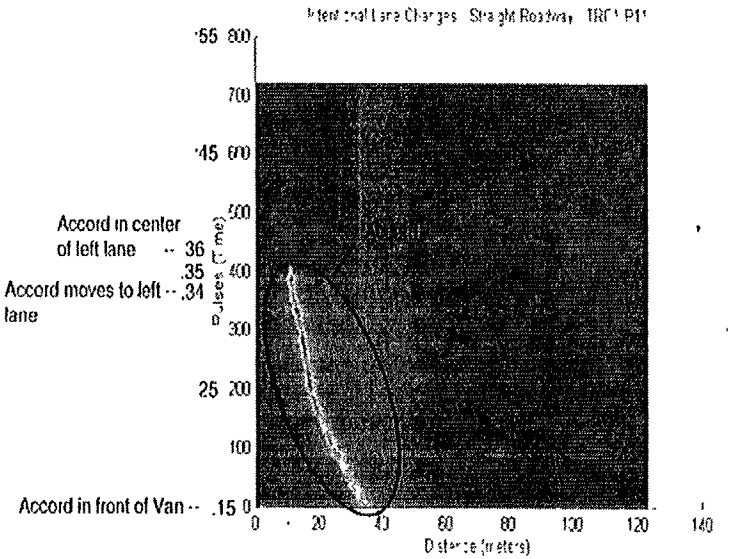

6.4 Intentional Lane Changes - Straight Roadway

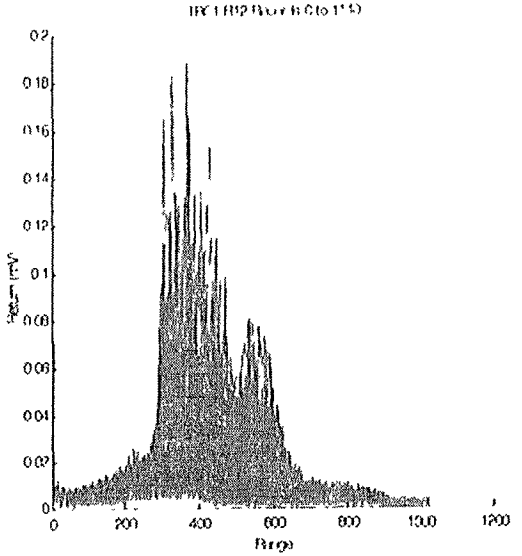

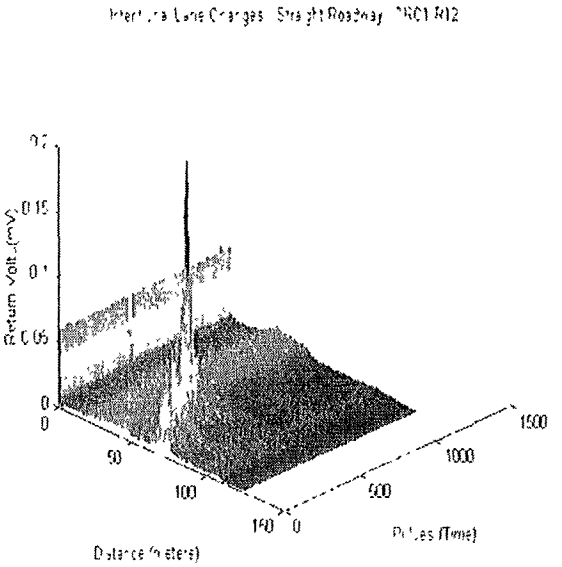

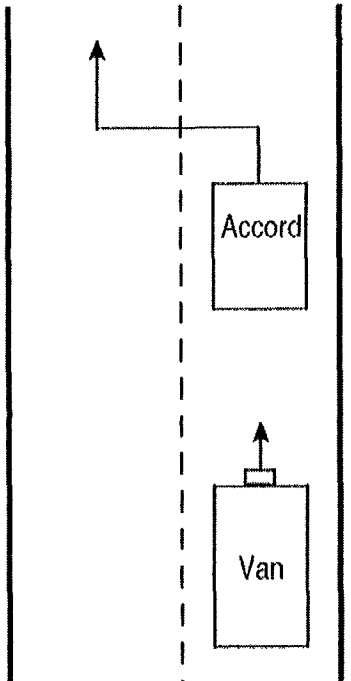

19:28:17 - Begin File

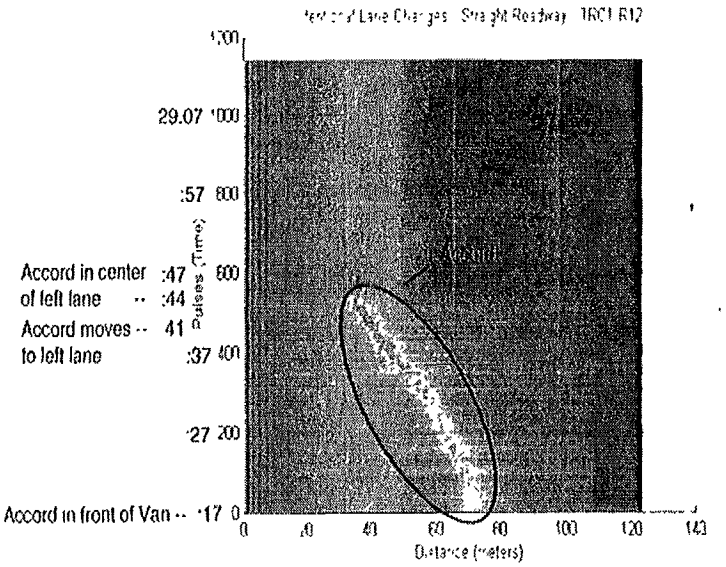

6.4 Intentional Lane Changes - Straight Roadway

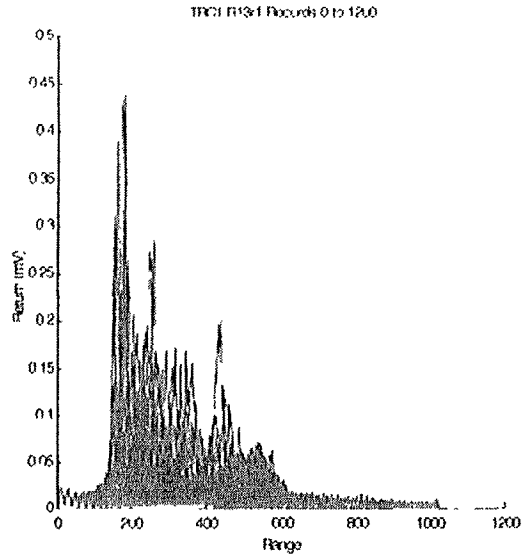

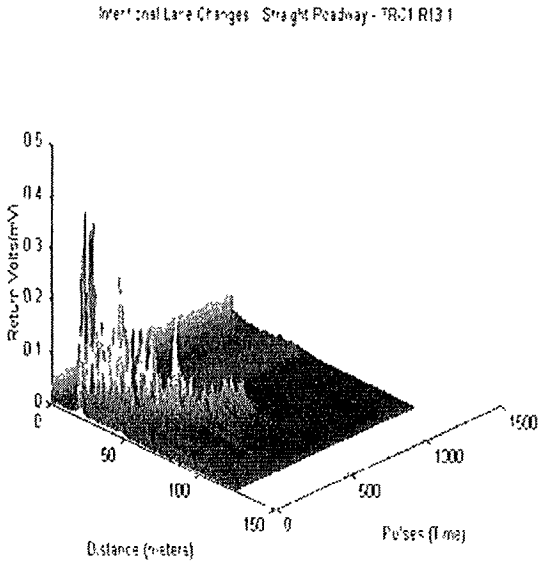

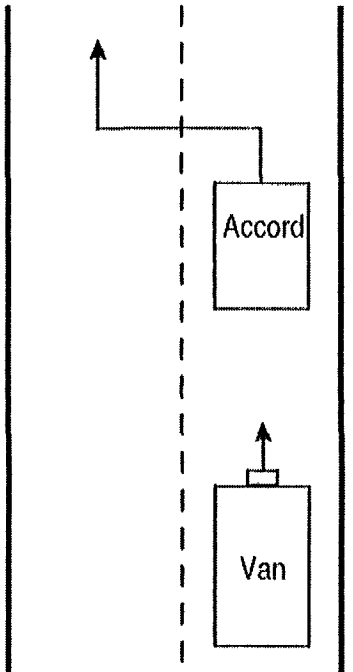

17:08:09 - Begin File

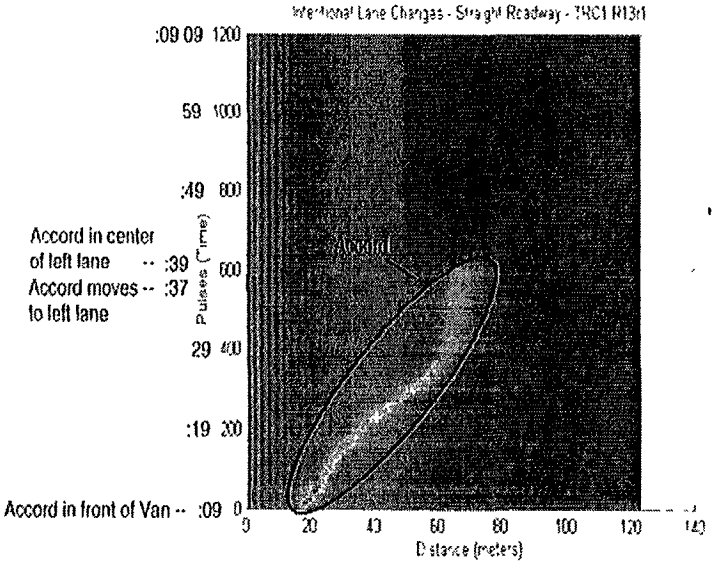

6.4 Intentional Lane Changes - Straight Roadway

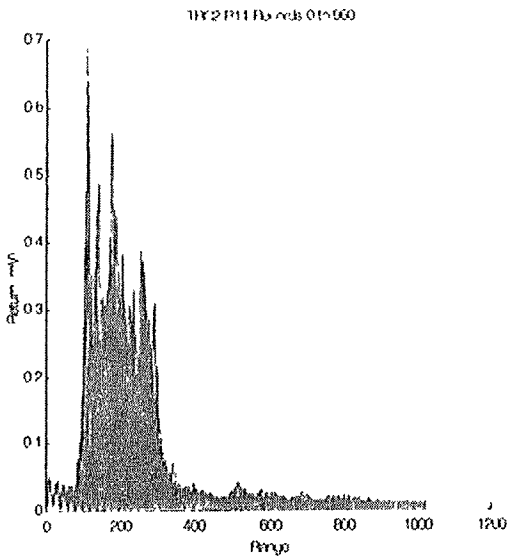

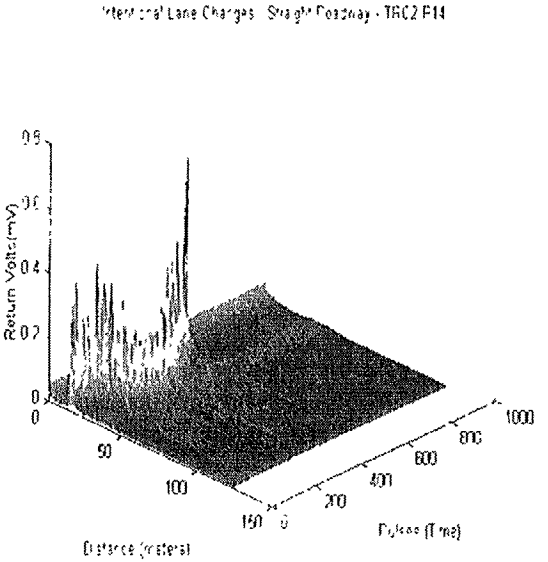

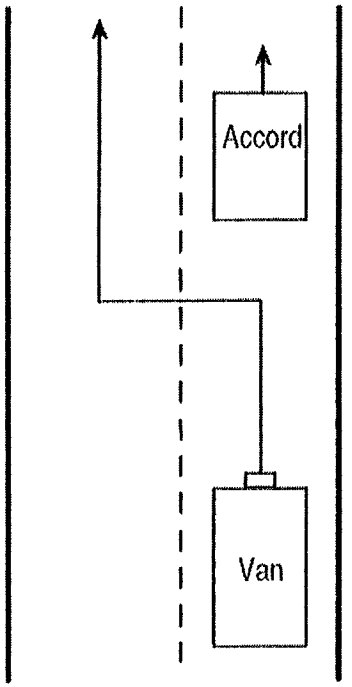

20:41:42 - Begin File

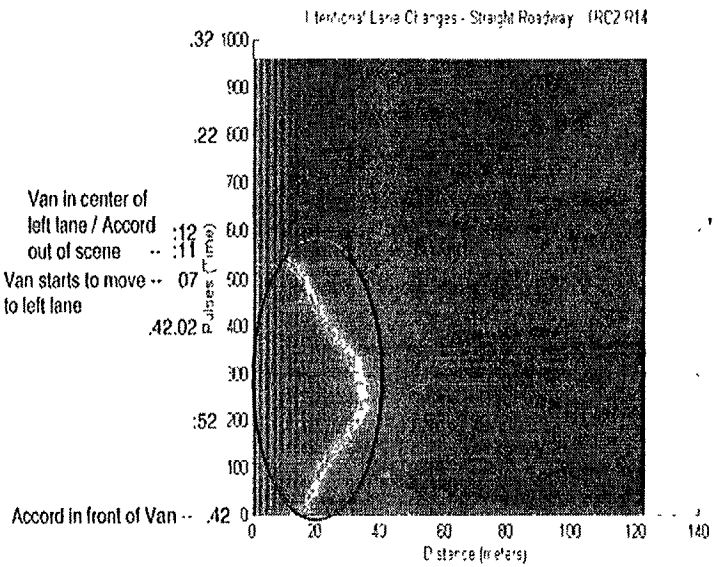

6.4 Intentional Lane Changes - Straight Roadway

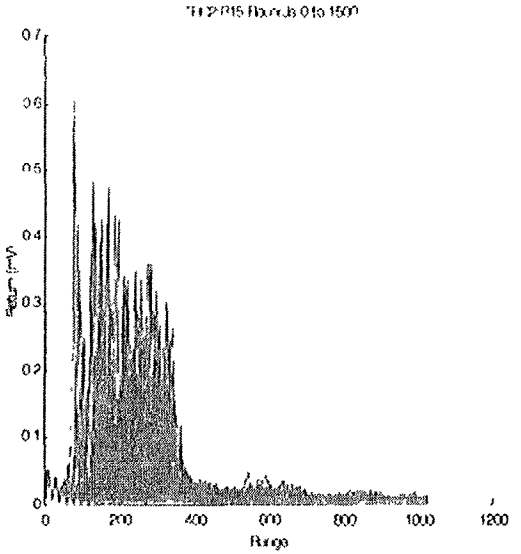

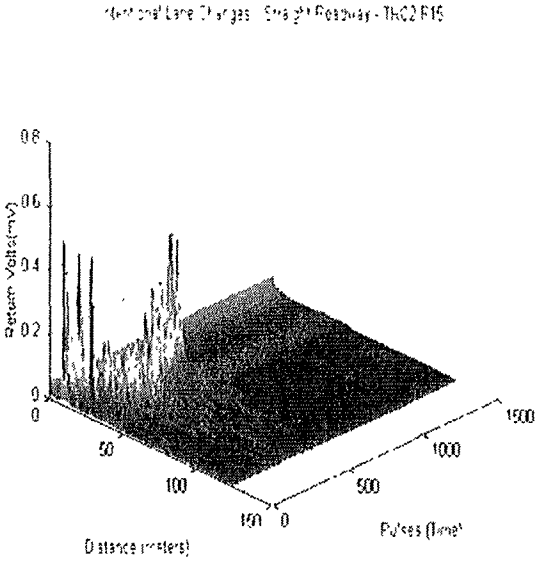

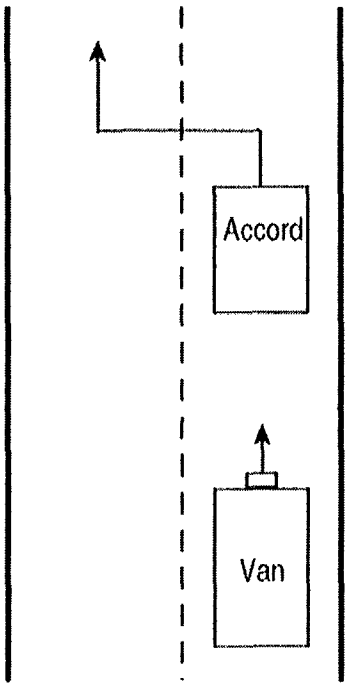

20:45:20 - Begin File

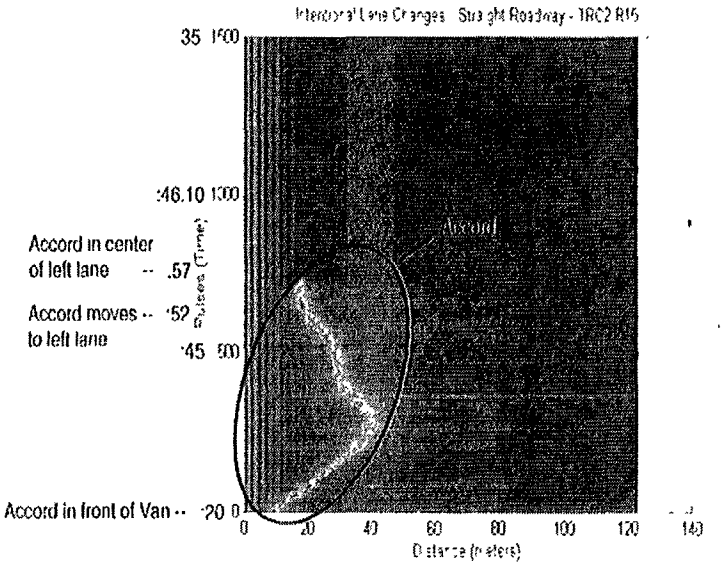

6.5 Tracking New Secondary - Straight Roadway

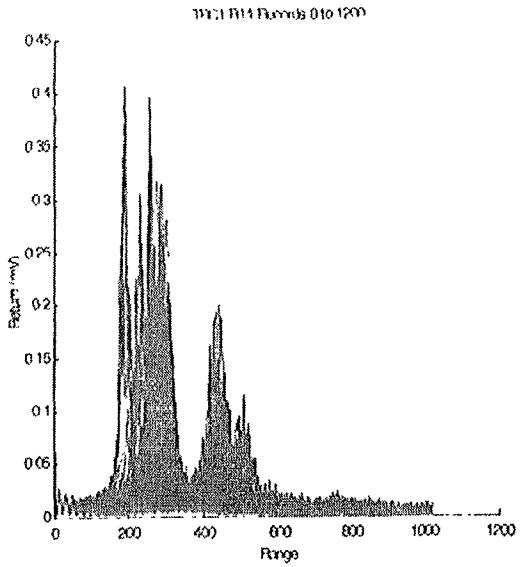

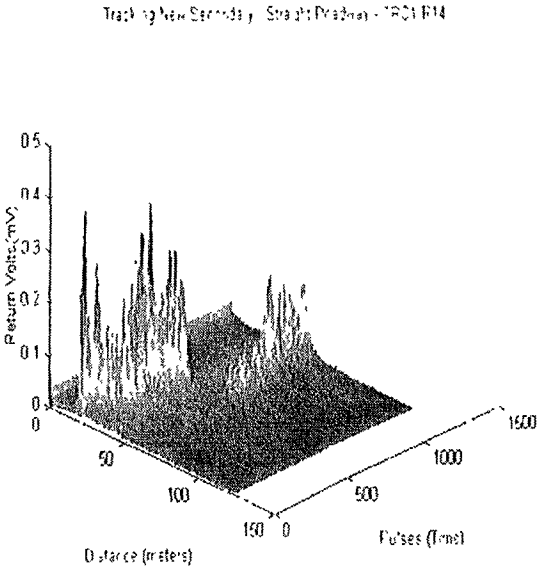

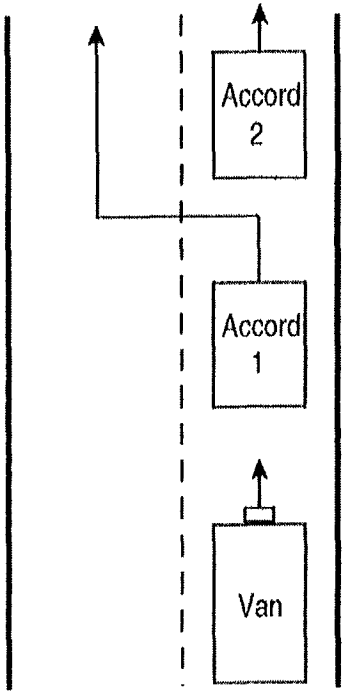

17:00:58 - Begin File

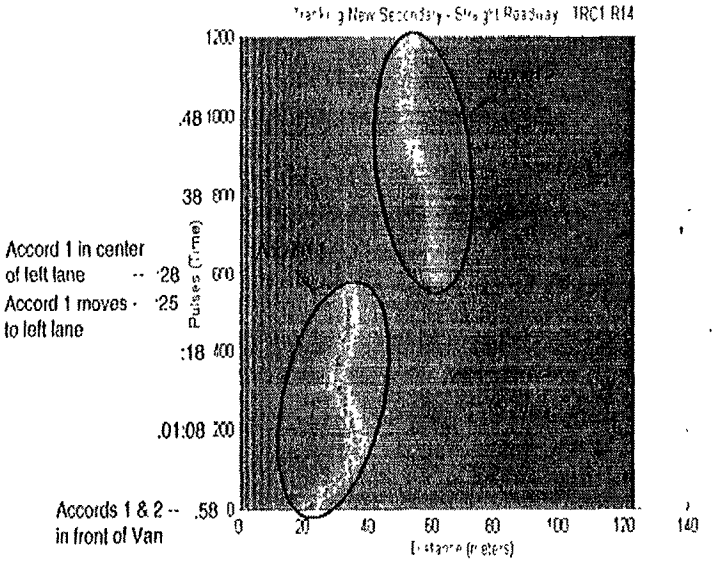

6.5 Tracking New Secondary - Straight Roadway

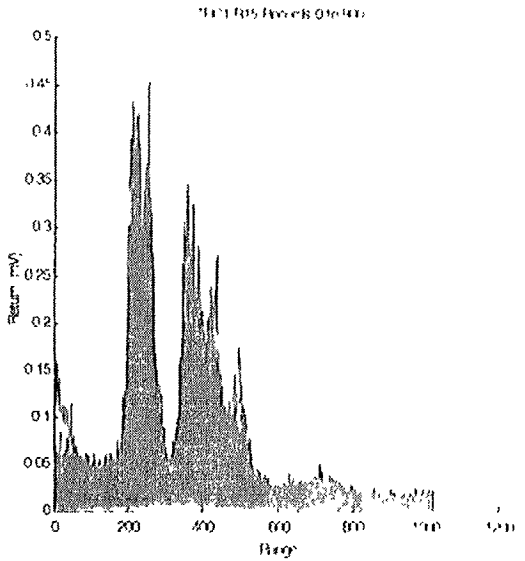

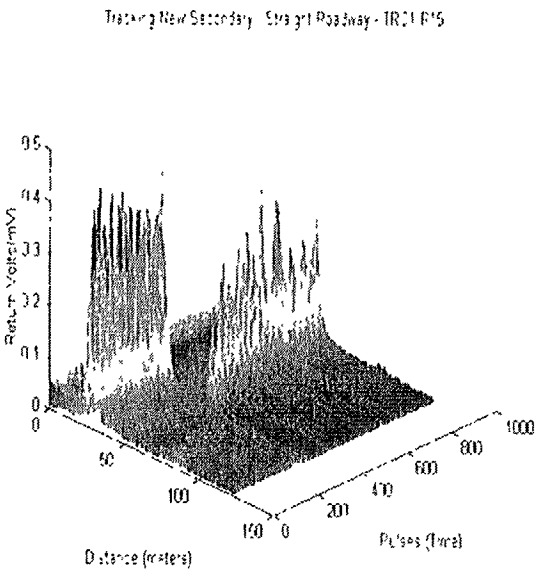

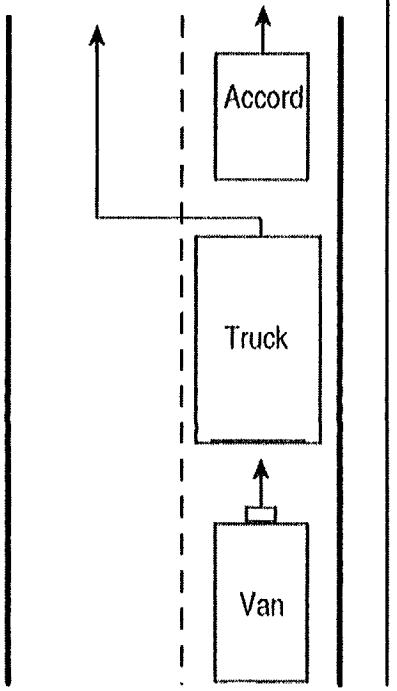

14:37:56 - Begin File

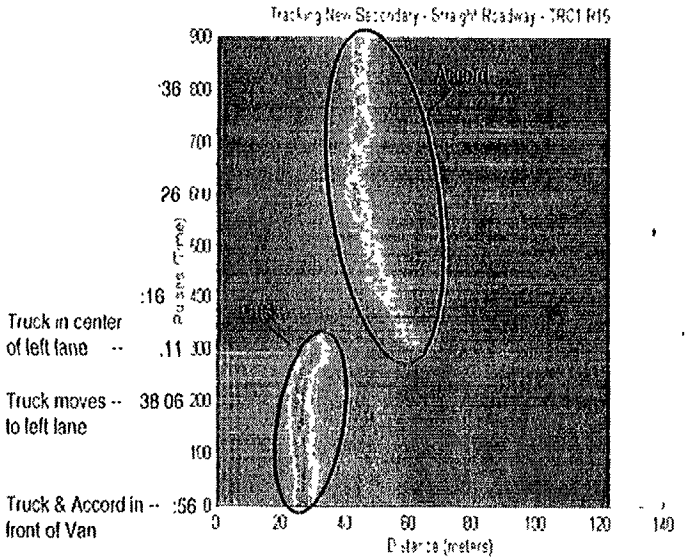

6.5 Tracking New Secondary - Straight Roadway

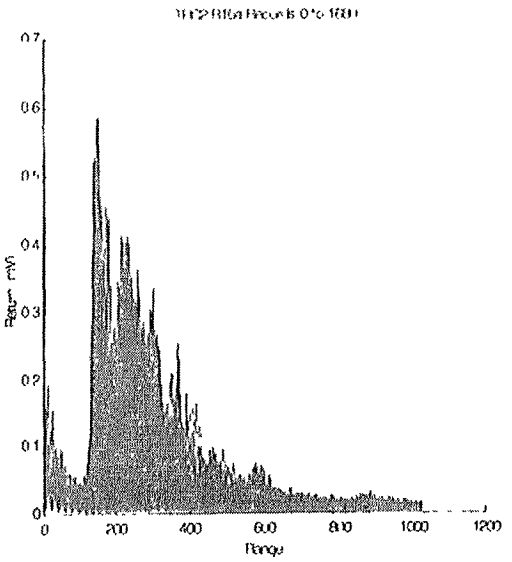

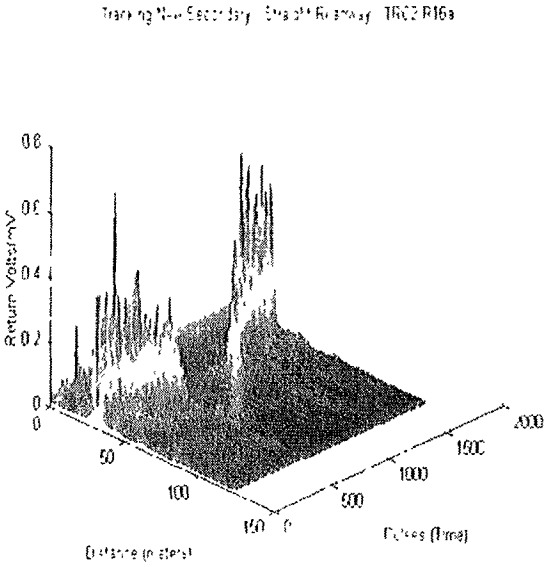

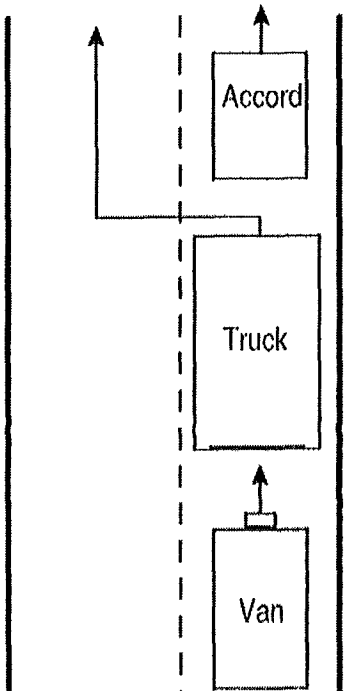

16:27:26 - Begin File

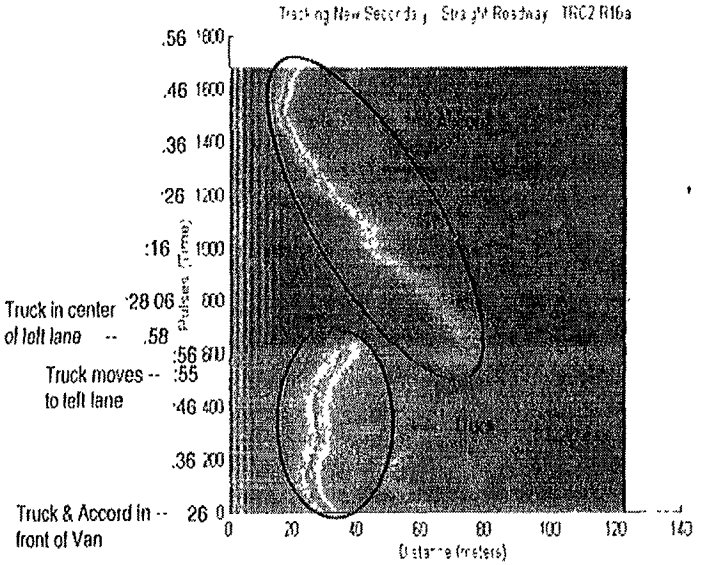

6.6 Tracking with a Cut-in-Straight Roadway

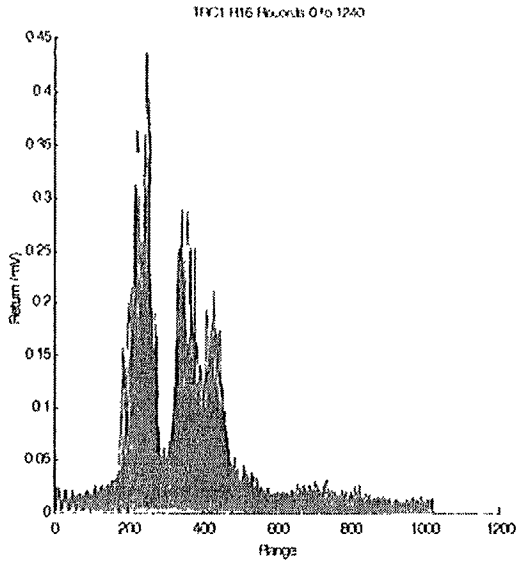

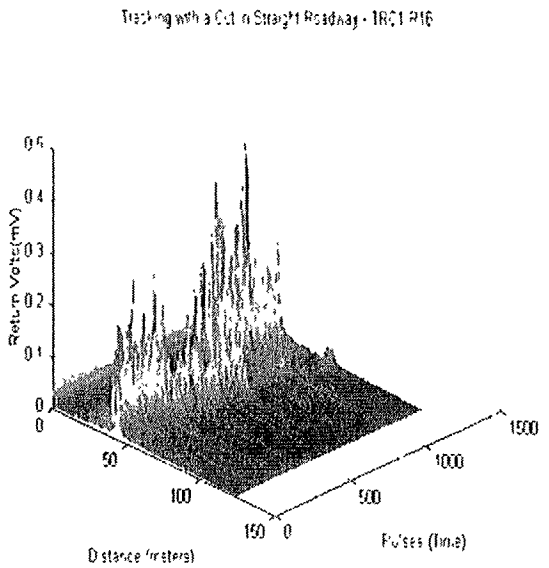

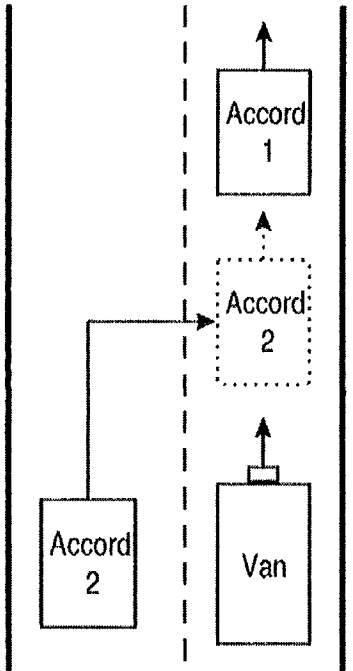

16:47:23 - Begin File

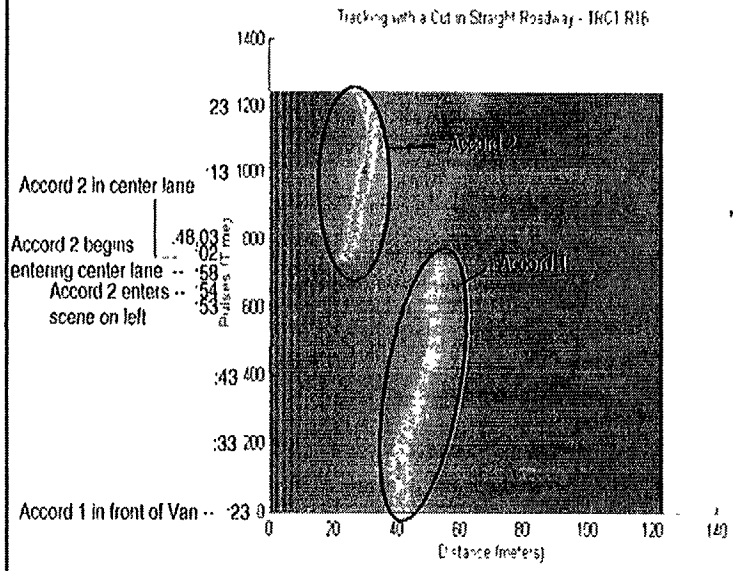

6.6 Tracking with a Cut-in-Straight Roadway

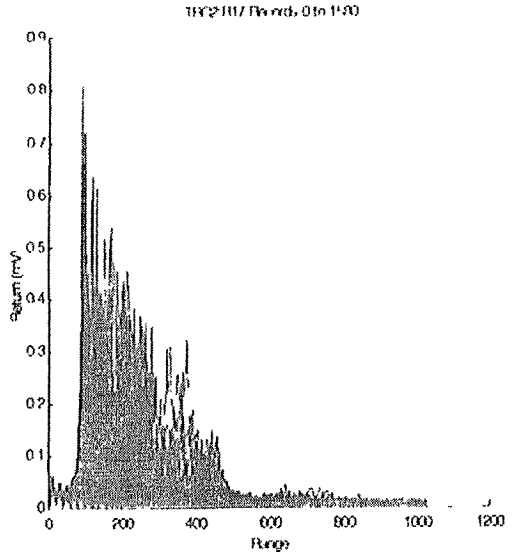

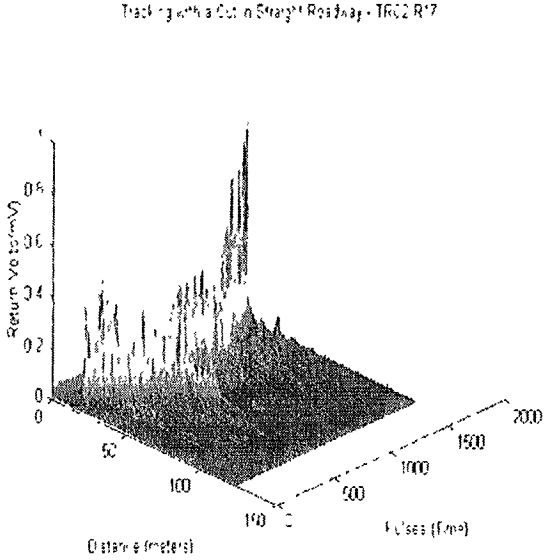

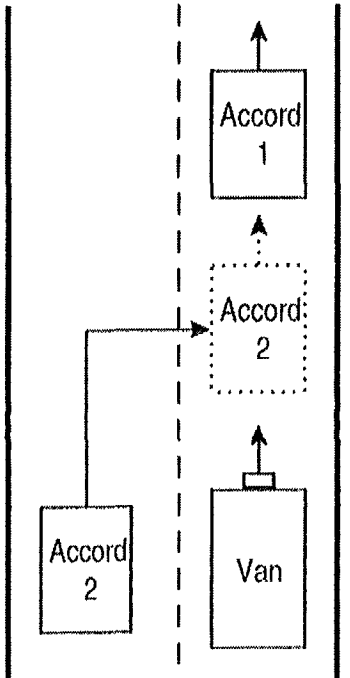

20:14:11 - Begin File

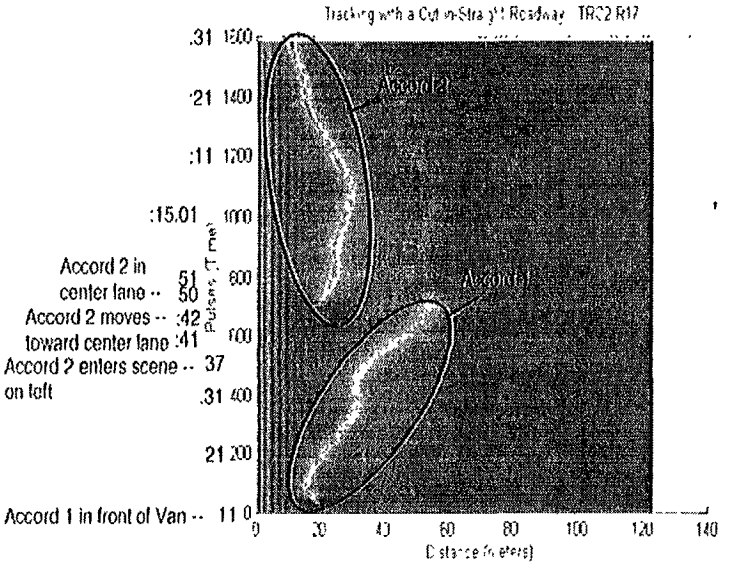

6.7 - Strong Vehicle Clutter in Range - Straight Roadway

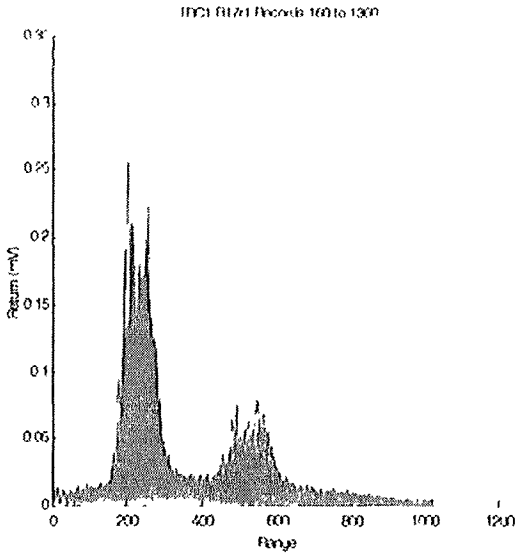

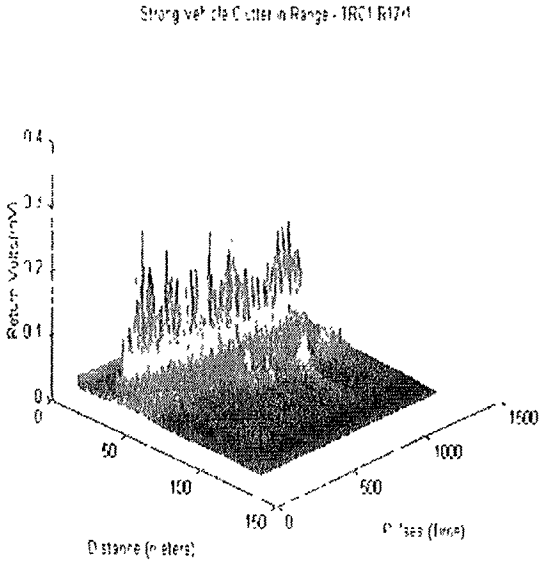

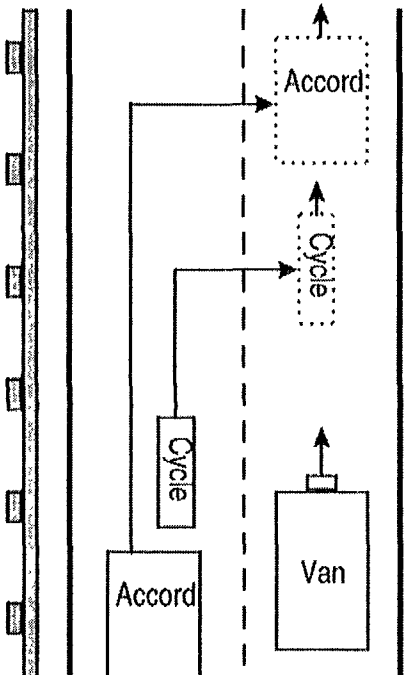

15:23:55 - Begin File

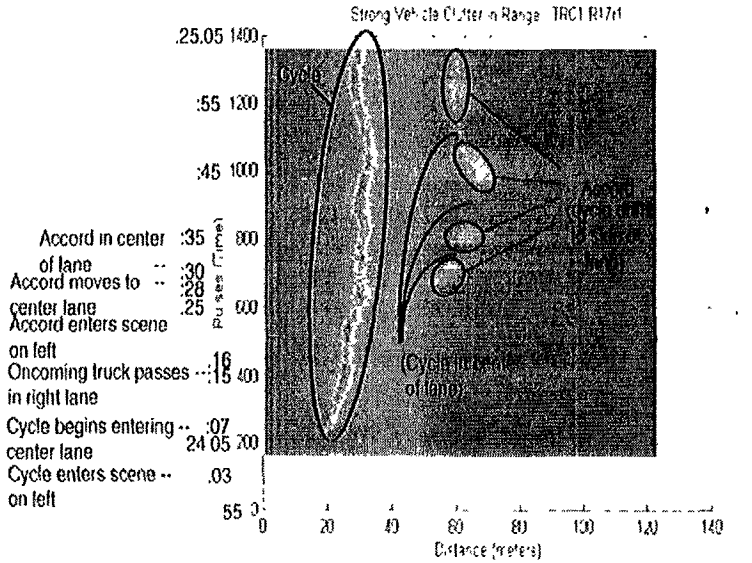

6.7 - Strong Vehicle Clutter in Range - Straight Roadway

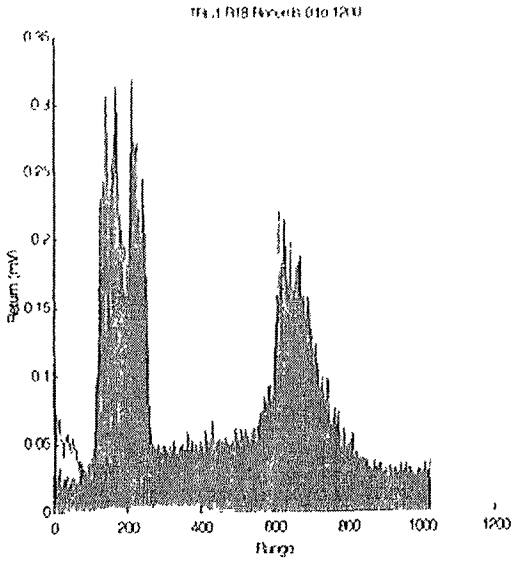

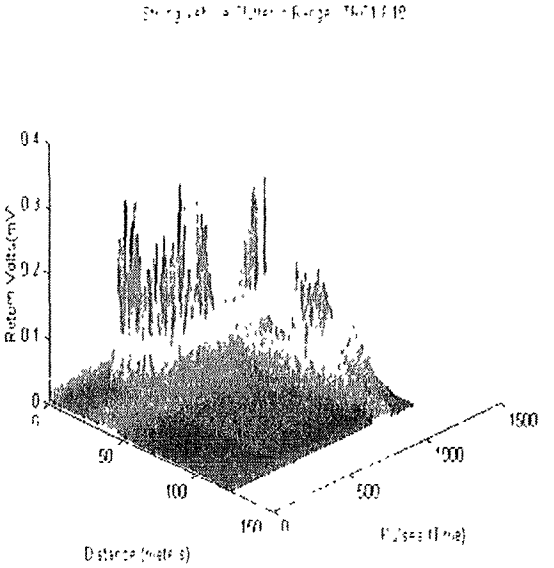

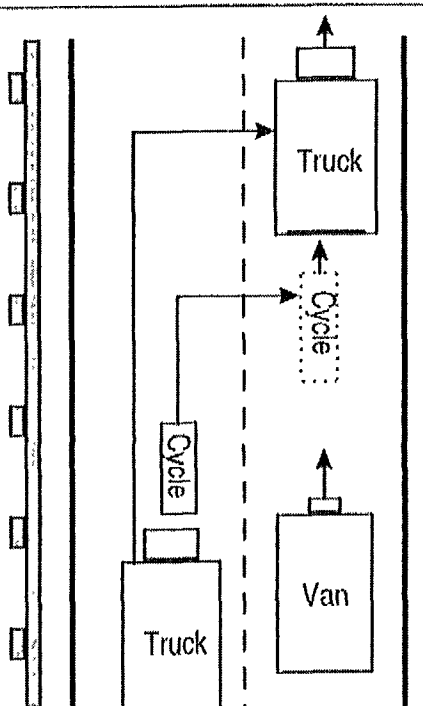

14:52:53 - Begin File

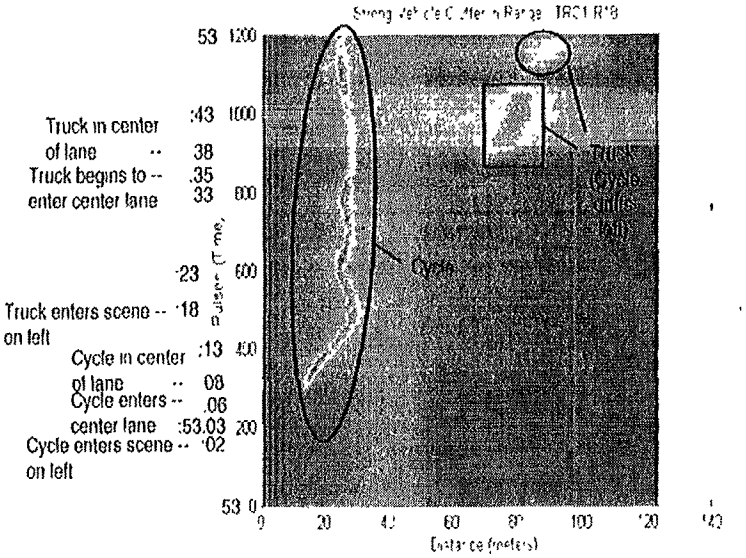

6.7 - Strong Vehicle Clutter in Range - Straight Roadway

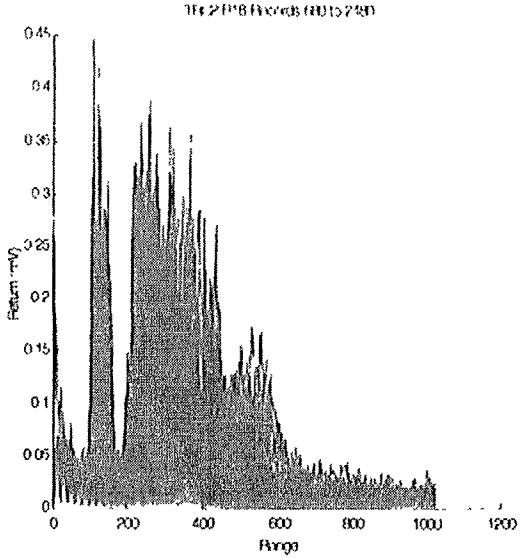

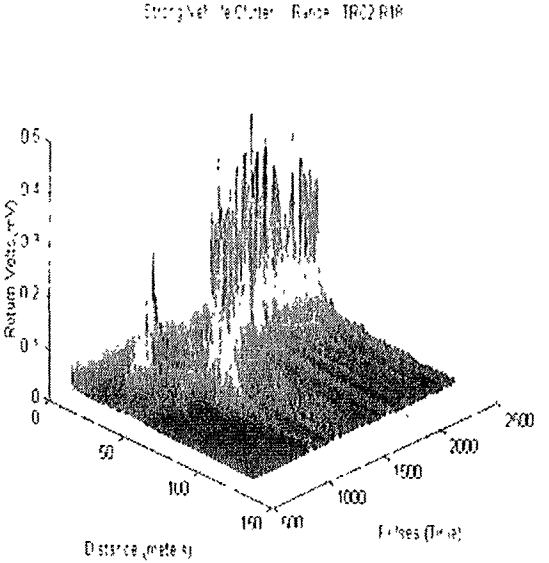

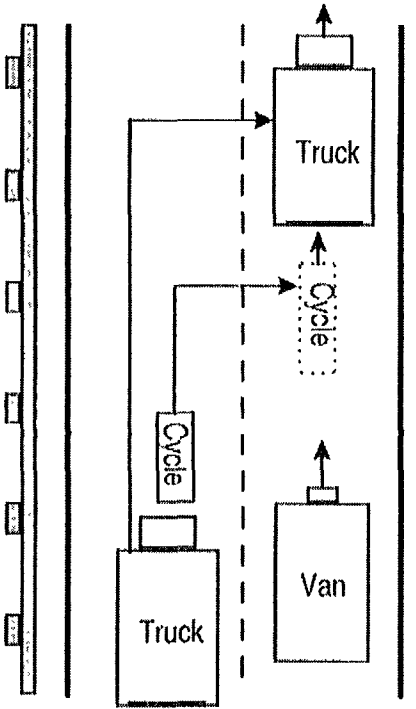

15:39:38 - Begin File

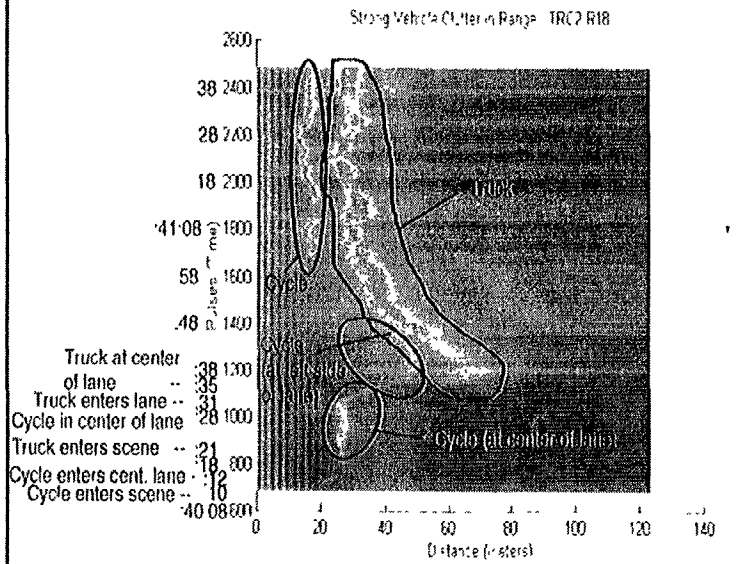

6.8 Vehicle Clutter in Azmuth

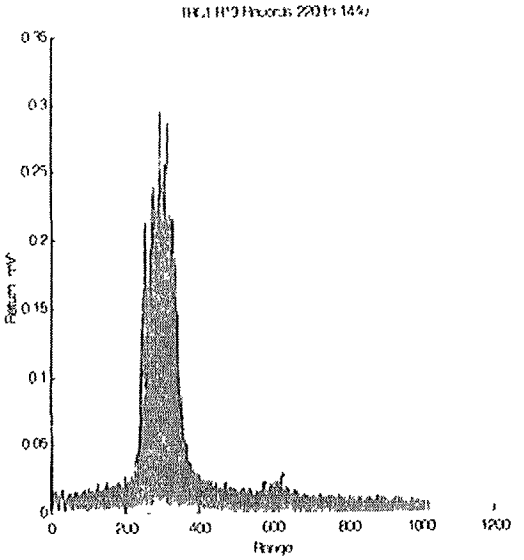

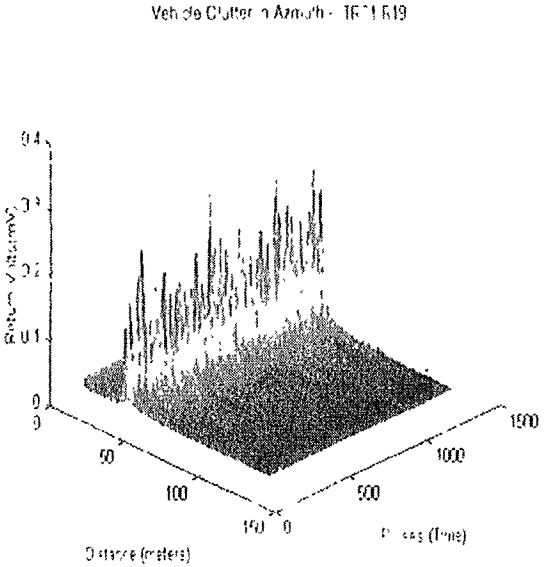

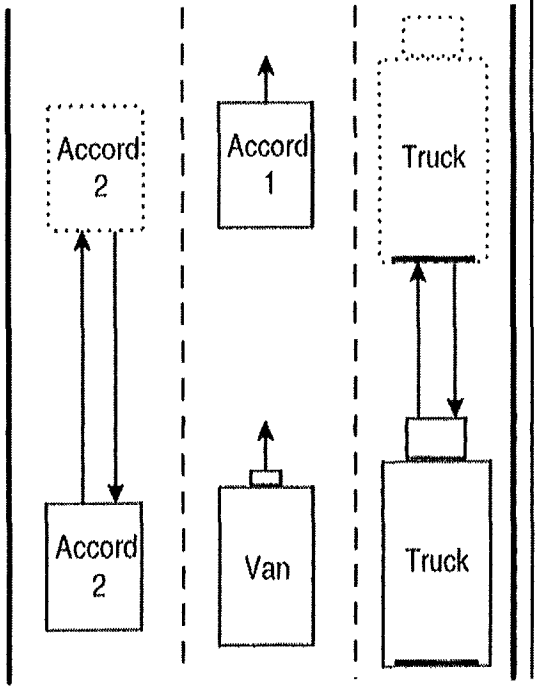

16:02:14 - Begin File

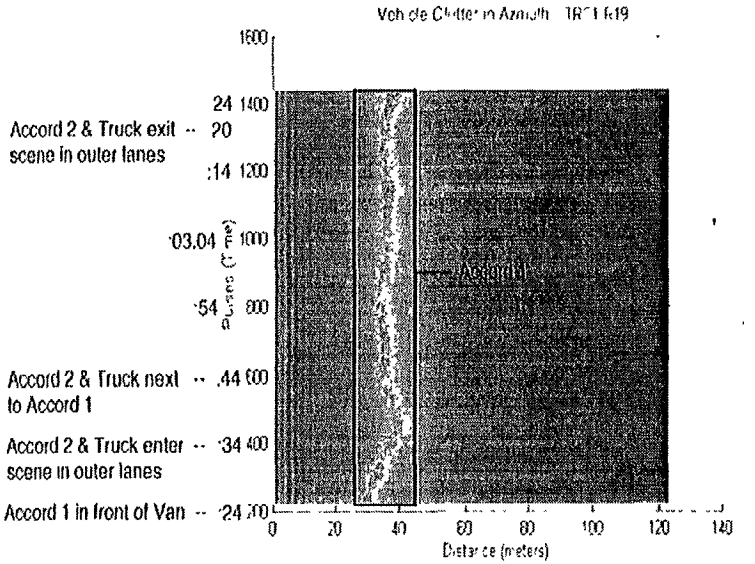

6.8 Vehicle Clutter in Azmuth

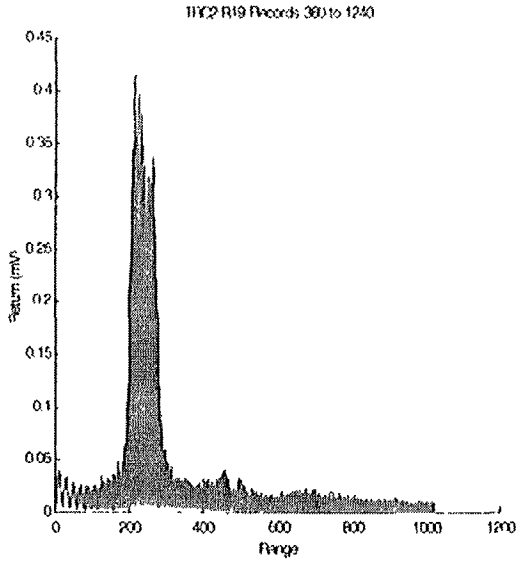

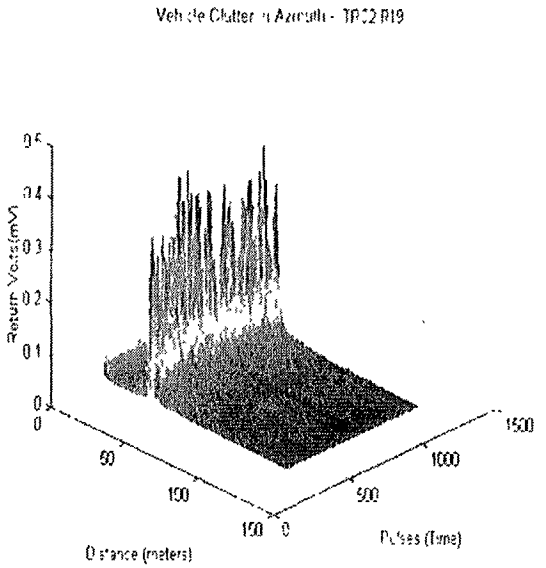

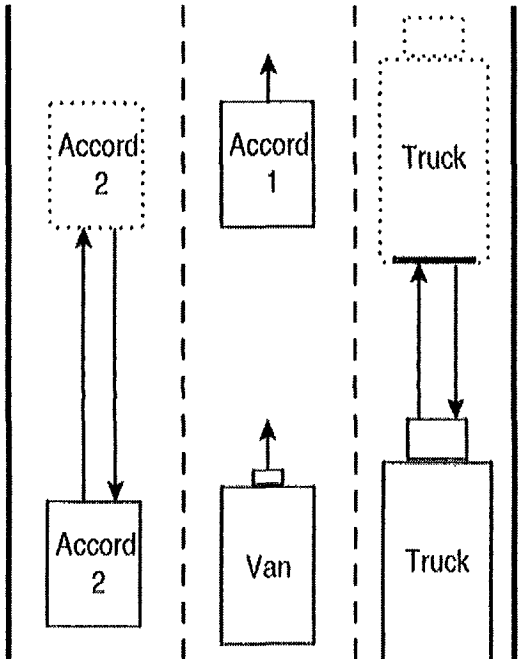

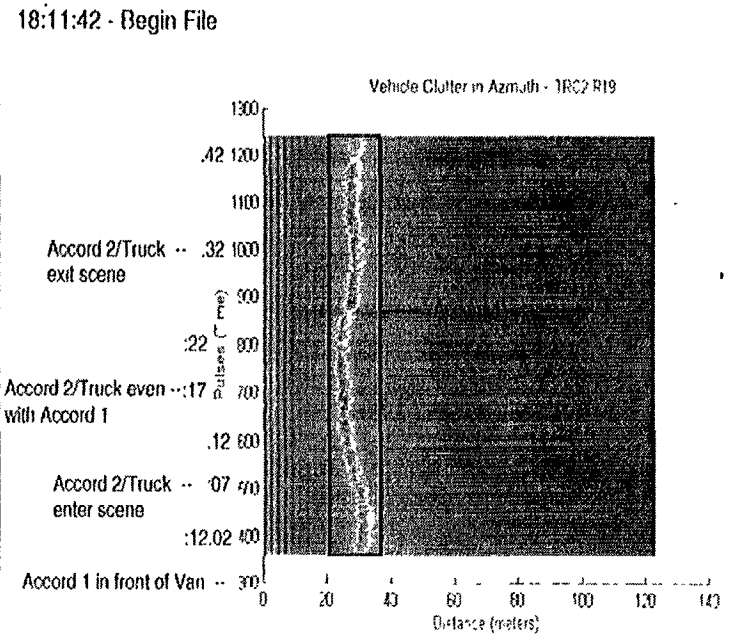

6.8 Vehicle Clutter in Azmuth

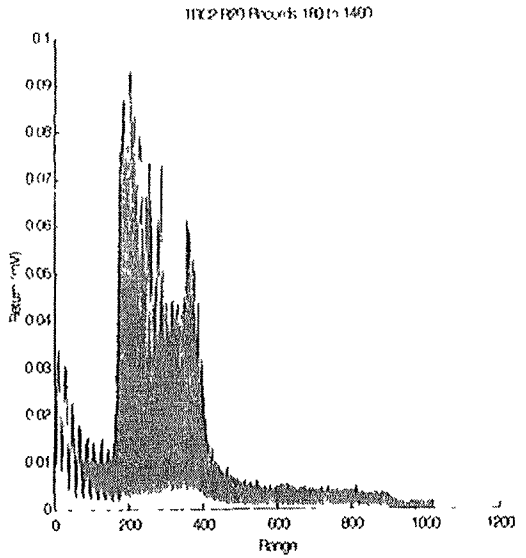

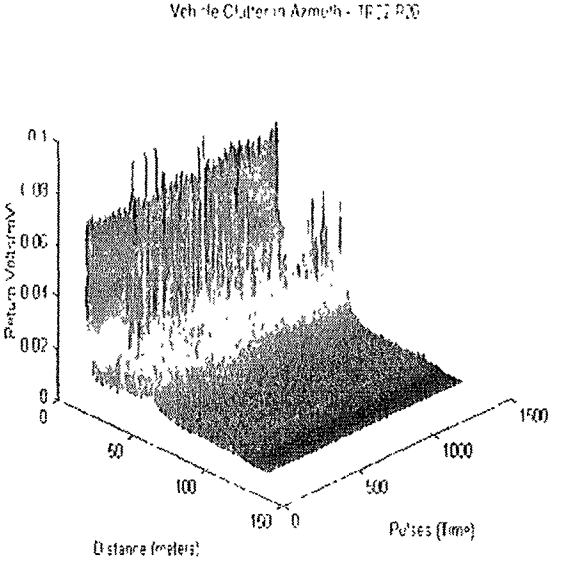

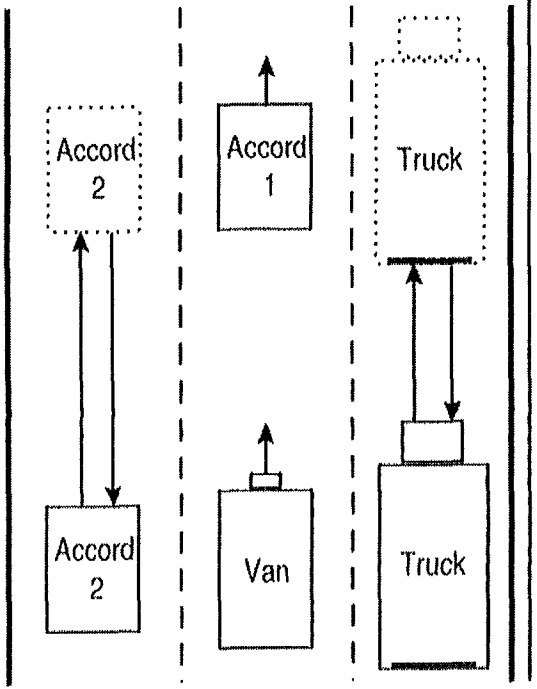

18:22:29 - Begin File

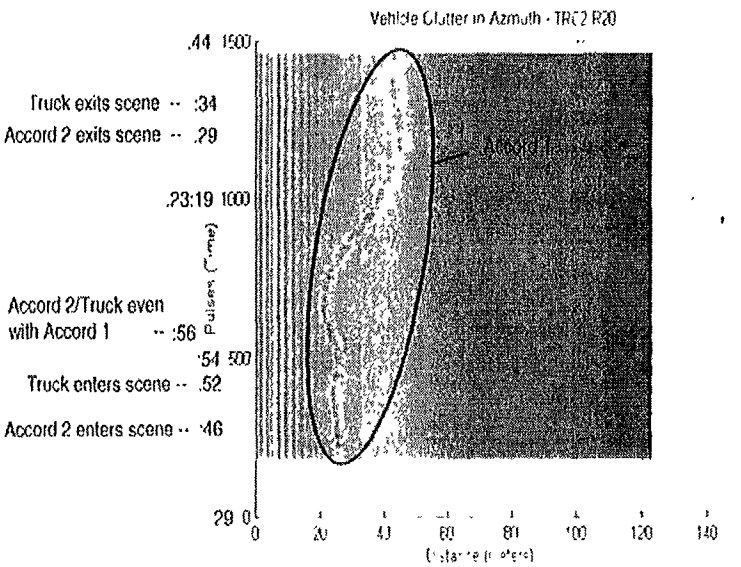

6.8 Vehicle Clutter in Azmuth

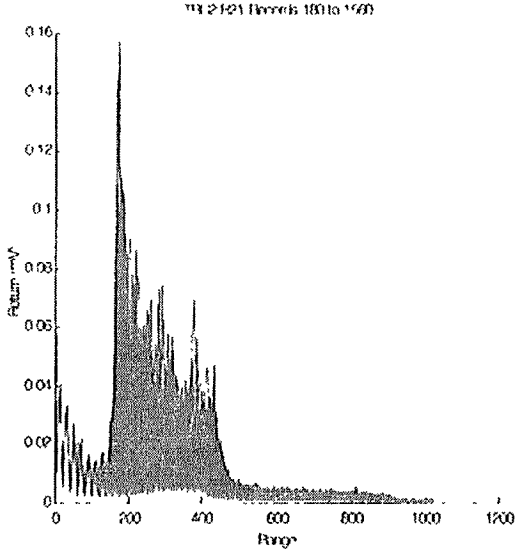

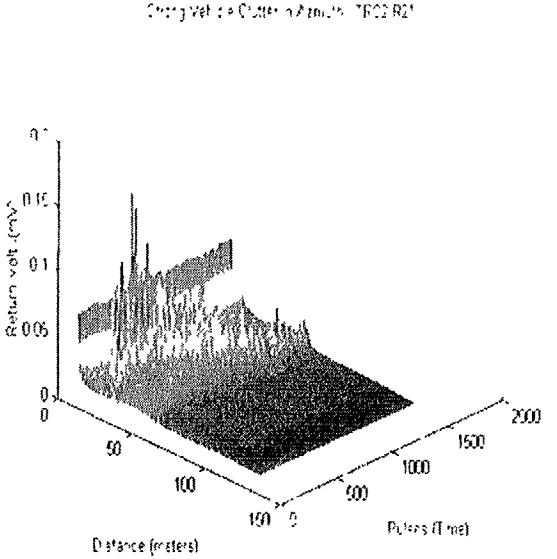

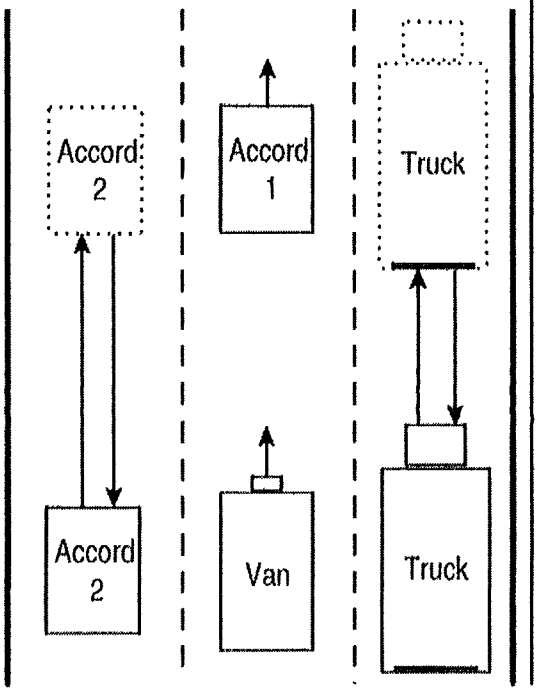

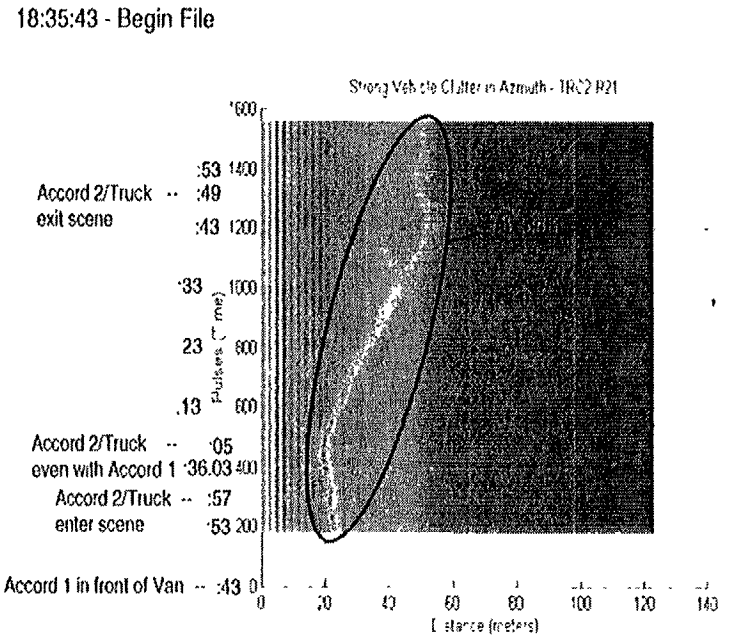

6.9 Merging Traffic - Straight Roadway

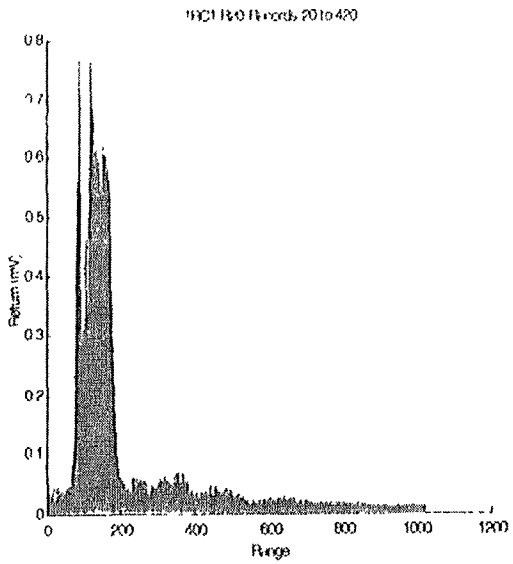

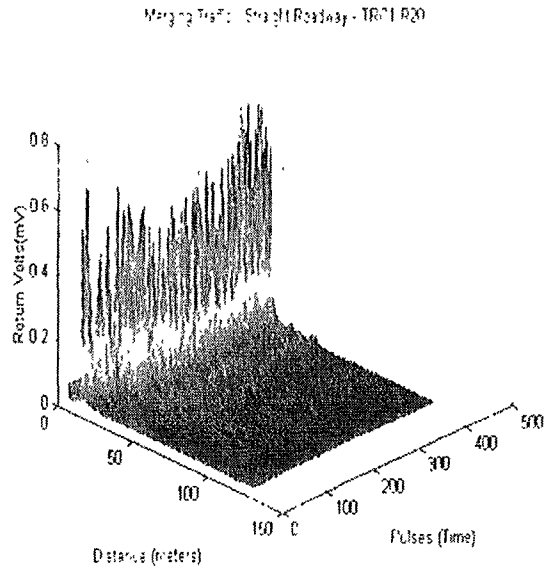

Accord 2 tries to merge between Van & Accord 1, but never does.

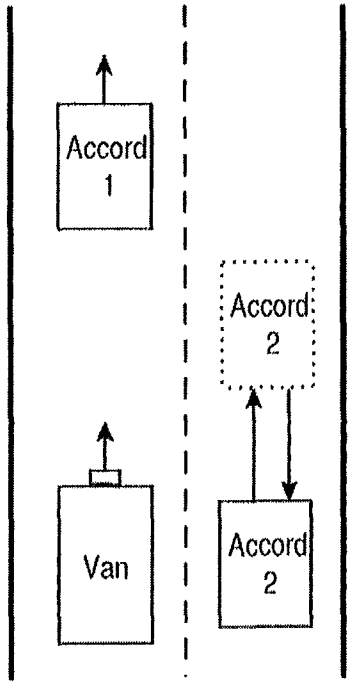

11:52:18 - Begin File

Accord 2 enters and exits scene from right -- :32

Accord 1 in front of Van -- :18

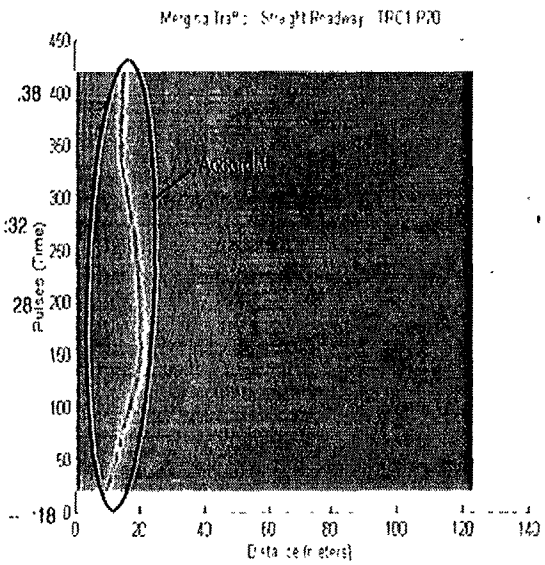

6.10 Vehicle Induced False Alarms - Curved Roadway

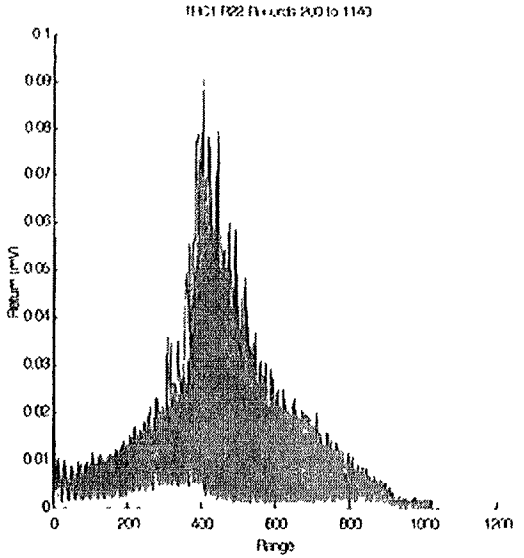

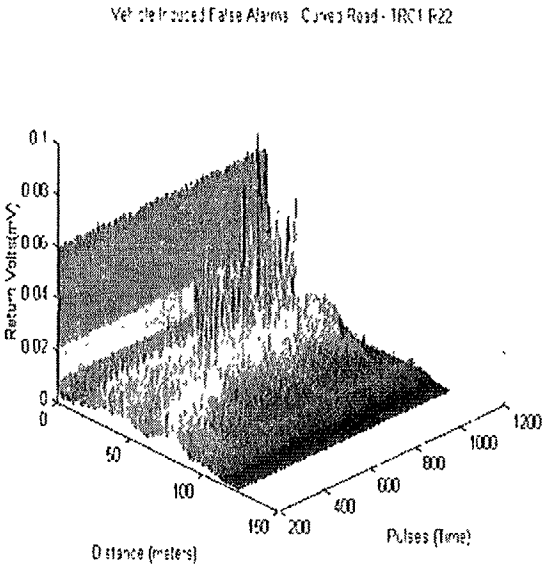

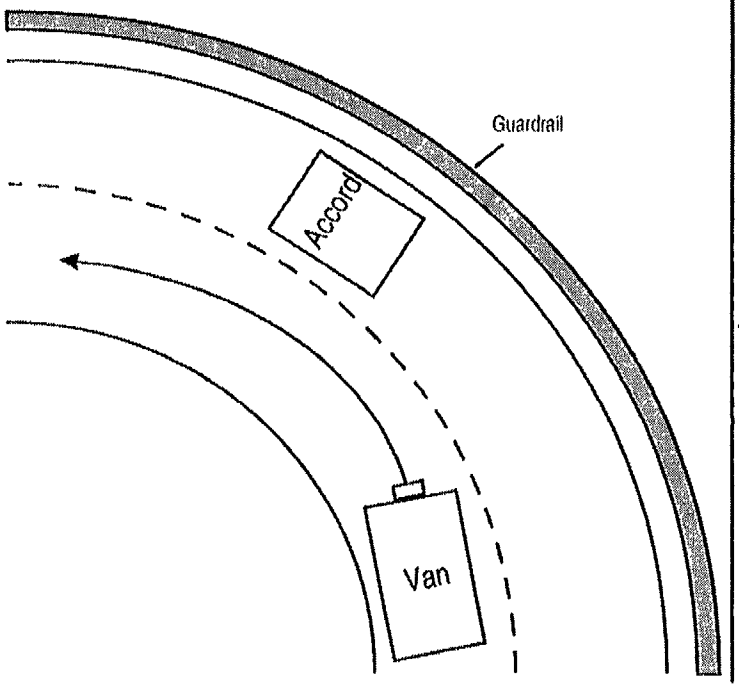

18:09:52 - Begin File

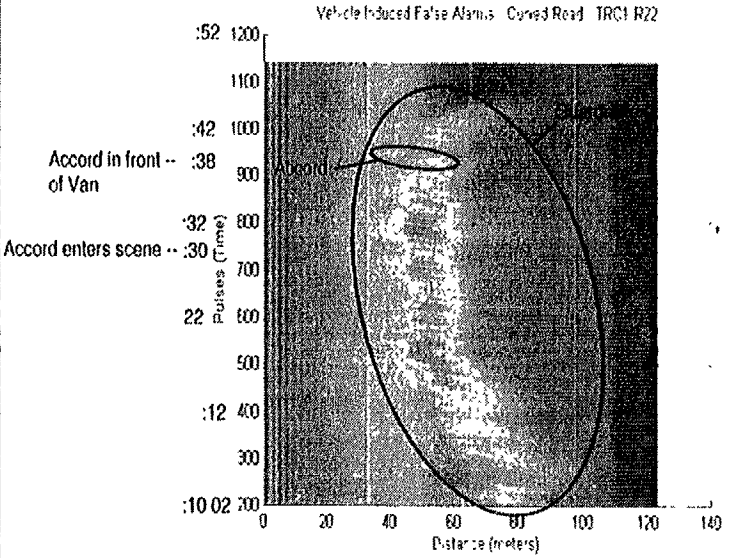

6.10 Vehicle Induced False Alarms - Curved Roadway

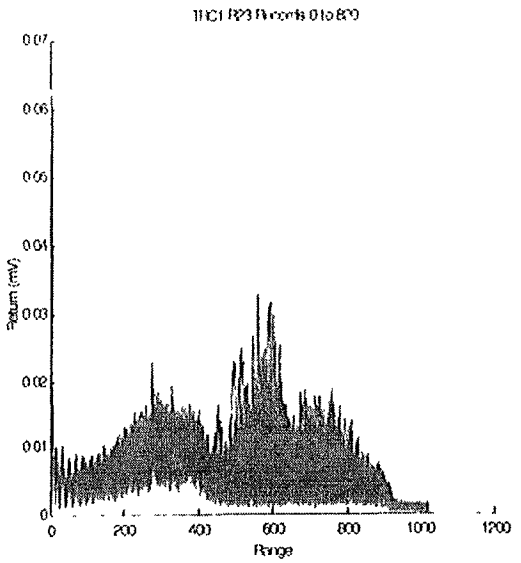

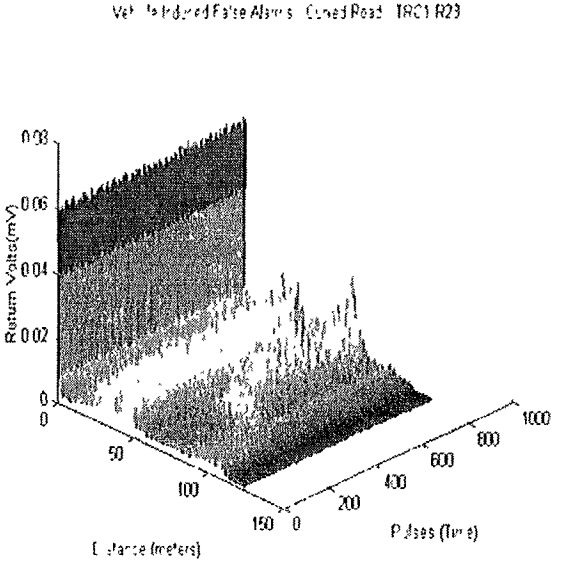

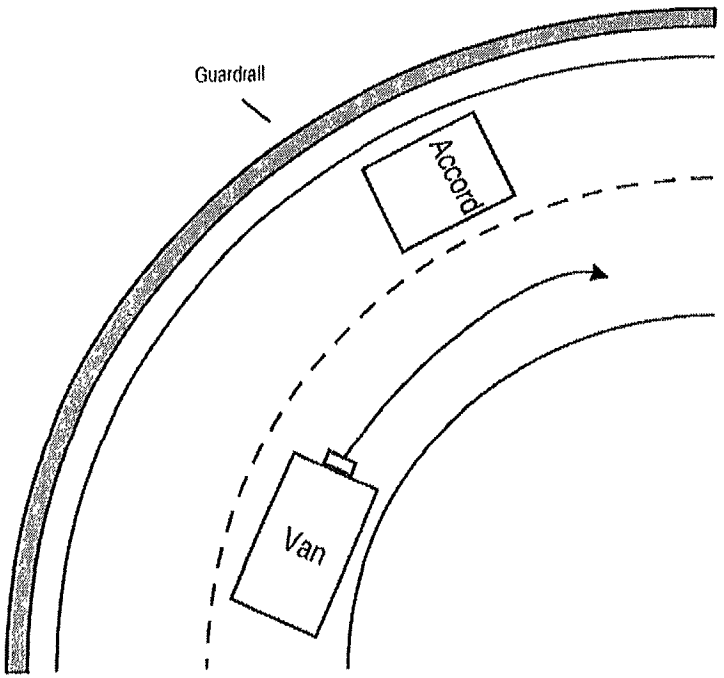

17:57:02 -Begin File

Accord in front of --
Van on curve
Accord enters scene --

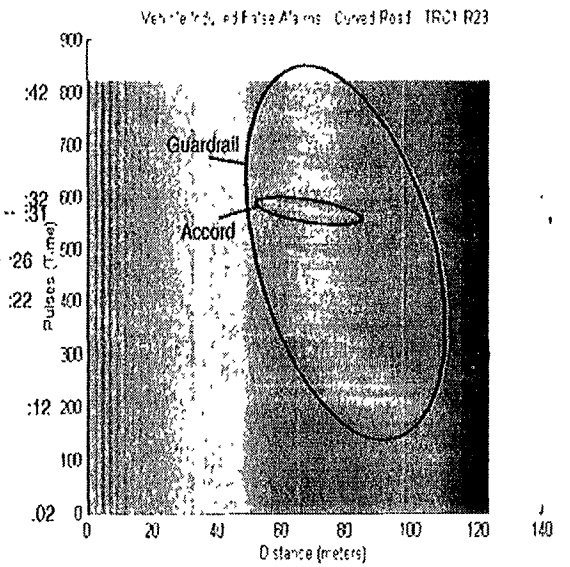

6.10 Vehicle Induced False Alarms - Curved Roadway

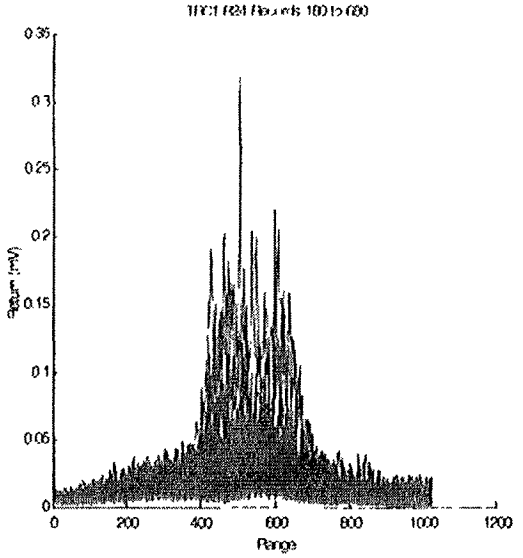

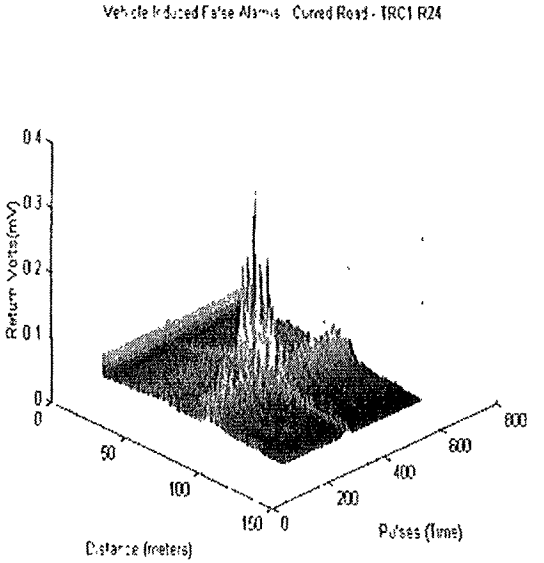

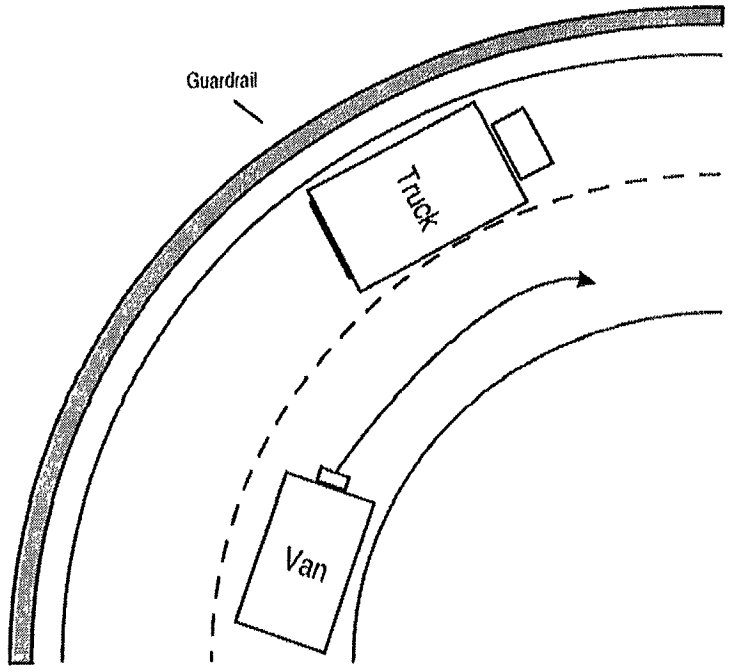

13:57:16 - Begin File

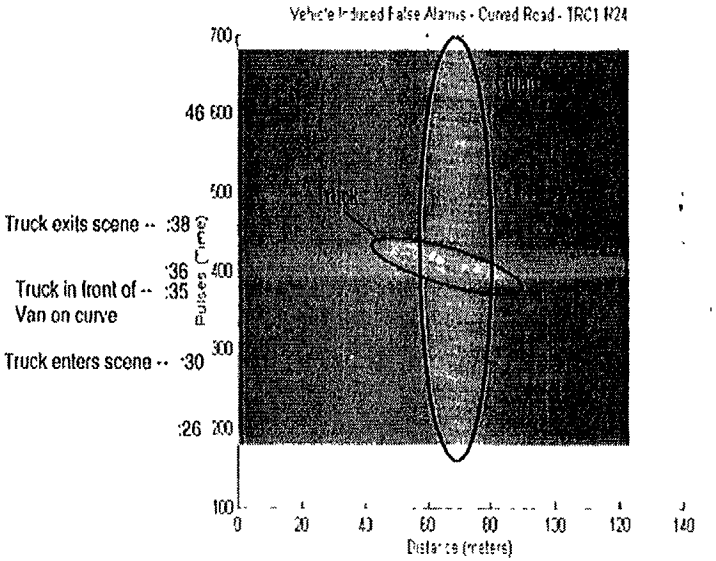

6.10 Vehicle Induced False Alarms - Curved Roadway

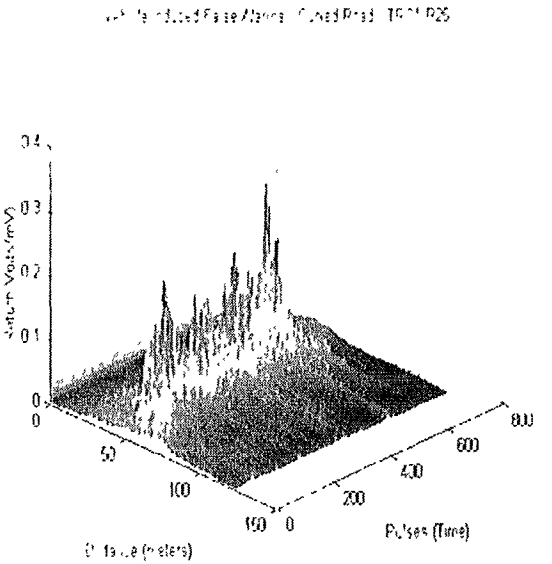

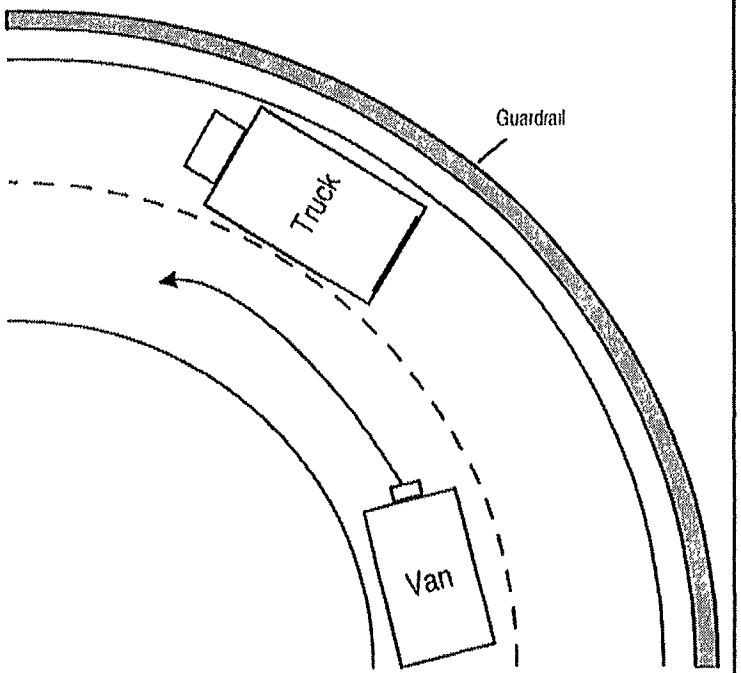

13:45:35 - Begin File

Truck in front of -- :00
Van on curve
Truck enters scene -- :55

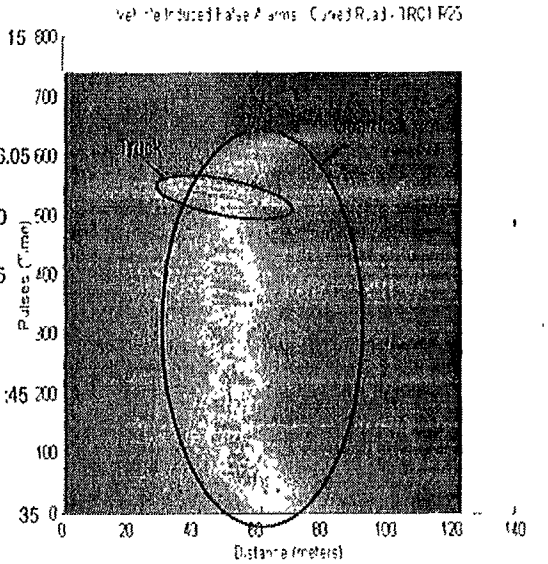

6.10 Vehicle Induced False Alarms - Curved Roadways

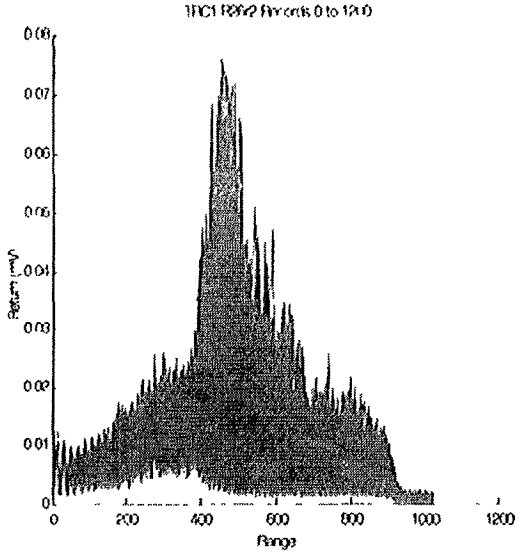

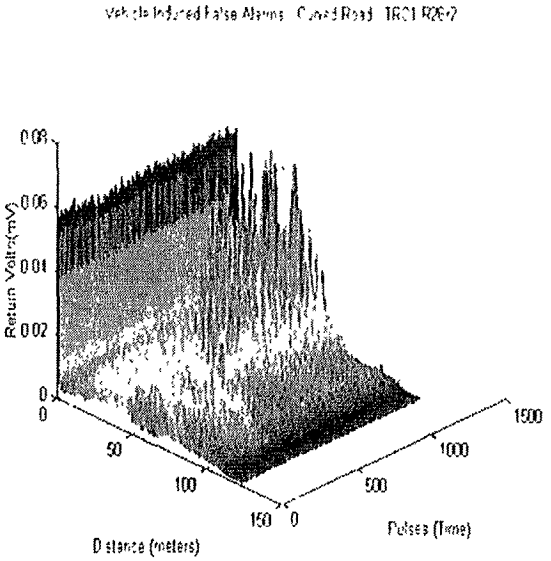

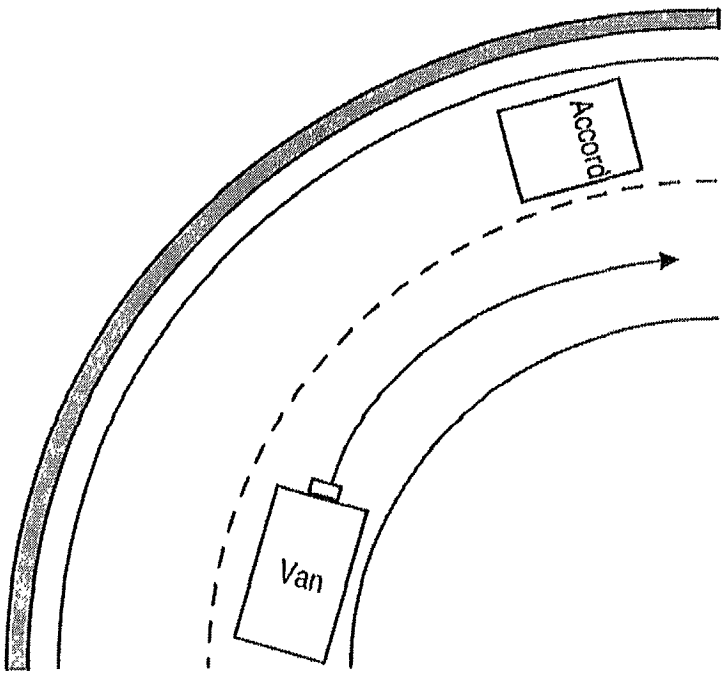

19:02:41 -Begin File

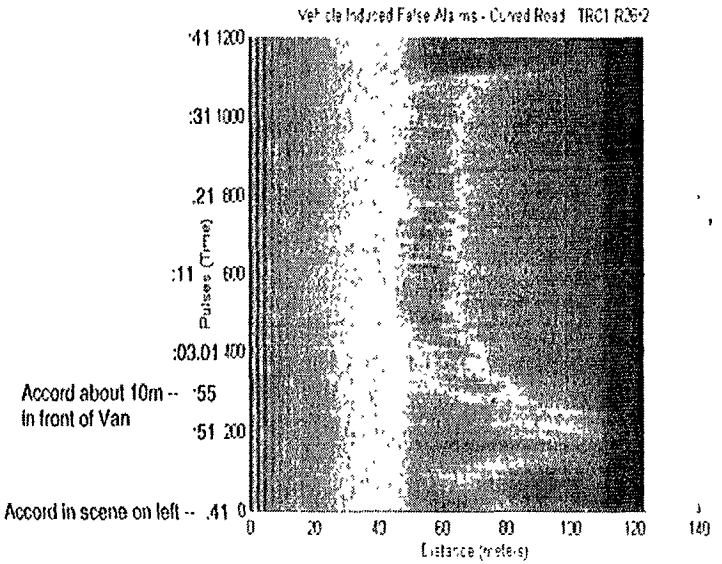

6.10 Vehicle Induced False Alarms - Curved Roadways

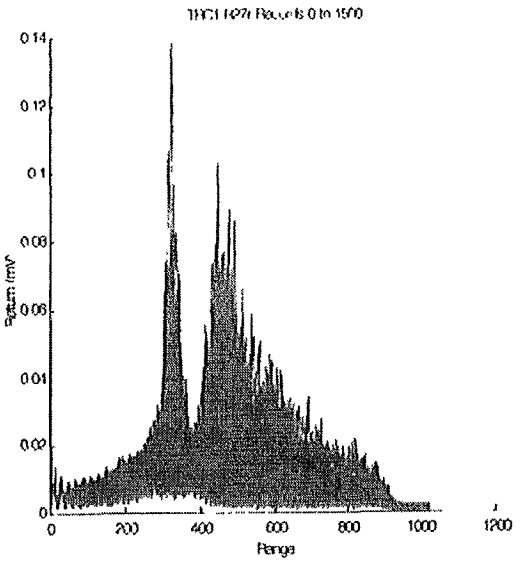

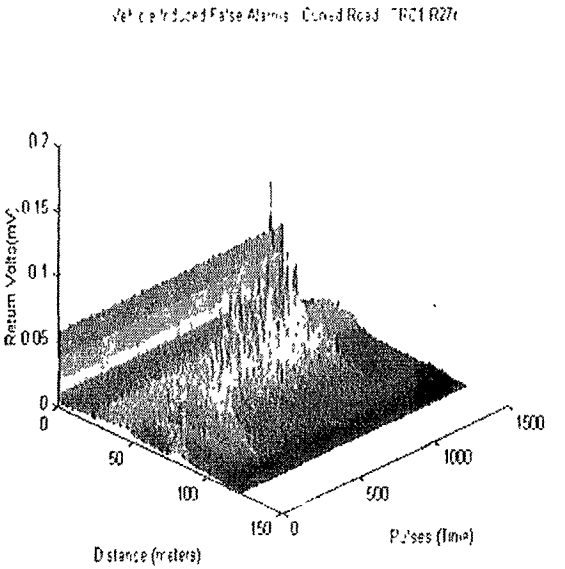

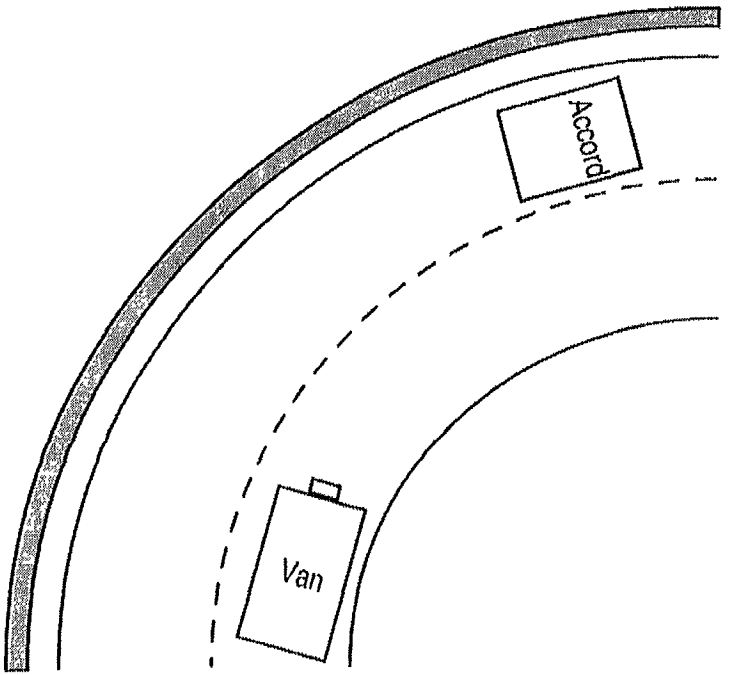

19:06:40 - Begin File

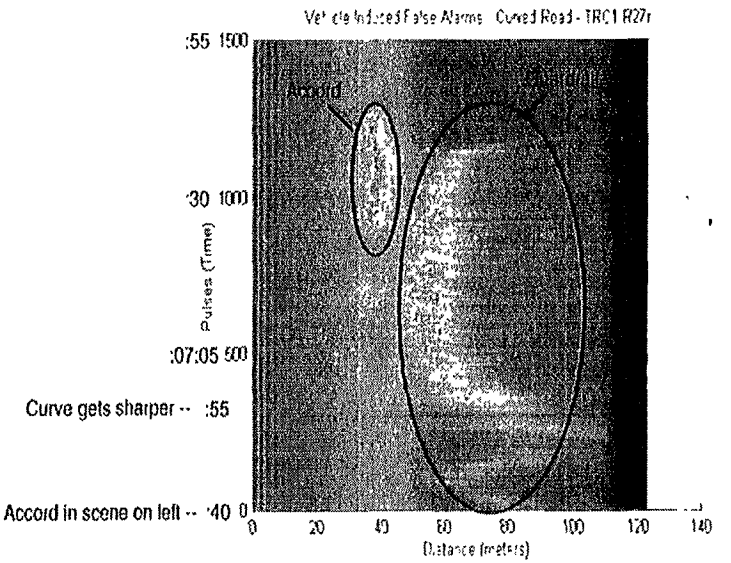

6.10 Vehicle Induced False Alarms - Curved Roadways

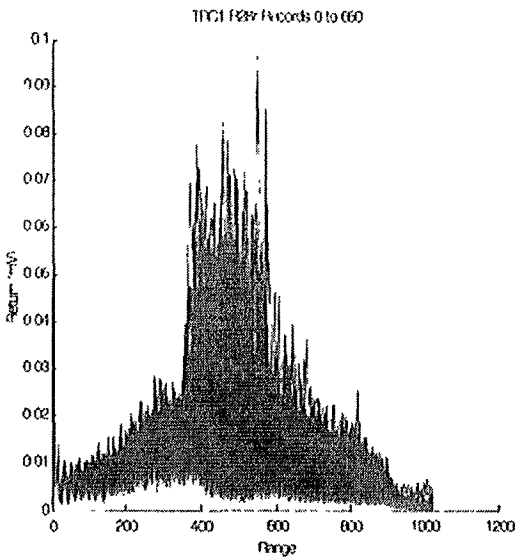

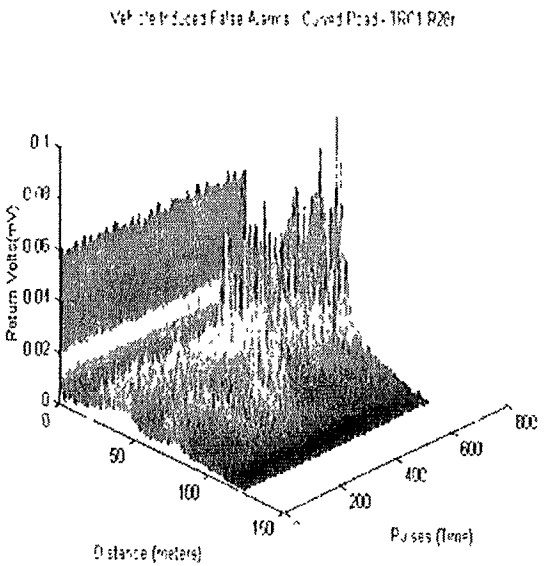

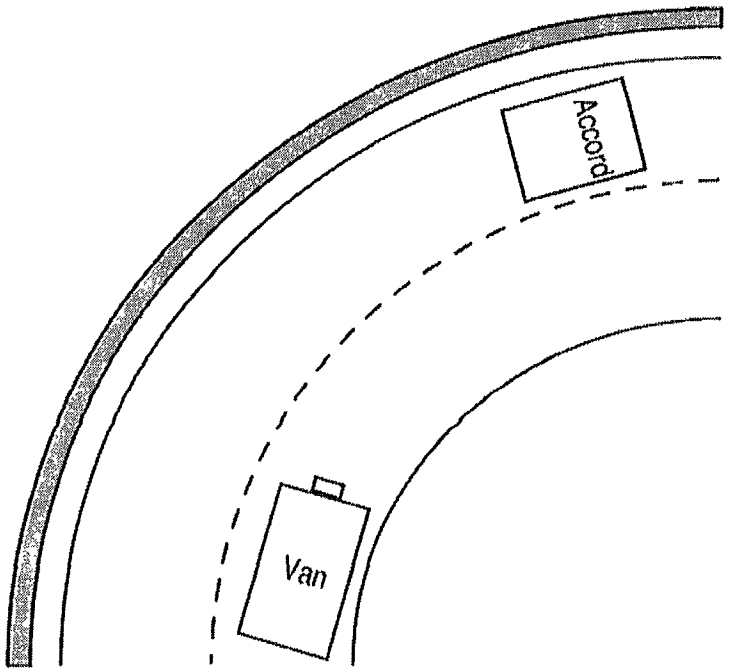

19:13:06 - Begin File

Curve gets sharper --

Accord in scene on left --

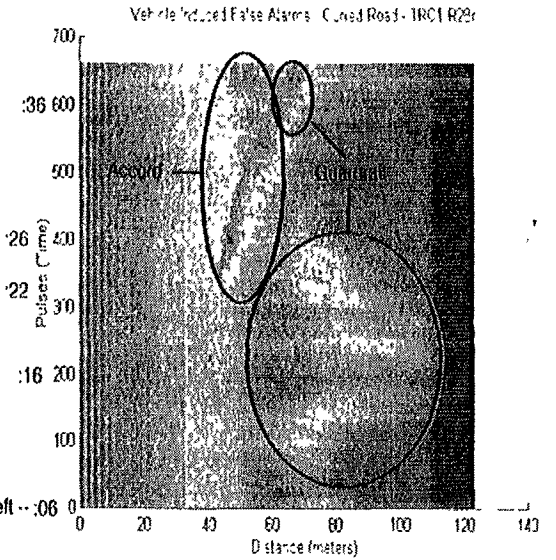

6.10 Vehicle Induced False Alarms - Curved Roads

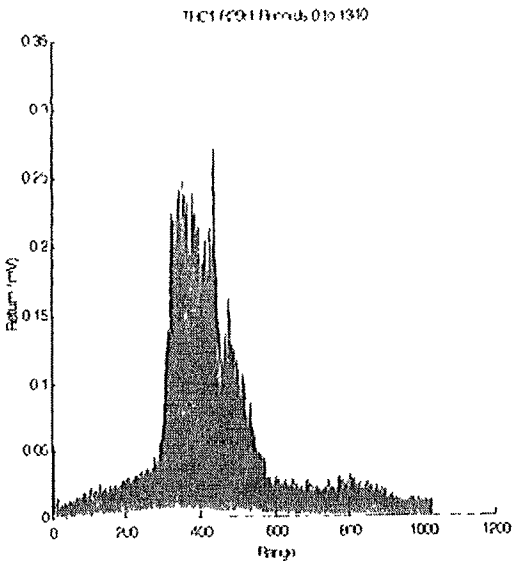

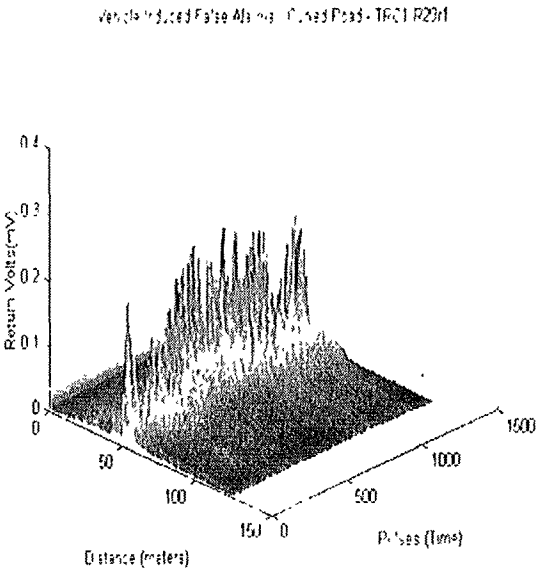

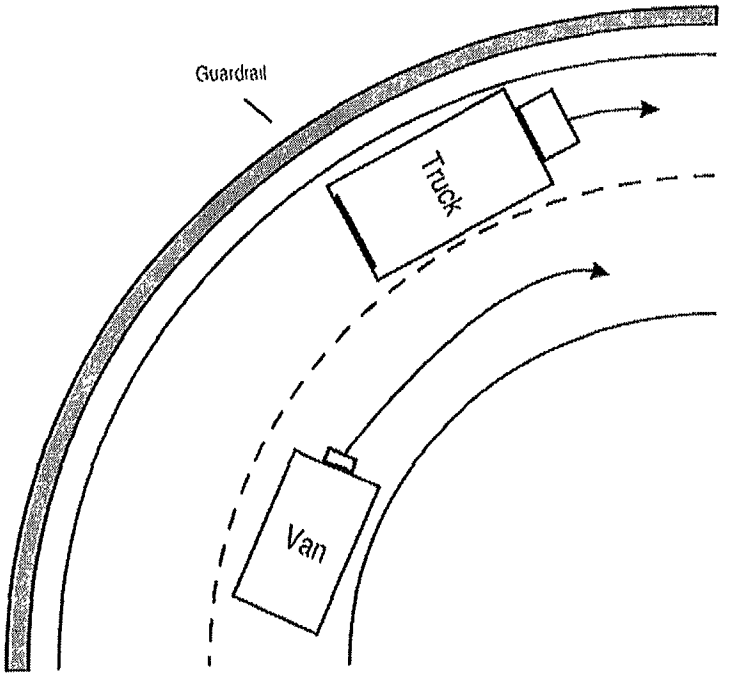

14:18:11 - Begin File

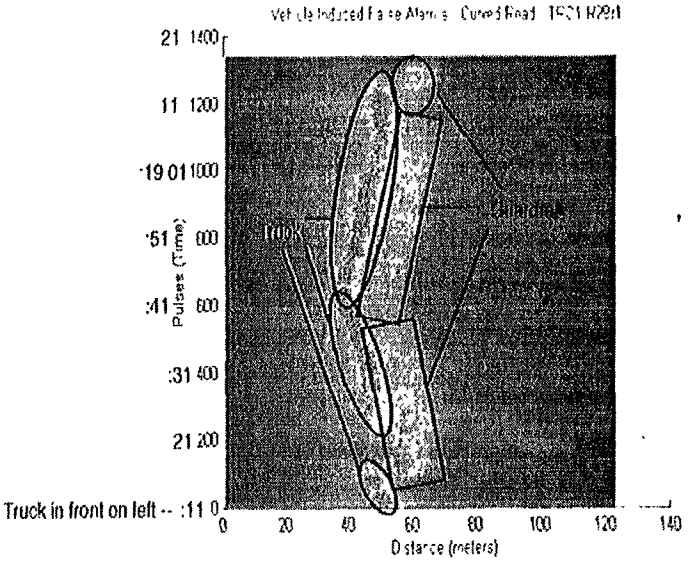

6.10 Vehicle Induced False Alarms - Curved Roads

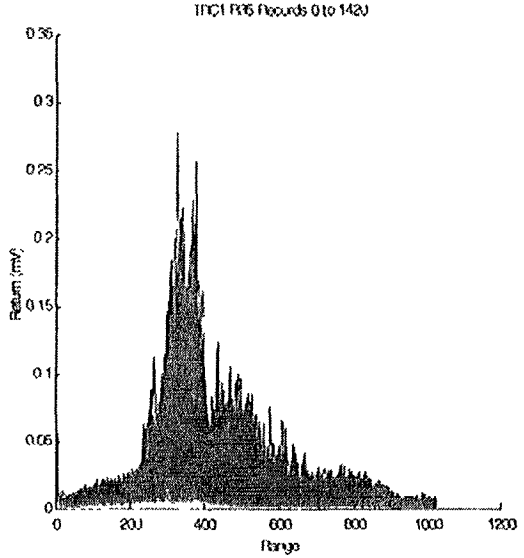

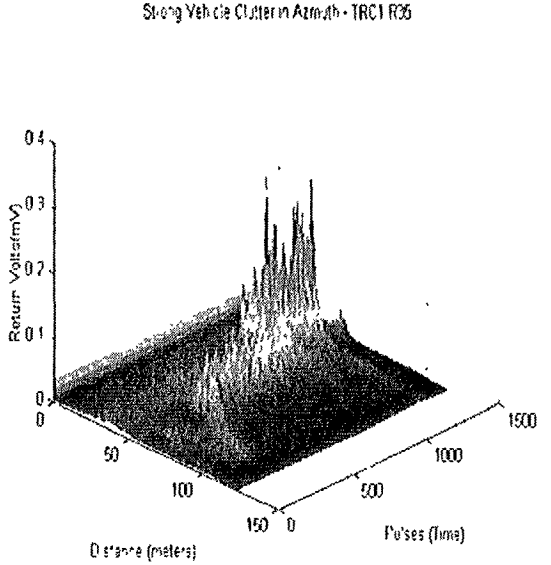

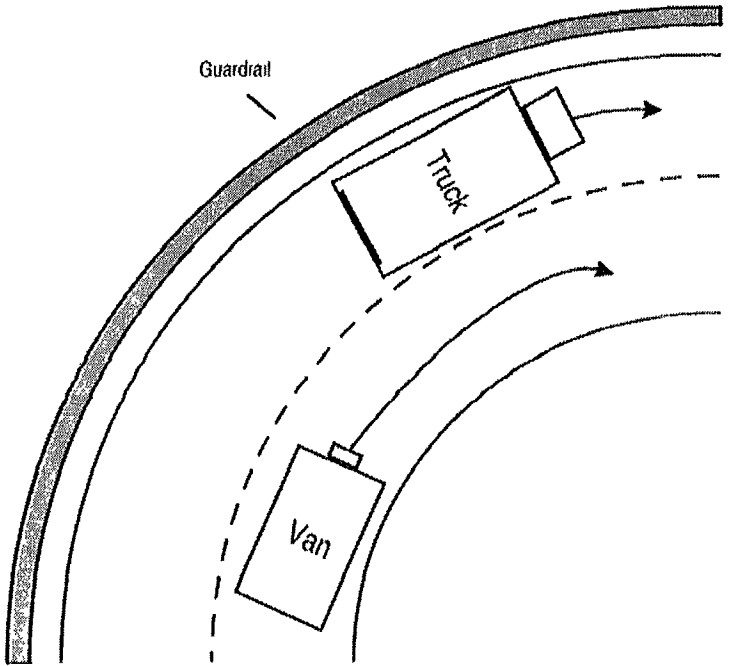

14:11:48 - Begin File

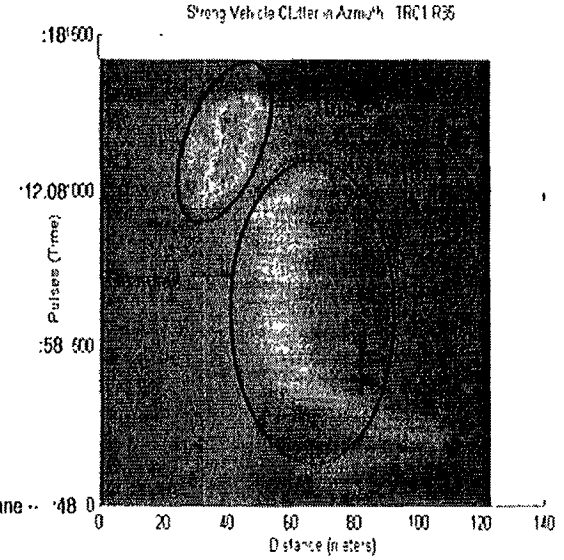

Truck in scene in left lane

6.10 Vehicle Induced False Alarms - Curved Roads

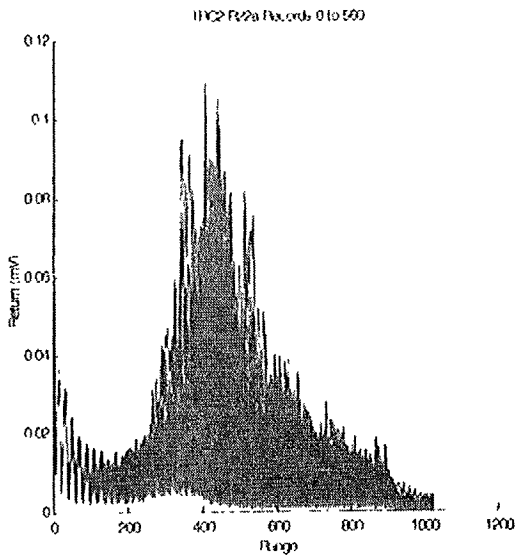

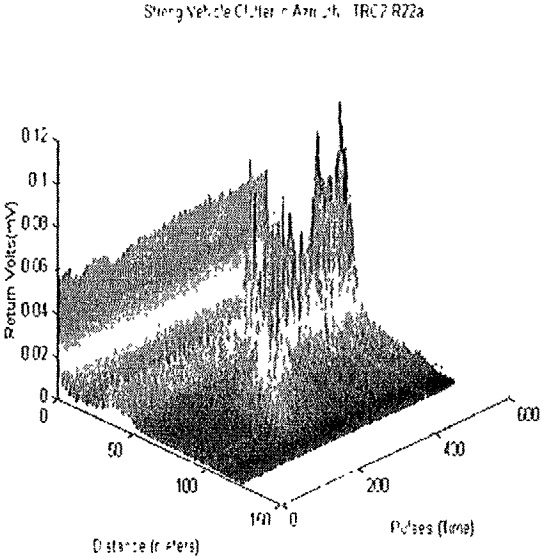

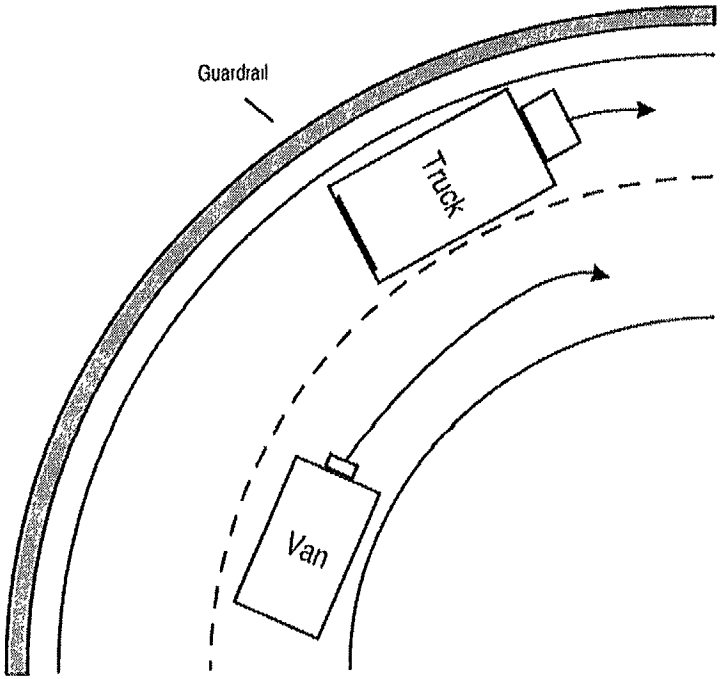

14:11:48 - Begin File

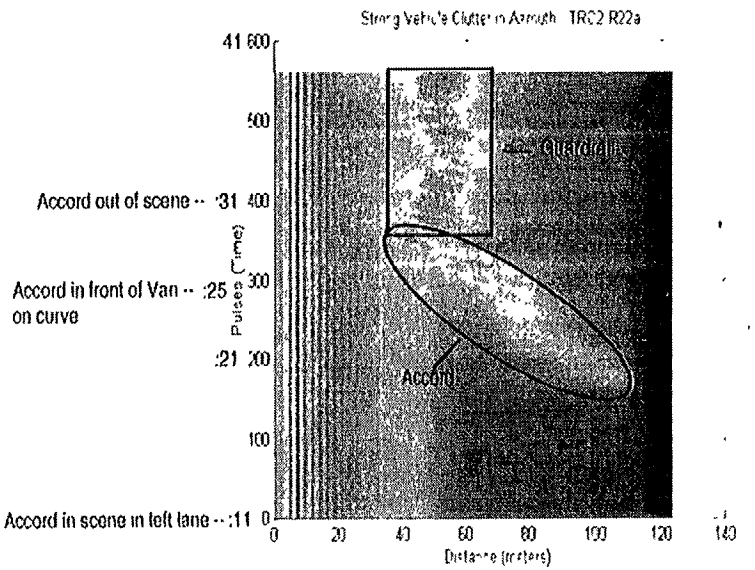

6.10 Vehicle Induced False Alarms - Curved Roads

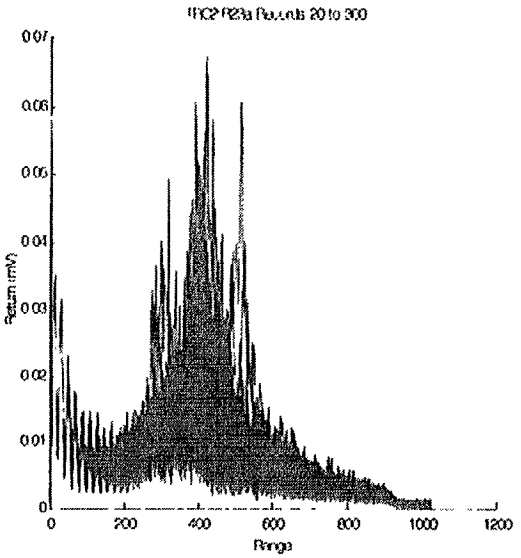

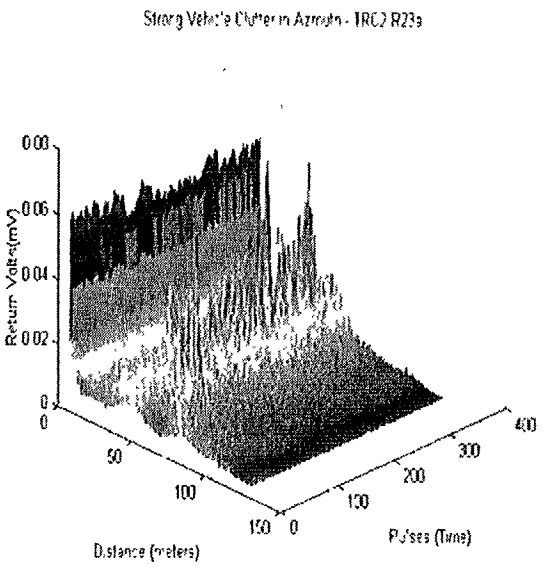

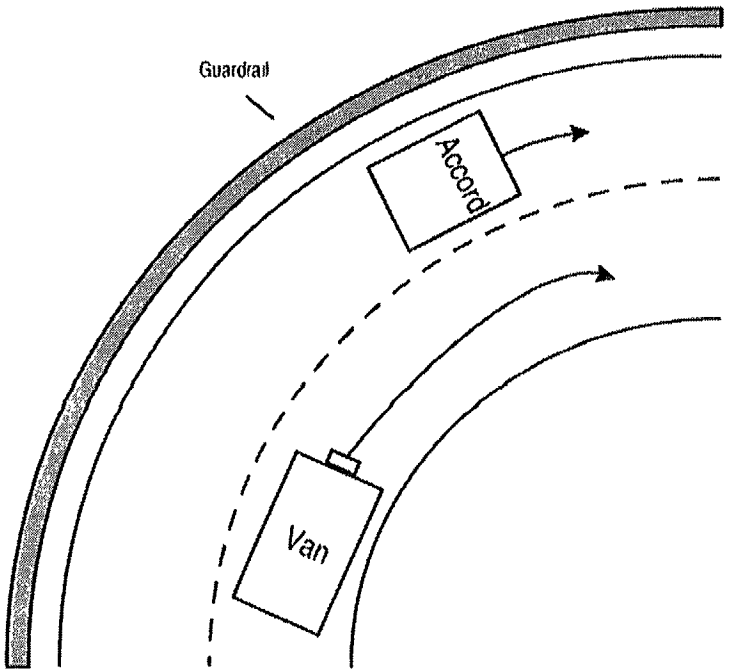

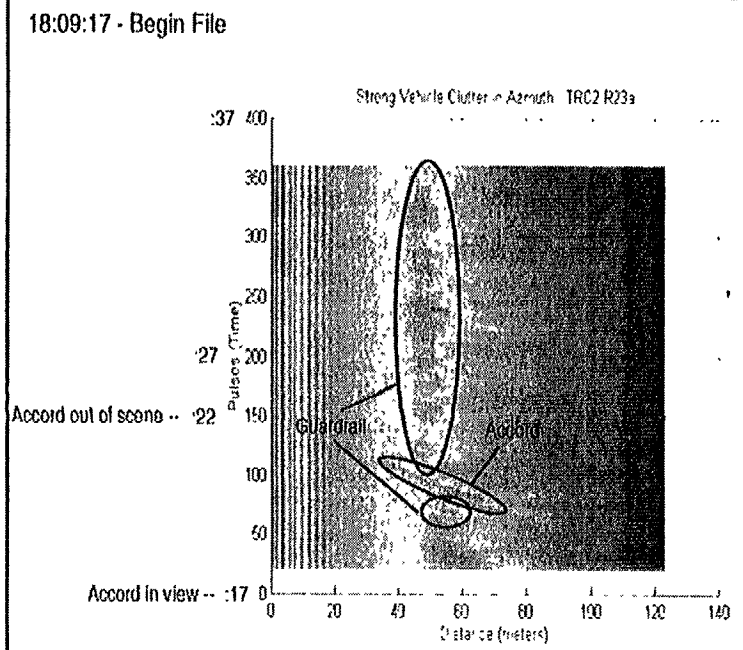

6.10 Vehicle Induced False Alarms - Curved Roads

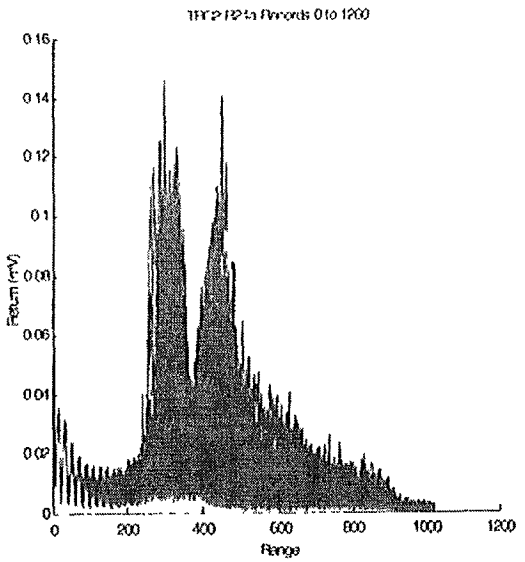

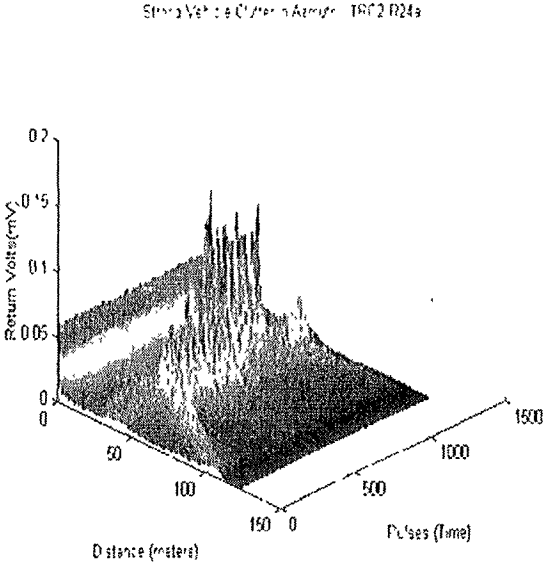

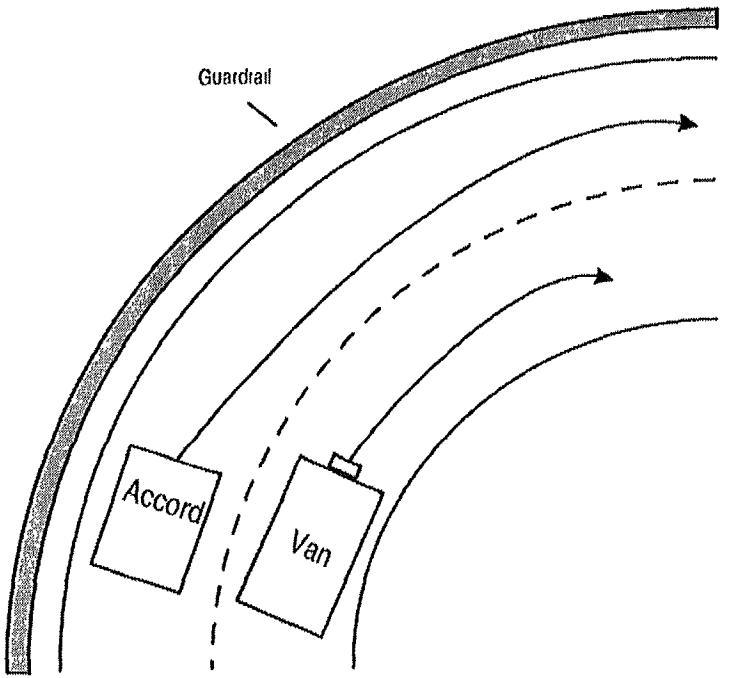

18:31:20 - Begin File

Accord enters scene --

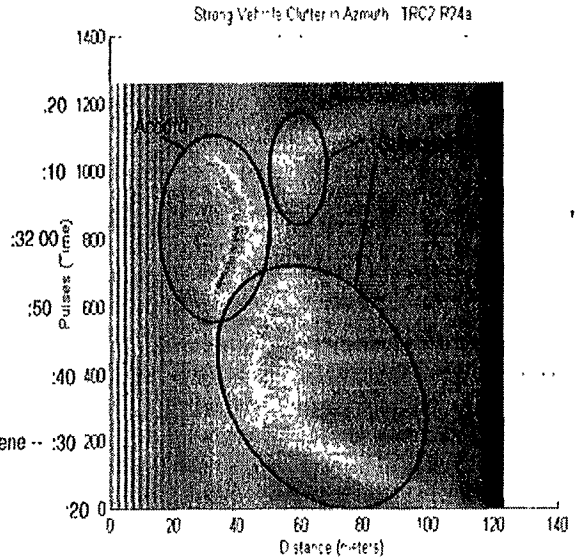

6.10 Vehicle Induced False Alarms - Curved Roads

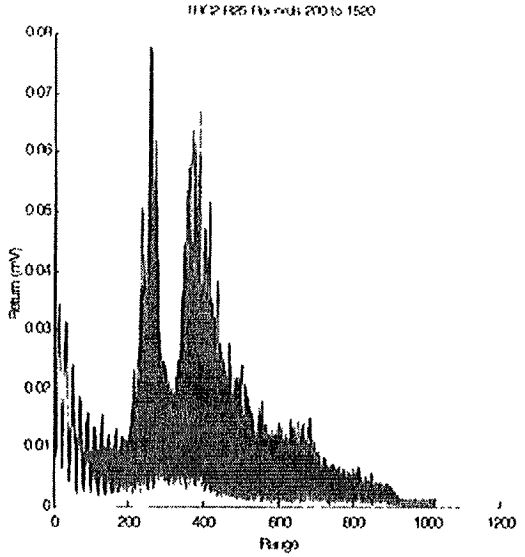

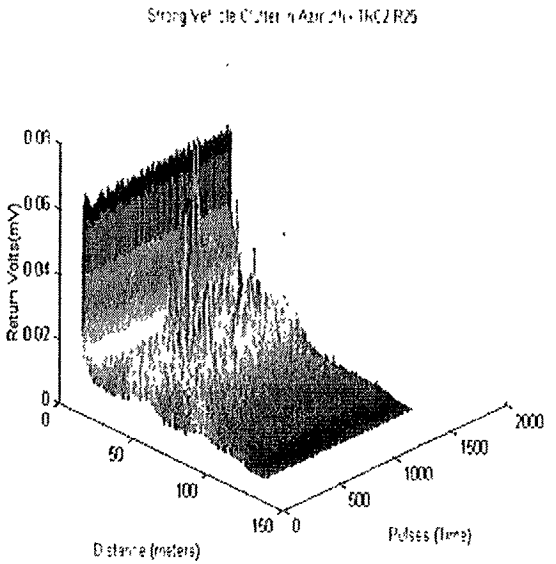

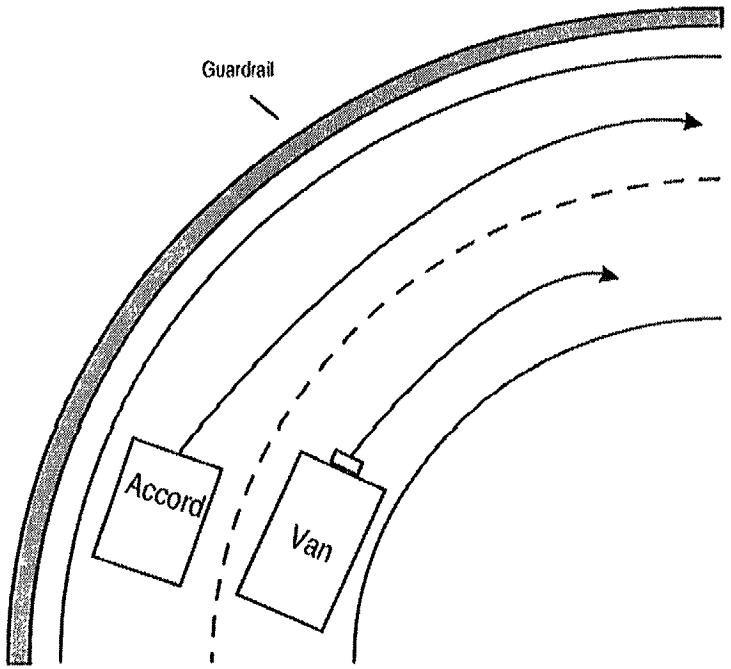

18:44:25 - Begin File

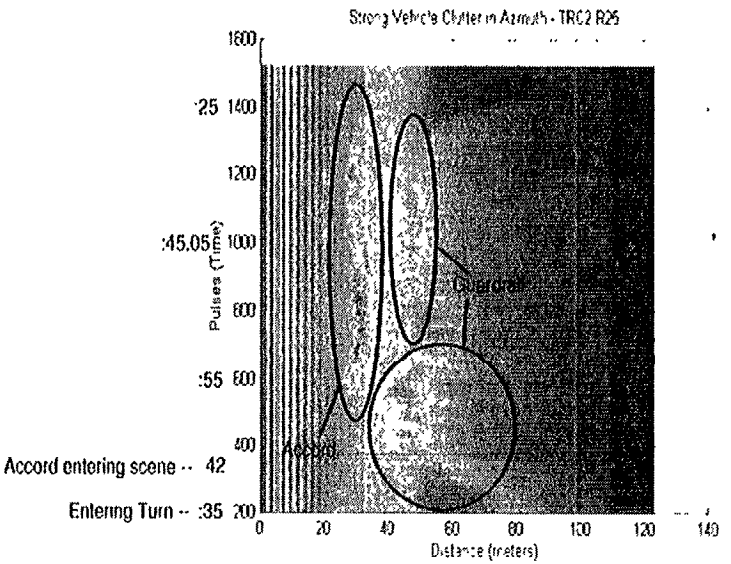

6.10 Vehicle Induced False Alarms - Curved Roads

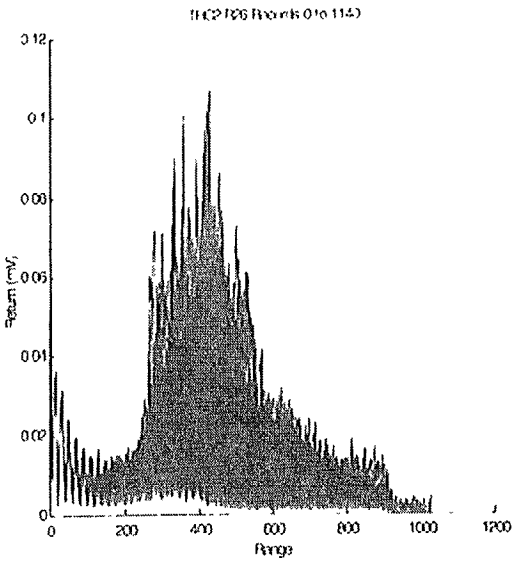

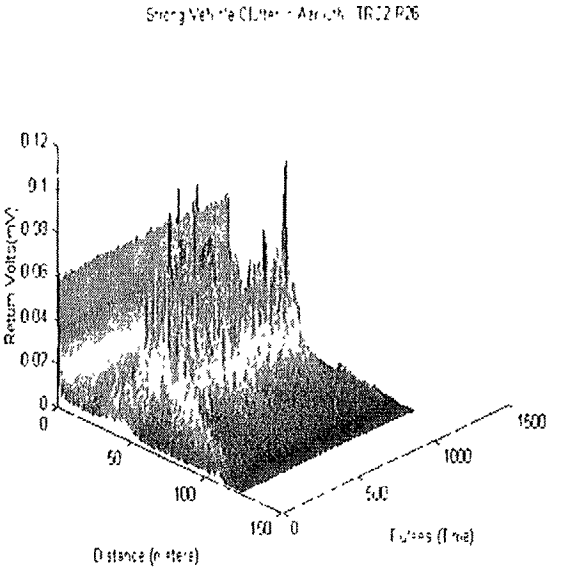

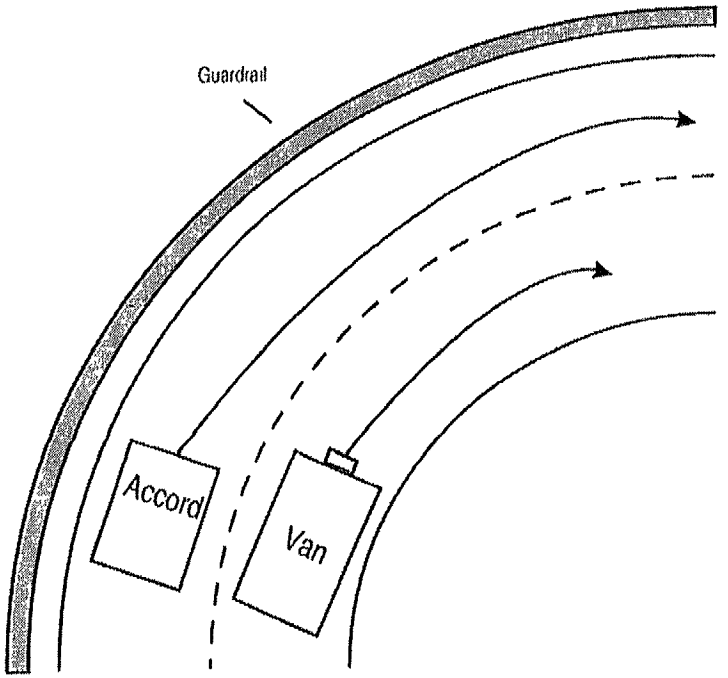

18:37:07 - Begin File

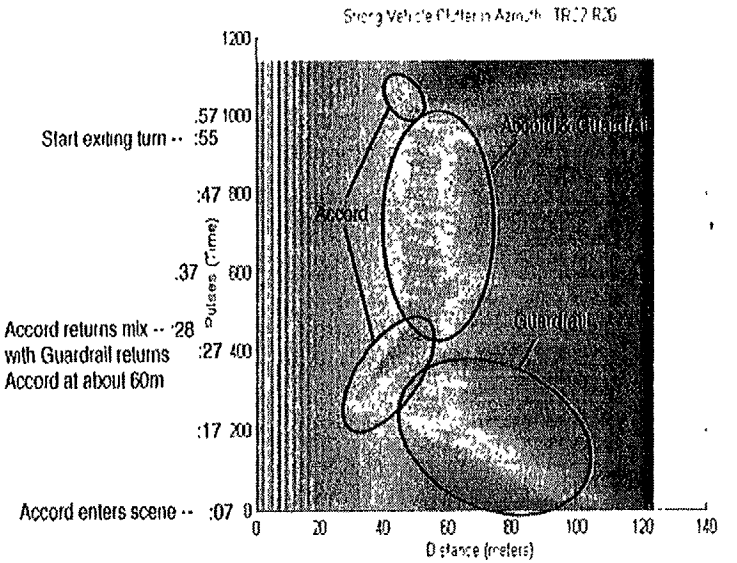

6.10 Vehicle Induced False Alarms - Curved Roads

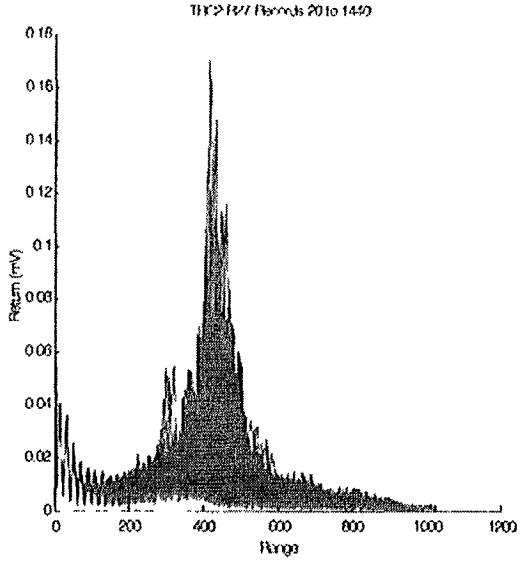

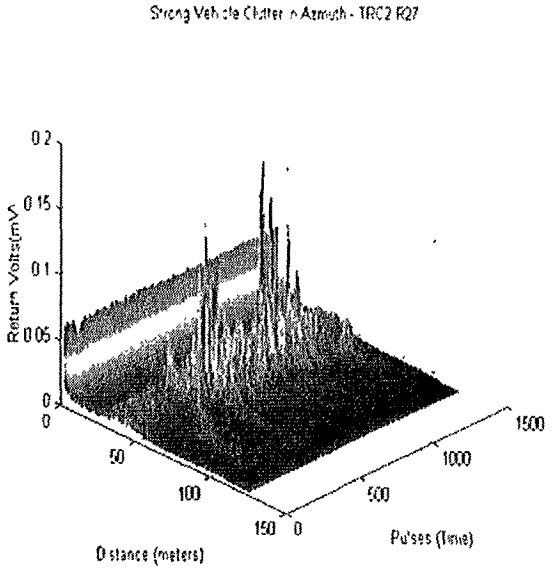

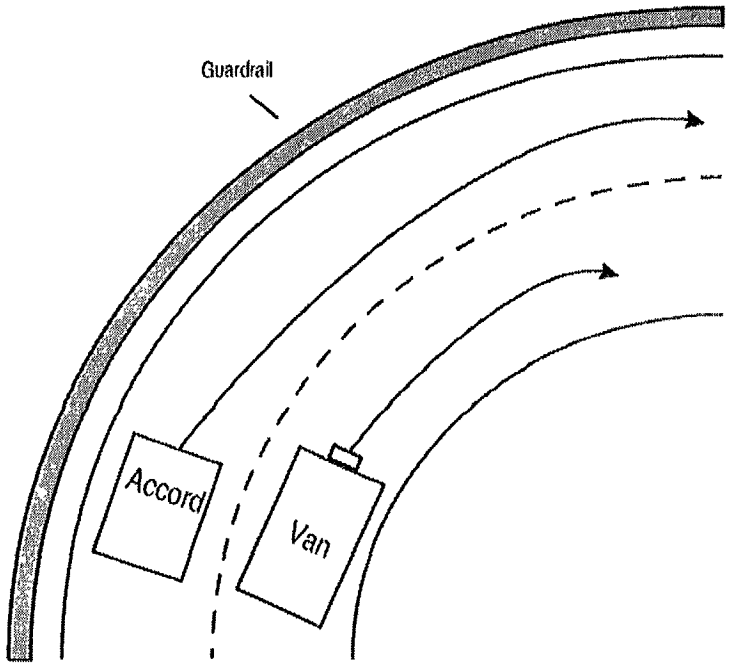

18:50:39 - Begin File

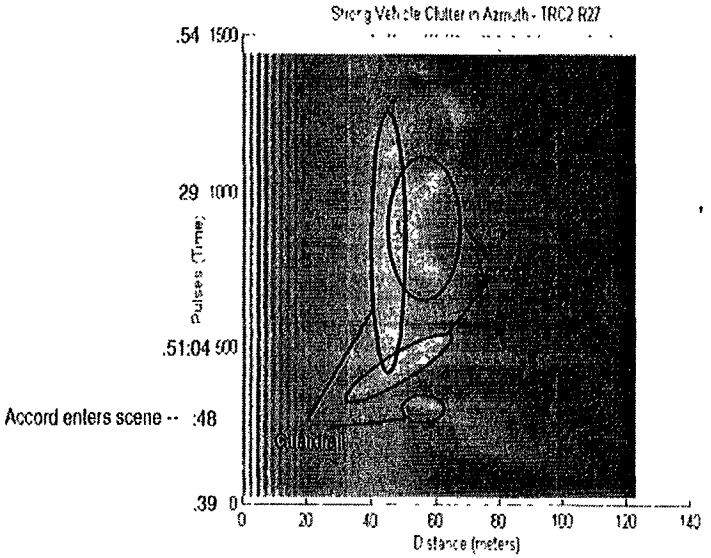

6.11 Tracking Through A Curve

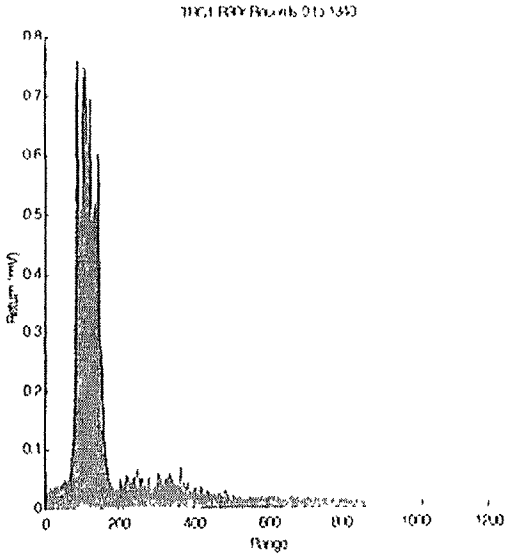

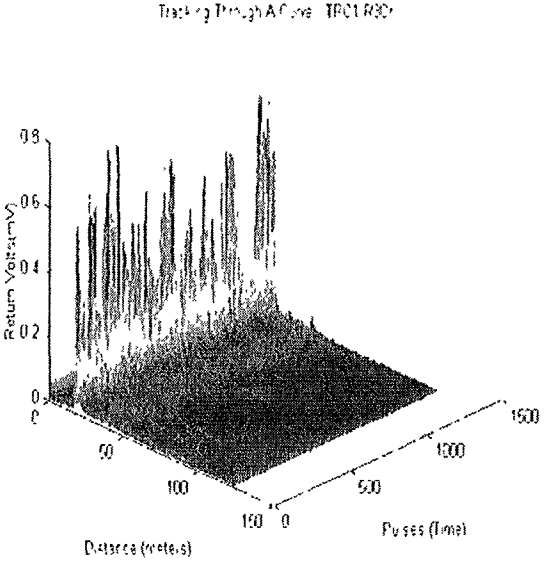

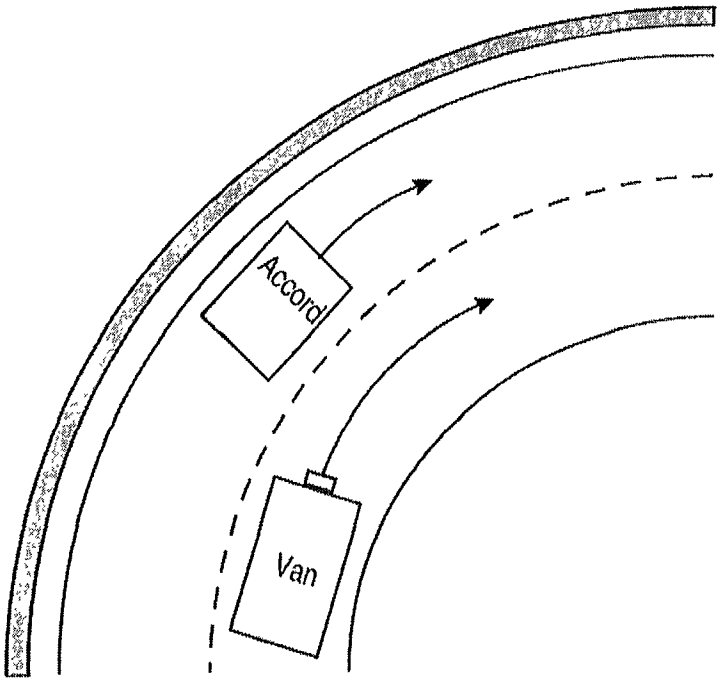

19:16:56 - Begin File

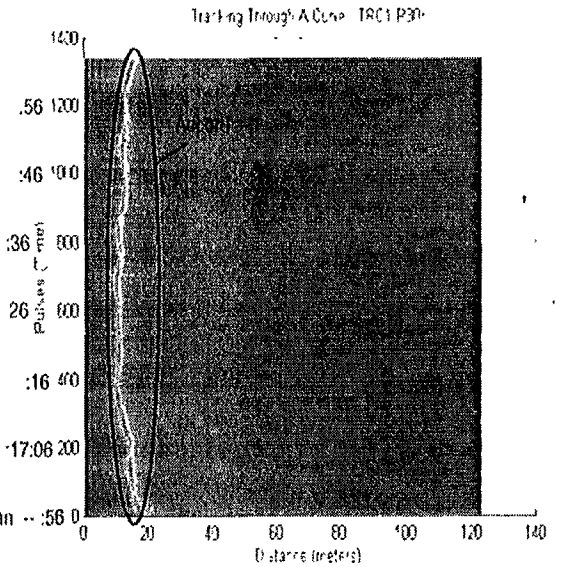

6.11 Tracking Through A Curve

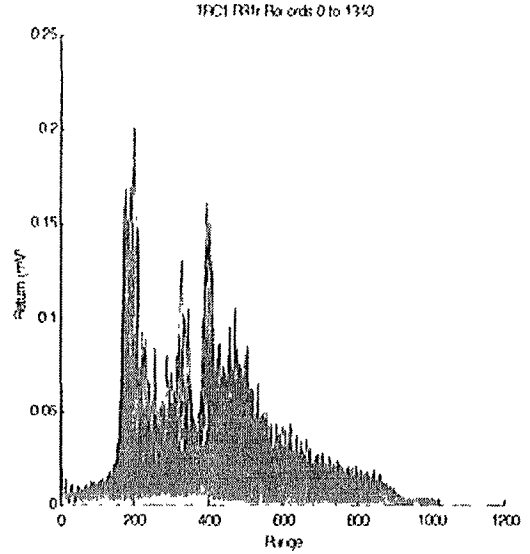

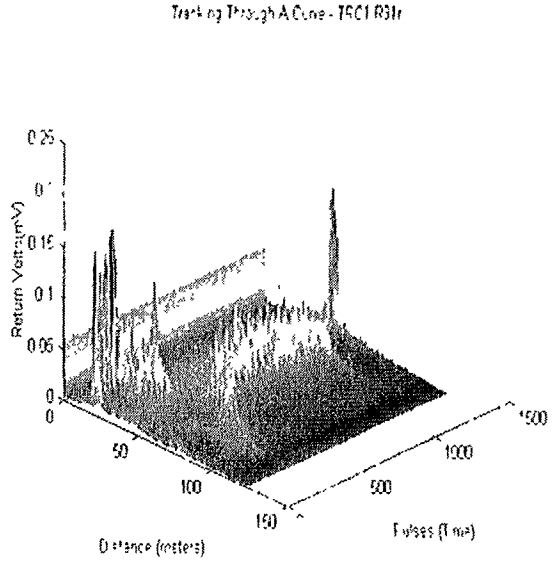

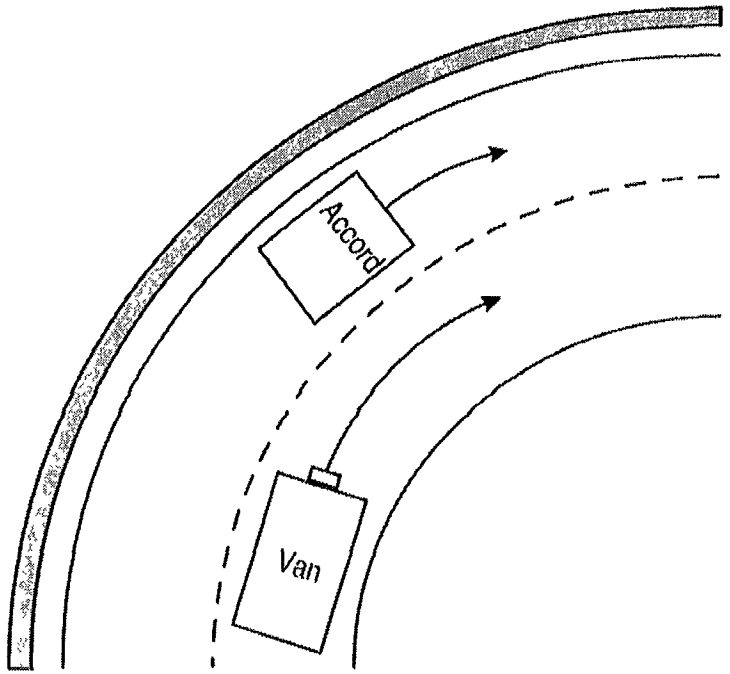

19:20:12 - Begin File

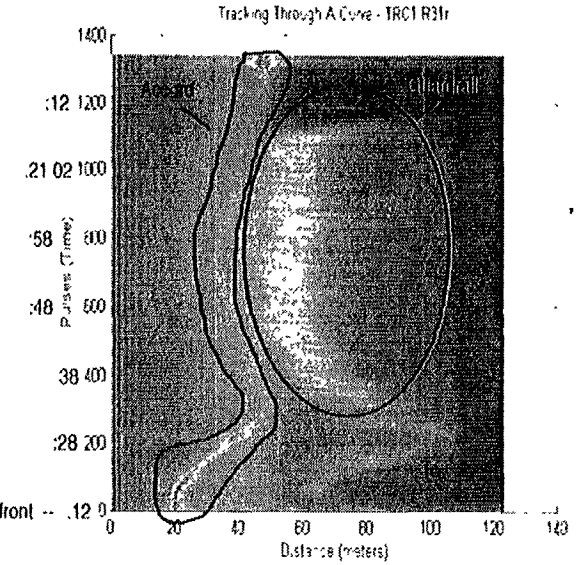

Accord 40m in front of Van

6.11 Tracking Through A Curve

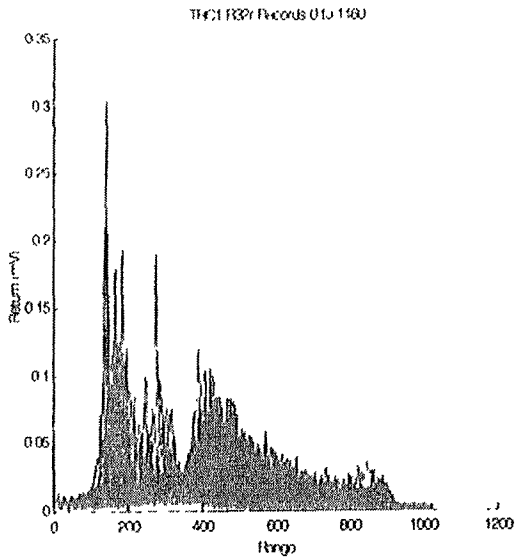

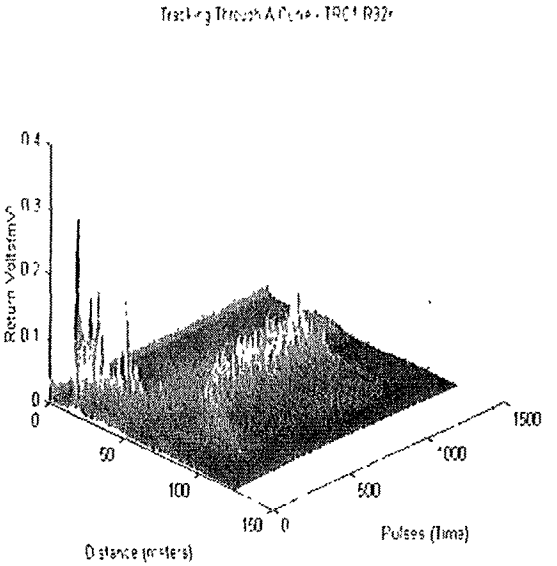

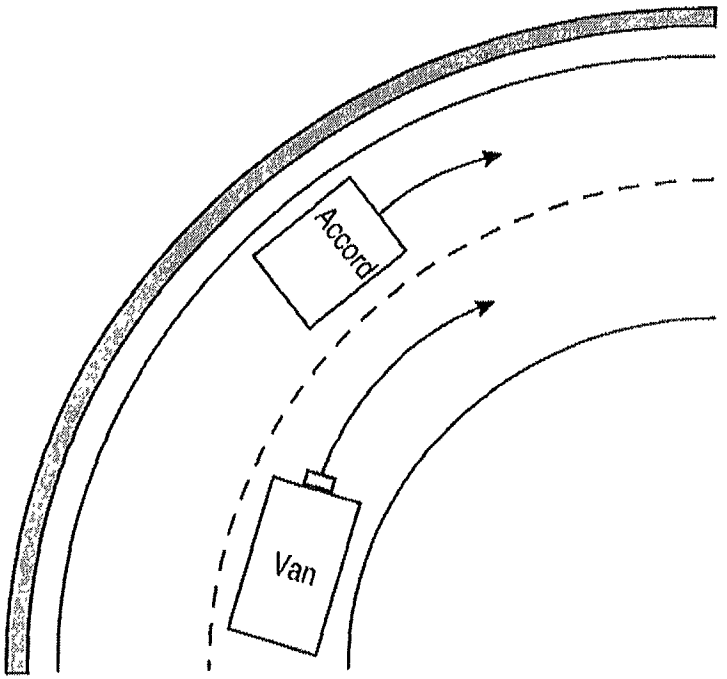

19:23:16 - Begin File

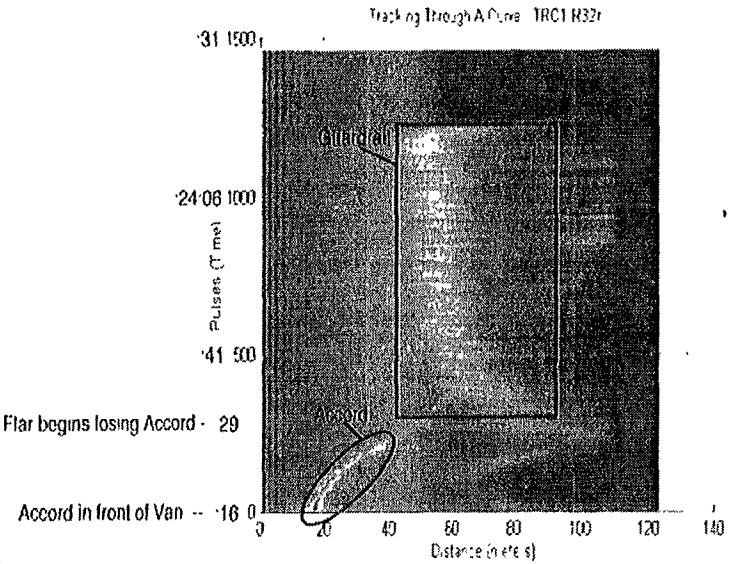

6.12 Vehicle Clutter in Azmuth - Curved Roadway

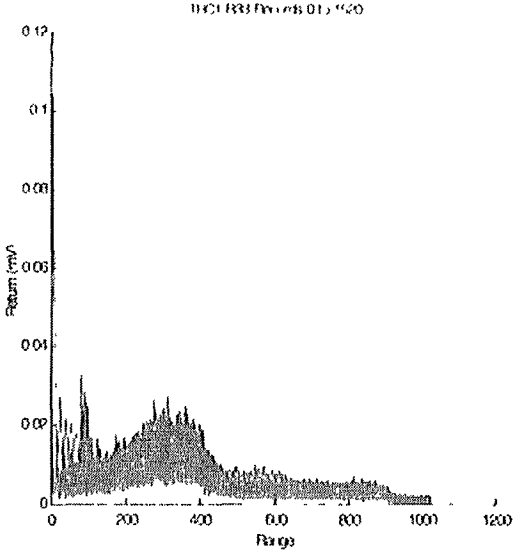

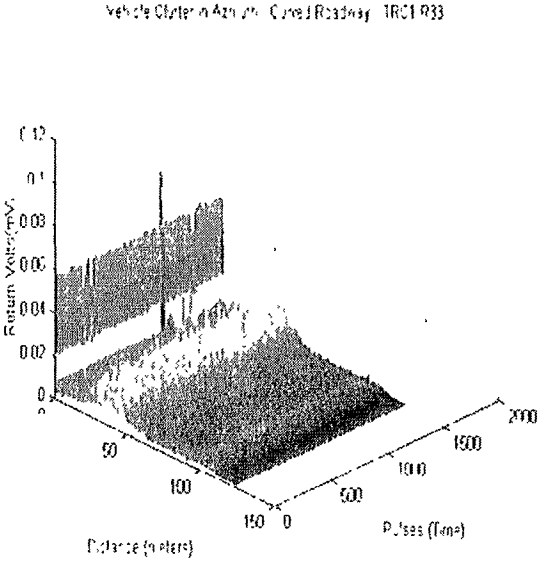

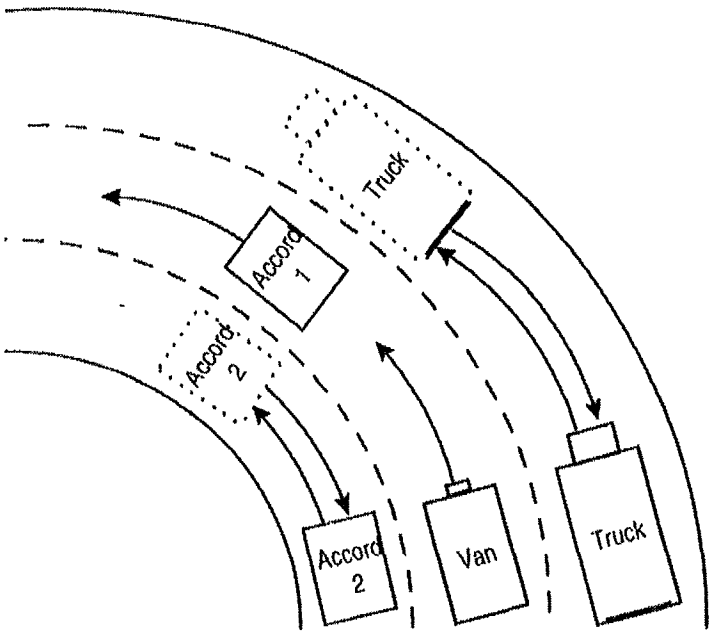

11:13:13 - Begin File

Truck/Accord 2 -- :21
exit scene

:14:13

Truck/Accord 2
even with Accord 1 -- :59
Accord 1 about 10m -- :57
in front of Van :53

Truck enters scene - :43

:33

Accord 1 in front of Van -- :13

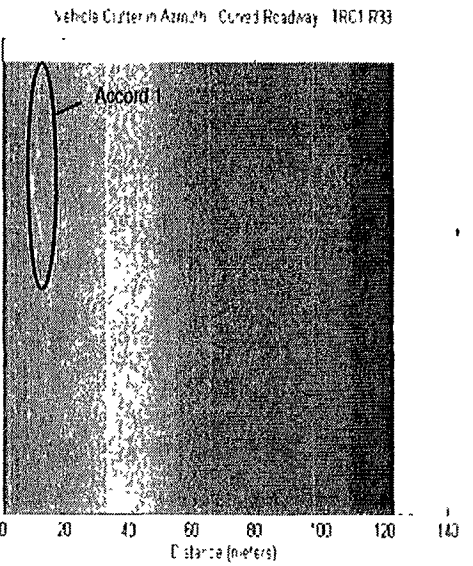

6.12 Vehicle Clutter in Azmuth - Curved Roadway

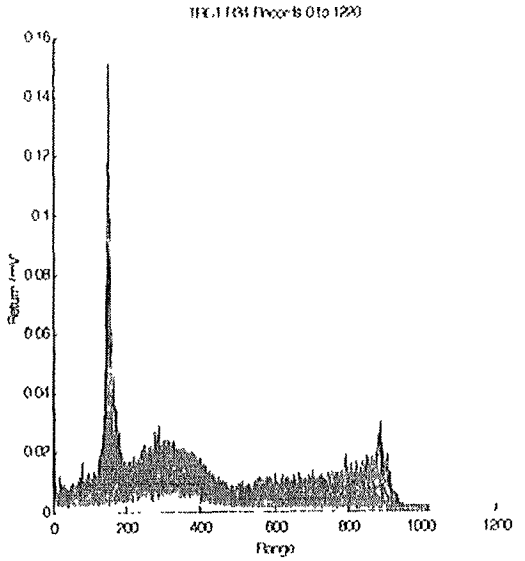

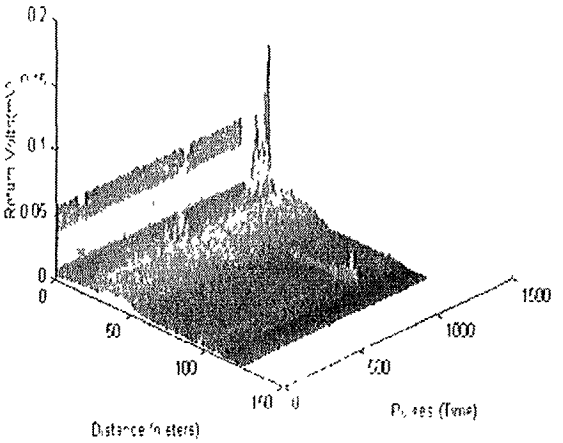

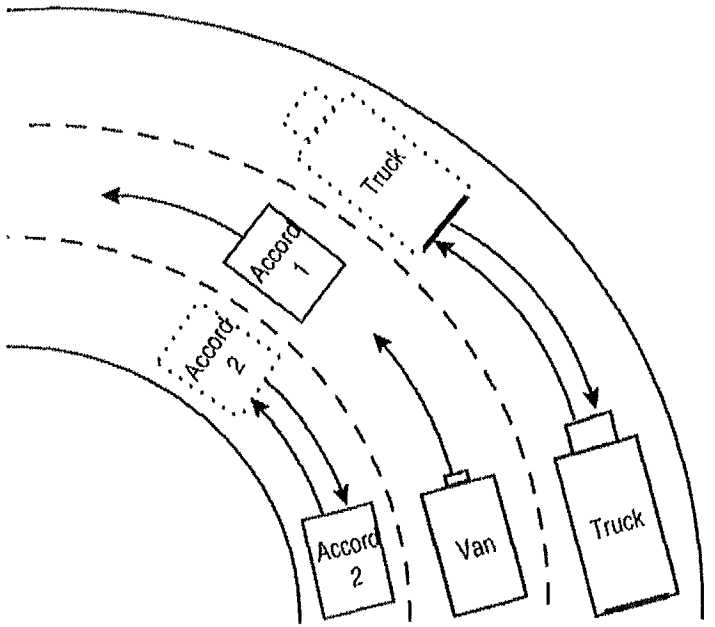

12:10:50 - Begin File

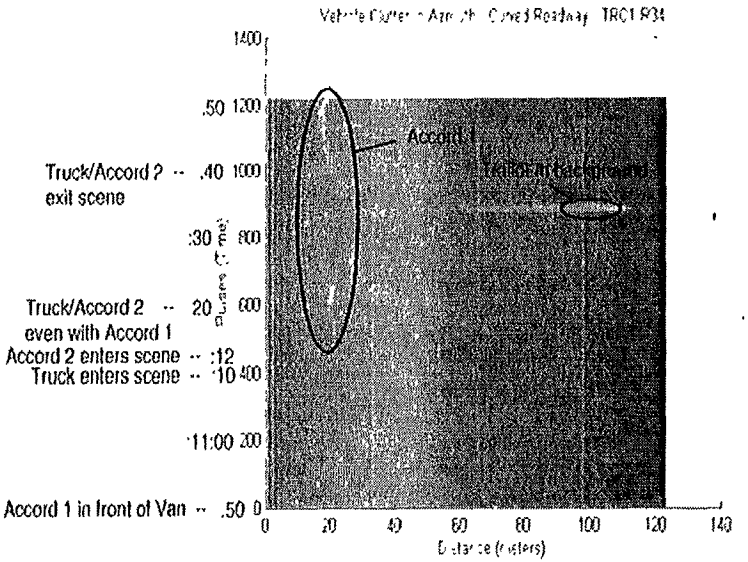

6.12 Vehicle Clutter in Azmuth - Curved Roadway

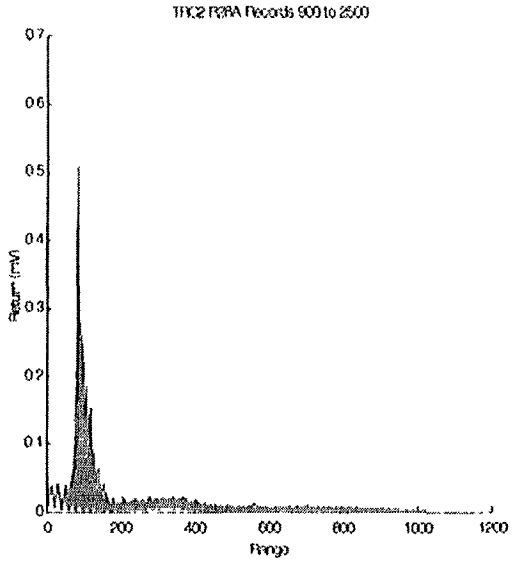

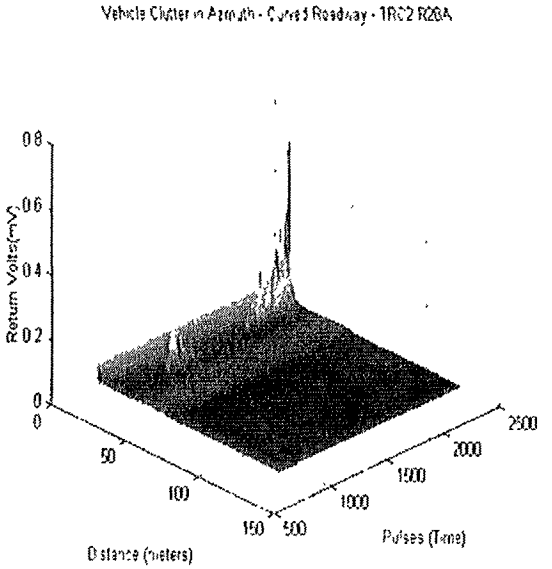

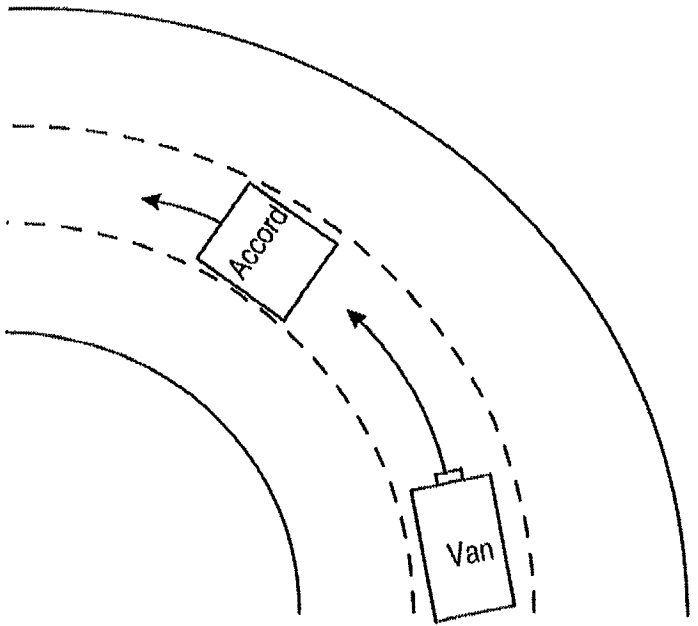

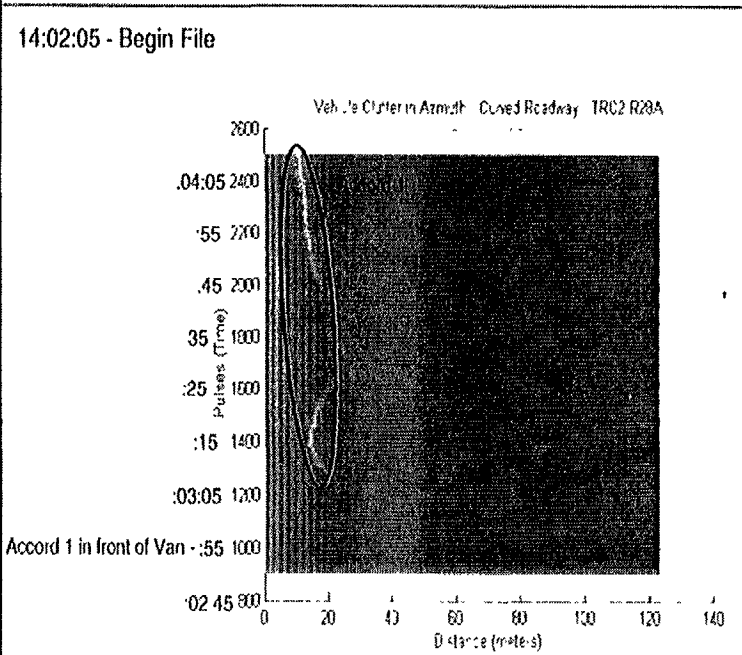

6.12 Vehicle Clutter in Azmuth - Curved Roadway

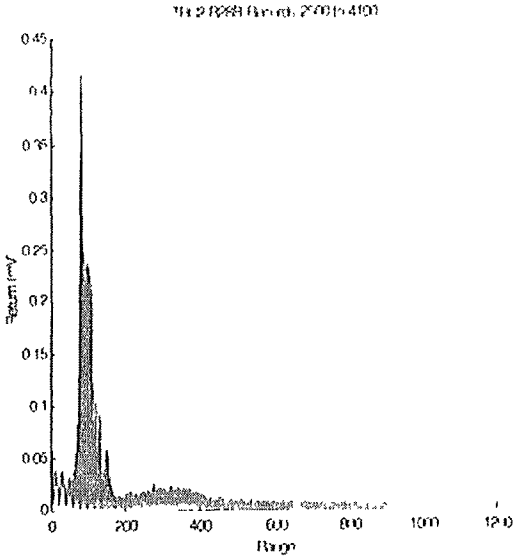

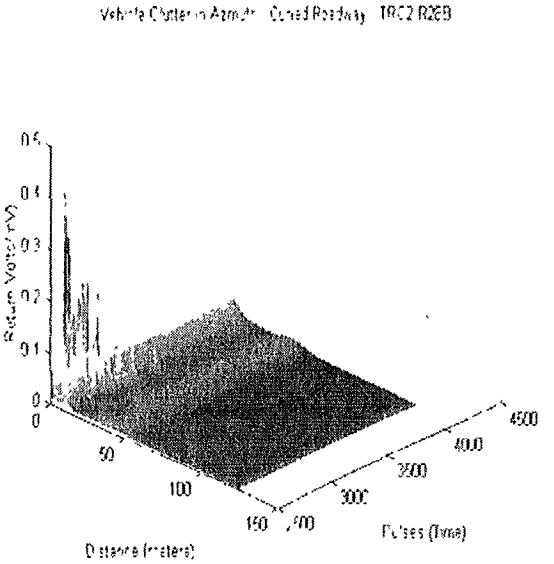

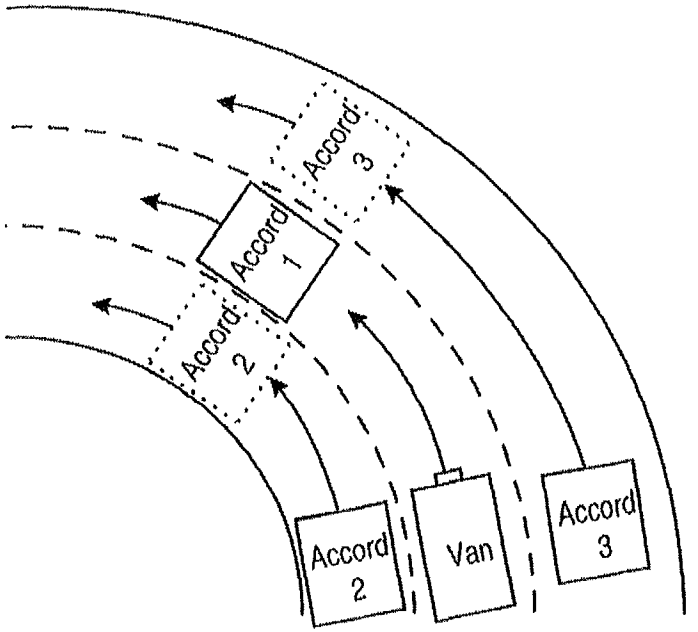

14:02:05 - Begin File

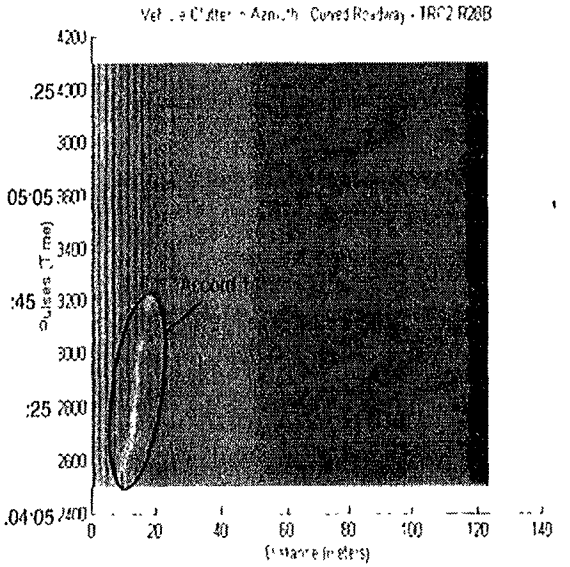

6.12 Vehicle-Clutter in Azmuth - Curved Roadway

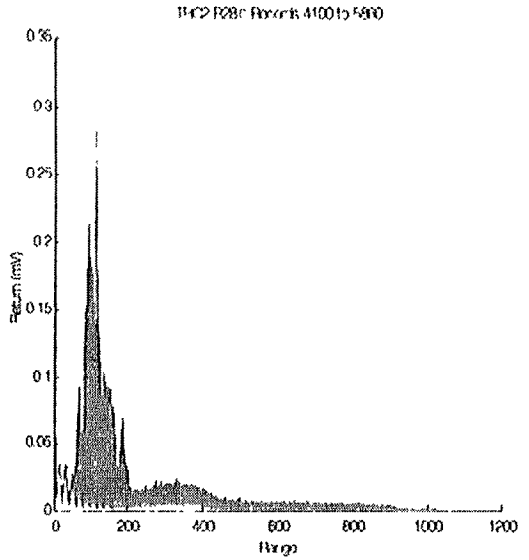

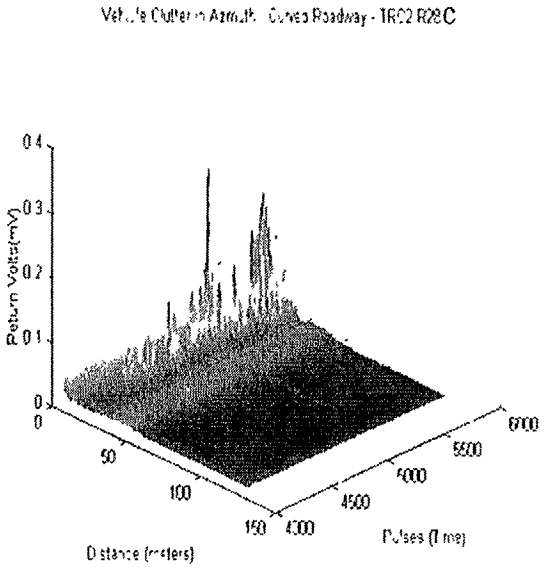

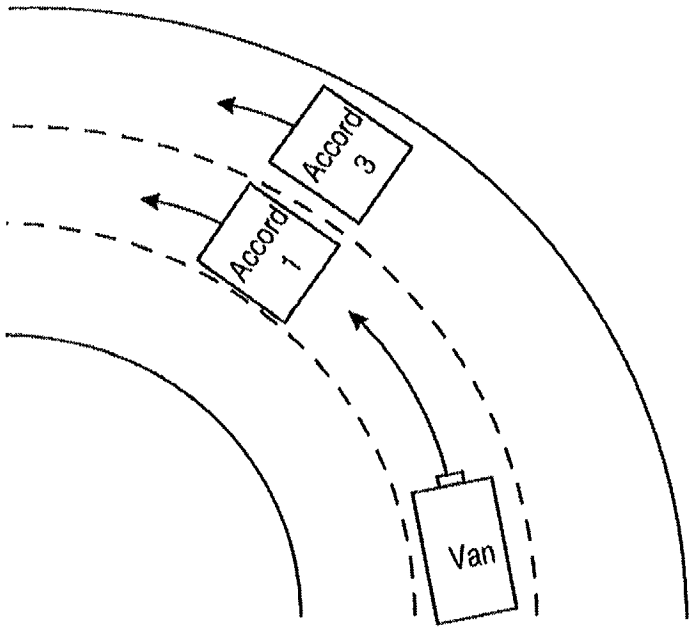

14:02:05 - Begin File

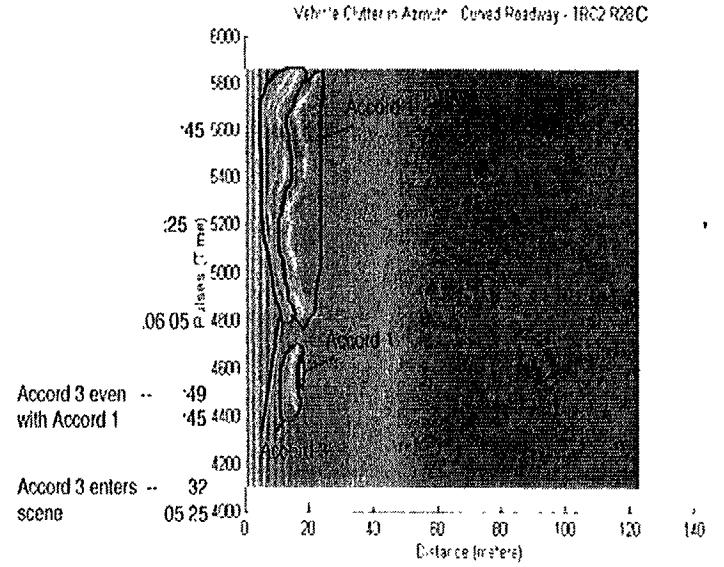

Accord 3 even with Accord 1

Accord 3 enters scene

6.12 Vehicle Clutter in Azmuth - Curved Roadway

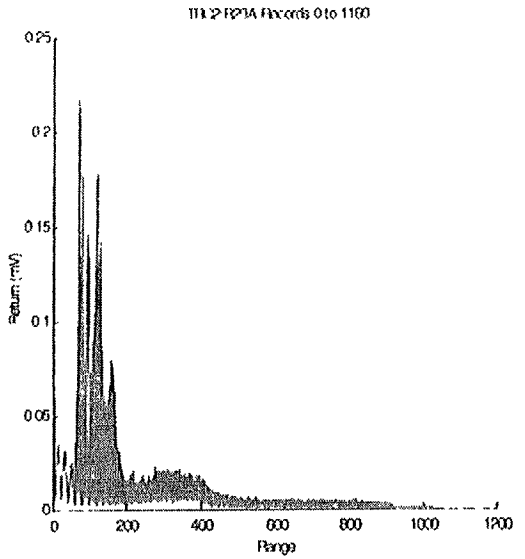

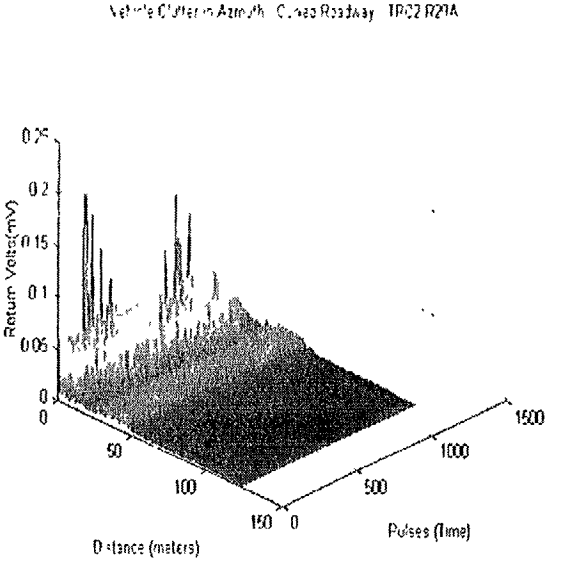

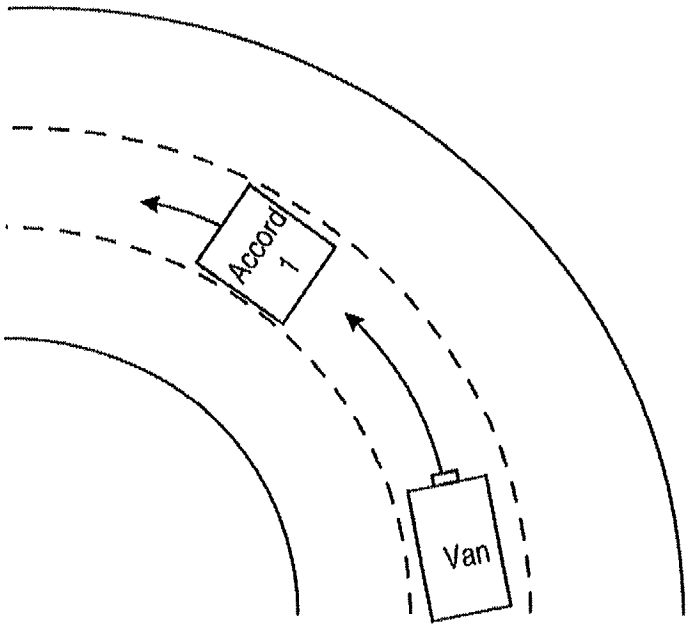

14:31:12 - Begin File

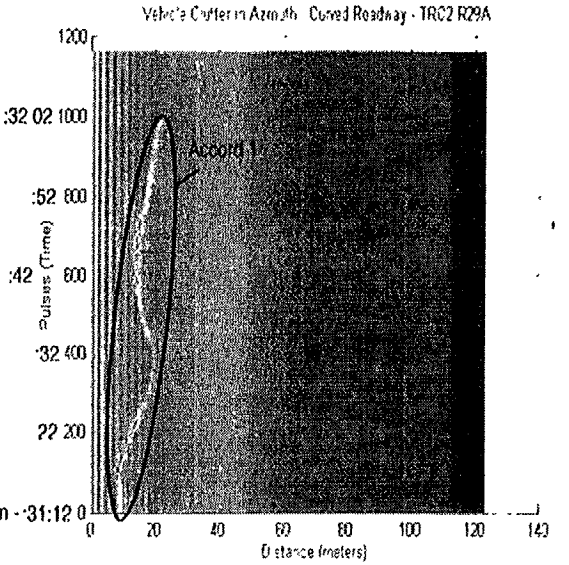

Accord 1 in front of Van - 31:12

6.12 Vehicle Clutter in Azmuth - Curved Roadway

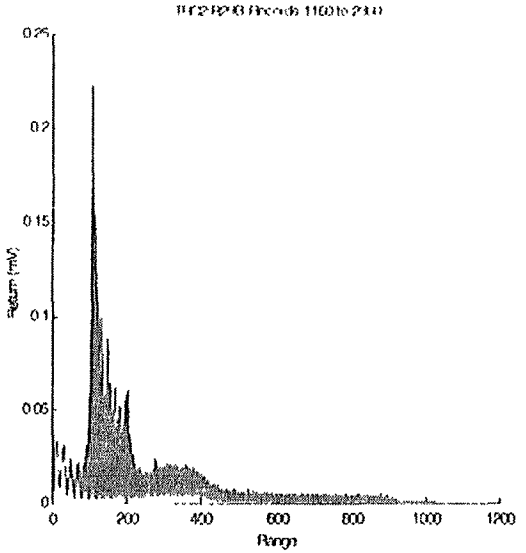

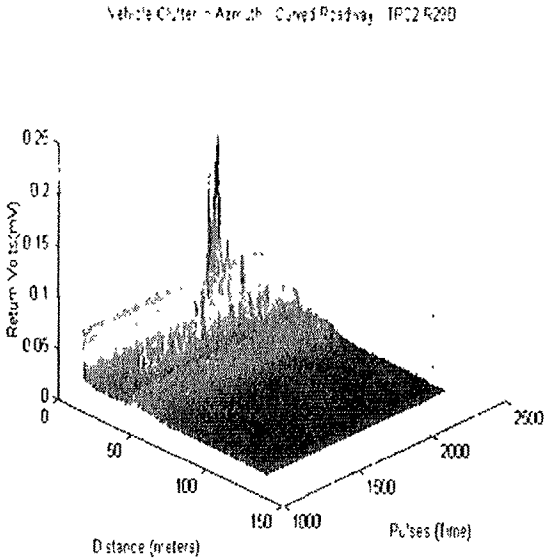

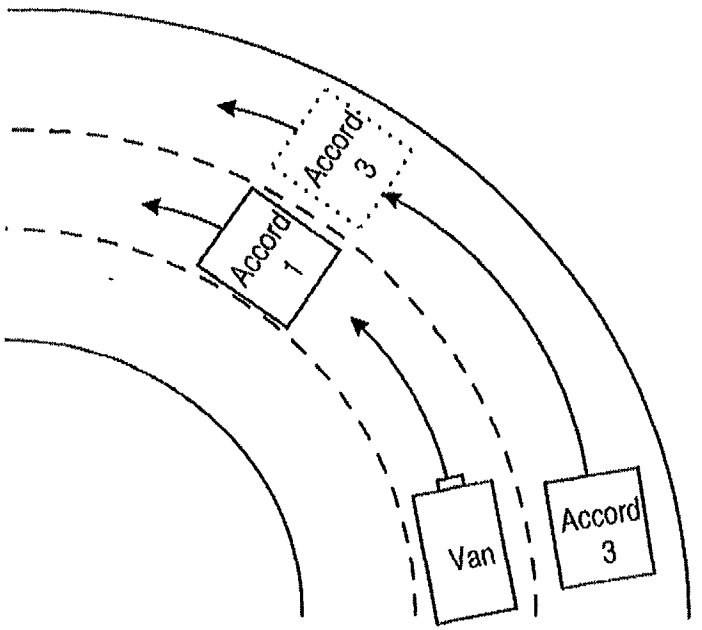

14:31:12 - Begin File

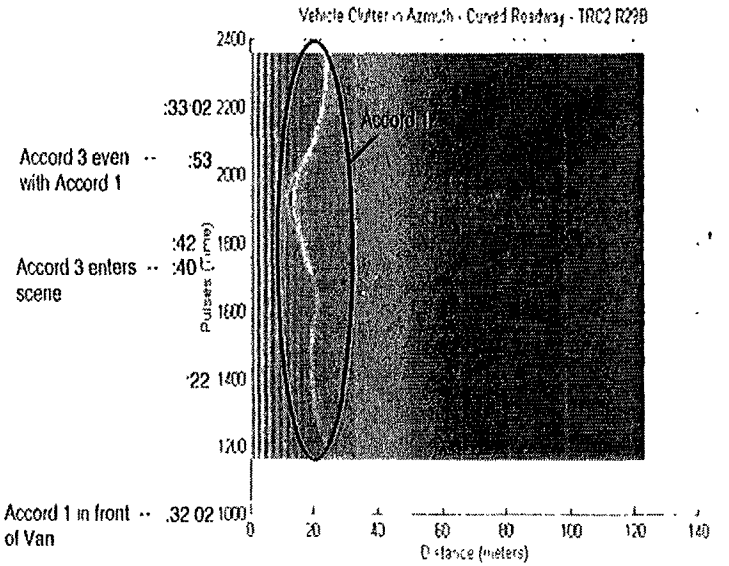

6.12 Vehicle Clutter in Azmuth - Curved Roadway

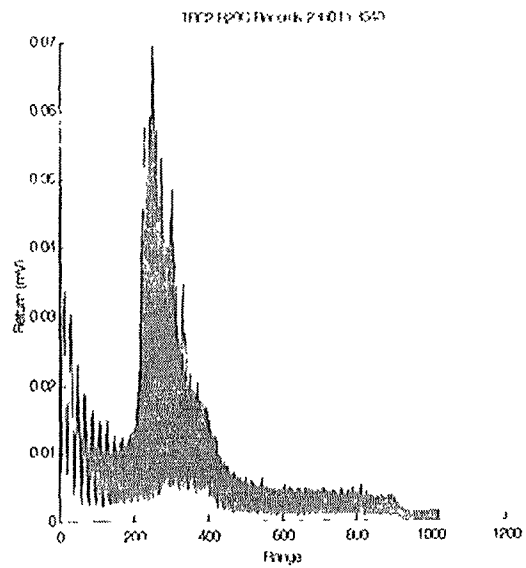

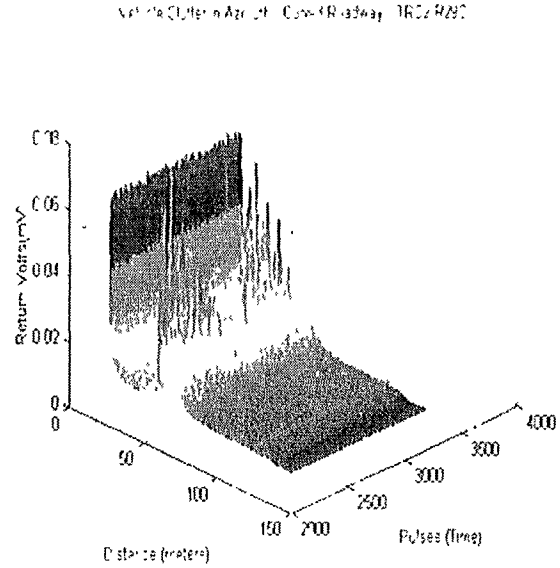

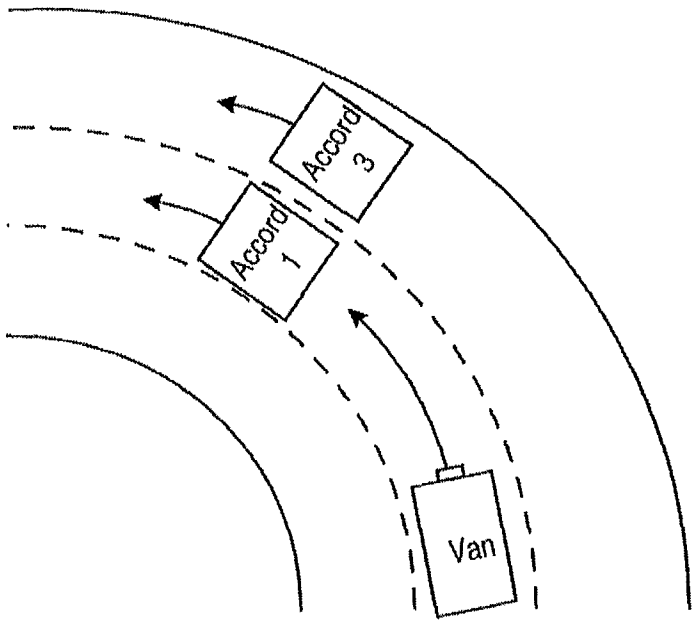

14:31:12 - Begin File

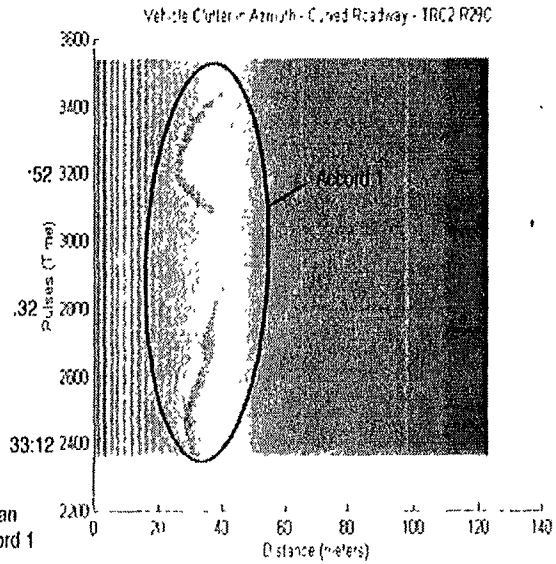

Accord 1 in front of Van
Accord 3 next to Accord 1

6.12 Vehicle Clutter in Azmuth - Curved Roadway

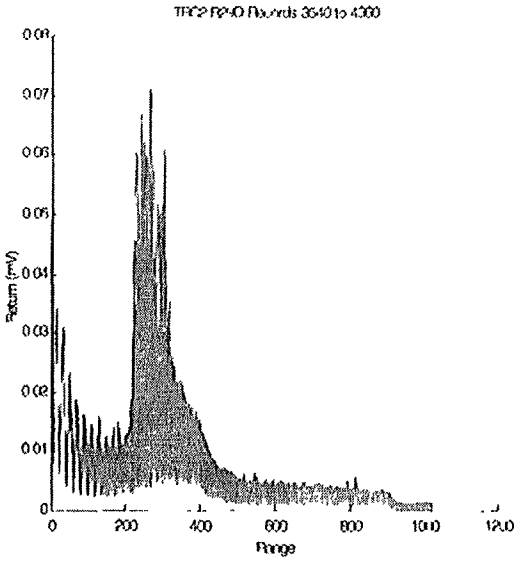

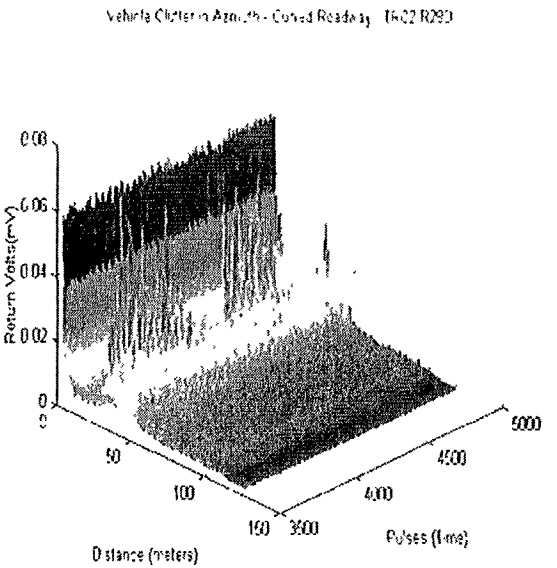

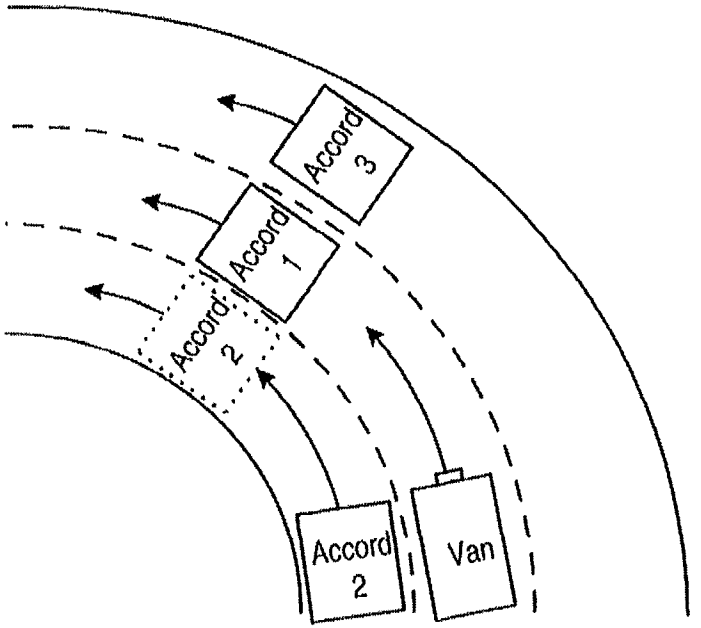

14:31:12 - Begin File

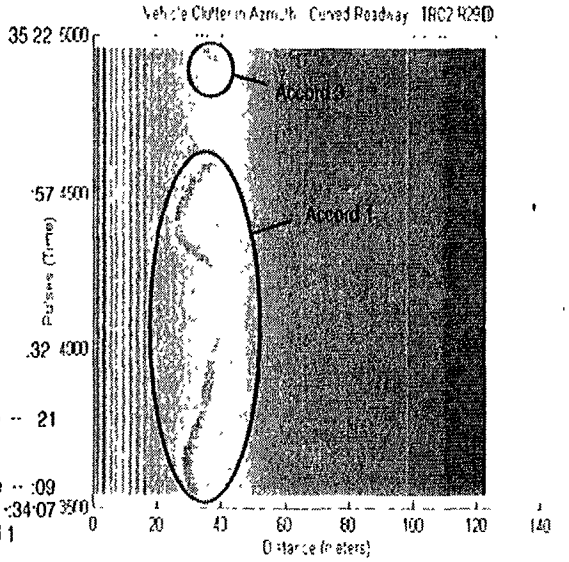

Accord 2 next to Accords 1 & 3 -- 21
Accord 2 enters scene -- :09
Accord 1 in front of Van -:34:07
Accord 3 next to Accord 1

6.12 Vehicle Clutter in Azmuth - Curved Roadway

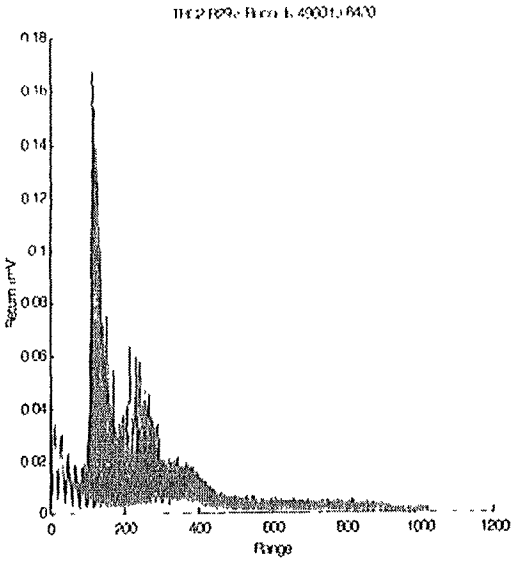

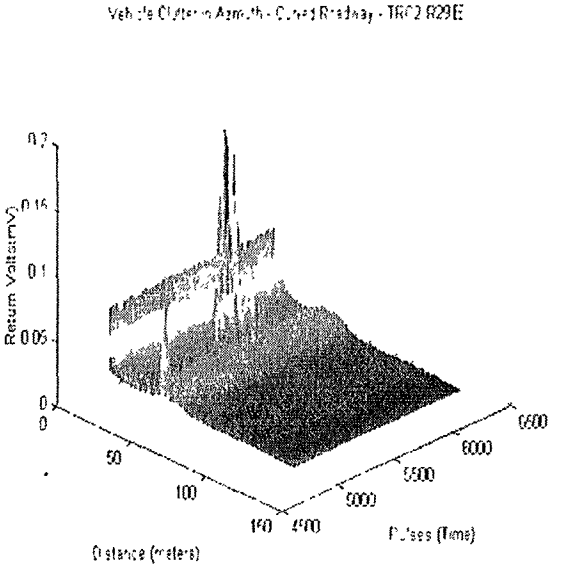

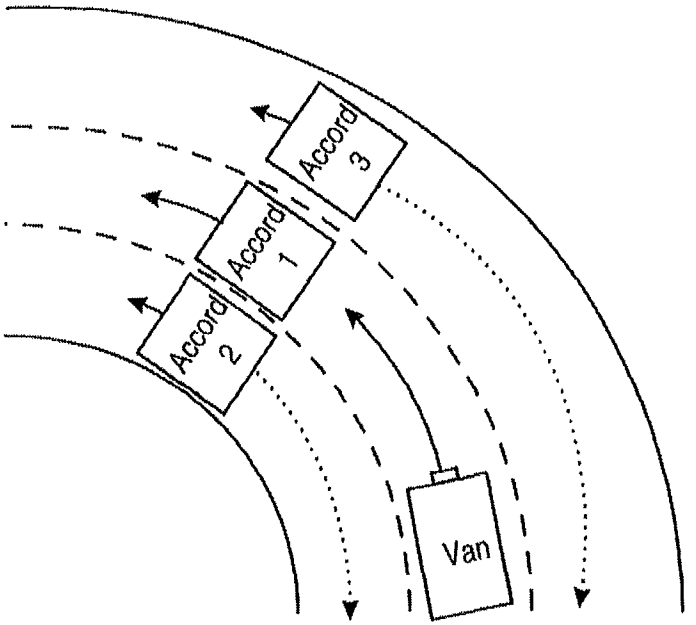

14:31:12 - Begin File

Accord 3 exits scene -- :35:41

Accords 1,2 & 3 in front of Van -- :35:22

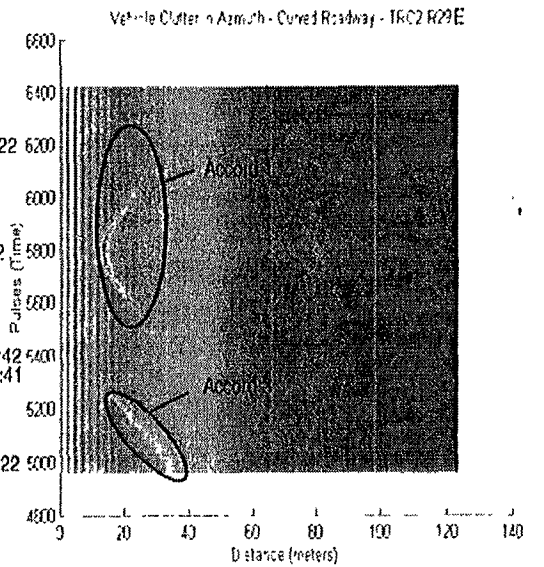

6.12 Vehicle Clutter in Azmuth - Curved Roadway

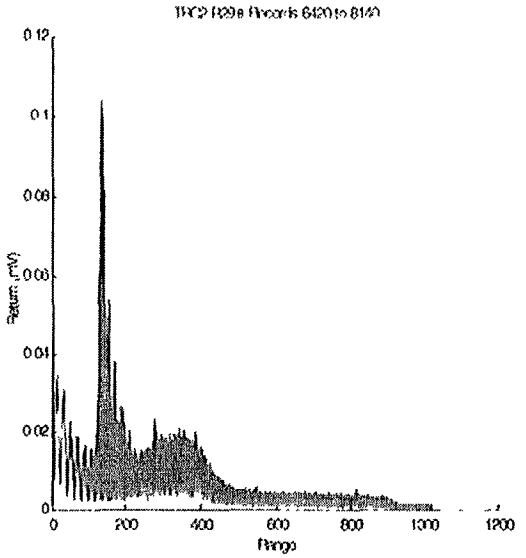

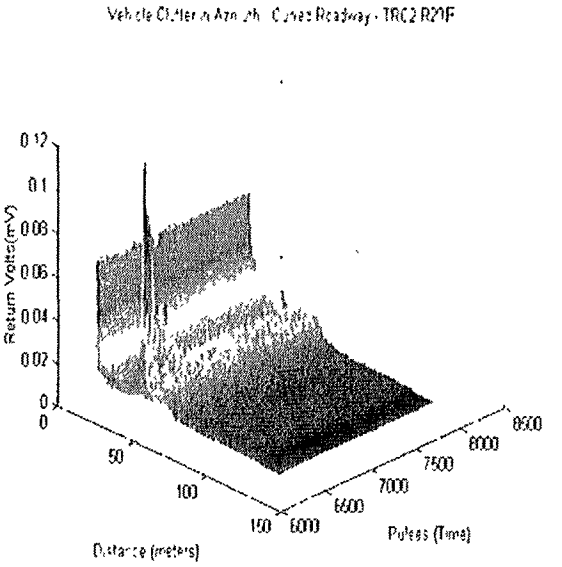

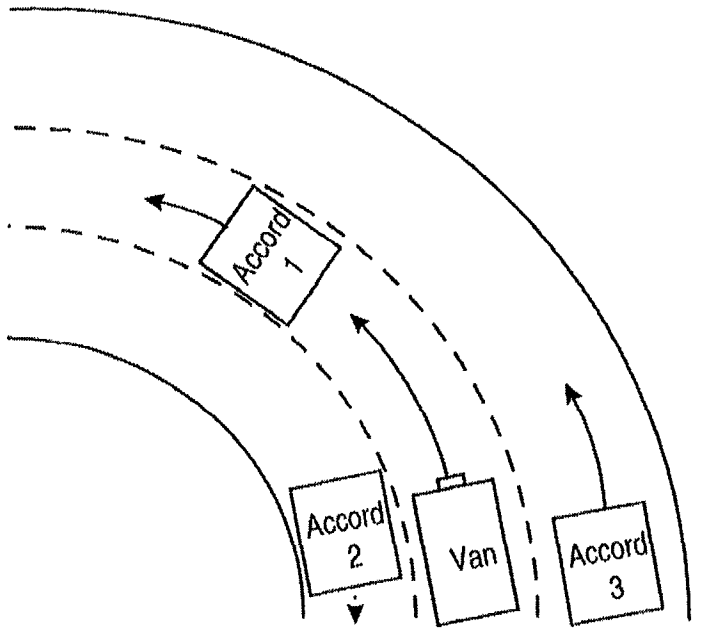

14:31:12 - Begin File

Accord 3 enters scene

Accord 1 in front

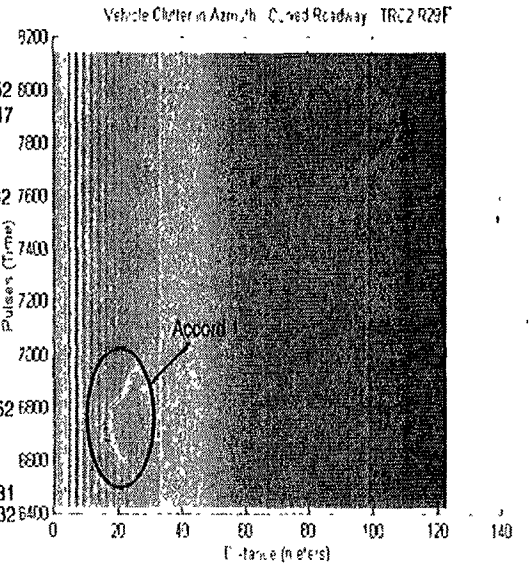

6.12 Vehicle Clutter in Azmuth - Curved Roadway

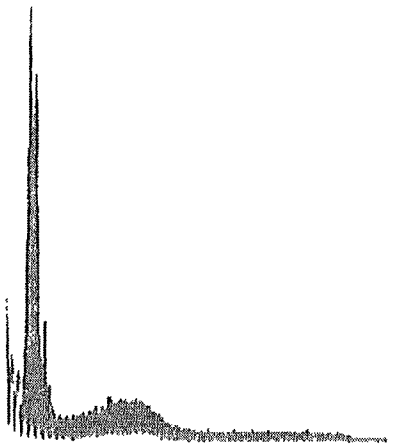

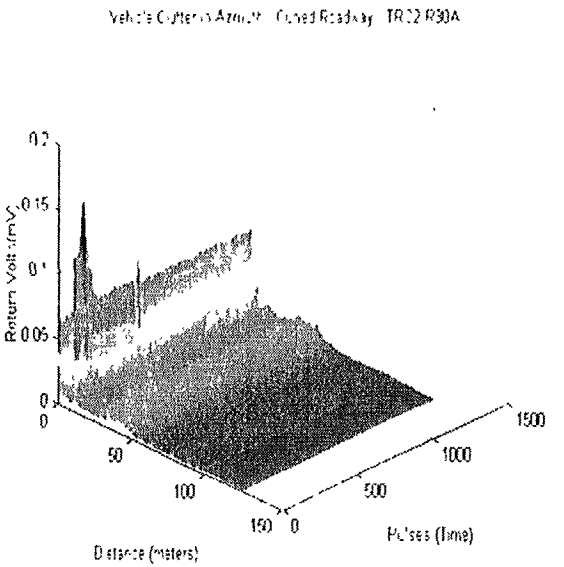

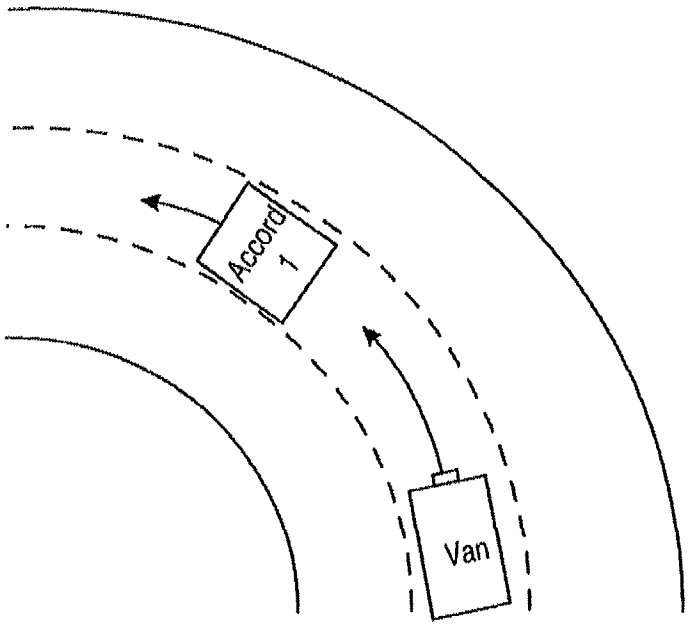

15:34:24 - Begin File

Accord 1 begins to move - :47

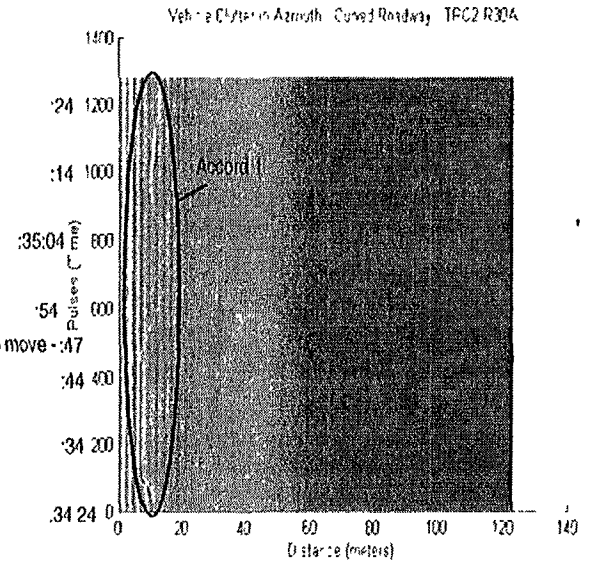

6.12 Vehicle Clutter in Azmuth - Curved Roadway

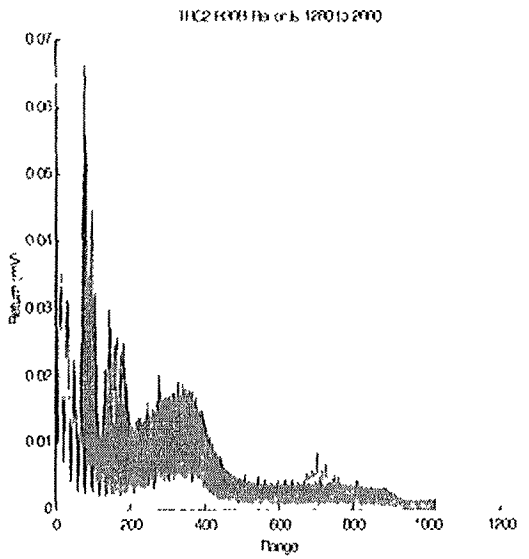

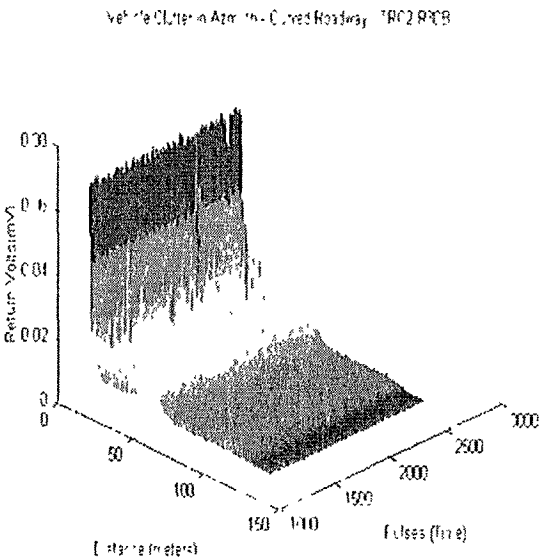

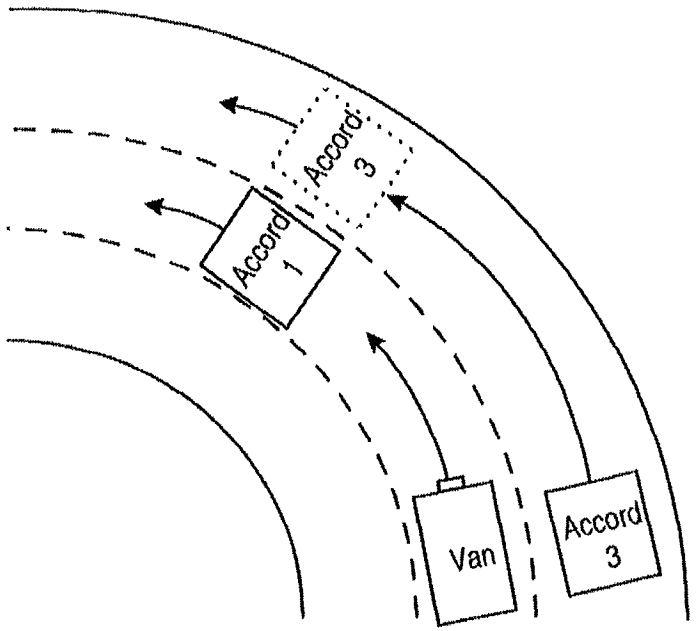

15:34:24 - Begin File

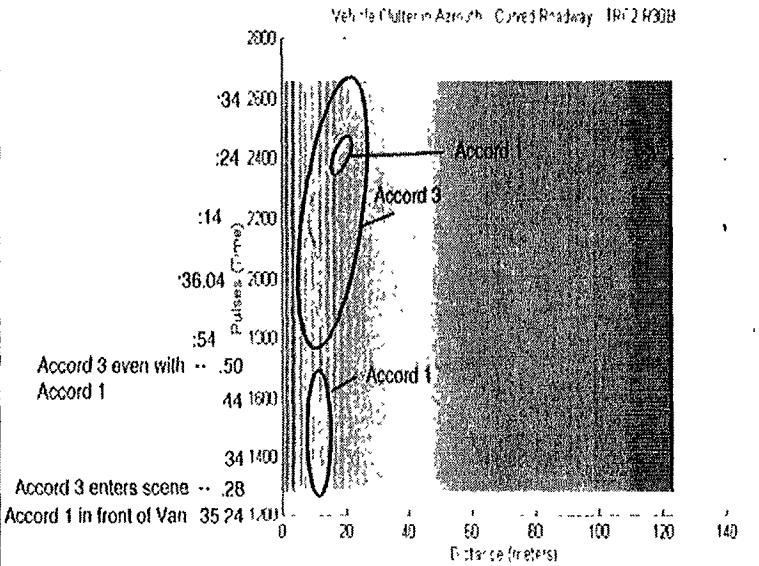

6.12 Vehicle Clutter in Azmuth - Curved Roadway

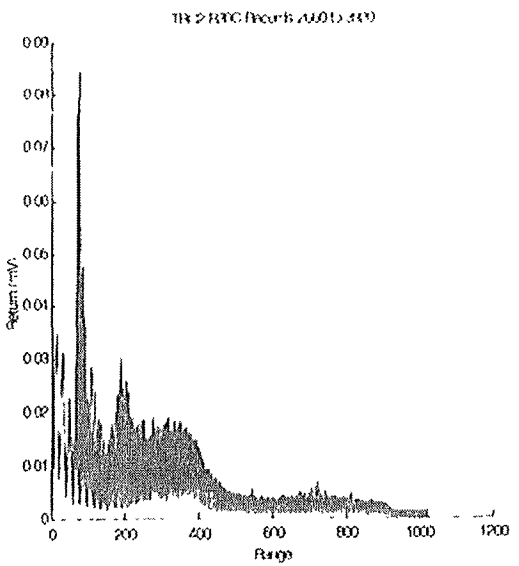

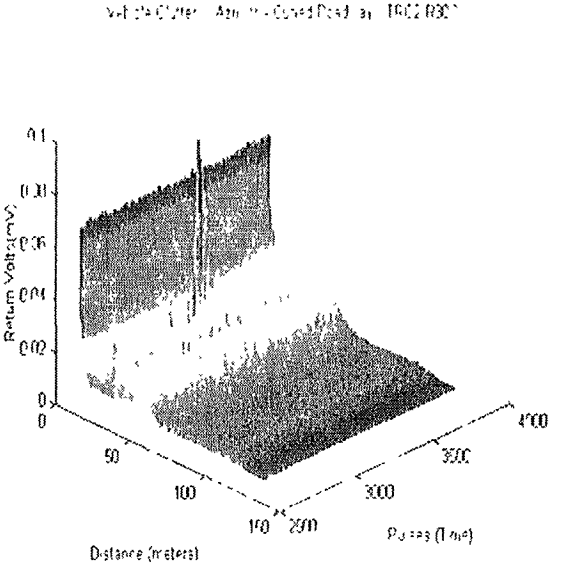

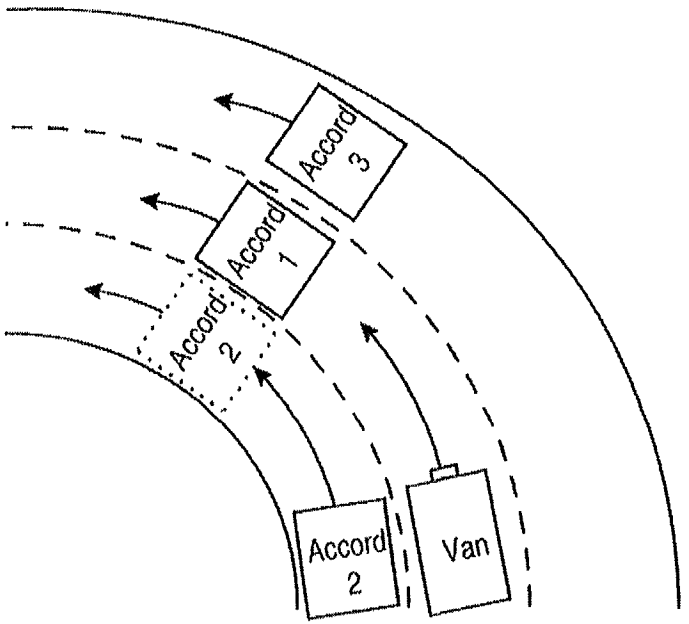

15:34:24 - Begin File

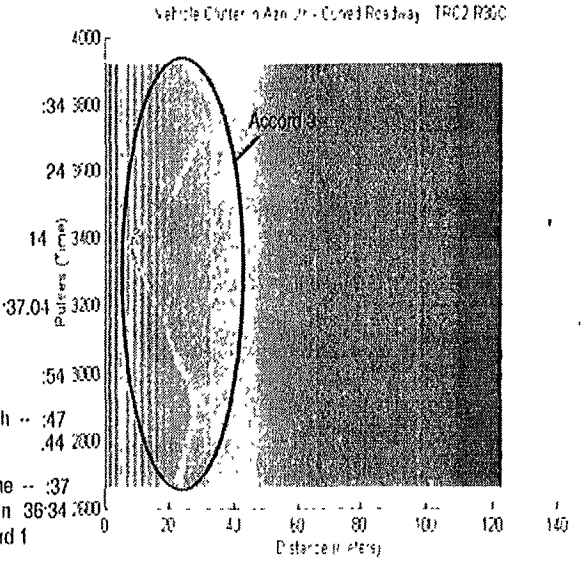

Accord 2 even with Accords 1 & 3 -- :47 :44

Accord 2 enters scene -- :37

Accord 1 in front of Van 36:34

Accord 3 next to Accord 1

6.12 Vehicle Clutter in Azmuth - Curved Roadway

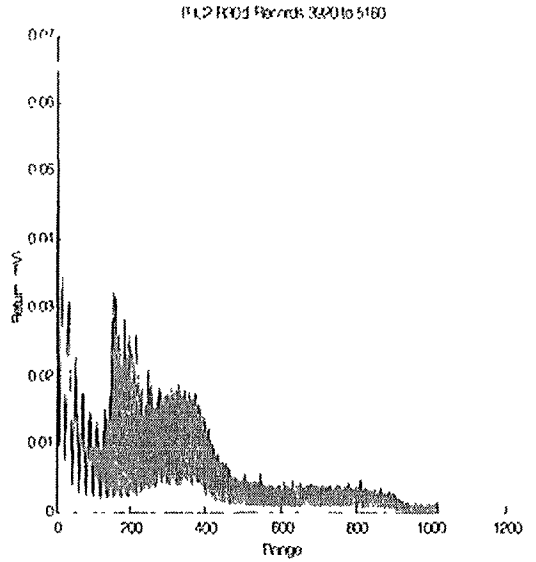

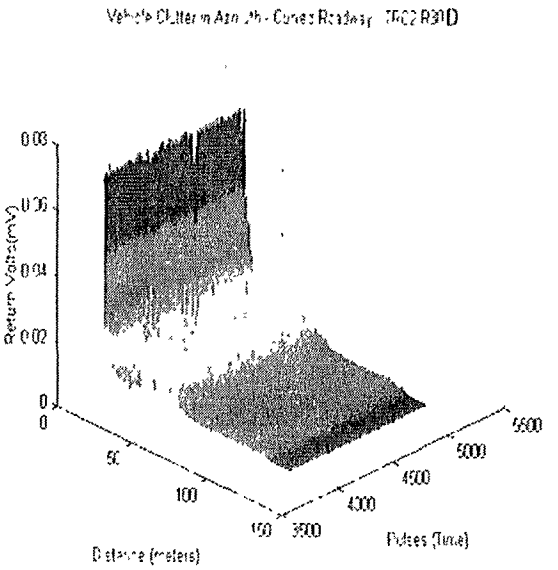

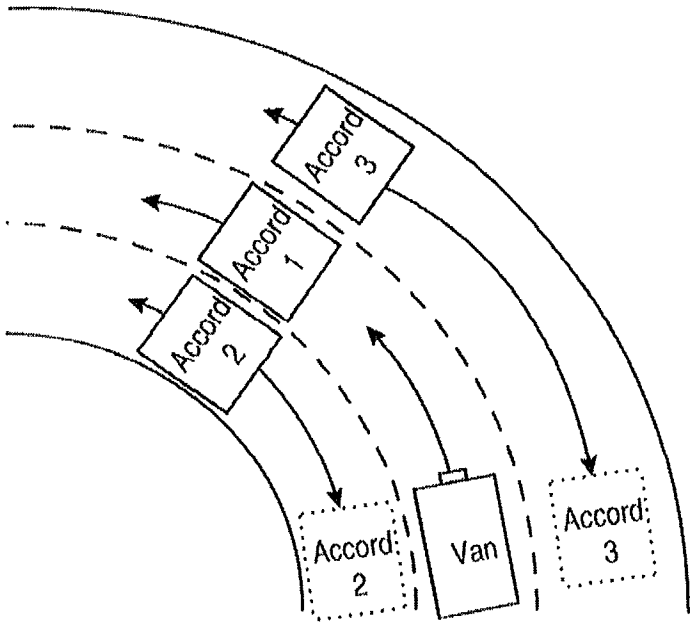

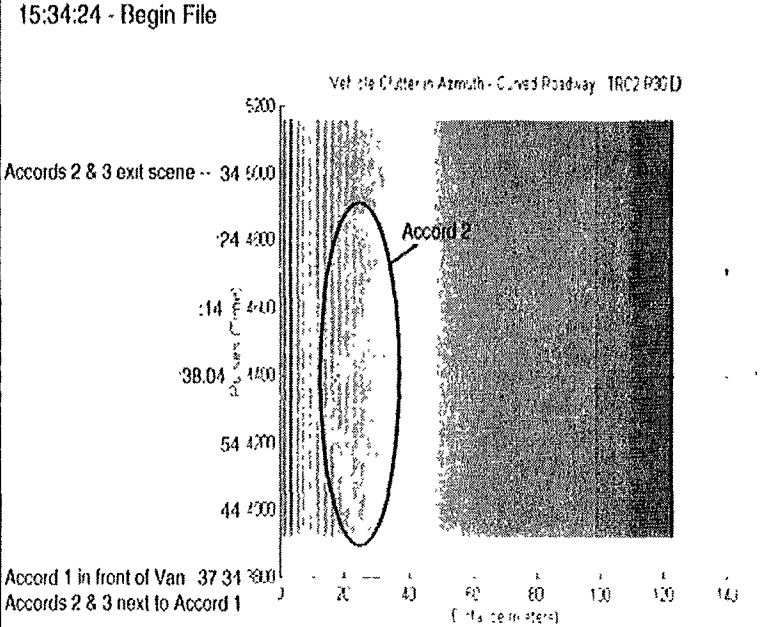

6.12 Vehicle Clutter in Azmuth - Curved Roadway

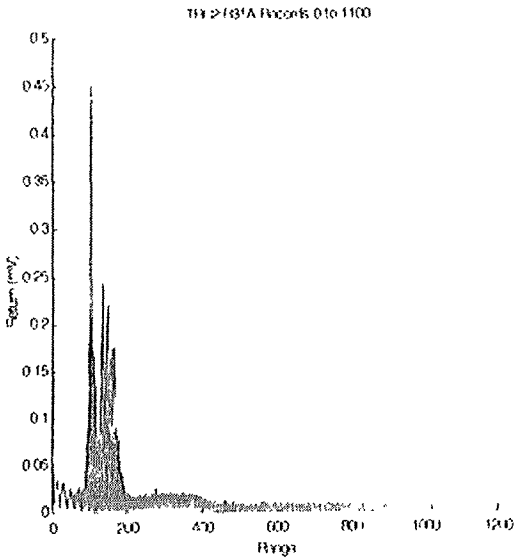

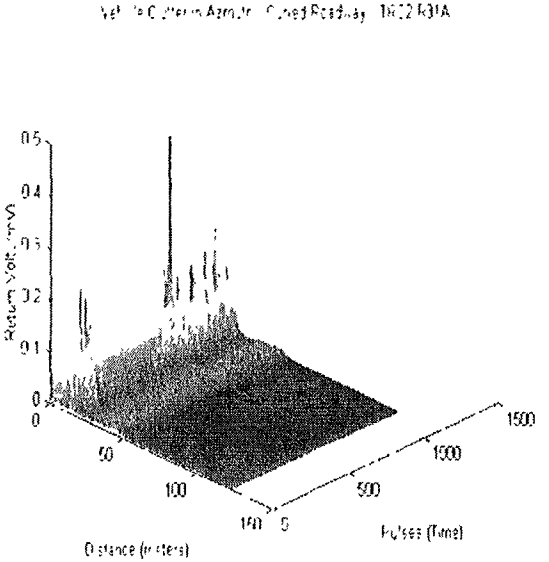

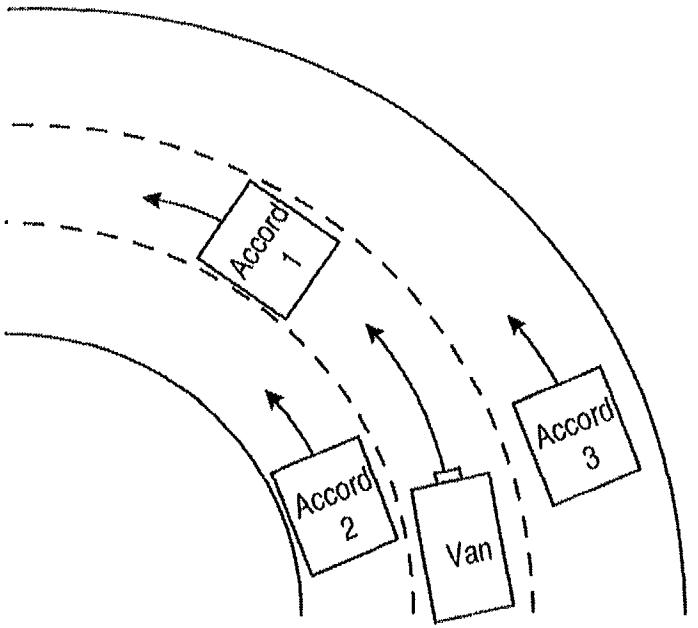

14:12:59 - Begin File

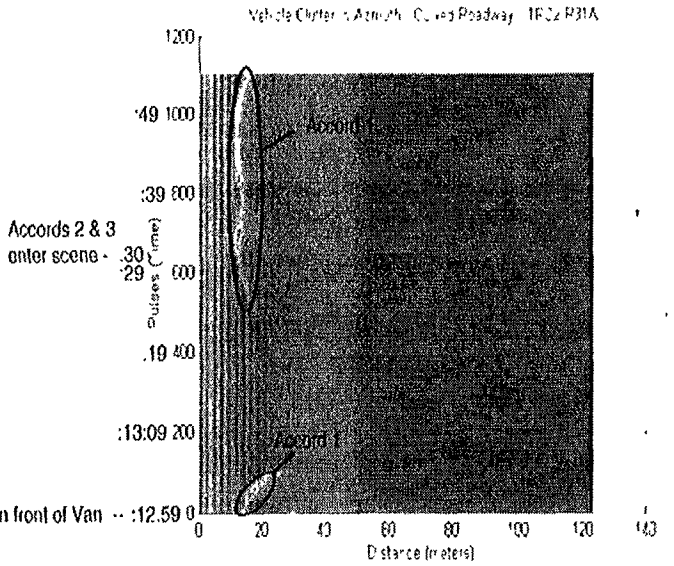

6.12 Vehicle Clutter in Azmuth - Curved Roadway

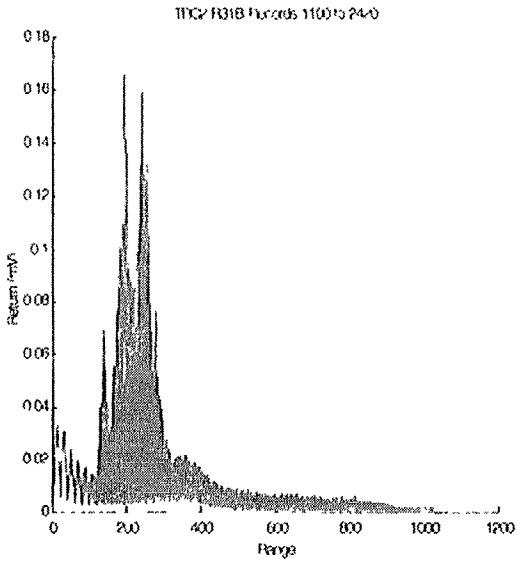

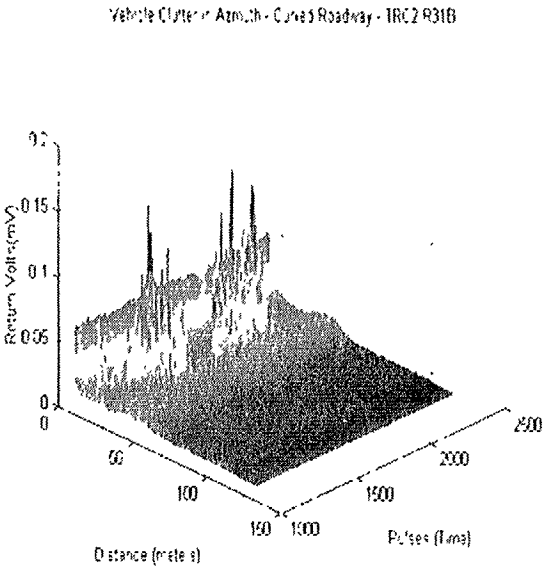

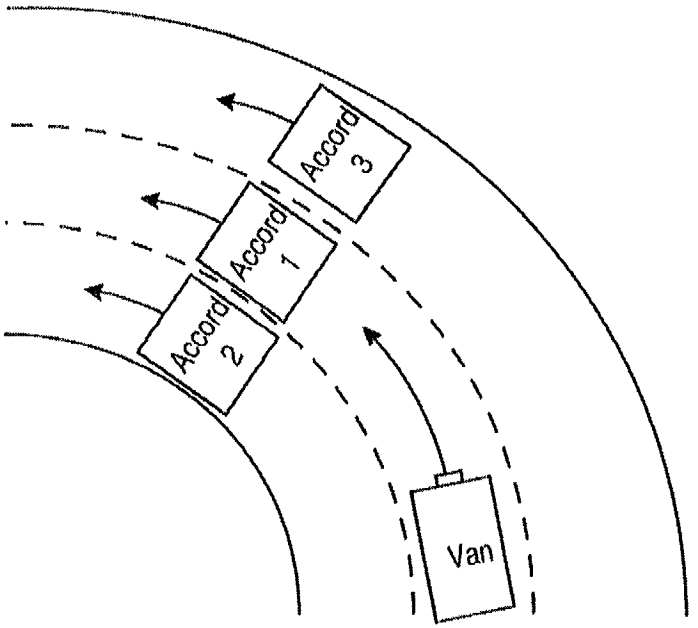

14:12:59 - Begin File

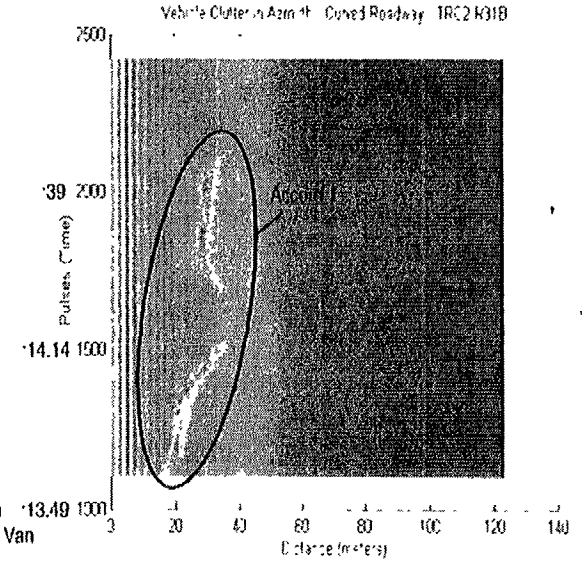

Accords 1,2,3 even
Accord 1 in front of Van

6.12 Vehicle Clutter in Azmuth - Curved Roadway

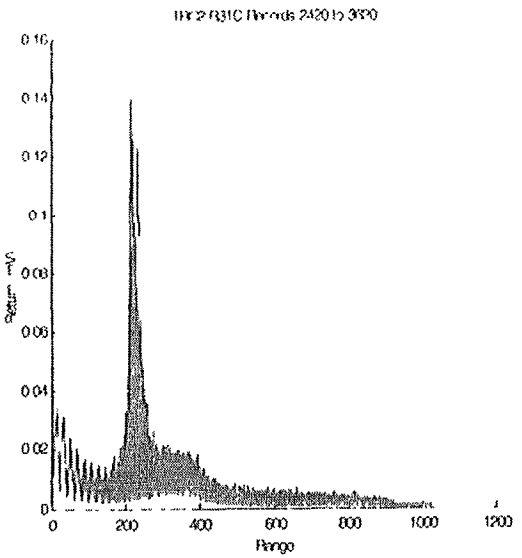

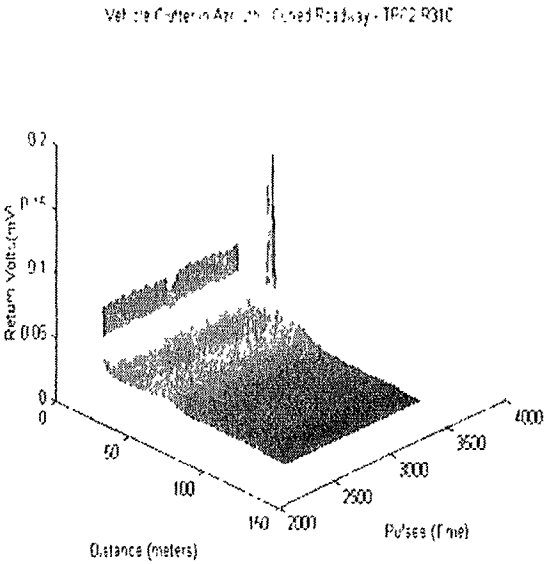

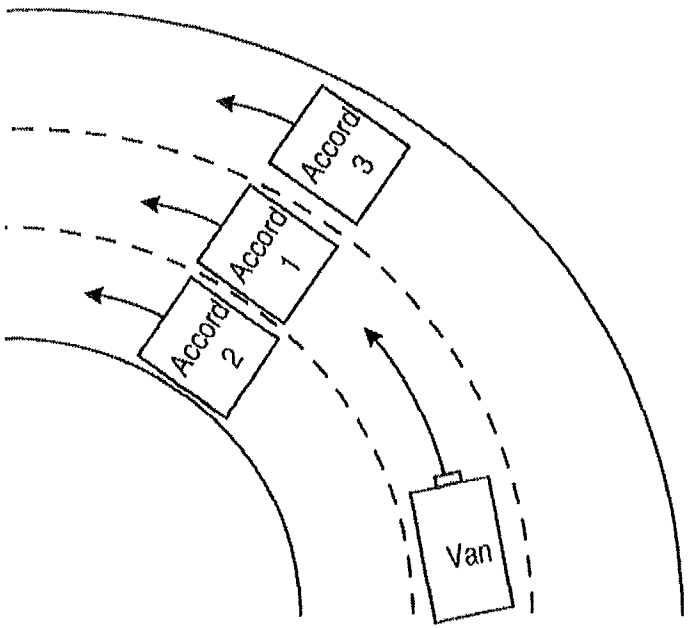

14:12:59 - Begin File

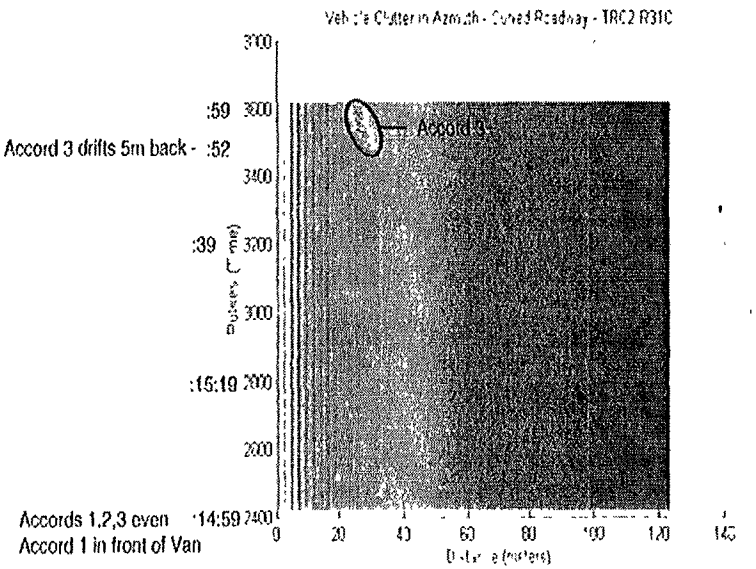

6.12 Vehicle Clutter in Azmuth - Curved Roadway

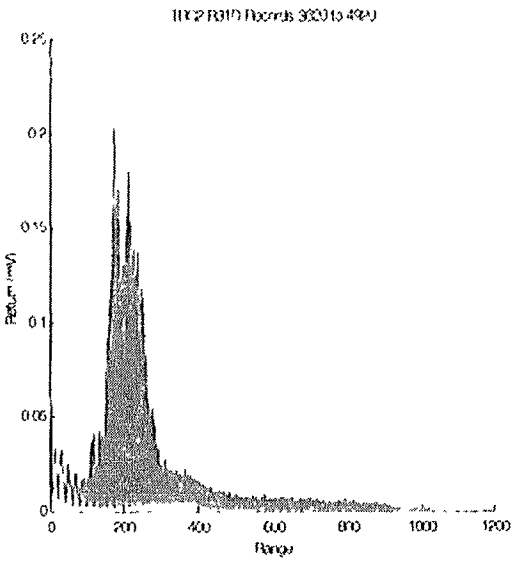

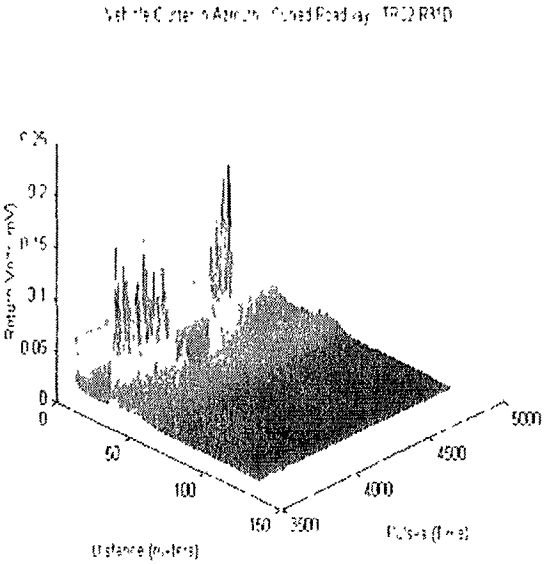

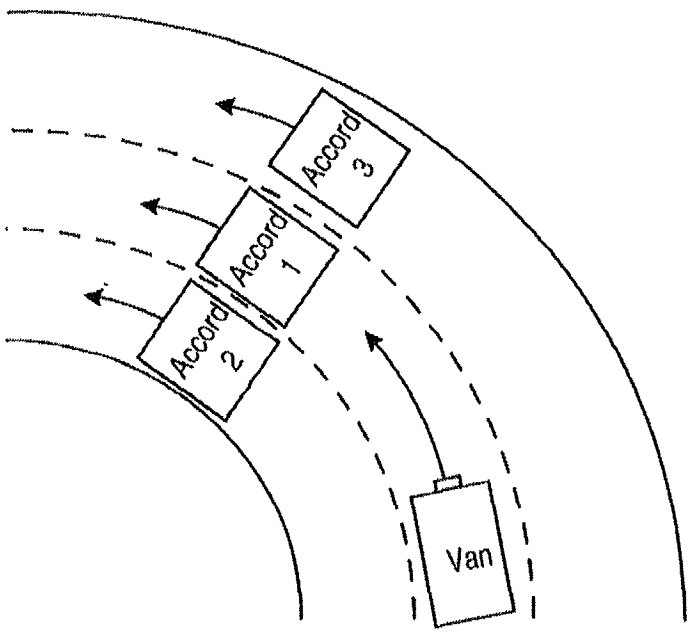

14:12:59 - Begin File

Accord 3 drifts back -- again from Accords 1,2

Accord 3 back in line -- with Accords 1,2

Accords 2,3 next to Accord 1
Accord 1 in front of Van

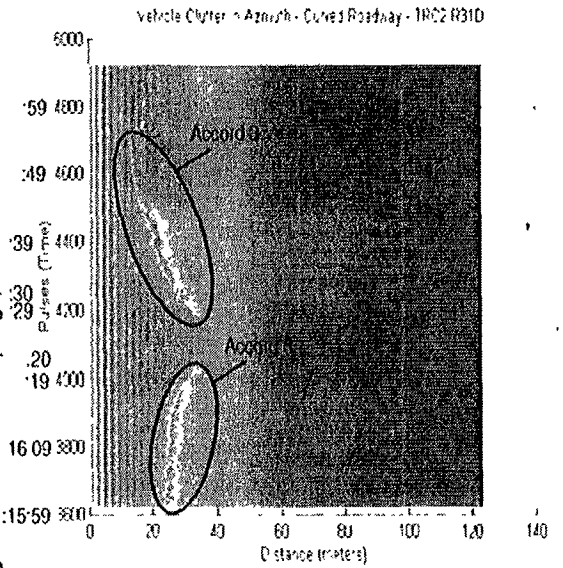

6.12 Vehicle Clutter in Azmuth - Curved Roadway

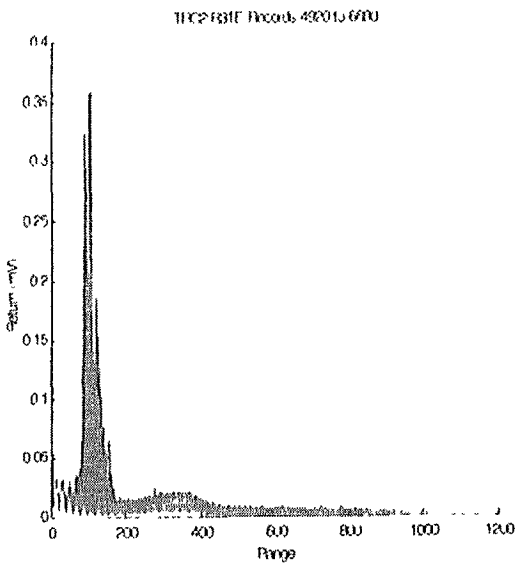

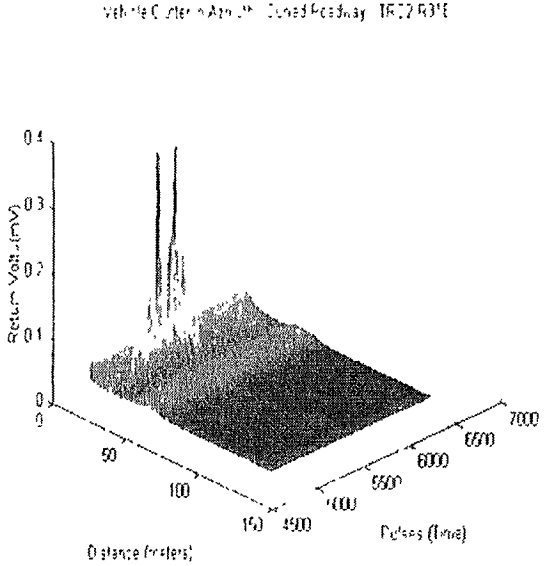

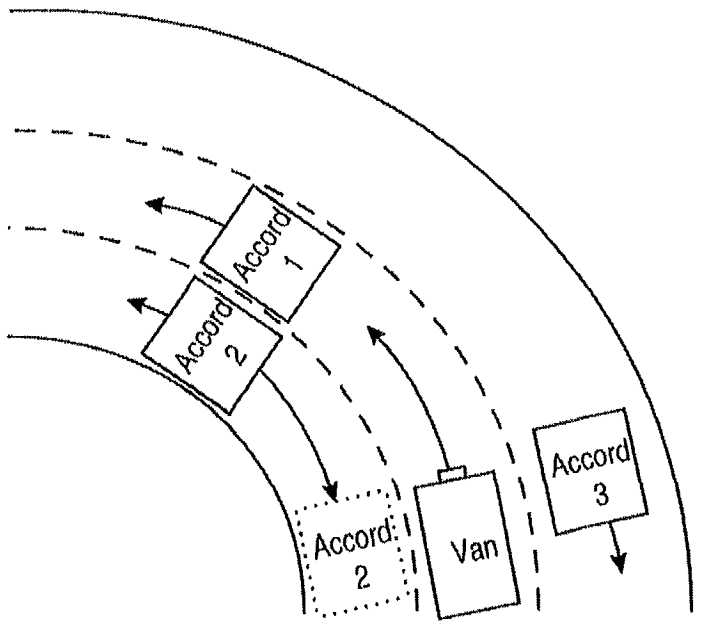

14:12:59 - Begin File